



Prolonged morphological expansion of spiny-rayed fishes following the end-Cretaceous

Ava Ghezelayagh^{1,18}  , Richard C. Harrington^{1,18}  , Edward D. Burress¹ , Matthew A. Campbell^{2,3}, Janet C. Buckner^{4,5}, Prosanta Chakrabarty⁶ , Jessica R. Glass⁷ , W. Tyler McCraney⁵, Peter J. Unmack⁸, Christine E. Thacker^{9,10} , Michael E. Alfaro⁵ , Sarah T. Friedman^{1,11}, William B. Ludt¹⁰, Peter F. Cowman¹² , Matt Friedman^{13,14} , Samantha A. Price¹⁵, Alex Dornburg¹⁶ , Brant C. Faircloth⁶ , Peter C. Wainwright¹¹  and Thomas J. Near^{1,17}

Spiny-rayed fishes (Acanthomorpha) dominate modern marine habitats and account for more than a quarter of all living vertebrate species. Previous time-calibrated phylogenies and patterns from the fossil record explain this dominance by correlating the origin of major acanthomorph lineages with the Cretaceous–Palaeogene mass extinction. Here we infer a time-calibrated phylogeny using ultraconserved elements that samples 91.4% of all acanthomorph families and investigate patterns of body shape disparity. Our results show that acanthomorph lineages steadily accumulated throughout the Cenozoic and underwent a significant expansion of among-clade morphological disparity several million years after the end-Cretaceous. These acanthomorph lineages radiated into and diversified within distinct regions of morphospace that characterize iconic lineages, including fast-swimming open-ocean predators, laterally compressed reef fishes, bottom-dwelling flatfishes, seahorses and pufferfishes. The evolutionary success of spiny-rayed fishes is the culmination of multiple species-rich and phenotypically disparate lineages independently diversifying across the globe under a wide range of ecological conditions.

Spiny-rayed fishes (Acanthomorpha) account for more than a quarter of all living vertebrates and are globally distributed across all types of aquatic ecosystem^{1–4}. Acanthomorphs are especially prevalent in modern nearshore marine habitats, with familiar representatives including sticklebacks, seahorses and commercially important species such as cod, tuna and flatfishes. Despite the scientific, economic and cultural importance of acanthomorphs, how spiny-rayed fishes diversified to become the dominant marine vertebrate lineage remains relatively unexplored.

The evolutionary success of acanthomorph fishes has repeatedly been linked to the Cretaceous–Palaeogene (K–Pg) mass extinction^{3,5–7}, which occurred 66 million years ago (Ma) and is understood to have laid the foundation for spectacular radiations of terrestrial vertebrates^{8–15}. The most inclusive lineages of acanthomorph fishes (for example, Syngnathiformes, Labriformes and Perciformes) originated before or during the Late Cretaceous^{3,16,17}, but Palaeogene fossils demonstrate that acanthomorph taxonomic diversity and morphological disparity increased substantially after the K–Pg event⁶. Phylogenomic analyses have raised the complementary proposal that the origins of many major acanthomorph lineages coincide with the K–Pg^{7,18}. However, the acanthomorph fossil record is sparse in the 20 million years around the end-Cretaceous^{6,16}, and

phylogenomic efforts so far have been limited by sampling designs that inadequately represent the group's staggering taxonomic richness^{7,18}. These factors have hindered resolution of the timing and patterns of acanthomorph diversification near the K–Pg; it remains uncertain if acanthomorph diversification in the Cenozoic was gradual or punctuated, whether lineage diversification is coupled with phenotypic disparity, and how individual lineages contributed to a collective pattern of acanthomorph diversification. A well-resolved, time-calibrated phylogeny that includes all major lineages is critical to understanding the evolutionary dynamics of spiny-rayed fishes across the K–Pg boundary and beyond.

The largest challenge to acanthomorph evolutionary studies is inferring a phylogeny of its more than 19,450 species¹⁴. The resolution of relationships within the subclade Percomorpha, which contains more than 95% of all acanthomorph species, has been particularly difficult. During most of the twentieth century, inferences of acanthomorph and percomorph relationships relied on anatomical characters that resulted in largely unresolved phylogenetic hypotheses¹⁹. Although these early morphological investigations defined major groups of acanthomorphs, their conclusions were dramatically upended by the introduction of phylogenies inferred from a relatively small number of Sanger-sequenced

¹Department of Ecology and Evolutionary Biology, Yale University, New Haven, CT, USA. ²Department of Animal Science, University of California, Davis, CA, USA. ³University of Alaska Museum of the North, Fairbanks, AK, USA. ⁴Department of Biology, University of Texas, Arlington, TX, USA. ⁵Department of Ecology and Evolutionary Biology, University of California, Los Angeles, CA, USA. ⁶Museum of Natural Science and Department of Biological Sciences, Louisiana State University, Baton Rouge, LA, USA. ⁷College of Fisheries and Ocean Sciences, University of Alaska Fairbanks, Fairbanks, AK, USA. ⁸Institute for Applied Ecology, University of Canberra, Canberra, Australian Capital Territory, Australia. ⁹Santa Barbara Museum of Natural History, Santa Barbara, CA, USA. ¹⁰Natural History Museum of Los Angeles County, Los Angeles, CA, USA. ¹¹Department of Evolution and Ecology, University of California, Davis, CA, USA. ¹²Queensland Museum, Townsville, Queensland, Australia. ¹³Department of Earth and Environmental Sciences, University of Michigan, Ann Arbor, MI, USA. ¹⁴Museum of Paleontology, University of Michigan, Ann Arbor, MI, USA. ¹⁵Department of Biological Sciences, Clemson University, Clemson, SC, USA. ¹⁶Department of Bioinformatics and Genomics, University of North Carolina, Charlotte, NC, USA. ¹⁷Peabody Museum of Natural History, Yale University, New Haven, CT, USA. ¹⁸These authors contributed equally: Ava Ghezelayagh, Richard C. Harrington. ✉e-mail: ava.ghezelayagh@gmail.com; richard.harrington@yale.edu

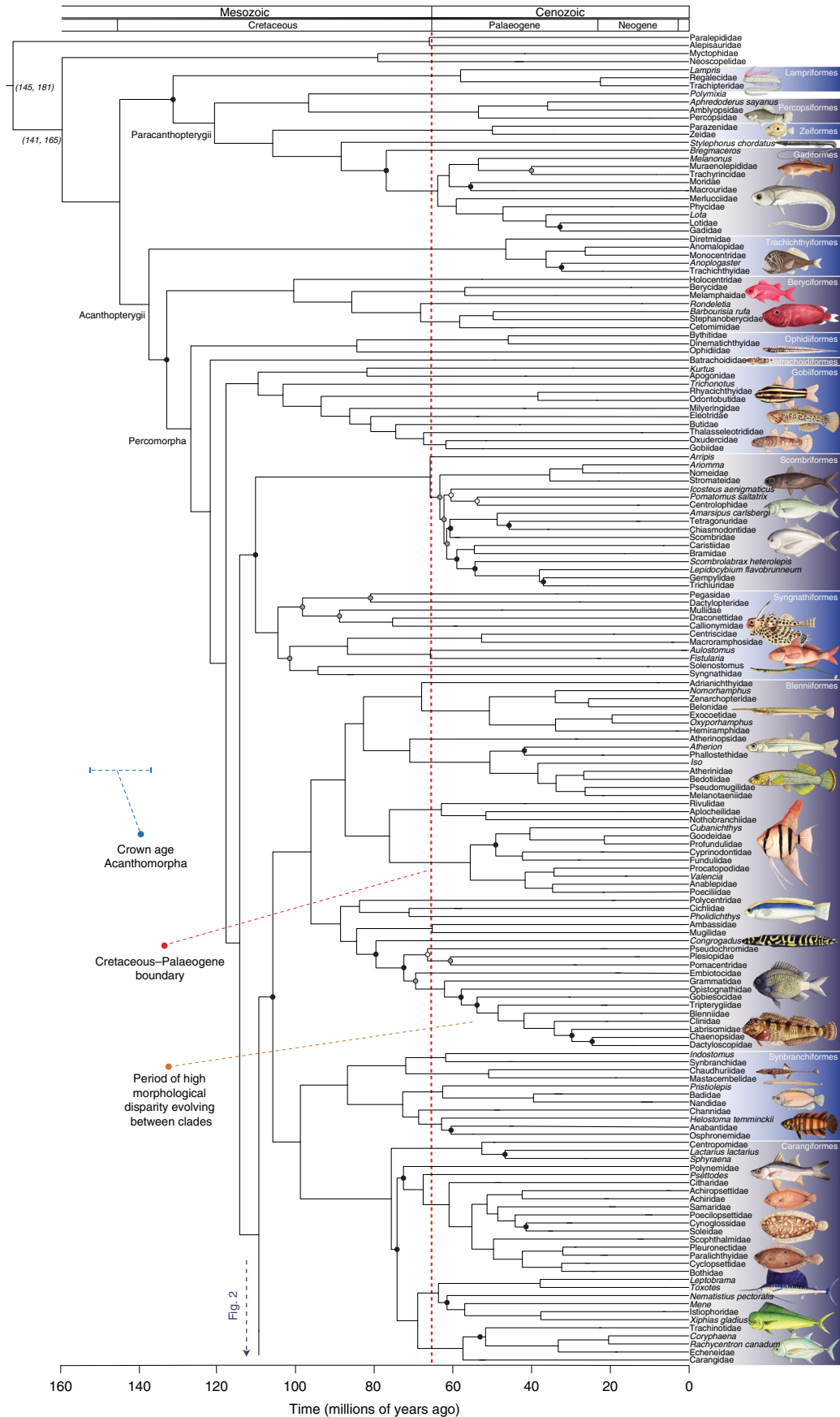


Fig. 1 | Time-calibrated phylogeny of Acanthomorpha, continued in Fig. 2. The phylogeny is condensed to represent taxonomic families at the tips. Monotypic families are represented by the species or genus name. Shaded tabs to the right of taxon labels identify inclusive taxonomic orders. Maximum likelihood bootstrap support (BSS) values for relationships are in Supplementary Figs. 1–15, but unmarked nodes have 100% BSS and nodes with BSS values <97% are indicated by light-grey circles. Nodes with black circles indicate subtending branches with sCF values lower than one or two site discordance (sDF) values, while nodes with dark-grey circles indicate lower sCF values and BSS values <97%. Horizontal grey bars at each node portray the 95% highest posterior density (HPD) credible interval of node age estimates. The blue shaded region reflects the 95% HPD credible interval of the crown age of Acanthomorpha. A vertical red dashed line marks the K-Pg. The red shaded region corresponds to the disparity through time plot in Fig. 2 and reflects a period of heightened among-clade morphological disparity in Acanthomorpha. Fish illustrations by Julie Johnson.

mitochondrial and nuclear genes^{3,17,20–22}. For instance, molecular phylogenies resolved the anglerfishes—long classified with the group of non-percomorph acanthomorphs that includes the economically important cods (Gadiformes)—well within Percomorpha as the sister lineage of the pufferfishes and their allies^{3,17,21}. In addition, molecular phylogenies have identified several major lineages of percomorphs that each encompass a large number of species and taxonomic families^{3,4,17}. As an example, one of these lineages discovered in molecular phylogenetic studies contains such ecologically and phenotypically disparate lineages as cichlids, blennies, guppies, flyingfishes, surfperches and mullets²². Despite this progress, the inter-relationships among and within the major lineages of percomorphs and acanthomorphs remain unresolved owing to limited informativeness in Sanger DNA sequence datasets and limited taxonomic sampling of previous phylogenomic analyses^{3,7,17,18,21–23}.

In this Article, we present the results of comprehensive phylogenomic analyses and estimates of divergence times for 1,084 species representing 308 of the 337 (91.4%) acanthomorph taxonomic families (Supplementary Table 1). We sampled nine species from Aulopiformes (lizardfishes), Myctophidae (lanternfishes) and Neoscolopelidae (blackchins) to serve as outgroups. Our phylogenomic inferences are based on a DNA sequence alignment of 989 ultraconserved element (UCE) loci, and our divergence time estimates were calibrated with 43 fossil constraints. We combine this new acanthomorph time tree with phenotypic data for 680 living acanthomorph species²⁴ to explore the evolutionary patterns of body shape disparity in spiny-rayed fishes.

Results and discussion

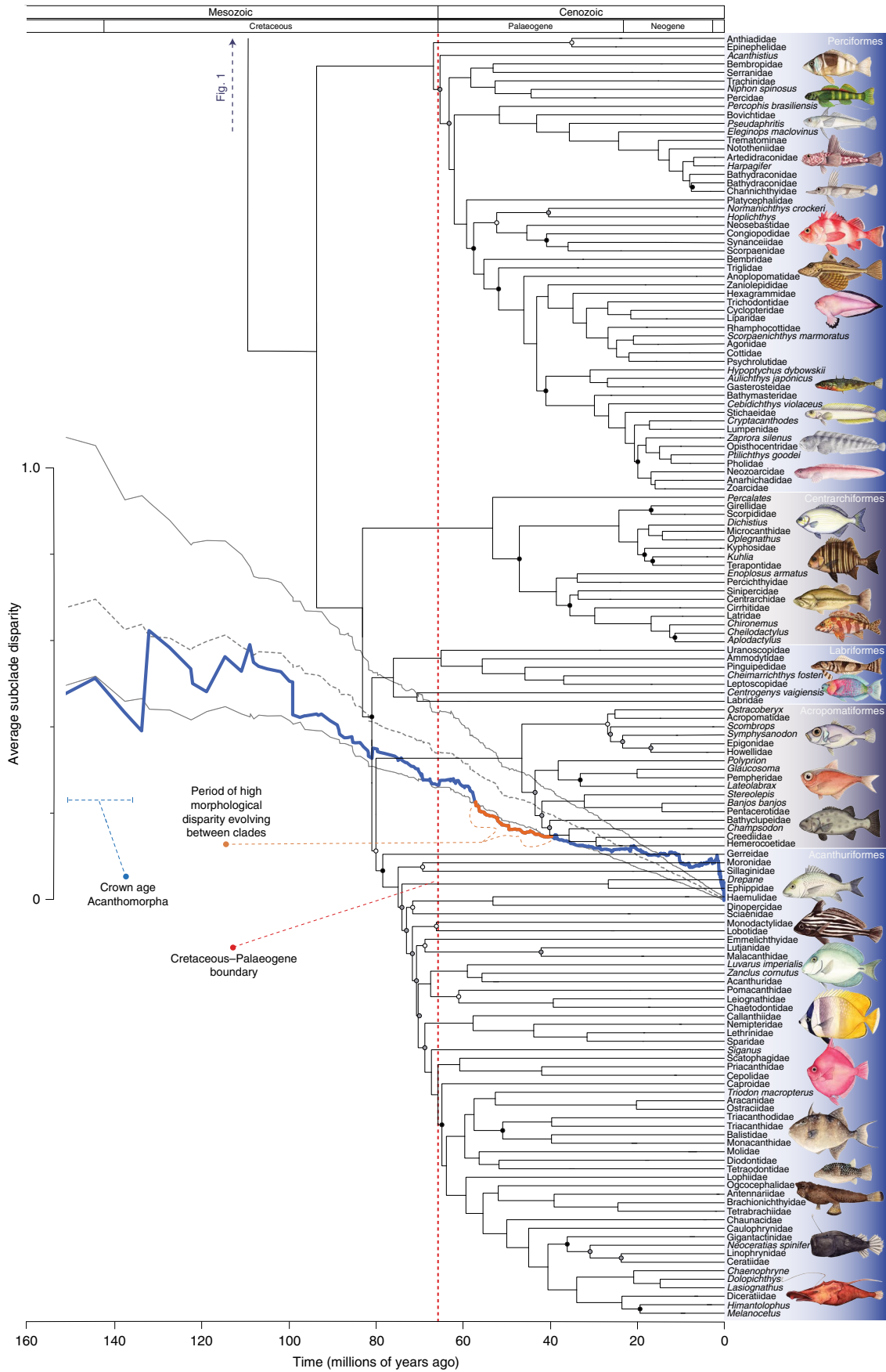
The results of the maximum likelihood analysis of the concatenated UCE dataset depart from previous efforts by yielding confident phylogenetic resolution of nearly all sampled families of acanthomorphs and percomorphs (Figs. 1 and 2 and Supplementary Figs. 1–25). The UCE phylogeny differs from a phylogenomic analysis of exon capture data¹⁸ in the identification of Paracanthopterygii as monophyletic and sister to Lampriformes, the resolution of a clade containing beardfishes (*Polymixia*) and Percopsiformes (troutperches, pirate perch and amblyopsis cavefishes), and the placement of Beryciformes (containing Berycoidei and Holocentridae) as the sister lineage of the species-rich Percomorpha, each supported by high bootstrap values and estimates of Bayesian concordance factors (Figs. 1 and 3). The phylogenies resulting from analyses of these concatenated exon markers also support the common ancestry

of Beryciformes and Percomorpha, and the deepest nodes within Paracanthopterygii are poorly supported¹⁸. Our results are consistent with earlier molecular analyses in regard to the resolution of major percomorph clades that each include a large number of taxonomic families^{3,7,17,18,21}. For example, our analyses resolve the percomorph subclade Acanthuriformes^{4,25} as a monophyletic group comprising more than 2,325 species that includes anglerfishes, pufferfishes, butterflyfishes and scores of other percomorph lineages that have long evaded resolution in morphological and molecular analyses (Fig. 2).

In addition to resolving major lineages and taxonomic families, the maximum likelihood UCE phylogeny reveals novel relationships among some of the most scientifically interesting lineages of percomorph fishes (Figs. 1 and 2 and Supplementary Figs. 1–25). For example, Sanger sequencing studies led to the discovery that the enigmatic coral reef-dwelling engineer gobies (*Pholidichthys*) are the sister lineage of cichlids^{3,17,22} (Fig. 1 and Supplementary Fig. 11). Whereas these Sanger analyses offered weak resolution beyond the monophyly of these two lineages, our maximum likelihood UCE phylogeny resolves the freshwater tropical African and South American leaffishes (Polycentridae) as the sister lineage of the *Pholidichthys*-cichlid clade, providing an opportunity for insight into the evolution of the remarkable species richness and key morphological novelties found in cichlid fishes. We also confidently resolve the nearshore rocky reef-dwelling false scorpionfish (*Centrogenys vaigiensis*) as the sister lineage to a clade of more than 630 species of wrasses and parrotfishes (Labridae) (Fig. 2 and Supplementary Fig. 21). Consistent with this discovery is that wrasses and *Centrogenys vaigiensis* share ancestral, highly modified components of the 'labroid' pharyngeal jaw apparatus²². This result thereby reduces the number of inferred independent evolutions of pharyngognathy, an advanced feeding mechanism that promotes trophic diversification by freeing the oral jaws from prey-processing functions^{22,26}.

Maximum likelihood concordance factor analyses using single-locus trees allow for a closer examination of node support and potential sources of discordance in the acanthomorph phylogeny. Phylogenetic inference on large, concatenated datasets of short sequences such as UCE loci are known to inflate nodal bootstrap support values^{27,28}. It is prudent to interpret high bootstrap support for difficult-to-resolve nodes or those supporting the resolution of contentious phylogenetic relationships with caution, distinguishing between the sampling variance that determines bootstrap support and the observed variance in the original data. We measure this underlying variation using site- and gene-concordance factors

Fig. 2 | Time-calibrated phylogeny and subclade disparity through time for Acanthomorpha, continued from Fig. 1. Continuation of the time-calibrated phylogeny condensed to represent taxonomic families at the tips. Shaded tabs to the right of taxon labels identify inclusive taxonomic orders. Maximum likelihood bootstrap support (BSS) values for relationships are in Supplementary Figs. 16–25, but unmarked nodes have 100% BSS and nodes with BSS values <97% are indicated by light-grey circles. Nodes with black circles indicate subtending branches with sCF values lower than one or two site discordance (sDF) values, while nodes with dark-grey circles indicate lower sCF values and BSS values <97%. Horizontal grey bars at each node portray the 95% highest posterior density (HPD) credible interval of node age estimates. The blue shaded region reflects the 95% HPD credible interval of the crown age of Acanthomorpha. A vertical red dashed line marks the K-Pg. The solid blue line shows observed average relative morphological disparity through time (DTT) for all of Acanthomorpha (represented in both Figs. 1 and 2), and the orange portion of the line, which corresponds to the vertical red shading, reflects the high among-clade disparity present in the early Eocene. The dashed black line and surrounding grey envelope represent the mean DTT and 95% confidence interval for Acanthomorpha as predicted under Brownian evolution, respectively. Fish illustrations by Julie Johnson.



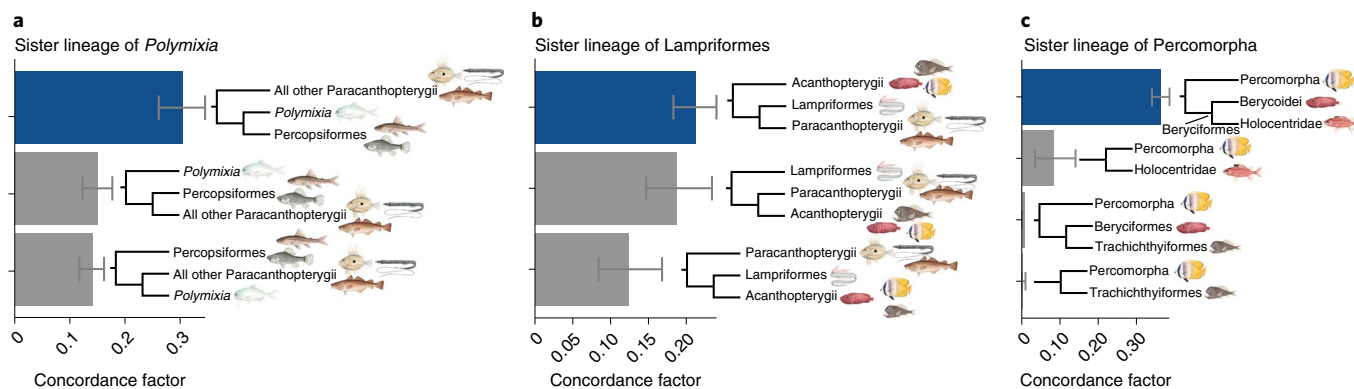


Fig. 3 | Bayesian concordance factor analyses used to compare alternative phylogenetic hypotheses concerning the sister taxa of three major acanthomorph lineages. BUCKy-inferred genome-wide posterior mean concordance factor estimates, with 95% confidence intervals, representing the proportion of $n = 250$ post-burnin gene trees exhibiting alternative topologies among major acanthomorph lineages. Lengths of blue bars reflect the posterior mean concordance factors for the topology represented in Figs. 1 and 2 and Supplementary Figs. 1–25, while lengths of grey bars represent the mean concordance factors of alternative topologies. Fish illustrations by Julie Johnson. **a**, Gene tree concordance for Percopsiformes, *Polymixia* and all other Paracanthopterygii. **b**, Lampriformes, Paracanthopterygii and Acanthopterygii. **c**, Alternative sister lineages of Percomorpha.

(sCF and gCF, respectively), or the proportion of alignment sites or gene trees in agreement with the branches in the acanthomorph phylogeny²⁸. We estimate low sCF and gCF values for acanthomorph relationships that are unique to the maximum likelihood analysis of the UCE dataset, as well as for acanthomorph lineages resolved as monophyletic with strong support from other lines of evidence (Figs. 1 and 2 and Extended Data Fig. 1). However, we observe many branches with very low gCF estimates and markedly higher sCF values (Extended Data Fig. 1a), as well as a positive correlation between branch length and congruence (Extended Data Fig. 1), indicating that incomplete lineage sorting is not the sole cause of gene tree conflict²⁸. Rather, the low gCF values and the observed phylogenetic incongruence are probably driven by weak phylogenetic signal in individual UCE loci, stochastic error or short subtending branches, all of which negatively impact the resolution of trees inferred from single loci^{28,29}. This result is consistent with the observation that individual UCE loci contain relatively little phylogenetic information despite having higher net phylogenetic informativeness than protein-coding genes^{30,31}. It also elucidates the topological differences in the phylogeny inferred using multi-species coalescent-based methods (Extended Data Fig. 2) and supports the use of concatenated alignments in our study.

As multiple processes likely drive the low gene concordance factor estimates for branches in the UCE phylogeny, low site concordance factor (sCF) values provide clearer evidence of incomplete lineage sorting. Approximately 12.8% of the UCE phylogeny's branches have higher site support for one or more alternative topologies (Figs. 1 and 2), and an additional 16.9% have sCF values similar to the site discordance factor (sDF) estimates (that is, sCF is higher than sDF by no more than 15%). The vast majority of these branches with low site support are within clades recognized as taxonomic families or represent otherwise uncontested relationships. Of note are the higher or imbalanced sDF values that highlight uncertainty in the common ancestry of Lampriformes and Paracanthopterygii (sCF 33.65%, sDF1 34.59% and sDF2 31.76%), the resolution of a clade containing Beryciformes and Percomorpha (sCF 28.63%, sDF1 46.96% and sDF2 24.41%), the identity of the earliest-diverging perciform lineages, and the resolution of Labriformes as the sister lineage of the clade comprising Acropomatiformes and Acanthuriformes (sCF 33.62%, sDF1 30.56% and sDF2 35.82%). The sDF values for several key branches within Scombriformes, Blenniiformes and Acanthuriformes are also higher than the site support for the relationships shown in Figs. 1 and 2, and there are

similar sCF and sDF estimates for the branches representing the common ancestry of *Polymixia* and Percopsiformes (sCF 37.78%, sDF1 27.63% and sDF2 34.58%), as well as *Centrogenys vaigiensis* and Labridae (sCF 34.11%, sDF1 33.53% and sDF2 32.35%). Despite these uncertainties, the maximum likelihood phylogeny inferred using the concatenated dataset of the UCE loci provides an important framework for resolving the phylogenetic relationships among lineages of acanthomorph and percomorph fishes (Figs. 1 and 2).

Divergence time estimates for Acanthomorpha resulting from relaxed molecular clock analyses calibrated with 43 well-justified fossil calibrations allow for unprecedented resolution of the timing and tempo of family-level lineage diversification (Figs. 1 and 2 and Extended Data Fig. 3). The median Bayesian posterior of stem lineage age estimates demonstrates that 80% of living acanthomorph taxonomic families originated after the K–Pg, during the Palaeocene through the early Miocene (~66–15 Ma) (Extended Data Fig. 4). This pattern of an extended period of lineage origination contrasts with earlier hypotheses of a clustered origin of these percomorph lineages shortly after the K–Pg mass extinction⁷. Although most of the acanthomorph taxonomic families originated in the Palaeogene, there is an indiscernible effect of the K–Pg mass extinction on acanthomorph lineage diversification rates, as we do not detect any statistically supported mass extinctions or tree-wide rate shifts (Extended Data Fig. 5). Moreover, stepping-stone simulations, used to evaluate the relative and absolute fits of competing diversification models to the observed time-calibrated phylogeny, strongly support a constant-rate birth–death model (Extended Data Fig. 6). These analyses are not impervious to type II error, but Bayesian estimates of the evolutionary rates of individual acanthomorph lineages are similarly homogeneous across the K–Pg and through the Cenozoic (Extended Data Fig. 7). We observe increases in speciation rates in only a few percomorph clades, such as branches in the phylogeny subtending the most recent common ancestors of Apogonidae (cardinalfishes), Pseudocrenilabrinae (African cichlids), Chaetodontidae (butterflyfishes), *Sebastes* (rockfishes) and Lycodinae (a lineage of eelpouts).

Although we reconstruct a history of constant rates of lineage diversification through most of acanthomorph history, body shape began diversifying sharply at the start of the Palaeogene (Fig. 2). Our analyses of morphological disparity through time highlight a period after the K–Pg event during which mean disparity is partitioned between clades more than expected under a Brownian model of evolution (Fig. 2 and Extended Data Fig. 8), indicating a

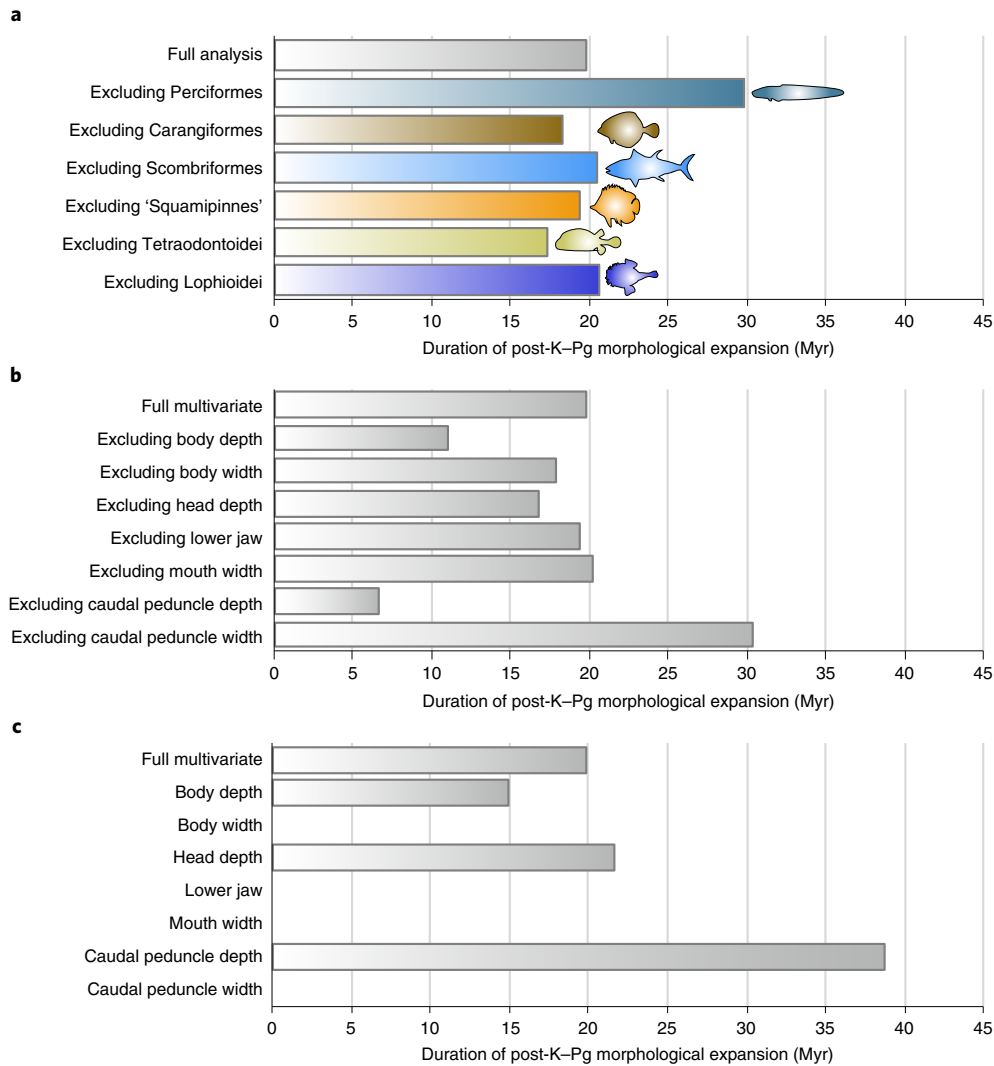


Fig. 4 | Robustness of DTT analyses. Effect of individual lineages or body shape traits on the length of the estimated period of among-clade morphological expansion after the K-Pg (that is, the period in which the observed disparity falls below that expected from a Brownian motion process). There is no single major lineage driving the duration of this period of phenotypic diversification, but the more pronounced contribution of depth measurements to this pattern indicates their importance over width measurements in the expansion of body shapes along the elongation axis. **a**, Duration of the period of morphological expansion when a single major lineage is excluded from the analysis. Note that not all major acanthomorph lineages are represented. 'Squamipinnes' refers to the acanthuriform clade in Supplementary Fig. 23 defined by *Chaetodon kleinii* and *Luvarus imperialis*, and Lophioidei and Tetraodontoidei are major subclades of Acanthuriformes. **b**, Duration of the period of morphological expansion when data for one of the seven body shape traits in the original analysis are excluded. **c**, Duration of the period of morphological expansion when the disparity through time analysis is based on a single body shape trait.

time during which subclades of Acanthomorpha evolved and maintained unique body plans³². This disparity through time analyses, repeated on a sample of 100 trees from the posterior distribution of BEAST time-trees, shows that the sudden diversification of acanthomorph body shapes began an average of five million years after the K-Pg and persisted until the early to mid-Eocene (~45–40 Ma) (Extended Data Fig. 8). This period of high among-clade phenotypic variation in the Palaeogene was not driven by a single clade, but occurred in several groups across Acanthomorpha (Figs. 1, 2 and 4a). The reconstructed history of phenotypic diversification is also unlikely an artefact of any topological uncertainties highlighted by the concordance factor analyses, as only 36 branches with sDF values greater than the sCF estimates bifurcate between 40 and 60 Ma. Divergences in body elongation, the lengthening of bodies relative to depth and width, contributes greatly to the pattern of the among-clade disparity detected in the disparity through time analyses (Fig. 4b,c and 5a). Elongation is one of the primary axes of body

shape variation in freshwater and marine fishes^{24,33}, and expansion along this axis is often coupled with niche divergence and transitions between pelagic, demersal and fully benthic habitats^{23,34}.

During the significant expansion of acanthomorph morphological disparity in the early Palaeogene, lineages established distinct regions of morphospace that correspond to iconic present-day ecomorphological types. These forms include the bottom-dwelling, side-lying flatfishes (Pleuronectoidei) and their sister lineage of speedy, predatory, pelagic fishes (Carangoidei), both within Carangiformes (Figs. 1 and 5 and Extended Data Fig. 9). Similarly, diverse sublineages of a clade of deep-bodied fishes (Acanthuriformes) were established in the late Palaeocene and early Eocene, including globose, deep-sea anglerfishes (Lophioidei), ocean sunfishes and rotund pufferfishes (Tetraodontoidei), and laterally compressed reef fishes such as butterflyfishes (Chaetodontidae), angelfishes (Pomacanthidae) and surgeonfishes (Acanthuridae) (Fig. 2). Subsequent phenotypic evolution followed a Brownian model, as acanthomorph clades

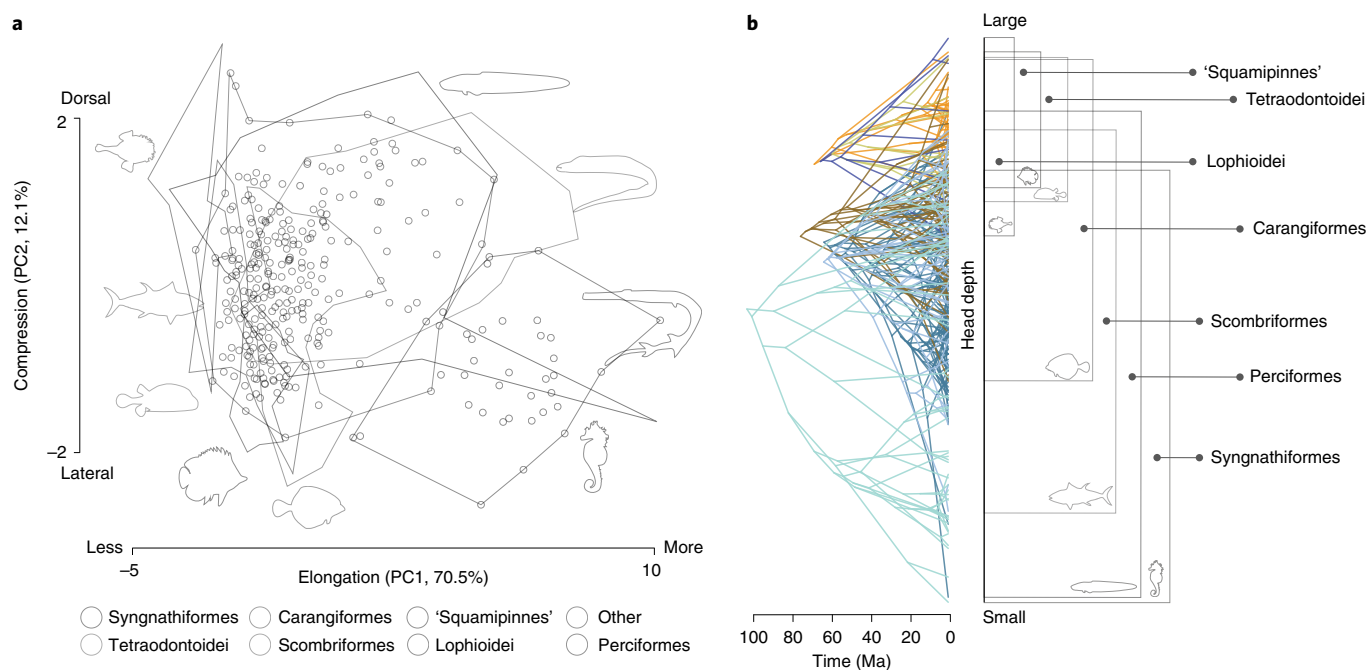


Fig. 5 | Changes in body elongation and compression. Patterns of acanthomorph morphological diversity. Note that not all major acanthomorph lineages are represented. 'Squamipinnes' refers to the acanthuriform clade in Supplementary Fig. 23 defined by *Chaetodon kleinii* and *Luvarus imperialis*, and Lophioidei and Tetraodontoidei are major subclades of Acanthuriformes. **a**, The first two principal components (PCs) of morphospace (elongation and compression), with seven major acanthomorph lineages colour-coded by taxon. The proportion of variance explained by PC1 is 70.5% and by PC2 is 12.1%. **b**, Phenogram depicting the evolutionary history of head depth (size-corrected), which is negatively correlated to standard length and can reveal patterns of elongation, across seven major acanthomorph lineages that arose around the K–Pg. Note that all major lineages except Syngnathiformes originate near the K–Pg boundary, but the three acanthuriform lineages 'Squamipinnes', Lophioidei and Tetraodontoidei have markedly different ancestral trait values from Carangiformes, Scombriformes and Perciformes.

within these well-recognized ecomorphs expanded their regions of morphospace occupation (Fig. 5b and Extended Data Fig. 9). This phenotypic diversification in some cases coincided with changes in geographic distribution and elevated rates of lineage diversification (Extended Data Fig. 7). Such a pattern is exemplified by Perciformes, which includes multiple radiations of large-mouthed predators found in habitats that range from nearshore polar habitats to tropical reefs and which repeatedly invaded both benthic and freshwater habitats. Though the evolutionary trajectories of specific spiny-rayed fish lineages are idiosyncratic (Fig. 5 and Extended Data Fig. 9), at a broader phylogenetic scale they each contribute to an overall pattern of elevated among-clade morphological disparity in Acanthomorpha during the early Cenozoic (Figs. 2 and 4 and Extended Data Fig. 8).

Our estimate of the timing of acanthomorph diversification at the onset of the Palaeogene adds an important perspective to patterns in the fossil record. Fossils suggest that acanthomorph taxonomic diversity and morphological disparity were low in the Late Cretaceous before the K–Pg event, after which both diversity and disparity increased^{6,16}. The precise timing of this morphological expansion and lineage diversification remained unclear owing to a scarcity of deposits yielding abundant and well-preserved teleost skeletons between the Campanian–Maastrichtian (~72 Ma) in the Late Cretaceous and the Palaeocene–Eocene boundary (~56 Ma) (refs. ^{6,16}). Though isolated acanthomorph otoliths are known throughout this interval, they are not well studied relative to those from Eocene and younger deposits³⁵. Our phylogenomic analyses shed light on acanthomorph diversification in the time corresponding to this gap in the fossil record, revealing that the origin of the high disparity observed among early Cenozoic fossil acanthomorphs probably began around 60 Ma and lasted for an interval of

approximately 15–20 Myr. The initiation of a steady accumulation of living families and a pattern of higher among-lineage morphological disparity following the K–Pg extends through much of the gap in the acanthomorph fossil record (Fig. 2), indicating that the rise of acanthomorph diversity in the early Eocene was probably a gradual process¹⁶.

Our results provide a new perspective to the presumed role of the K–Pg as a catalyst of vertebrate morphological and lineage diversification. We do not corroborate the observation⁷ that acanthomorph lineage diversification rates increased after this global mass extinction (Extended Data Fig. 5). The approximately 15–20 Myr period following the K–Pg during which body shape trait space was highly partitioned among clades was probably coincident with the origin of much of the ecomorphological disparity that characterizes the diversity of living spiny-rayed fishes (Figs. 2 and 5b and Extended Data Figs. 8 and 9). These ecomorphological types acted as a reservoir of diversity, setting the stage for more recent, phylogenetically or geographically localized radiations, including endothermic pelagic tunas, Antarctic notothenioids, parrotfishes on coral reefs, and African Rift Lake cichlids^{36–39}. Our findings indicate the remarkable diversity of spiny-rayed fishes is the product of several species-rich and morphologically disparate lineages that diversified throughout most regions of the world in nearly every available marine and freshwater habitat.

Methods

Detailed descriptions of most procedures are available in Supplementary Information.

Taxon sampling and procurement of sequence data. This study incorporates UCE sequence data from 1,109 specimens, including 9 outgroup taxa and 1,075 acanthomorph species spanning 308 recognized taxonomic families in

Acanthomorpha (Supplementary Table 1). UCE data for 360 specimens came from five previous phylogenomic studies (Supplementary Table 1), and UCE sequences for 96 species were extracted from whole genome shotgun sequence data published in the National Center for Biotechnology Information (NCBI) GenBank.

We generated new sequence data from 647 specimens representing 628 species of acanthomorphs and six outgroups, largely following the protocols for library preparation and target enrichment described by Faircloth et al.⁴⁰ and Alfaro et al.⁷. We isolated DNA from muscle or fin tissue following the standard protocol for Qiagen's DNeasy Blood and Tissue kits. After using a Qubit fluorometer (Life Technologies) to quantify 1 μ l of all DNA extractions and visualizing DNA through agarose gel electrophoresis in sodium borate buffer, we sheared approximately 500 ng of genomic DNA from each sampled specimen using a QSonica Q800R3 sonicator to obtain fragment sizes between 300 and 600 nt.

We followed commercial protocols for dual indexing of genomic libraries with Kapa HyperPrep kits (Kapa Biosystems) and Illumina TruSeq iTru5 and iTru7 adapters⁴¹. We performed dual-step SPRI bead clean-ups with 80% EtOH washes for all purification steps, including a 0.8 \times clean-up after the ligation of adapters. We amplified DNA libraries using 25 μ l KAPA HiFi HotStart ReadyMix (Kapa Biosystems), 5 μ l of 5 μ M Illumina TruSeq iTru5 and iTru7 dual-indexed primers⁴¹, and 5 μ l ddH₂O using the following thermocycler settings: 98 °C for 45 s; 13 cycles of 98 °C for 15 s, 60 °C for 30 s, 72 °C for 60 s; and a final extension of 72 °C for 5 min. We purified PCR products using 1.0 \times SPRI beads and rehydrated libraries in 25 μ l of 10 mM Tris-HCl. After library quantification with a Qubit fluorometer, we pooled 80 ng of each sample into groups of nine, dried the pools in a vacuum and rehydrated with 4.9 μ l of 10 mM Tris-HCl.

We used a bait set from Arbor Biosciences designed to target 1,314 UCE loci in acanthomorph fishes for target enrichment of UCE loci⁷. For 24 h at 65 °C, we allowed pooled libraries to hybridize with 100 ng Arbor Biosciences myBaits, 500 ng custom blocking oligos, 500 ng commercially available human Cot-1 DNA (Arbor Biosciences) and 1% sodium dodecyl sulfate. After hybrid enrichment, we performed 2.0 \times bead clean-ups on all pools, during which we removed all residue of the final wash buffer, allowed samples to dry on the magnetic rack and rehydrated samples with 30 μ l of ddH₂O. We combined these bead-bound enriched libraries with 25 μ l HiFi HotStart ReadyMix polymerase (Kapa Biosystems), 5 μ l of each Illumina TruSeq primer mix and 5 μ l ddH₂O. Samples then underwent a PCR with 16 amplification cycles using the same temperature and time settings that were used earlier for library amplification. We performed 1.0 \times bead clean-ups to purify the reaction products, and rehydrated pools in 33 μ l ddH₂O. We quantified the enriched pools, diluted them to 2.5 ng μ l⁻¹, affirmed their size distribution using a Bioanalyzer (Agilent Technologies) and quantified each pool via qPCR using a commercial kit (Kapa Biosystems). Using the Bioanalyzer's estimates of mean fragment sizes and the qPCR results, we adjusted sample concentrations to 10 nM and created an equimolar pool of all enriched libraries. Libraries were sequenced using 150 bp paired-end sequencing on Illumina HiSeq platforms.

Data processing and phylogenetic analyses. We used the PHYLUCE v.1.7.1 (refs. ^{40,42}) computer package to process raw read data, remove potential paralogs, conduct de novo assembly and construct alignments of UCE loci. We generated two separate alignments of UCE loci present in at least 75% of the samples: one consisting of all 1,109 specimens (1,084 species) and another including only a subset of the 702 species that overlapped with the taxon sampling of a previously published morphological dataset. The 1,084- and 702-taxon alignments consisted of 987 loci (383,250 bp) and 989 loci (499,957 bp), respectively.

Using these two 75% complete data matrices, we conducted multiple phylogenetic analyses using maximum likelihood methods in IQ-TREE v.1.7 (ref. ⁴³) and RAxML-ng v.0.9.0 (ref. ⁴⁴). We topologically constrained the divergence time analyses represented in Figs. 1 and 2 with phylogenies inferred in IQ-TREE using single-partition alignments of the 702-taxon and 1,084-taxon datasets. Both of these tree searches assumed the GTR + Gamma model of molecular evolution and used ultrafast bootstrap approximation to generate 1,000 bootstrap replicates and 1,000 replicates of the Shimodaira-Hasegawa approximate likelihood ratio test (SH-aLRT). We used the program TOPD v.4.6 (ref. ⁴⁵) to ensure the phylogenies inferred using different partitioning schemes and maximum likelihood programs presented similar tree topologies.

We also used IQ-TREE's ModelFinder Plus and ultrafast bootstrap approximation options to infer maximum likelihood gene trees for each UCE locus. In TreesShrink⁴⁶, we used a false-positive tolerance rate parameter (α) of 0.05 to identify and remove potentially aberrant sequences from the single-gene alignments. We re-aligned filtered alignments using MAFFT v.7.130b (ref. ⁴⁷) and used them to repeat inference of gene trees in IQ-TREE. We employed the resulting gene trees to generate a summary species tree in ASTRAL-III v.5.6.3 (ref. ⁴⁸). Additionally, we applied these gene trees in IQ-TREE 2 (ref. ⁴⁹) to calculate the percentage of decisive gene trees (gCF) that are consistent with each branch in the single-partition IQ-TREE phylogeny²⁸. To calculate stable sCF values for every internal branch, we randomly subsampled 100 quartets from our concatenated alignment. We performed correlation analyses between branch lengths and maximum likelihood concordance factor values using base R functions after log-transforming branch lengths (results in the legend of Extended Data Fig. 1).

We also applied Bayesian methods to understand the degree of topological discordance along the backbone of the acanthomorph tree. For an 82-taxon sample that represented the major acanthomorph subclades, we generated alignments using MAFFT and inferred gene tree distributions for each locus. We ran these tree searches in MrBayes v.3.2.7 (ref. ⁵⁰) for 2 million generations, assuming a GTR + Gamma model of molecular evolution. We measured topological discordance between these Bayesian gene trees by estimating genome-wide concordance factors in BUCKY⁵¹ using an α value of 1.0.

Divergence time estimation. We estimated divergence times for the 702- and 1,084-taxon phylogenies in BEAST v.2.5 (refs. ⁵²⁻⁵⁴) using reduced datasets of randomly subsampled UCE loci^{36,55}. For both phylogenies, we repeated dating analyses on three different alignments of 30 loci. For each of these alignments, we accounted for site-specific variation in evolutionary patterns by selecting the best-fit partitioning schemes using PartitionFinder2 v.2.1.1 (ref. ⁵⁶). We performed at least three replicate analyses for each 30-locus dataset. We ran all BEAST analyses under a relaxed log-normal clock model and a birth-death tree model, using the IQ-TREE phylogenies inferred from the single-partition, 702- and 1,084-taxon alignments as topological constraints. We used 43 fossil constraints (detailed in Supplementary Information) to assign minimum age priors and ran BEAST analyses for a minimum of 200 million generations after discarding a burnin of 200 million iterations. We used Tracer v.1.7.1 (ref. ⁵⁷) to assess convergence of parameters across replicate MCMC chains and ensure there were no directional trends in parameter estimates. For each set of random loci, we combined replicate analyses in LogCombiner and constructed maximum clade credibility (MCC) trees using TreeAnnotator in BEAST v.1.8.4 (ref. ⁵⁸), with summarized node heights rescaled to reflect the posterior median heights. MCC trees for the 702-taxon datasets were summarized from 10,000 post-burnin, randomly sampled trees, while MCC trees for the 1,084-taxon datasets were summarized from 1,200 such trees.

Diversification rate analyses. We removed all outgroup and duplicate taxa from the 1,084-taxon MCC tree displaying the highest effective sample size and used this pruned tree for all diversification rate analyses. We used TESS⁵⁹ to conduct stepping-stone simulations that estimated the marginal likelihoods of eight birth-death models, allowing us to calculate Bayes factors and assess the competing models' relative and absolute fits to the time-calibrated phylogeny of Acanthomorpha. We examined tree-wide speciation, extinction and net-diversification rates using TESS's CoMET model. For this analysis, we accounted for our incomplete sampling, specified a uniform sampling strategy and ran three replicate reversible-jump MCMC chains until effective sample size values were ≥ 200 . CoMET runs were checked for within- and between-analysis convergence of the diversification rate parameters as described in Supplementary Information. Using the same time-calibrated phylogeny, we also inferred rate heterogeneity across lineages using BAMM v.2.5.0 (ref. ⁶⁰). BAMM analyses accounted for the incomplete sampling of taxonomic families and other major representative clades and used empirically determined rate priors identified by the R package BAMMtools v.2.1.6 (ref. ⁶¹). We ran 23 MCMC chains with different combinations of parameters in BAMM, each for 100 million generations, and we identified the rate shifts along specific branches that were predicted by at least 16 of these analyses.

Phylogenetic comparative methods. We pruned a body trait dataset of teleost fishes²⁴ to include maximum body depth, maximum fish width, head depth, lower jaw length, mouth width, minimum caudal peduncle depth and minimum caudal peduncle width for the 680 species that matched the species represented in the 702-taxon UCE phylogeny. To correct for body size, we regressed log-transformed trait values against log-transformed standard fish lengths and calculated phylogenetic residuals in PHYTOOLS⁶². We assessed disparity through time using GEIGER⁶³ and the time-calibrated IQ-TREE phylogeny. We repeated disparity through time analyses on 100 randomly sampled time trees from the posterior distribution generated in BEAST, and we summarized the mean and 95% confidence interval for the 1.0 My time interval after the K-Pg during which average subclade disparity first dropped below the value simulated under Brownian evolution, as well as the proportion of trees through time that strayed from the Brownian prediction. We tested the sensitivity of disparity through time analyses to the exclusion of body shape traits and of major clades that arose immediately around the K-Pg boundary. Finally, we used PHYTOOLS to visualize body shape morphospace using principal component analysis and to generate phenograms that visualize the evolutionary histories of the following seven major lineages: Scombriformes, Syngnathiformes, Carangiformes, Perciformes, Lophioidae (in Acanthuriformes), Tetraodontoidae (in Acanthuriformes) and 'Squamipinnis' (referring to the acanthuriform clade in Supplementary Fig. 23 defined by *Chaetodon kleinii* and *Luvarus imperialis*).

Reporting summary. Further information on research design is available in the Nature Research Reporting Summary linked to this article.

Data availability

NCBI BioSample Accession numbers corresponding to sequence data are listed in Supplementary Table 1. New raw sequence data are available for download from the NCBI Sequence Read Archive (SRA), under BioProject ID PRJNA758064.

Sequence alignments, partitioning schemes, phylogenetic trees, phenotypic trait data and other related data files are available on the corresponding Dryad Digital Repository: <https://datadryad.org/stash/share/-vfd5XqnNuJ1BHG7s2nBDw2nRRyK80Rc4BAtrAkkoU>.

Code availability

Analyses relied on open-source programs, and scripts used for data analysis are available on the Dryad Digital Repository: <https://datadryad.org/stash/share/-vfd5XqnNuJ1BHG7s2nBDw2nRRyK80Rc4BAtrAkkoU>.

Received: 6 May 2021; Accepted: 19 May 2022;

Published online: 14 July 2022

References

- Fricke, R., Eschmeyer, W. N. & Fong, J. D. *Eschmeyer's Catalog of Fishes: species by family/subfamily (1 September 2021)* <https://researcharchive.calacademy.org/research/ichthyology/catalog/SpeciesByFamily.asp> (2021).
- Wainwright, P. C. & Longo, S. J. Functional innovations and the conquest of the oceans by acanthomorph fishes. *Curr. Biol.* **27**, R550–R557 (2017).
- Near, T. J. et al. Phylogeny and tempo of diversification in the superradiation of spiny-rayed fishes. *Proc. Natl Acad. Sci. USA* **110**, 12738–12743 (2013).
- Dornburg, A. & Near, T. J. The emerging phylogenetic perspective on the evolution of actinopterygian fishes. *Annu. Rev. Ecol., Evolution, Syst.* **52**, 427–452 (2021).
- Chen, W.-J. et al. New insights on early evolution of spiny-rayed fishes (Teleostei: Acanthomorpha). *Front. Mar. Sci.* **1**, 53 (2014).
- Friedman, M. Explosive morphological diversification of spiny-finned teleost fishes in the aftermath of the end-Cretaceous extinction. *Proc. R. Soc. B* **277**, 1675–1683 (2010).
- Alfaro, M. E. et al. Explosive diversification of marine fishes at the Cretaceous–Palaeogene boundary. *Nat. Ecol. Evolution* **2**, 688–696 (2018).
- Meredith, R. W. et al. Impacts of the Cretaceous terrestrial revolution and KPg extinction on mammal diversification. *Science* **334**, 521–524 (2011).
- Stadler, T. Mammalian phylogeny reveals recent diversification rate shifts. *Proc. Natl Acad. Sci. USA* **108**, 6187–6192 (2011).
- Venditti, C., Meade, A. & Pagel, M. Multiple routes to mammalian diversity. *Nature* **479**, 393–396 (2011).
- Liu, L. et al. Genomic evidence reveals a radiation of placental mammals uninterrupted by the KPg boundary. *Proc. Natl Acad. Sci. USA* **114**, E7282–E7290 (2017).
- Slater, G. J. Phylogenetic evidence for a shift in the mode of mammalian body size evolution at the Cretaceous–Palaeogene boundary. *Methods Ecol. Evol.* **4**, 734–744 (2013).
- Jetz, W. & Pyron, R. A. The interplay of past diversification and evolutionary isolation with present imperilment across the amphibian tree of life. *Nat. Ecol. Evolution* **2**, 850–858 (2018).
- Longrich, N. R., Bhullar, B.-A. S. & Gauthier, J. Mass extinction of lizards and snakes at the Cretaceous–Paleogene boundary. *Proc. Natl Acad. Sci. USA* **109**, 21396–21401 (2012).
- Jarvis, E. D. et al. Whole-genome analyses resolve early branches in the tree of life of modern birds. *Science* **346**, 1320 (2014).
- Patterson, C. An overview of the early fossil record of acanthomorphs. *Bull. Mar. Sci.* **52**, 29–59 (1993).
- Betancur-R, R. et al. The tree of life and a new classification of bony fishes. *PLOS Curr.* <https://doi.org/10.1371/currents.tol.53ba26640df0cceaee75bb165c8c26288> (2013).
- Hughes, L. C. et al. Comprehensive phylogeny of ray-finned fishes (Actinopterygii) based on transcriptomic and genomic data. *Proc. Natl Acad. Sci. USA* **115**, 6249–6254 (2018).
- Johnson, G. D. & Patterson, C. Percomorph phylogeny: a survey of acanthomorphs and a new proposal. *Bull. Mar. Sci.* **52**, 554–626 (1993).
- Near, T. J. et al. Resolution of ray-finned fish phylogeny and timing of diversification. *Proc. Natl Acad. Sci. USA* **109**, 13698–13703 (2012).
- Miya, M. et al. Major patterns of higher teleostean phylogenies: a new perspective based on 100 complete mitochondrial DNA sequences. *Mol. Phylogenet. Evol.* **26**, 121–138 (2003).
- Wainwright, P. C. et al. The evolution of pharyngognath: a phylogenetic and functional appraisal of the pharyngeal jaw key innovation in labroid fishes and beyond. *Syst. Biol.* **61**, 1001–1027 (2012).
- Ribeiro, E., Davis, A. M., Rivero-Vega, R. A., Ortí, G. & Betancur-R, R. Post-Cretaceous bursts of evolution along the benthic-pelagic axis in marine fishes. *Proc. R. Soc. B* **285**, 20182010 (2018).
- Price, S. A. et al. Building a body shape morphospace of teleostean fishes. *Integ. Comp. Biol.* **59**, 716–730 (2019).
- Smith, W. L., Stern, J. H., Girard, M. G. & Davis, M. P. Evolution of venomous cartilaginous and ray-finned fishes. *Integ. Comp. Biol.* **56**, 950–961 (2016).
- Liem, K. Evolutionary strategies and morphological innovations: cichlid pharyngeal jaws. *Syst. Zool.* **22**, 425–441 (1973).
- Chan, K. O., Hutter, C. R., Wood, P. L., Grismer, L. L. & Brown, R. M. Larger, unfiltered datasets are more effective at resolving phylogenetic conflict: Introns, exons, and UCEs resolve ambiguities in Golden-backed frogs (Anura: Ranidae; genus *Hylarana*). *Mol. Phylogenet. Evol.* **151**, 106899 (2020).
- Minh, B. Q., Hahn, M. W. & Lanfear, R. New methods to calculate concordance factors for phylogenomic datasets. *Mol. Biol. Evol.* **37**, 2727–2733 (2020).
- Simion, P., Delsuc, F. & Philippe, H. in *Phylogenetics in the genomic era* (eds C. Scornavacca, F. Delsuc & N. Galtier) 2.1:1–2.1:34 (no commercial publisher, authors open access book, 2020).
- Gilbert, P. S. et al. Genome-wide ultraconserved elements exhibit higher phylogenetic informativeness than traditional gene markers in percomorph fishes. *Mol. Phylogenet. Evol.* **92**, 140–146 (2015).
- Alda, F., Ludt, W. B., Elias, D. J., McMahan, C. D. & Chakrabarty, P. Comparing ultraconserved elements and exons for phylogenomic analyses of Middle American cichlids: when data agree to disagree. *Genome Biol. Evol.* <https://doi.org/10.1093/gbe/evab161> (2021).
- Harmon, L. J., Schulte, J. A., Larson, A. II & Losos, J. B. Tempo and mode of evolutionary radiation in iguanian lizards. *Science* **301**, 961–964 (2003).
- Claverie, T. & Wainwright, P. C. A morphospace for reef fishes: elongation is the dominant axis of body shape evolution. *PLoS ONE* **9**, e112732 (2014).
- Friedman, S. T. et al. Body shape diversification along the benthic–pelagic axis in marine fishes. *Proc. R. Soc. B* **287**, 20201053 (2020).
- Schwarzhan, W. & Stringer, G. Fish otoliths from the Late Maastrichtian Kemp Clay (Texas, USA) and the Early Danian Clayton Formation (Arkansas, USA) and an assessment of extinction and survival of teleost lineages across the K–Pg boundary based on otoliths. *Riv. Ital. Paleontol. Strat.* **126**, 395–446 (2020).
- Friedman, M. et al. A phylogenomic framework for pelagiarian fishes (Acanthomorpha: Percomorpha) highlights mosaic radiation in the open ocean. *Proc. R. Soc. B* **286**, 20191502 (2019).
- Price, S. A., Holzman, R., Near, T. J. & Wainwright, P. C. Coral reefs promote the evolution of morphological diversity and ecological novelty in labrid fishes. *Ecol. Lett.* **14**, 462–469 (2011).
- McGee, M. D. et al. The ecological and genomic basis of explosive adaptive radiation. *Nature* **586**, 75–79 (2020).
- Daane, J. M. et al. Historical contingency shapes adaptive radiation in Antarctic fishes. *Nat. Ecol. Evolution* <https://doi.org/10.1038/s41559-019-0914-2> (2019).
- Faircloth, B. C. et al. Ultraconserved elements anchor thousands of genetic markers spanning multiple evolutionary timescales. *Syst. Biol.* **61**, 717–726 (2012).
- Glenn, T. C. et al. Adapterama I: universal stubs and primers for 384 unique dual-indexed of 147,456 combinatorially-indexed Illumina libraries (iTru & iNext). *PeerJ* **7**, e7755 (2019).
- Faircloth, B. C. PHYLUCES is a software package for the analysis of conserved genomic loci. *Bioinformatics* **32**, 786–788 (2016).
- Nguyen, L. T., Schmidt, H. A., von Haeseler, A. & Minh, B. Q. IQ-TREE: a fast and effective stochastic algorithm for estimating maximum likelihood phylogenies. *Mol. Biol. Evol.* **32**, 268–274 (2015).
- Kozlov, A. M., Darrriba, D., Flouri, T., Morel, B. & Stamatakis, A. RAxML-NG: a fast, scalable and user-friendly tool for maximum likelihood phylogenetic inference. *Bioinformatics* **35**, 4453–4455 (2019).
- Puigbò, P., Garcia-Vallvé, S. & McInerney, J. O. TOPDFMTS: a new software to compare phylogenetic trees. *Bioinformatics* **23**, 1556–1558 (2007).
- Mai, U. & Mirarab, S. TreeShrink: fast and accurate detection of outlier long branches in collections of phylogenetic trees. *BMC Genomics* **19**, 23–40 (2018).
- Katoh, K. & Standley, D. M. MAFFT multiple sequence alignment software Version 7: improvements in performance and usability. *Mol. Biol. Evol.* **30**, 772–780 (2013).
- Zhang, C., Rabiee, M., Sayyari, E. & Mirarab, S. ASTRAL-III: polynomial time species tree reconstruction from partially resolved gene trees. *BMC Bioinformatics* **19**, 15–30 (2018).
- Minh, B. Q. et al. IQ-TREE 2: new models and efficient methods for phylogenetic inference in the genomic era. *Mol. Biol. Evol.* **37**, 1530–1534 (2020).
- Ronquist, F. et al. MrBayes 3.2: efficient Bayesian phylogenetic inference and model choice across a large model space. *Syst. Biol.* **61**, 539–542 (2012).
- Ane, C., Larget, B., Baum, D. A., Smith, S. D. & Rokas, A. Bayesian estimation of concordance among gene trees. *Mol. Biol. Evol.* **24**, 412–426 (2007).
- Bouckaert, R. et al. BEAST 2.5: an advanced software platform for Bayesian evolutionary analysis. *PLoS Comput. Biol.* **15**, e1006650 (2019).
- Gernhard, T. The conditioned reconstructed process. *J. Theor. Biol.* **253**, 769–778 (2008).
- Drummond, A. J., Ho, S. Y. W., Phillips, M. J. & Rambaut, A. Relaxed phylogenetics and dating with confidence. *PLoS Biol.* **4**, 699–710 (2006).

55. Harrington, R. C. et al. Phylogenomic analysis of carangimorph fishes reveals flatfish asymmetry arose in a blink of the evolutionary eye. *BMC Evol. Biol.* **16**, 224 (2016).
56. Lanfear, R., Frandsen, P. B., Wright, A. M., Senfeld, T. & Calcott, B. PartitionFinder 2: new methods for selecting partitioned models of evolution for molecular and morphological phylogenetic analyses. *Mol. Biol. Evol.* **34**, 772–773 (2017).
57. Rambaut, A., Drummond, A. J., Xie, D., Baele, G. & Suchard, M. A. Posterior summarization in Bayesian phylogenetics using Tracer 1.7. *Syst. Biol.* **67**, 901–904 (2018).
58. Drummond, A. J., Suchard, M. A., Xie, D. & Rambaut, A. Bayesian phylogenetics with BEAUti and the BEAST 1.7. *Mol. Biol. Evol.* **29**, 1969–1973 (2012).
59. Höhna, S., May, M. R. & Moore, B. R. TESS: an R package for efficiently simulating phylogenetic trees and performing Bayesian inference of lineage diversification rates. *Bioinformatics* **32**, 789–791 (2016).
60. Rabosky, D. L. Automatic detection of key innovations, rate shifts, and diversity-dependence on phylogenetic trees. *PLoS ONE* **9**, e89543 (2014).
61. Rabosky, D. L. et al. BAMMtools: an R package for the analysis of evolutionary dynamics on phylogenetic trees. *Methods Ecol. Evol.* **5**, 701–707 (2014).
62. Revell, L. J. phytools: an R package for phylogenetic comparative biology (and other things). *Methods Ecol. Evol.* **3**, 217–223 (2012).
63. Harmon, L. J., Weir, J. T., Brock, C. D., Glor, R. E. & Challenger, W. GEIGER: investigating evolutionary radiations. *Bioinformatics* **24**, 129–131 (2008).

Acknowledgements

We thank J. Johnson for the fish illustrations in Figs. 1–3 and Extended Data Fig. 3, and the numerous undergraduate and graduate researchers from the University of California, Davis and Clemson University who helped collect morphological data. Portions of this research were conducted with high-performance computational resources provided by Louisiana State University (<http://www.hpc.lsu.edu>). We are grateful to the ichthyology curators and staff of the following collections for granting access to the tissues and specimens that made this study possible: Smithsonian National Museum of Natural History (Washington, DC), University of Florida Museum of Natural History (Gainesville), Scripps Institution of Oceanography (La Jolla), South African Institute for Aquatic Biodiversity (Grahamstown), Southeastern Louisiana University Museum of Biology (Hammond), American Museum of Natural History (New York), Australian Museum (Sydney), Academy of Natural Sciences (Philadelphia), Field Museum of Natural History (Chicago), California Academy of Sciences (San Francisco), Cornell University Museum of Vertebrates (Ithaca), University of Tennessee David A. Etnier Ichthyological Collection (Knoxville), Burke Museum of Natural History and Culture (Seattle), Academia Sinica (Taipei), Biodiversity Research Museum (Taipei), Natural History Museum and Institute (Chiba), Australian National Fish Collection (Hobart), Kyoto University Museum, Mie University Fish Collection of the Fisheries Research Laboratory (Shima), Hokkaido University Museum (Sapporo), Illinois Natural History Survey (Champaign), Kagoshima University Museum (Korimoto), University of Kansas Biodiversity Institute (Lawrence), Natural History Museum of Los Angeles County, Universidade Estadual Paulista (São Paulo), Louisiana Museum of Natural History (Baton Rouge), Harvard Museum of Comparative Zoology (Cambridge),

Museo Nacional de Ciencias Naturales (Madrid), Museo Nacional de Historia Natural (Santiago), North Carolina Museum of Natural Sciences (Raleigh), National Museum of Natural History (New Delhi), Museum of New Zealand Te Papa Tongarewa (Wellington), Museum Victoria (Melbourne), National Museum of Nature and Science (Tokyo), Museums and Art Galleries of the Northern Territory (Darwin), University of Tokyo Ocean Research Institute, Queensland Museum (Brisbane), Royal Ontario Museum (Toronto), Seikai National Fisheries Research Institute (Nagasaki), Universitetsmuseet i Bergen (Hordaland), University of Copenhagen Zoological Museum, and Peabody Museum of Natural History (New Haven). Funding: Authors were independently funded by the National Institute of Health Predoctoral Training Program in Genetics T32 GM 007499 (to A.G.), the Bingham Oceanographic Fund maintained by the Peabody Museum of Natural History, Yale University (to T.J.N.), the Australian Research Council DECRA Fellowship DE170100516 (to P.F.C.), start-up funds from Louisiana State University (to B.C.F.) and the following National Science Foundation grants: NSF DEB-1556953 (to S.A.P. and P.C.W.), NSF DEB-1655624 (to B.C.F.), NSF DEB-1701323 (to P.C. and W.B.L.), NSF DEB-1830127 (to S.A.P.), NSF DEB-1839915 (to P.C.), NSF DEB-2017822 (to M.F.) and NSF IOS-1755242 (to A.D.).

Author contributions

The project was conceived and designed by T.J.N., A.G., R.C.H., J.R.G., B.C.F. and P.C.W. A.G., R.C.H., J.R.G., M.A.C., J.C.B., W.T.M., M.E.A., W.B.L., B.C.F., P.F.C. and T.J.N. organized and executed the collection of UCE sequence data. S.A.P., S.T.F. and P.C.W. coordinated and collected morphological data. A.G., R.C.H., B.C.F. and A.D. carried out phylogenetic analyses. A.G. and R.C.H. performed phylogenetic divergence dating analyses, and A.G. performed analyses of lineage diversification rates. E.D.B. and P.C.W. performed morphological comparative analyses. C.E.T., P.C., W.B.L., P.F.C., P.J.U., A.D. and B.C.F. aided in the interpretation of certain phylogenetic or taxonomic results, and M.F. contributed palaeontological insights into some results. A.G., R.C.H., A.D. and T.J.N. wrote the first draft of the manuscript. All authors contributed to the writing and editing of the final draft of the manuscript.

Competing interests

The authors declare no competing interests.

Additional information

Extended data is available for this paper at <https://doi.org/10.1038/s41559-022-01801-3>.

Supplementary information The online version contains supplementary material available at <https://doi.org/10.1038/s41559-022-01801-3>.

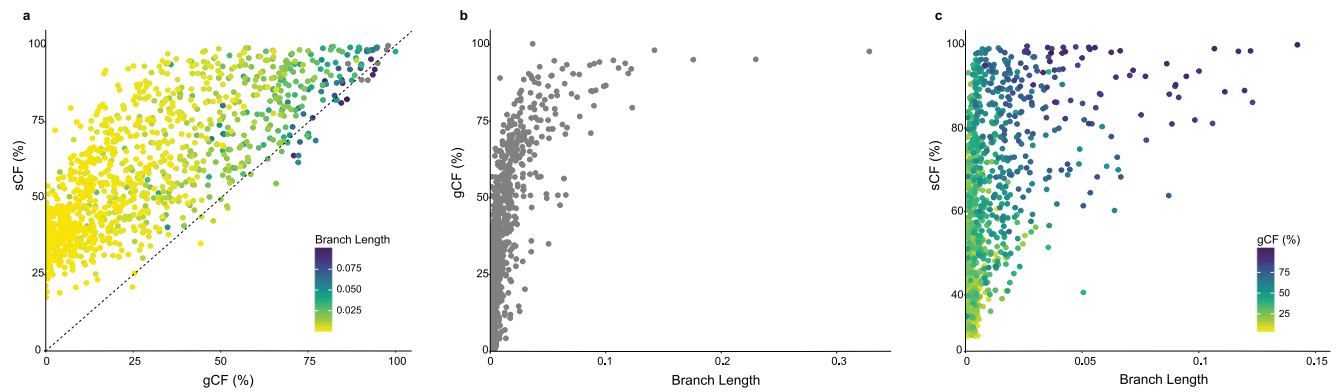
Correspondence and requests for materials should be addressed to Ava Ghezelayagh or Richard C. Harrington.

Peer review information *Nature Ecology & Evolution* thanks Ole Seehausen and the other, anonymous, reviewer(s) for their contribution to the peer review of this work.

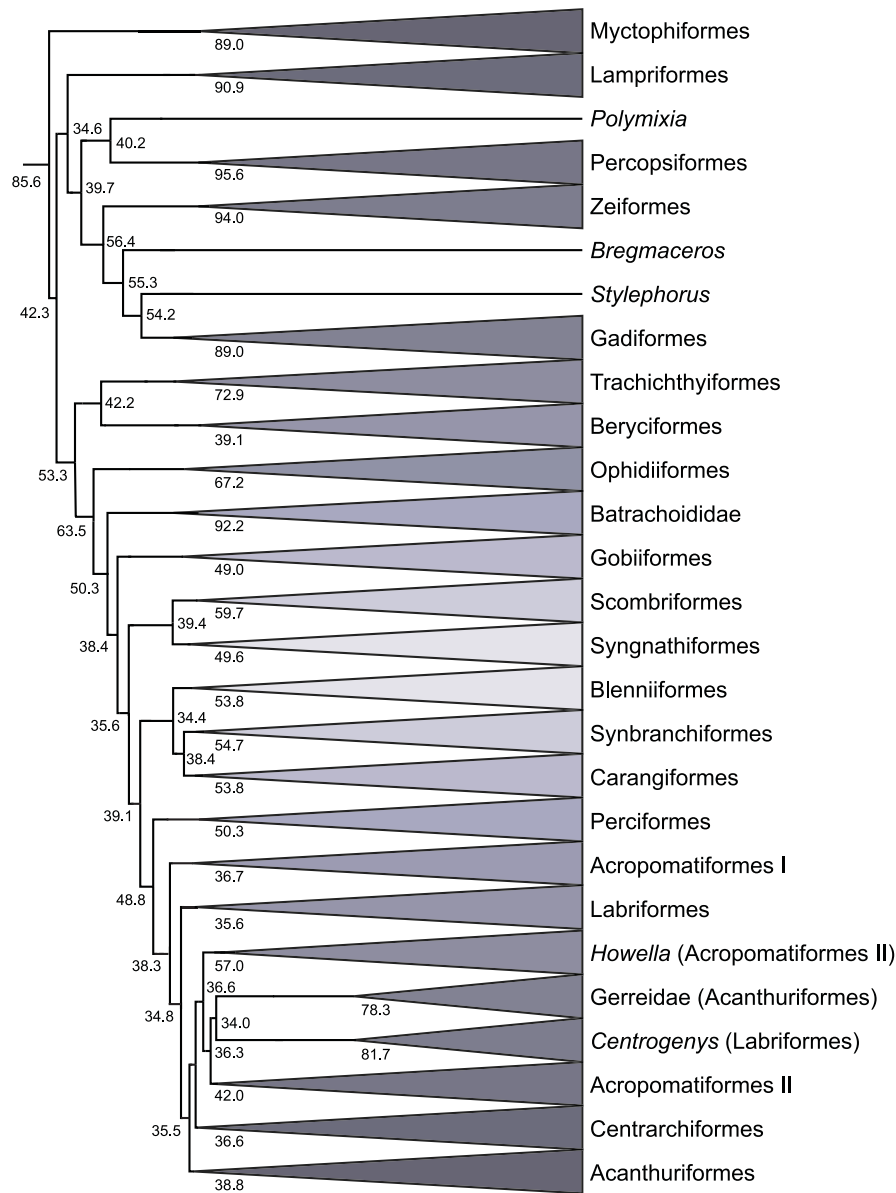
Reprints and permissions information is available at www.nature.com/reprints.

Publisher's note Springer Nature remains neutral with regard to jurisdictional claims in published maps and institutional affiliations.

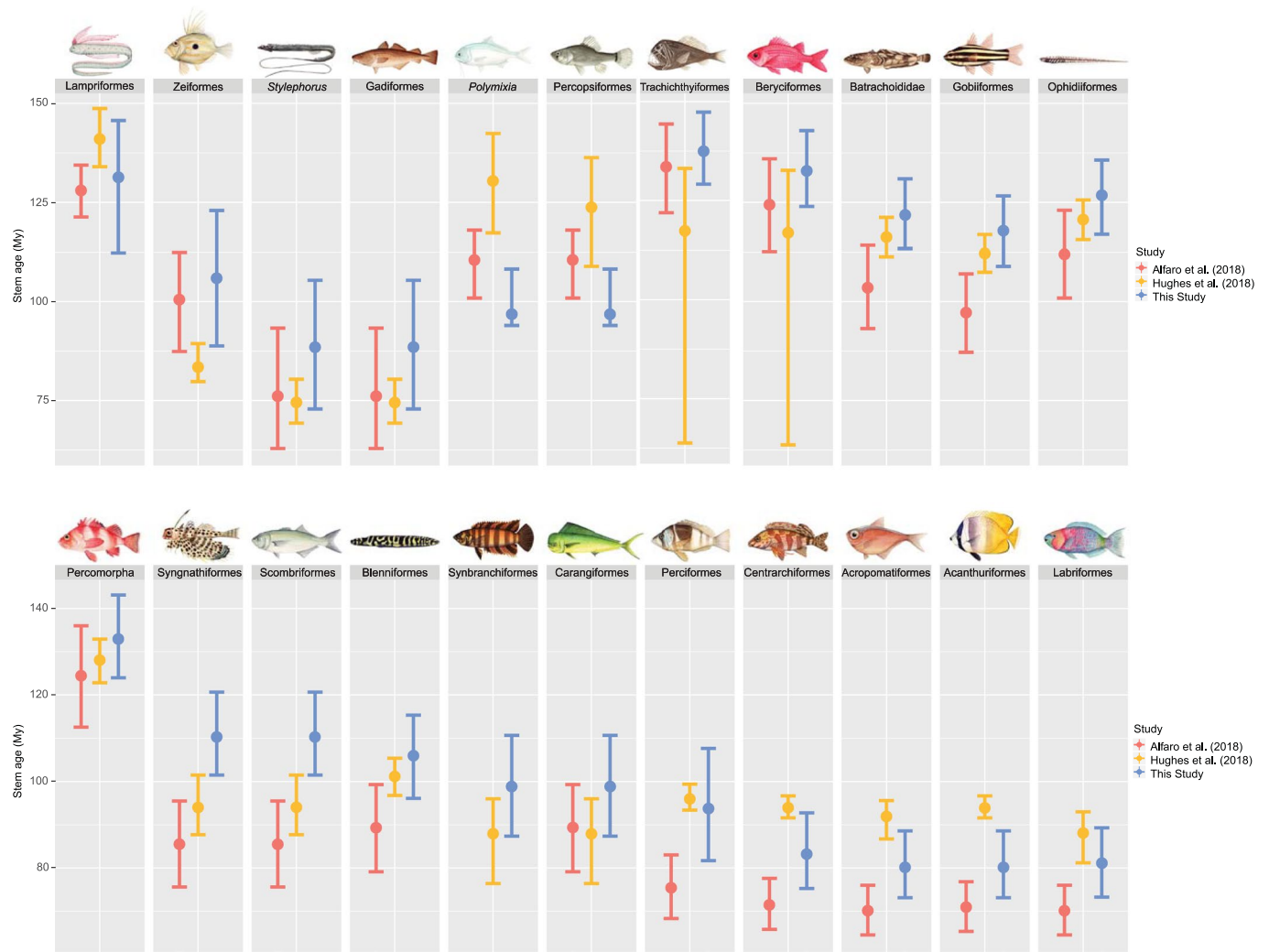
© The Author(s), under exclusive licence to Springer Nature Limited 2022



Extended Data Fig. 1 | Relationships among gene concordance factor (gCF) values, site concordance factor values (sCF) and branch lengths (substitutions per sequence site) along all branches of the acanthomorph phylogeny represented in Supplementary Figs. 1–25. Note that unlike gCF values, site concordance and discordance values sum to 100% because their calculations allow for only three possible resolutions of a branch. Branch lengths have a positive, logarithmic correlation with gCF and sCF. A one percent increase in branch lengths leads to a 0.1413 increase in the natural log of gCF (Standard Error = 0.2925, y-intercept = 108.3323, R-squared = 0.6791) and a 0.0905 change in the natural log of sCF (Standard Error = 0.3416, y-intercept = 109.851, R-squared = 0.3889). These correlation analyses were performed using base R functions after log-transforming branch lengths; all branches were included in these calculations. **a.** Relationship between gCF and sCF, with points colored by branch lengths. The dashed black line with a slope of 1 demonstrates dissimilar levels of conflict among loci and sites, suggesting that the low gCF values are not just caused by genuine discordance in the gene trees. Eleven gray points reflect extremely long branches with lengths greater than 0.1 nucleotide substitutions per site (greater than the upper 99th percentile). **b.** Logarithmic relationship between branch lengths and gCF. **c.** Relationship between branch lengths and sCF values, with points colored by gCF values. Not shown are three points with very long branches (0.176–0.328 substitutions per sequence sites), all of which have sCF and gCF values >94%.

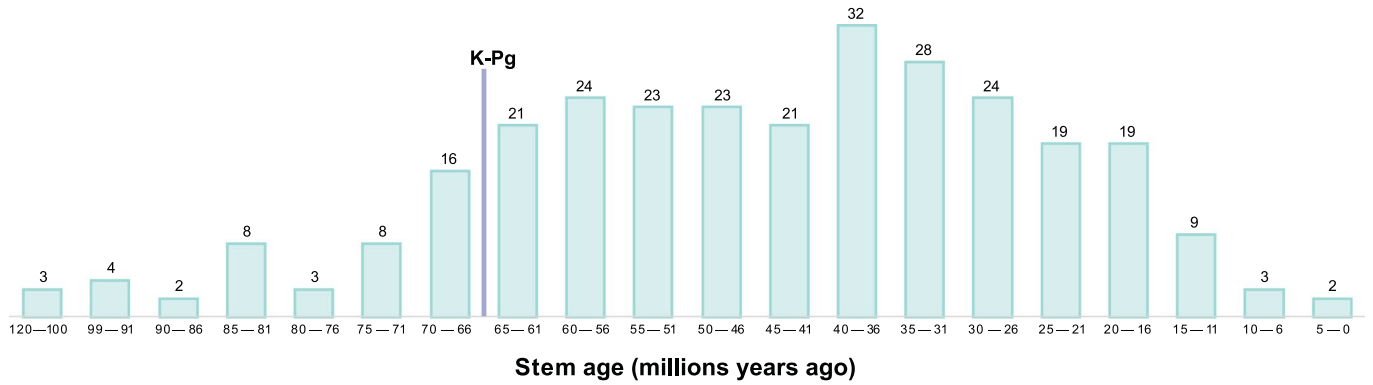


Extended Data Fig. 2 | ASTRAL-III summary species tree inferred using individual gene trees. Collapsed species tree inferred under the multi-species coalescent model (the uncollapsed tree can be found in the study's Dryad repository). Local posterior probability values at nodes do not measure support for bipartitions, but rather are a function of the frequencies of the represented quartet topologies among all gene trees. 'Acropomatiformes I' refers to the clade containing *Champsodon*, Creediidae, and Hemerochetidae while 'Acropomatiformes II' includes all other acropomatiform taxa according to Supplementary Table 3.

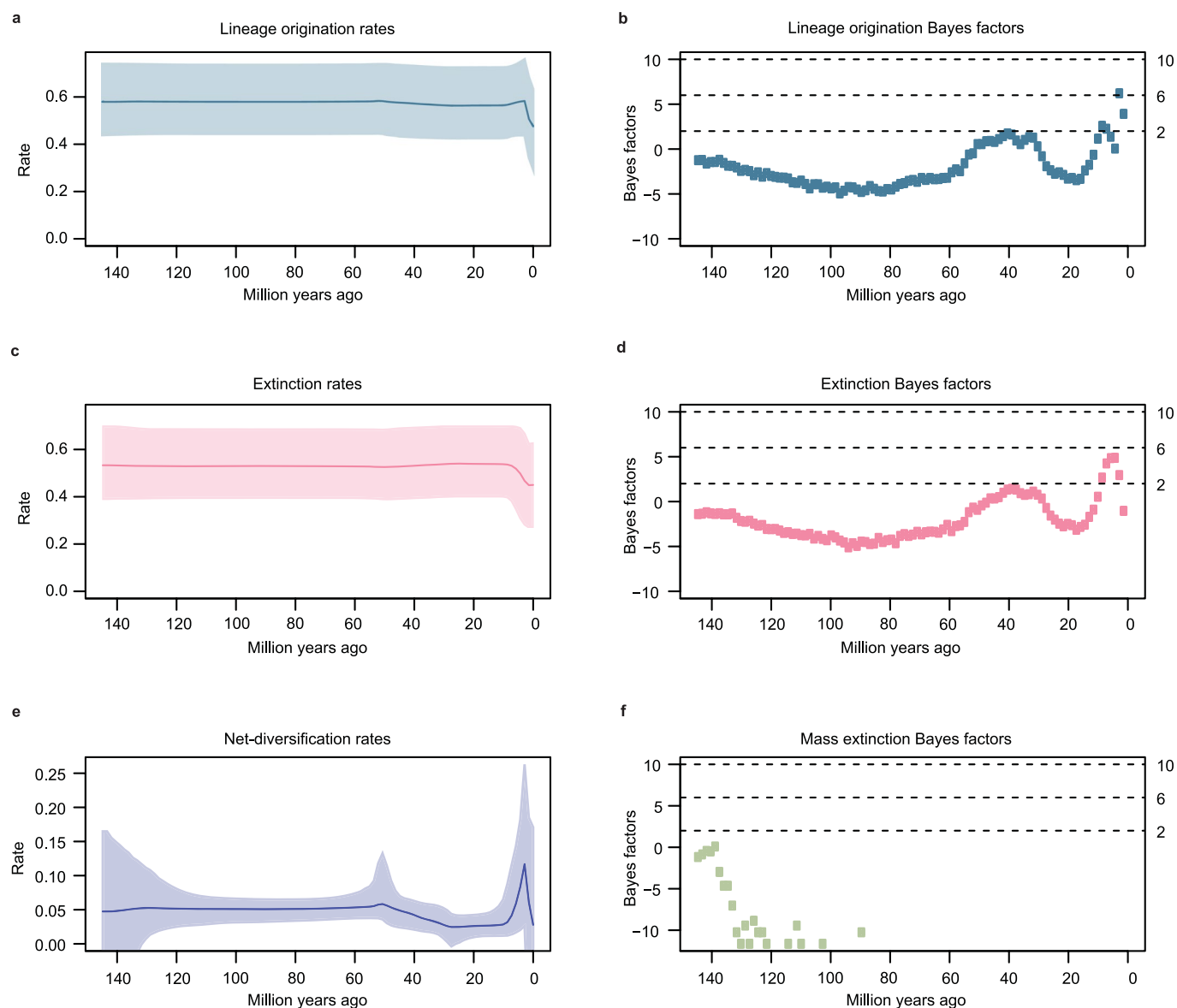


Extended Data Fig. 3 | Median stem age estimates and 95% Highest Posterior Density (HPD) credible intervals for 22 major acanthomorph clades, as reported in the following 3 phylogenomic studies: Alfaro *et al.*⁷, Hughes *et al.*¹⁸ and this study. Estimates for this study are the raw node heights reported in the 1,084-taxon time tree represented in Figs. 1 and 2. The 95% HPD credible interval of stem ages for most of the represented clades overlap with previous estimates, but we observe some major discrepancies, likely due to differences in tree topologies and taxon sampling. Fish illustrations by Julie Johnson.

Number of lineages classified as taxonomic families



Extended Data Fig. 4 | Acanthomorph lineages classified as taxonomic families underwent a steady period of increased origination beginning at the K-Pg boundary. Bar plot of the estimated number of lineages classified as taxonomic families originating during 5 million year bins. Note that the amounts of time represented by the first two bars are greater than the 5 million years represented by all other bars.

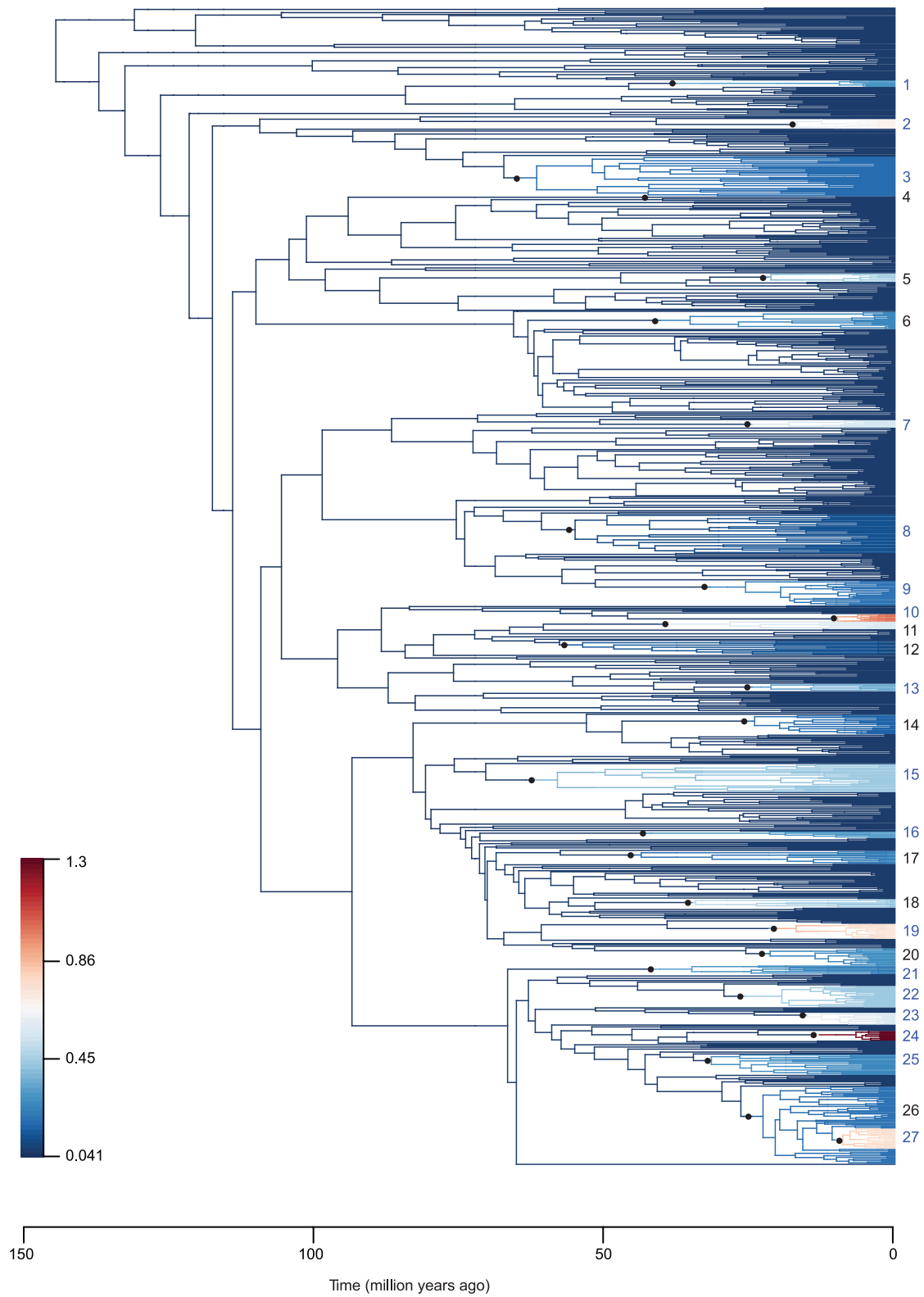


Extended Data Fig. 5 | TESS-CoMET analyses suggest constant tree-wide diversification rates through most of the history of Acanthomorpha. In **b**, **d**, and **e**, horizontal dashed lines and the right-hand y-axis mark statistical support cutoffs for rate shifts, with $2 \leq \text{BF} < 6$ considered to be low support, $6 \leq \text{BF} < 10$ considered to be moderate support and ≥ 10 considered to be high support. The rate shifts observed in **a**, **c**, and **e** over the last 10 million years are likely an artifact of the CoMET model (see **Supplementary Information** for further discussion). **a**, Posterior mean (blue line) and 95% credible interval (blue shading) for acanthomorph lineage origination (that is speciation) rates through time. **b**, Bayes factor (BF) support for a shift in lineage origination rate at every 1 Myr time period. **c**, Posterior mean (pink line) and 95% credible interval (pink shading) for acanthomorph lineage extinction rates through time. **d**, Bayesian support (in BF) for a shift in extinction rate at every 1 Myr time period. **e**, Posterior mean (violet line) and 95% credible interval (violet shading) for acanthomorph net-diversification (origination minus extinction) rates through time. Though this plot suggests that there is a small shift in net-diversification rate -50 Mya, there is no statistical support for such a shift (see **b** and **d**). **f**, There is no statistical support (in BF) for a mass extinction event in Acanthomorpha at any 1 Myr time period.

Model 1 (Null)	Model 2 (Alternative)	2ln(BF)
Constant BD Uniform Sampling	Mass Extinction BD Diversified Sampling	55,487.1
Episodic BD (shift at 50 mya) Uniform Sampling	Mass Extinction BD Diversified Sampling	55,480.7
Decreasing Speciation Rate BD Uniform Sampling	Mass Extinction BD Diversified Sampling	55,477.2
Episodic BD (shift at 50 mya) Diversified Sampling	Mass Extinction BD Diversified Sampling	54,609.6
Decreasing Speciation Rate BD Diversified Sampling	Mass Extinction BD Diversified Sampling	50,634.5
Constant BD Diversified Sampling	Mass Extinction BD Diversified Sampling	49,838.1
Constant BD Uniform Sampling	Mass Extinction BD Uniform Sampling	29,863.0
Episodic BD (shift at 50 mya) Uniform Sampling	Mass Extinction BD Uniform Sampling	29,856.6
Decreasing Speciation Rate BD Uniform Sampling	Mass Extinction BD Uniform Sampling	29,853.1
Episodic BD (shift at 50 mya) Diversified Sampling	Mass Extinction BD Uniform Sampling	28,985.5
Mass Extinction BD Uniform Sampling	Mass Extinction BD Diversified Sampling	25,624.1
Decreasing Speciation Rate BD Diversified Sampling	Mass Extinction BD Uniform Sampling	25,010.4
Constant BD Diversified Sampling	Mass Extinction BD Uniform Sampling	24,214.0
Constant BD Uniform Sampling	Constant BD Diversified Sampling	5,649.0
Episodic BD (shift at 50 mya) Uniform Sampling	Constant BD Diversified Sampling	5,642.6
Decreasing Speciation Rate BD Uniform	Constant BD Diversified Sampling	5,639.1
Constant BD Uniform Sampling	Decreasing Speciation Rate BD Diversified Sampling	4,852.6
Episodic BD (shift at 50 mya) Uniform Sampling	Decreasing Speciation Rate BD Diversified Sampling	4,846.2
Decreasing Speciation Rate BD Uniform Sampling	Decreasing Speciation Rate BD Diversified Sampling	4,842.7
Episodic BD (shift at 50 mya) Diversified Sampling	Constant BD Diversified Sampling	4,771.5
Episodic BD (shift at 50 mya) Diversified Sampling	Decreasing Speciation Rate BD Diversified Sampling	3,975.1
Constant BD Uniform Sampling	Episodic BD (shift at 50 mya) Diversified Sampling	877.5
Episodic BD (shift at 50 mya) Uniform Sampling	Episodic BD (shift at 50 mya) Diversified Sampling	871.1
Decreasing Speciation Rate BD Uniform Sampling	Episodic BD (shift at 50 mya) Diversified Sampling	867.6
Decreasing Speciation Rate BD Diversified Sampling	Constant BD Diversified Sampling	796.4
Constant BD Uniform Sampling	Decreasing Speciation Rate BD Uniform Sampling	9.9
Constant BD Uniform Sampling	Episodic BD (shift at 50 mya) Uniform Sampling	6.4
Episodic BD (shift at 50 mya) Uniform Sampling	Decreasing Speciation Rate BD Uniform Sampling	3.5

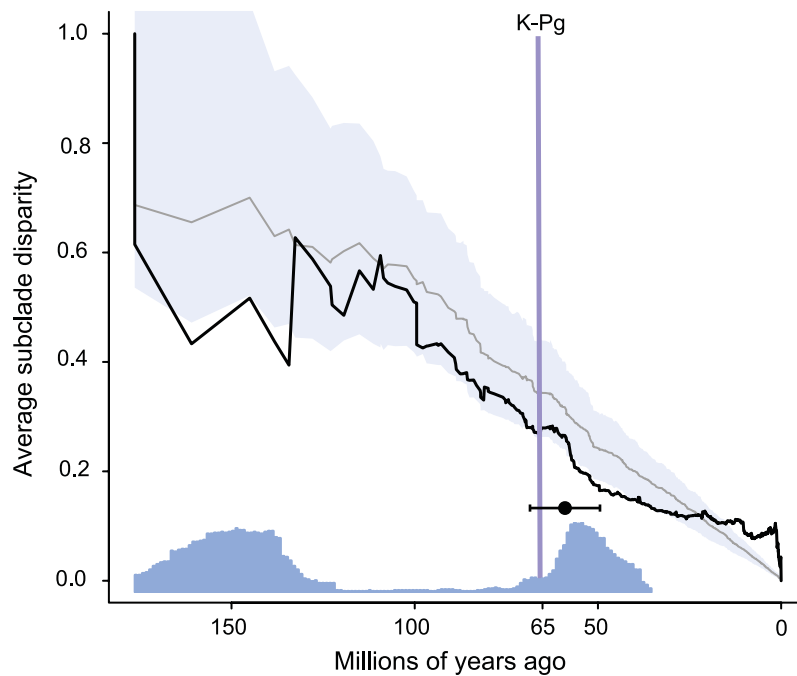
Extended Data Fig. 6 | See next page for caption.

Extended Data Fig. 6 | Pairwise comparisons of 8 birth-death (BD) branching process models. TESS calculated Bayes Factors ($2\ln(\text{BF})$) from the pairwise comparisons of marginal likelihoods for 8 birth-death (BD) branching-process models with the following priors: 1.) constant diversification rate with uniform (random) sampling, 2.) constant diversification rate with diversified sampling (sampling results in even coverage of all clades), 3.) decreasing speciation rate with uniform sampling, 4.) decreasing speciation rate with diversified sampling, 5.) constant diversification rate with a rate shift 50 Mya ('Episodic BD') with uniform sampling, 6.) constant diversification rate with a rate shift 50 Mya ('Episodic BD') with diversified sampling, 7.) constant speciation rate with a single mass extinction event occurring at any point in time ('Mass Extinction BD') with uniform sampling, and 8.) constant speciation rate with a single mass extinction event occurring at any point in time ('Mass Extinction BD') with diversified sampling. Observations of the pairwise comparisons note strong preference for a model that assumes uniform (random) sampling and strong support for either a constant rate BD model, or an episodic BD model that assumes a shift 50 mya. There is moderate Bayesian support ($2\ln(\text{BF}) = 6.4$) that among the models assuming uniform sampling, the constant rate model is preferred over the model with a shift 50 Mya.

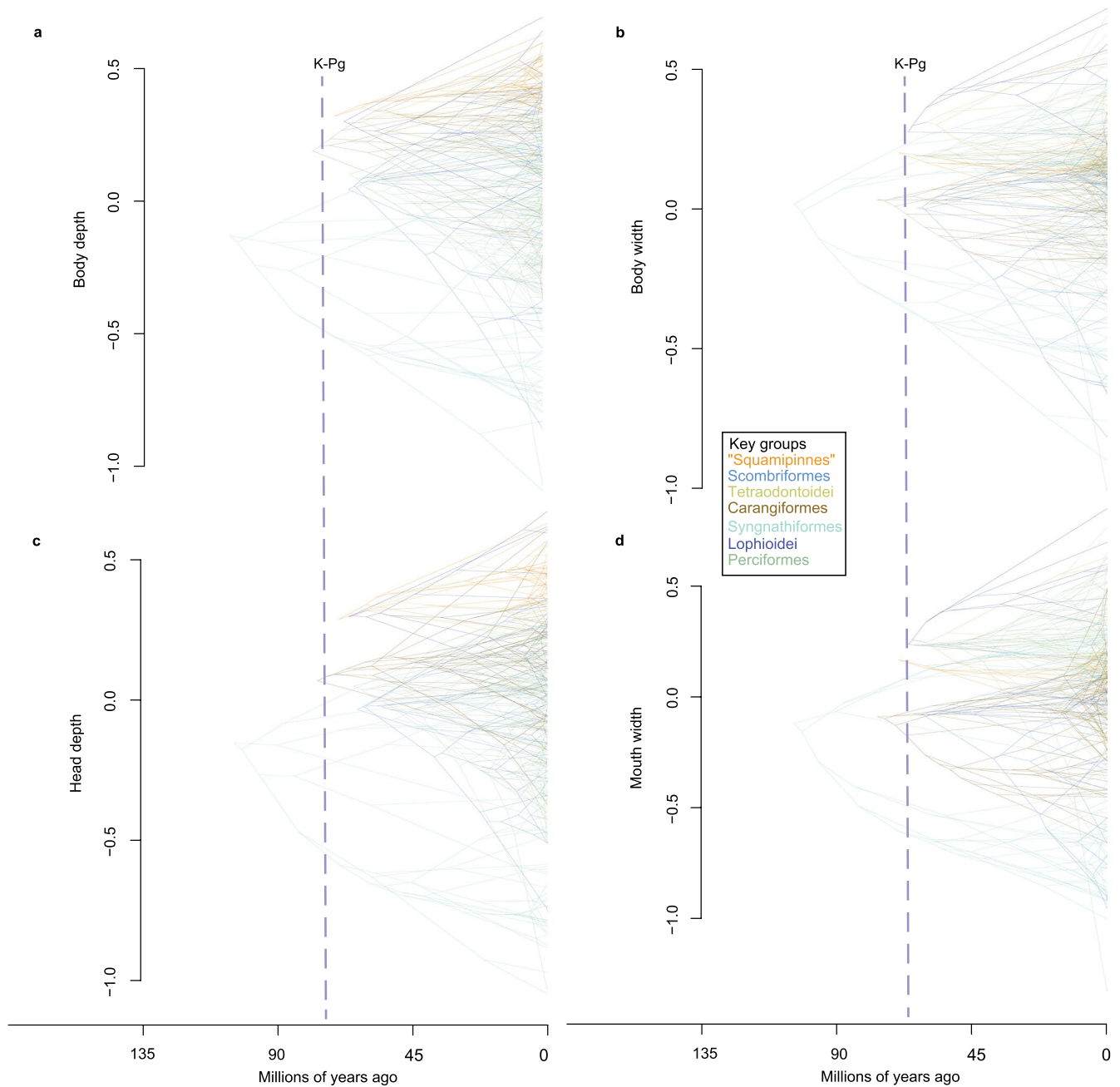


Extended Data Fig. 7 | See next page for caption.

Extended Data Fig. 7 | Visual summary of shifts in speciation rates inferred using BAMM. The configuration presented here is the maximum shift credibility (MSC) configuration for an analysis that expected 15 rate shifts under the prior. Darker red colors depict relatively fast rates, while darker blue colors depict relatively slow rates. Rate shifts along branches are denoted with filled, black circles and assigned identifying numbers. Shifts in speciation rate are estimated to have occurred on the branches leading to the following 27 clades: 1.) Dinematchthyidae, 2.) Apogonidae (to the exclusion of *Pseudamia*), 3.) Gobiidae and Oxudercidae, 4.) *Solenostomus*, 5.) *Parupeneus* and *Pseudopeneus* (in Mullidae), 6.) *Ariomma*, Nomeidae and Stromateidae, 7.) Mastacembelidae, 8.) the clade defined by Scopthalmidae and Soleidae, 9.) Carangidae (to the exclusion of *Seriola*), 10.) Pseudocrenilabrinae (in Cichlidae), 11.) Pomacentridae, 12.) the clade defined by Gobiesocidae and Dactyloscopidae, 13.) Poeciliidae, 14.) the clade defined by Scorpididae and Terapontidae, 15.) Labridae, 16.) Sciaenidae, 17.) the clade defined by Nemipteridae and Sparidae, 18.) Tetraodontidae, 19.) Chaetodontidae, 20.) Acanthuridae (to the exclusion of *Prionurus* and *Naso*), 21.) Anthiinae and Epinephelidae, 22.) darters (Etheostomatinae), 23.) the clade defined by Nototheniidae and Channichthyidae, 24.) *Sebastes*, 25.) the clade defined by Trichodontidae and Psychrolutidae, 26.) the clade defined by Stichaeidae and Zoarcidae and 27.) the clade defined by *Bothrocara* and *Lycodes concolor* (in Zoarcidae). Shifts labelled with blue rather than black numbers are estimated to have occurred by 16 of the 23 BAMM analyses conducted in this study. Although shift number 20 and shift number 26 are labelled in black, the vast majority of BAMM analyses predicted a rate shift in nearby branches leading to slightly more inclusive clades (specifically Acanthuridae to the exclusion of *Naso*, and all of Lycodinae, respectively).



Extended Data Fig. 8 | Mean relative disparity through time (DTT) for all of Acanthomorpha, calculated using the combined data for seven phenotypic measurements and repeated on a sample of 100 trees from the posterior distribution of time-trees. The gray line and blue shaded region indicate the median and 95% confidence interval (CI) expected under a Brownian motion model (BM) of evolution, respectively, and the solid black line indicates the observed pattern of disparity. This is the same plot visualized in Fig. 2, but note that the earliest portion of the DTT plot that includes the outgroup is not shown in Fig. 2. Acanthomorph body shapes radiated for approximately 15–20 million years in the aftermath of the K-Pg, followed by within-lineage phenotypic diversification. The blue histogram along the x-axis shows the proportion of time-calibrated trees for which the null hypothesis is rejected ($P < 0.05$) and the observed disparity falls outside of the BM model's 95% CI in each one-million-year interval. The inset, black box-and-whisker plot depicts the mean ($\pm 95\%$ CI) of the initial time point at which the observed disparity dropped below that expected from BM following the K-Pg.



Extended Data Fig. 9 | Phenograms depicting the evolutionary history of four size-corrected phenotypic traits (body depth and width, head depth, and mouth width) across seven major lineages that arose around the K-Pg. The vertical dashed line marks the K-Pg boundary. Note that not all major acanthomorph lineages are represented in these plots and that Lophioidei and Tetraodontoidei are major subclades of Acanthuriformes. 'Squamipinnes' refers to the acanthuriform clade in Supplementary Fig. 23 defined by *Chaetodon kleinii* and *Luvarus imperialis*.

Supplementary information

**Prolonged morphological expansion of
spiny-rayed fishes following the end-
Cretaceous**

In the format provided by the
authors and unedited

1. Supplementary Methods

a. Taxon sampling

The phylogenetic analyses included UCE sequence data sampled from 1,109 specimens that include 1,084 species. For this study, we collected new UCE sequence data from 653 specimens. We retrieved UCE loci from the remaining 456 specimens at NCBI from previous studies of acanthomorph phylogeny¹⁻⁵ or from whole genomic data (Supplementary Table 1). This study included representatives of all currently recognized acanthomorph taxonomic orders, 307 of the 331 (92.7%) described taxonomic families of Acanthomorpha and 276 of the 290 (95.2%) families of Percomorpha⁶. Based on previous phylogenetic analyses^{7,8}, we sampled two species of Aulopiformes and seven species of Myctophiformes as outgroups for the phylogenetic analyses: *Notolepis coatsi*, *Alepisaurus ferox*, *Scopelengys tristis*, *Neoscopelus macrolepidotus*, *Neoscopelus microchir*, *Dasyscopelus selenops*, *Benthoosema glaciale*, *Notoscopelus caudispinosus*, and *Ceratospelus warmingii*. We sampled phenotypic data from 680 of the 1,075-acanthomorph species sampled in the UCE inferred phylogeny. We inferred phylogenies from the UCE dataset for an inclusive taxon sampling of 1,084 species and for a set of 702 species that included the 680 for which corresponding morphological data was obtained. We refer to these UCE datasets and resulting phylogenies as the 1,084- and 702-taxon datasets and trees, respectively.

b. Library preparation, target enrichment, and sequencing

We isolated DNA from tissue biopsies using Qiagen DNeasy Blood and Tissue kits following the manufacturer's protocol. We used a Qubit fluorometer (Life Technologies) to quantify 1-2 uL of all DNA extractions. We sheared approximately 500 ng of genomic DNA from each sampled specimen using a QSonica Q800R3 sonicator to obtain fragment sizes between 300-600 bp. For library preparation and target enrichment of UCE loci, we followed protocols described in a previous study³ using Kapa HyperPrep kits (Kapa Biosystems) and Illumina TruSeq iTru5 and iTru7 adapters for dual indexing of genomic libraries⁹. We used a bait set from Arbor Biosciences designed to target 1,314 UCE loci in acanthomorph fishes for target-enrichment of UCE loci³. Enriched libraries were sequenced using 150 bp paired-end sequencing on Illumina HiSeq platforms.

c. Assembly and alignment construction

For 96 species, we harvested UCE loci sequences from existing whole genomic data (Supplementary Table 1). We downloaded genomes from NCBI and converted to 2bit format using faToTwoBit from the UCSC Genome Browser Downloads (<https://hgdownload.cse.ucsc.edu/admin/exe/>). We then located UCE loci in each genome assembly by running the PHYLUCE v.1.7.1^{10,11} program `run_multiple_lastzs_sqlite.py` with default parameters and the FASTA file containing the UCE bait sequences. From each assembly, we extracted the identified UCE loci along with ± 500 bp of sequence from each flank using `phyluce_probe_slice_sequence_from_genomes.py` with default parameters.

To process raw read data generated by our own sequencing efforts, construct assemblies, identify orthologous UCE sequences, and construct alignments for each UCE locus, we used the PHYLUCE computer package^{10,11}, which uses parallel wrapper functions around external programs to perform tasks required to process high-throughput DNA sequence data. We used the `illumiprocessor` parallel wrapper program (<https://github.com/faircloth-lab/illumiprocessor>) to implement Trimmomatic¹², which removes adapter index sequences and low-quality bases from demultiplexed raw reads. We constructed assemblies for each sample using *trinity* v.r2013-02-25¹³ and used the PHYLUCE program `phyluce_assembly_match_contigs_to_probes` to identify which assembled contigs represented UCE sequences by matching them to a FASTA file containing the UCE bait sequences, and to remove reciprocal and non-reciprocal duplicates.

We used PHYLUCE programs to infer a separate set of alignments and phylogenies for the 702 species including the sampling of morphological data and the full 1,109 specimen sampling using the same protocols. We generated alignments for each UCE locus using MAFFT v7.130b¹⁴ and trimmed with trimAL v1.4.rev¹⁵. For further downstream phylogenetic analyses, we retained UCE loci that included at least 75% of the total specimens in both the 1,084- and 702-taxon datasets.

d. Phylogenetic analyses

We inferred phylogenies for both the 1,084-taxon and 702-taxon datasets using maximum likelihood methods as implemented in IQ-TREE v. 1.7¹⁶ and RAxML-ng 0.9.0¹⁷. In IQ-TREE, we ran tree searches using ultrafast bootstrap approximation until 1,000 bootstrap replicates and

1,000 replicates of the Shimodaira-Hasegawa approximate likelihood ratio test (SH-aLRT) were generated¹⁸. Phylogenies inferred in IQ-TREE using the unpartitioned alignments described above served as the topological constraints for subsequent divergence time analyses. Maximum likelihood tree searches conducted in IQ-TREE used the ModelFinderPlus¹⁹ option, which applies a relaxed hierarchical clustering search algorithm to determine partitioning schemes and models of molecular evolution.

Before conducting analyses in RAxML-ng v0.9.0¹⁷, we determined partitioning schemes using PartitionFinder2 v2.1.1²⁰, with units of partitioning based on individual UCE loci. We identified these partitioning schemes using a relaxed hierarchical clustering search algorithm with a maximum cluster size set to 1000 data blocks, the Bayesian Information Criterion method for partition model comparison, and GTR+Gamma as the model of molecular evolution. We removed all fully undetermined columns from our partitioned, concatenated alignment using RAxML-ng, compressed the alignment, and converted to binary. We performed maximum likelihood tree searches on these alignments using the extended majority rule criterion method implemented with the autoMRE command to continue bootstrapping until convergence.

We compared the tree topologies inferred in the concatenated analyses described above using the program TOPD_v4.6²¹. Phylogenies based on the 1,084-species dataset (IQ-TREE single-partition, IQ-TREE multiple partitions, and RAxML-ng multiple partitions) were compared to one another, and separate analyses compared the three phylogenies inferred from the 702-taxon dataset. We utilized TOPD to calculate partition metrics, i.e., TOPD's "Split" method²², and path length metrics, i.e., TOPD's "Nodal" method²³. We produced lists of taxa with different phylogenetic positions among the compared trees using TOPD's "Disagree" method, which removes a single taxon at each iteration and calculates the reduction in trees' split distance.

We inferred a summary species tree in ASTRAL-III v5.6.3²⁴, using maximum likelihood gene trees for each UCE locus generated with IQ-TREE v 1.6.12. For individual gene tree inference, we applied the ModelFinder Plus¹⁹ option to determine the optimal model of molecular evolution as well as the ultrafast bootstrap approximation with a maximum of 10,000 bootstrap iterations. We used TreeShrink²⁵ to identify abnormally long branch lengths in the individual UCE gene trees and to minimize the impact of misspecified sequences. We used a false positive tolerance rate parameter (α) of 0.05 in our TreeShrink filtering to automate the

removal of potentially aberrant sequences from the UCE alignment. We re-aligned the TreeShrink-pruned alignments using MAFFT v7.130b¹⁴ and re-inferred gene trees using IQ-TREE, as above. We used these gene trees to infer a species tree in ASTRAL-III.

e. Bayesian concordance factor analyses

To evaluate the phylogenetic discordance among individual UCE gene trees, we used IQ-TREE to estimate maximum likelihood gene- and site-concordance factors (gCF and sCF, respectively; methods are described in the main text) and BUCKy²⁶ to estimate Bayesian genome-wide concordance factors. We compared alternative phylogenetic hypotheses among the major lineages of Acanthomorpha using these concordance factors. BUCKy estimates the frequency of topological partitions that occur in a sample of Bayesian gene tree posterior distributions and provides an estimate for their genome-wide frequency and 95% confidence intervals. Because the number of possible topological relationships among taxa increases non-linearly as the number of species included in the analysis increases, large taxonomic datasets are intractable for thorough concordance factor analyses with BUCKy. We therefore used a reduced taxonomic dataset of 82 species that represent each of the major subclades of Acanthomorpha to reduce computational burden. For this reduced dataset, we generated alignments of the 82 species using MAFFT (Supplementary Table 1). We used MrBayes v. 3.2.7²⁷ to infer a Bayesian gene tree distributions for each UCE locus. We ran MrBayes analyses with a GTR+Gamma molecular evolutionary model for 2 million generations, with trees sampled every 2,000 generations. Using the BUCKy program mbsum, we discarded the first 75% of sampled trees from the posterior sample of each UCE locus as burnin, summarized branching patterns in the remaining post-burnin posterior distribution, and used an alpha value of 1.0 for concordance factor estimation. These gene tree posterior distributions were then used for subsequent BUCKy estimation of concordance factors.

f. Divergence-time estimation

We estimated divergence times for both the 702- and 1,084-taxon phylogenies using BEAST v.2.5²⁸ following a protocol used in other UCE studies where BEAST analyses were run using reduced datasets of 30 UCE loci^{1,5,29}. We constrained the phylogeny used in the BEAST runs using the IQ-TREE analyses of the 1,084- and 702-taxon datasets. For both datasets, we

performed BEAST analyses on three different sets of 30 loci, each randomly drawn without replacement from the entire set of ~1,000 UCE loci. Exploratory BEAST analyses using sets of 25 and 50 loci yielded similar divergence time estimates, justifying the moderately computationally expensive analyses using the 30 locus datasets. For each subset of 30 loci, we determined the optimum partitioning scheme using the relaxed hierarchical clustering algorithm in PartitionFinder2 v. 2.1.1²⁰. For divergence dating analyses performed in BEAST, we employed a relaxed lognormal clock model and a birth-death tree model. We assigned minima for age priors using forty-three fossil occurrences, described below. For each 30-locus dataset, we ran at least three replicate analyses for a minimum of 200 million generations beyond a total burnin of 200 million generations. As MCMC chains progressed, we accepted suggestions provided by BEAST for improving operators' tuning parameter values. We used Tracer v.1.7.1 to observe effective sample size (ESS) values for posterior parameter estimates, to assess convergence among replicate MCMC chains, and to check for directional trends in parameter estimates³⁰. Though the large size of the phylogenies created computational limits that resulted in moderate ESS values for some parameters, most parameter estimates reached ESS values well above 200. Some analyses were run up to 900 million generations in length to obtain adequate ESS values and ensure no directional trends in and unimodal distributions of parameter estimates. We used LogCombiner in BEAST v.1.8.4^{31,32} to remove a burnin, and trees from each replicate run were randomly thinned. We thinned the sets of 1,084-species trees such that a total of 1,200 trees would remain across all runs, with an equal number of trees from each replicate contributing to the final summary trees. We randomly thinned the sets of 702-species trees such that 10,000 total trees remained across replicate runs. For each set of loci, we used LogCombiner to combine trees from replicate runs and TreeAnnotator in BEAST v.1.8.4 (Drummond et al. 2012) to estimate maximum clade credibility trees.

g. Diversification rate analyses

We performed diversification rate analyses on the time-calibrated 1,084-taxon phylogeny that was run for the most generations and therefore had the highest ESS values for posterior parameter estimates. Species diversity of acanthomorph lineages used to determine sampling fractions for all diversification rate analyses were based on numbers of species presented in Eschmeyer's Catalog of Fishes⁶, which at the time of the analyses included 19,219 species of

Acanthomorpha. We removed all outgroups and duplicate samples of the same species before performing diversification rate analyses, leaving a phylogeny consisting of 1,075 acanthomorph species and a sampling fraction of 0.056. We performed stepping-stone simulations within TESS³³ to estimate the marginal likelihoods of eight birth-death models and evaluate their fit to the acanthomorph time-calibrated phylogeny. Competing models included those with constant diversification rates, with episodically changing rates, or with decreasing speciation rates. Variants of the constant rate model with and without a mass extinction event were also tested to assess the potential impact of the K-Pg mass extinction on acanthomorph diversification. We tested variants of the competing models that accommodated the effects of incomplete taxon sampling by correcting for uniform (random) or diversified sampling methods.

Using the simulated marginal likelihoods of candidate models, we calculated Bayes factors and compared the relative fits of models to the acanthomorph phylogeny (Extended Data Fig. 6). With the exception of the models assuming a decreasing speciation rate, we ran stepping-stone simulations for 10,000 iterations with 1,000 power posteriors (stepping stones) and a burn-in period of 3,000 generations. Due to limited computational resources, we ran the simulations of marginal likelihoods for the decreasing speciation rate (i.e., continuous) models for 2,000 iterations (a burn-in of 500 generations was removed) with 100 power posteriors. This test of relative model fit greatly favored models assuming uniform (random) sampling methods over diversified methods (Extended Data Fig. 6), informing our model selection in downstream TESS analyses.

We extracted the three branching process-models that were most favored in the tests of relative model fit and assessed their absolute fit to the acanthomorph phylogeny using posterior-predictive simulations. We compared the predictive distributions of the gamma statistic, number of taxa, and lineage-through-time (LTT) plots to the empirical estimates.

We inferred the global speciation, extinction and net-diversification rates through time using the CoMET model as employed by TESS. For CoMET analyses represented in Extended Data Fig. 5, we specified a uniform (random) sampling strategy ($\rho = 0.056$), conditioned the model on taxa survival, discarded a burn-in of 30,000 iterations, and ran three replicate reversible-jump MCMC chains until the effective sample size (ESS) reached 500 or greater. We assessed convergence within each CoMET run by calculating the effective sample sizes and

Geweke diagnostics for the diversification rate, and we assessed convergence of multiple runs using the Rubin-Gelman test.

We inferred global diversification rates and examined rate heterogeneity across clades using BAMM v.2.5.0³⁴. Our analyses corrected for incomplete sampling by accounting for the sampling fractions of 304 major representative clades, most of which are taxonomic families, in accordance with the number of species described by Eschmeyer's Catalog of Fishes⁶. We also used the information on species diversity to appropriately adjust these clade-specific sampling fractions for non-monophyletic taxonomic groups. As in the TESS analyses, we set the global sampling fraction for all BAMM analyses to 0.056. We identified appropriate rate priors using the function `setBAMMpriors` in the R package `BAMMtools` v.2.1.6³⁵, accounting for incomplete taxon sampling.

We ran Markov chain Monte Carlo simulations for 100 million generations under the default settings. We also used default settings for MCMC scaling operators and move frequencies. We ran BAMM 23 times, each time under different conditions that might be appropriate for a medium-sized tree consisting of ~1,000 taxa. Runs tested different combinations of numbers of MCMC chains (2 or 4), temperature increment parameters ($\Delta T = 0.05$ or 0.1) and expected number of diversification rate shifts (1, 5, 10, 15, 20, 25, 30, 35, 40 and 45). We tested the effect of changing the number of expected shifts—despite the `setBAMMpriors` function in `BAMMtools` recommending an input of just one expected shift—because preliminary runs suggested that the number of diversification rate shifts is greater than 20. For each analysis, we compared Bayes factors for competing prior models with different numbers of expected rate shifts.

h. Body shape trait data

We pruned a body trait dataset to the 680 species that matched those in the 702-species UCE phylogeny³⁶. The body shape dataset included maximum body depth, maximum fish width, head depth, lower-jaw length, mouth width, minimum caudal-peduncle depth, and minimum caudal-peduncle width. We measured maximum body depth as the maximum linear distance from the dorsal to ventral margin of the body, anywhere in the region between the posterior edge of the operculum to the anterior portion of the caudal peduncle. We measured maximum fish width as the maximum width anywhere along the body. We measured head depth as the vertical distance

from the dorsal to ventral margins of the head passing through the center of the eye. We measured lower jaw length as the linear distance from the anterior end of the lower jaw to the articular-quadrato joint. We measured mouth width as the linear distance between the left and right articular-quadrato joints. We measured minimum caudal peduncle depth as the minimum vertical distance from the dorsal to ventral margin of the caudal peduncle. We measured minimum caudal peduncle width as the narrowest point along the caudal peduncle. Lastly, we measured fish standard length as the linear distance from the anterior tip of the upper jaw to the posterior edge of the hypural plate or to the posterior end of the vertebral column (i.e., in species that lack a hypural plate). There were no repeat measurements for samples or species. We accounted for size by regressing log-transformed lengths against log-transformed standard fish length and calculating phylogenetic residuals using the `phyl.resid` function implemented in PHYTOOLS³⁷. We used this matrix of residuals for seven traits for phylogenetic comparative analyses using a multivariate framework.

i. Disparity through time analyses

We assessed disparity through time (DTT) using the `dtm` function implemented in GEIGER³⁸. We incorporated uncertainty in divergence times by repeating analyses across 100 trees randomly sampled from the posterior distribution. Since we were specifically interested in patterns around and following the K-Pg boundary, we summarized disparity through time in 1 My intervals as the proportion of trees in which the observed subclade disparity fell below that expected from a Brownian motion process (i.e., the expected pattern if the clade is undergoing significant between-clade ecological divergence) (results in Fig. 2 and Extended Data Fig. 8). Focusing on the time following the K-Pg boundary, we statistically summarized the 1 My time interval during which the observed subclade disparity first dropped below that expected from a Brownian motion process (results in Extended Data Fig. 8). We tested the sensitivity of disparity through time analyses to body shape traits and to the inclusion of major clades by repeating all analyses to the exclusion of clades that arose immediately around the K-Pg boundary and to the exclusion of each trait, as well as repeating the analyses for each trait separately in a univariate framework (results in Fig. 4). We also visualized the evolutionary histories of the following focal lineages using the phenogram function implemented in PHYTOOLS³⁷: Carangiformes, Lophioidei, Perciformes, Scombriformes, “Squamipinnes” (here defined as the clade containing *Chaetodon*

kleinii and *Luvarus imperialis*), Syngnathiformes, and Tetraodontoidei. We visualized body shape morphospace using principal component analysis (PCA) with the `prcomp` function. Since the traits had different variances, we scaled all traits prior to performing PCA.

2. Fossil calibrations for relaxed clock BEAST analyses

i. Node: Stem lineage Lampriformes, dating the most recent common ancestor (MRCA) of *Lampris guttatus* and *Stylephorus chordatus*, which is the MRCA of Lampriformes and all other paracanthopterygians. *First occurrence*: †*Aipichthys minor*. Sannine Limestone, Hadjula, Lebanon. *Resolution in phylogenetic analyses*: †*Aipichthys minor* is resolved as a lampriform stem lineage in parsimony analyses of morphological characters^{39,40}. *Stratigraphy*: The Hadjula fish beds are located below reported occurrence of *Mantelliceras mantelli*, which defines the first complete ammonite zone of the Late Cretaceous. The top of the *Mantelliceras mantelli* Zone is dated at 98.0 Ma⁴¹, from which we derive a minimum age for *Aipichthys*. *Minimum age*: 98.0 Ma. *Prior setting*: lognormal prior, minimum age 98.0 Ma, mean=1.0, S.D.=1.25, upper 95% CI: 119.0 Ma¹.

ii. Node: Stem lineage Polymixiiformes, dating the MRCA of *Polymixia lowei* and *Aphredoderus sayanus*, which subtends the MRCA of *Polymixia* and Percopsiformes. *First occurrence*: †*Homonotichthys dorsalis*. Lower Chalk of Sussex and Kent, UK⁴². *Resolution in phylogenetic analyses*: none. *Character states*: four full-sized branchiostegals; anterior branchiostegals reduced and forming support for chin barbel^{42,43}. *Stratigraphy*: middle-upper Cenomanian, zone of *Holoaster subglobosus*, corresponding to the late Cenomanian^{42,44,45}. The minimal age for †*Homonotichthys dorsalis* is provided by the age of Cenomanian-Turonian boundary, which is dated as 93.9 Ma⁴¹. *Absolute age estimate*: 93.6 Ma (28). *Prior setting*: lognormal prior, minimum age 93.6 Ma, mean = 1.06, S.D.=1.25, upper 95% CI: 116.35 Ma³.

iii. Node: Stem lineage Aphredoderidae, dating the MRCA of *Aphredoderus sayanus* and *Typhlichthys subterraneus*, which subtends the MRCA of Aphredoderidae and Amblyopsidae. *First occurrence*: †*Trichophanes foliarum*. Florissant Formation, Colorado, USA⁴⁶. *Resolution in phylogenetic analyses*: †*Trichophanes* and *Aphredoderus* form a clade in a maximum parsimony

analysis of 47 morphological characters⁴⁷. *Character states*: ventral margins of lachrymal and infraorbitals spiny; alveolar process of premaxilla divided into separate segments⁴⁶⁻⁴⁸.

Stratigraphy: The upper Priabonian Florissant Roadcut is dated radiometrically using ⁴⁰Ar/³⁹Ar isotope ratios as 34.07 Ma⁴⁹. *Absolute age estimate*: 34.1 Ma. *Prior setting*: lognormal prior, minimum age 34.1 Ma, mean=1.0, S.D.= 1.347, upper 95% CI: 59.0 Ma⁷.

iv. Node: Stem lineage *Zenopsis*, dating the MRCA of *Zenopsis* and *Zeus*. *First occurrence*:

†*Zenopsis clarus*, †*Z. tyleri*, and †*Z. hoernesii*. Lower Maikopian series, Psheka Horizon of the Belaya River, Caucasus⁵⁰, and Lower Dysodylic shales, Strujinoasa-Drăgușina and Piatra Neamț, Romania⁵¹; Lower Dysodylic shales, Piatra Neamț, Romania⁵¹; Laško (Tüffer), Slovenia⁵¹.

Resolution in phylogenetic analyses: maximum parsimony analysis of 45 morphological characters resulted in a phylogeny where †*Zenopsis clarus*, †*Z. tyleri*, and †*Z. hoernesii*, and *Z. oblongus* are resolved in a clade⁵². *Character states*: slender lachrymal; pelvic-fin spines absent; buckler-like plates present along ventral midline of abdomen, and along dorsal ridge from middle of spinous to end of soft dorsal fin⁵². *Stratigraphy*: lower Rupelian [P18], lower Khadumian regional stage⁵³. *Absolute age estimate*: 32.0 Ma⁵⁴. *Prior setting*: lognormal prior, minimum age 32.0 Ma, mean=1.0, S.D.= 0.33, upper 95% CI: 36.7 Ma⁷.

v. Node: Stem lineage Lampridae, dating the MRCA of *Lampris guttatus* and *Zu elongatus*, which is the MRCA of Lampriformes. *First occurrence*: †*Turkmene finitimus*. Danatinsk Suite, Uyly-Kushlyuk locality, Turkmenistan^{55,56}. *Resolution in phylogenetic analysis*: none.

Character states: first dorsal fin pterygiophore strongly reclined posteriorly; enlarged pectoral fins inserting high on flank; shoulder girdle broad ventrally, with expanded coracoid; long parapophyses absent from abdominal vertebrae⁵⁶. *Stratigraphy*: uppermost Thanetian-lowermost Ypresian⁵⁷. *Absolute age estimate*: 55.8 Ma⁵⁴. *Prior setting*: lognormal prior, minimum age 55.8 Ma, mean=1.0, S.D.= 1.411, upper 95% CI: 83.5 Ma⁷.

vi. Node: Stem lineage Holocentridae, dating the MRCA of *Myripristis violacea* and *Rondeletia loricata*, which subtends the MRCA of Holocentridae and Berycoidei. *First occurrence*: †*Stichocentrus liratus* from the Sannine Limestone, Hadjula, Lebanon⁵⁸. *Resolution in phylogenetic analyses*: none. *Character states*: The penultimate anal-fin spine of

†*Stichocentrus* is enlarged and represents a synapomorphy of holocentroids^{43,59}. *Stratigraphy*: See discussion for Calibration i, †*Aipichthys minor*. *Absolute age estimate*: 98.0 Ma. *Prior setting*: lognormal prior, minimum age 98.0 Ma, mean=1.0, S.D.= 0.8, upper 95% CI: 108.0 Ma¹.

vii. Node: Stem lineage Myripristinae, dating the MRCA of *Myripristis violacea* and *Sargocentron coruscum*, which subtends the MRCA of Holocentridae. *First occurrence*: †*Eoholocentrum macrocephalum*, †*Berybolcensis leptacanthus*, and †*Tenuicentrum pattersoni*. Pesciara beds of ‘Calcarei nummulitici’, Bolca, Italy⁶⁰⁻⁶². *Resolution in phylogenetic analyses*: analysis of 72 morphological characters resolve †*Eoholocentrum*, †*Berybolcensis*, and †*Tenuicentrum* as stem-lineage Myripristinae⁶³. *Character states*: tooth-bearing platform expanded and overhangs lateral side of dentary near symphysis; premaxillary tooth field curves dorsally toward ascending process at symphysis; edentulous ectopterygoid (†*Berybolcensis* and †*Tenuicentrum*); spinous procurrent caudal-fin rays reduced to four in the upper and three in the lower lobe (†*Berybolcensis* and †*Tenuicentrum*)⁶³. *Stratigraphy*: upper Ypresian [NP14]^{64,65}. *Absolute age estimate*: 50 Ma⁵⁴. *Prior setting*: lognormal prior, minimum age 50.0 Ma, mean=1.0, S.D.= 0.6, upper 95% CI: 57.3 Ma⁷.

viii. Node: Crown lineage Syngnathiformes, dating the MRCA of *Pegasus volitans* and *Syngnathus scovelli*, which subtends the MRCA of Syngnathiformes. *First occurrence*: †*Gasterorhamphosus zuppichinii*. “Calcarei di Melissano”, Porto Selvaggio, Lecce province, Italy⁶⁶. *Resolution in phylogenetic analyses*: none, but Orr⁶⁷ argues that †*Gasterorhamphosus* is a stem lineage of a clade containing Macrorhamphosidae and Centriscidae. *Character states*: anal-fin spine absent; enlarged dorsal-fin spine with serrated posterior margin; elongated tubular snout; pleural ribs absent; cleithrum bears enlarged posterodorsal process; rod-like anteroventral process of coracoid; pectoral rays simple^{67,68}. *Stratigraphy*: uppermost Campanian-lowermost Maastrichtia⁶⁹. *Absolute age estimate*: 69.71 Ma¹. *Prior setting*: lognormal prior, minimum age 69.71 Ma, mean=1.0, S.D.= 0.785, upper 95% CI: 79.6 Ma¹.

ix. Node: Stem lineage Centriscidae, dating the MRCA of *Aeoliscus strigatus* and *Macroramphosus gracilis*, which subtends the MRCA of Centriscidae. *First occurrence*: †*Paramphisile weileri* and †*Paraeoliscus robinetae*. Pesciara beds of ‘Calcarei nummulitici’,

Bolca, Italy⁷⁰. *Resolution in phylogenetic analyses*: none. *Character states*: caudal fin directed posteroventrally (†*Paraeoliscus*); dorsal spine jointed distally⁶⁷. *Stratigraphy*: See discussion for Calibration viii †*Eoholocentrum macrocephalum*. *Absolute age estimate*: 50 Ma⁵⁴. *Prior setting*: lognormal prior, minimum age 50.0 Ma, mean=1.0, S.D.= 0.6, upper 95% CI: 57.3 Ma⁷.

x. Node: Crown lineage *Ariomma*, dating the MRCA of *Ariomma indica* and *A. melana*. *First occurrence*: †*Ariomma geslini* from the diatomites of St Eugène, Chelif Basin, Algeria⁵. *Resolution in phylogenetic analyses*: none. *Character states*: extension of pleural ribs onto caudal vertebrae^{71,72}, and a distinctive pattern of anal-fin skeleton shared with *A. bondi* and *A. melana*, consisting of anterior pterygiophores that bend posteriorly, overlapping the similarly curved shafts of successive pterygiophores^{72,73}. *Stratigraphy*: Details presented in Friedman et al.⁵. *Absolute age estimate*: 5.94 Ma. *Prior setting*: lognormal prior, minimum age 5.94 Ma, mean=1.0, S.D.= 1.299, upper 95% CI: 28.96 Ma⁵.

xi. Node: stem lineage Stromateidae, dating the MRCA of *Pampus argenteus* and *Ariomma indica*, which subtends the MRCA Stromateidae and the clade that comprises *Ariomma* and Nomeidae. *First occurrence*: †*Pinichthys pulcher* from the Pshakha Horizon †*Planorbella* Beds, Lower Maikop Caucasus⁷⁴. *Resolution in phylogenetic analyses*: none. *Character states*: †*Pinichthys* has a stellate, bony base of papillae in the region expected to bear pharyngeal sacs⁷⁵. Synapomorphies of stromateiod displayed by †*Pinichthys* include: a continuous dorsal fin; a ventral articulation between the coracoid and ventral tip of the cleithrum; and an elongated first anal fin pterygiophore that is strongly reclined⁷⁶. †*Pinichthys* differs from extant lineages of Stromateidae by having well-developed pelvic fins in adults and lacking extension of the first anal fin pterygiophore posterior to the first haemal spine⁵. †*Pinichthys* is interpreted as a stem-lineage stromateiod, which is consistent with previous interpretations⁷⁴. *Stratigraphy*: Details presented in Friedman et al.⁵. *Absolute age estimate*: 32.02 Ma. *Prior setting*: lognormal prior, minimum age 32.02 Ma, mean=1.0, S.D.= 1.2, upper 95% CI: 51.6 Ma⁵.

xii. Node: stem lineage Chiasmodontidae, dating the MRCA of *Kali kerberti* and *Tetragonurus atlanticus*, which subtends the MRCA of Chiasmodontidae and *Tetragonurus*. *First occurrence*: †*Bannikovichthys paelignus* from the fish-bearing laminates of Toricella Paligna, Italy⁷⁷.

Resolution in phylogenetic analyses: none. *Character states*: The hypothesis that †*Bannikovichthys* is related to living Chiasmodontidae is based on an absence of scales, elongated opercles, delicate ossification of the interopercle and subopercle, and enlarged hourglass-shaped radials⁷⁷. The relationships of †*Bannikovichthys* among living chiasmodontids is uncertain, so it is conservatively treated as a stem-lineage taxon⁵. *Stratigraphy*: Details presented in Friedman et al.⁵. *Absolute age estimate*: 11.9 Ma. *Prior setting*: lognormal prior, minimum age 11.9 Ma, mean=1.0, S.D.= 1.454, upper 95% CI: 41.56 Ma⁵.

xiii. Node: within crown of *Scomber*, dating the MRCA of *Scomber australasicus* and *Scomber japonicus*. *First occurrence*: *Scomber colias* from the Raz-el-Aïn, Oran, Algeria. *Resolution in phylogenetic analyses*: This fossil is attributed to the living species *Scomber colias*, which is resolved as the sister lineage of *S. japonicus* in a molecular phylogenetic analysis⁷⁸. *Stratigraphy*: Details presented in Friedman et al.⁵. *Absolute age estimate*: 5.94 Ma. *Prior setting*: lognormal prior, minimum age 5.94 Ma, mean=1.0, S.D.= 1.255, upper 95% CI: 27.4 Ma⁵.

xiv. Node: stem lineage *Scomber*, dating the MRCA of *Scomber australasicus* and *Rastrelliger kanagurta*. *First occurrence*: †*Scomber saadii* from the Padbeh Formation of Istehbanât, Iran⁷⁹. *Resolution in phylogenetic analyses*: None. *Character states*: †*Scomber saadii* exhibits serrations on the teeth that is a synapomorphy of *Scomber*^{78,80}. *Stratigraphy*: Details presented in Friedman et al.⁵. *Absolute age estimate*: 33.9 Ma. *Prior setting*: lognormal prior, minimum age 33.9 Ma, mean=1.0, S.D.= 1.02, upper 95% CI: 48.45 Ma⁵.

xv. Node: stem lineage *Acanthocybium*, dating the MRCA of *Acanthocybium solandri* and *Scomberomorus maculatus*. *First occurrence*: †*Palaeocybium proosti* from the London Clay Formation, Isle of Sheppey, UK⁸¹. *Resolution in phylogenetic analysis*: none. *Character states*: †*Palaeocybium* and *Acanthocybium* share closely spaced teeth with blunt tips and the holotype specimen shows an elongate lower jaw that is similar to *Acanthocybium* and *Scomberomorus*⁸²⁻⁸⁴. *Stratigraphy*: Details presented in Friedman et al.⁵. *Absolute age estimate*: 50.5 Ma. *Prior setting*: lognormal prior, minimum age 50.5 Ma, mean=1.0, S.D.= 0.5, upper 95% CI: 56.72 Ma⁵.

xvi. Node: stem lineage Sardini + Thunnini, dating the MRCA of *Scomberomorus maculatus* and *Euthynnus affinis*. *First occurrence*: †*Eocoelopoma portentosum* from the Danatinsk Formation, Turkmenistan⁸⁵. *Resolution in phylogenetic analyses*: None. *Character states*: Details presented in Friedman et al.⁵. *Stratigraphy*: Details presented in Friedman et al.⁵. *Absolute age estimate*: 54.17 Ma. *Prior setting*: lognormal prior, minimum age 54.17 Ma, mean=1.0, S.D.= 0.698, upper 95% CI: 62.71 Ma⁵.

xvii. Node: stem lineage Thunnus, dating the MRCA of *Thunnus orientalis* and *Auxis rochei*, which is the MRCA of Thunnini. *First occurrence*: †*Thunnus abchasicus* from the Kuma Horizon, Pshakha River, Caucasus⁸⁶. *Resolution in phylogenetic analyses*: None. *Character states*: †*Thunnus abchasicus* exhibits several synapomorphies of *Thunnus* that include the presence of small oral teeth and the shortened preural vertebrae⁸⁶. The presence of a spine in the second dorsal fin suggests that †*T. abchasicus* is a stem lineage *Thunnus*⁸⁵. *Stratigraphy*: Details presented in Friedman et al.⁵. *Absolute age estimate*: 38.62 Ma. *Prior setting*: lognormal prior, minimum age 38.62 Ma, mean=1.0, S.D.= 0.91, upper 95% CI: 50.78 Ma⁵.

xviii. Node: stem lineage Promethichthys, dating the MRCA of *Promethichthys prometheus* and *Diplospinus multistriatus*. *First occurrence*: †*Hemithyrsites maicopicus* from the Upper Maikop of the Kurdzhips River, Adygea, Caucasus⁸⁵. *Resolution in phylogenetic analyses*: None. *Character states*: Derived traits shared by *Promethichthys* and †*Hemithyrsites maicopicus* include reduction of the pelvic fin to a single spine and the presence of two pairs of dorsal and anal finlets⁸⁵. *Stratigraphy*: Details presented in Friedman et al.⁵. *Absolute age estimate*: 15.97 Ma. *Prior setting*: lognormal prior, minimum age 15.97 Ma, mean=1.0, S.D.= 0.986, upper 95% CI: 29.67 Ma⁵.

xix. Node: Stem lineage Channidae, dating the MRCA of *Channa micropeltes* and *Helostoma temminckii*, which subtends the MRCA of Channidae and a clade containing Helostoma, Anabantidae, and Osphronemidae. *First occurrence*: †*Anchichanna kuldanensis* from the Ganda Kas Area, Kuldana Formation, Kala Chitta Hills, Pakistan⁸⁷. *Resolution in phylogenetic analyses*: None. *Character states*: †*Anchichanna kuldanensis* exhibits the Channidae synapomorphy of the outer wall of the auditory bulla formed mainly by the prootic, but is likely

a stem-lineage taxon because it does not share synapomorphies with either *Channa* or *Parachanna*⁸⁷. *Stratigraphy*: The Kuldana Formation and other vertebrate fossil localities of the Kala Chitta Hills straddle the Ypresian-Lutetian boundary⁸⁸. *Absolute age estimate*: 41.3 Ma. *Prior setting*: lognormal prior, minimum age 41.3 Ma, mean=1.0, S.D.= 1.31, upper 95% CI: 64.7 Ma⁸⁹.

xx. Node: Stem lineage Sphyraenidae, dating the MRCA of *Sphyraena jello* and *Lactarius lactarius*. *First occurrence*: †*Sphyraena bolcensis*, Pesciara beds of ‘Calcari nummulitici’, Bolca, Italy^{90,91}. *Resolution in phylogenetic analyses*: None. *Character states*: three ‘T’-shaped, sutured predorsals or spineless pterygiophores⁹²; elongate gape; upper jaw non-protrusible; enlarged fangs on dentary, premaxilla, and palatine. *Stratigraphy*: upper Ypresian [NP14]^{64,65}. *Absolute age estimate*: 50.0 Ma⁶⁵. *Prior setting*: lognormal prior, minimum age 50.0 Ma, mean=1.0, S.D.= 0.5999, upper 95% CI: 57.3 Ma⁹³.

xxi. Node: Stem lineage Mene, dating the MRCA of *Mene maculata* and *Xiphias gladius*. *First occurrence*: †*Mene purdyi*, ‘Mancora Formation’, Perú⁹⁴; †*M. triangulum*, Danatinsk Suite, Uyly-Kushlyuk locality, Turkmenistan^{55,57}; and †*Mene* sp., ‘Stolle Klint clay’, Ølst Formation, Denmark⁹⁵. *Resolution in phylogenetic analyses*: None. *Character states*: frontal vault; many small infraorbitals; all anal fin rays short, with anteriormost rays plate like; anal fin spines absent; postcleithrum broad and contacts first anal fin pterygiophore; disc-like body with deep ventral keel; greatly elongated second anal fin ray⁹⁴. *Stratigraphy*: uppermost Thanetian-lowermost Ypresian [NP14]^{57,95}. *Absolute age estimate*: 55.2 Ma⁹⁶. *Prior setting*: lognormal prior, minimum age 55.2 Ma, mean=1.0, S.D.= 0.92, upper 95% CI: 67.5 Ma^{1,93}.

xxii. Node: Stem lineage Carangidae, dating the MRCA of *Caranx caninus* and *Trachinotus goodei*, which subtends the MRCA of the clade comprising Carangidae, *Coryphaena*, *Rachycentron*, Scomberoidinae, and Trachinotinae. *First occurrence*: †*Archaeus oblongus*. Danatinsk Suite, Uyly-Kushlyuk locality, Turkmenistan⁵⁵. *Resolution in phylogenetic analyses*: None. *Character states*: broad gap between second and third anal-fin spines⁹⁷. *Stratigraphy*: uppermost Thanetian-lowermost Ypresian⁵⁷. *Absolute age estimate*: 55.8 Ma⁵⁴. *Prior setting*: lognormal prior, minimum age 55.8 Ma, mean=1.0, S.D.= 0.661, upper 95% CI: 63.9 Ma⁹³.

xxiii. Node: Stem lineage Caranginae, dating the MRCA of *Caranx caninus* and *Seriola dumerili*, which subtends the MRCA of Carangidae. *First occurrence*: †*Eastmanalepes primaevus*, Pesciara beds of ‘Calcari nummulitici’, Bolca, Italy⁹⁸. *Resolution in phylogenetic analyses*: None. *Character states*: lateral line scales modified as thick scutes^{97,99}. *Stratigraphy*: upper Ypresian [NP14]⁶⁴. *Absolute age estimate*: 49.0 Ma¹. *Prior setting*: lognormal prior, minimum age 49.0 Ma, mean=1.0, S.D.= 0.1, upper 95% CI: 52.2 Ma^{1,93}.

xxiv. Node: Stem lineage Echeneioidei, dating the MRCA of *Echeneis naucrates* and *Scomberoides lysan*, which subtends the MRCA of the clade comprising Echeneidae, *Coryphaena*, *Rachycentron*, Scomberoidinae, and Trachinotinae. *First occurrence*: †*Ductor vestenae* from the Pesciara locality of Bolca, Italy^{90,91}. *Resolution in phylogenetic analyses*: parsimony and Bayesian analyses of morphology and combined molecular and morphological datasets resolve †*Ductor vestenae* as either a stem echeneioid or as the sister the clade containing *Rachycentron* and *Coryphaena*¹⁰⁰. We follow the conservative consideration of †*Ductor vestenae* as a stem-lineage taxon, as used in Harrington et al.¹. *Character states*: Discussed in Friedman et al.¹⁰⁰. *Stratigraphy*: upper Ypresian [between NP14 and SPZ11]⁶⁴. *Absolute age estimate*: 49.0 Ma¹. *Prior setting*: lognormal prior, minimum age 49.0 Ma, mean=1.0, S.D.= 0.1, upper 95% CI: 52.2 Ma¹.

xxv. Node: Stem lineage Echeneidae, dating the MRCA of *Echeneis naucrates* and *Coryphaena hippurus*, which subtends the MRCA of clade containing Echeneidae, *Coryphaena*, and *Rachycentron*. *First occurrence*: unnamed Echeneidae undet. from the Frauenweiler clay pit, Germany¹⁰¹. *Resolution in phylogenetic analyses*: None. *Character states*: no supraneurals; multiple anal fin pterygiophores insert anterior to first haemal spine; spinous dorsal fin modified as adhesion disc^{100,102}. *Stratigraphy*: See discussion in Harrington et al.¹. *Absolute age estimate*: 29.62 Ma¹. *Prior setting*: lognormal prior, minimum age 29.62 Ma, mean=1.0, S.D.= 0.87, upper 95% CI: 41.0 Ma¹.

xxvi. Node: Stem lineage Scomberoides, dating the MRCA of *Scomberoides lysan* and *Trachinotus goodei*, which subtends the MRCA of Scomberoidinae and Trachinotinae. *First*

occurrence: Scomberoides spinosus from the Upper Maikop at Chernaya Rechka, Caucasus⁵⁷. *Resolution in phylogenetic analyses:* None. *Character states:* *Scomberoides spinosus* exhibits two synapomorphies of Scomberoidinae: 26 versus 24 vertebrae and posterior rays of the dorsal and anal fin developed as finlets^{97,99,103}. *Stratigraphy:* See discussion in Harrington et al.¹. *Absolute age estimate:* 19.3 Ma¹. *Prior setting:* lognormal prior, minimum age 19.3 Ma, mean=1.0, S.D.= 1.095, upper 95% CI: 35.8 Ma¹.

xxvii. Node: Stem lineage Citharidae, dating the MRCA of *Gymnachirus melas* and *Scophthalmus rhombus*, which subtends the MRCA of Citharidae and all other pleuronectoids except *Psettodes*. *First occurrence:* †*Eobothus minimus* from the Pesciara beds of ‘Calcari nummulitici’, Bolca, Italy^{104,105}. *Resolution in phylogenetic analyses:* †*Eobothus* is the sister lineage of *Citharus*¹⁰⁴. *Character states:* complete orbital asymmetry; dorsal fin extends above orbit; hook-shaped urohyal; parahypural not in articulation with pural centrum 1; long neural spine on preural centrum 2¹⁰⁴. *Stratigraphy:* See discussion in Harrington et al.¹. *Absolute age estimate:* 49.0 Ma¹. *Prior setting:* lognormal prior, minimum age 49.0 Ma, mean=1.0, S.D.= 0.68, upper 95% CI: 57.3 Ma¹.

xxviii. Node: Stem lineage of the clade containing Soleidae and Cynoglossidae, dating the MRCA of *Aseraggodes xenicus* and *Poecilopsetta plinthus*. *First occurrence:* †*Eobuglossus eocenicus* from the Mokkatam Formation, Djebel Turah, Egypt¹⁰⁶. *Resolution in phylogenetic analyses:* none. *Character states:* †*Eobuglossus* shows derived cranial features limited to Soleidae, including blind side preopercular canal terminating on ventral margin of preopercular and convex portion of blind side dentary anterior to angulo-articular^{106,107}. *Stratigraphy:* See discussion in Harrington et al.¹. *Absolute age estimate:* 41.2 Ma¹. *Prior setting:* lognormal prior, minimum age 41.9 Ma, mean=1.0, S.D.= 0.4, upper 95% CI: 46.4 Ma¹.

xxix. Node: Stem lineage Bothidae, dating the MRCA of *Bothus pantherinus* and *Cyclopsetta frimbriata*, which subtends the MRCA of the clade containing Bothidae and Cyclopsettidae. *First occurrence:* †*Oligobothus pristinus* from the Lower Dysodilic shales, Piatra Neamț, Romania¹⁰⁸. *Resolution in phylogenetic analyses:* None. *Character states:* myorhabdoi present¹⁰⁸. *Stratigraphy:* See discussion in Harrington et al.¹. *Absolute age estimate:* 29.62 Ma¹.

Prior setting: lognormal prior, minimum age 29.62 Ma, mean=1.0, S.D.= 0.06, upper 95% CI: 32.6 Ma¹.

xxx. Node: Stem lineage Pleuronectidae, dating the MRCA of *Pleuronichthys cornutus* and *Paralichthys albigutta*, which subtends the MRCA of the clade containing Pleuronectidae and Paralichthyidae. *First occurrence*: †*Oligopleuronectes germanicus* from the Frauenweiler fossil site, Germany¹⁰⁹. *Resolution in phylogenetic analyses*: None. *Character states*: Suggested as a member of Pleuronectidae based on †*Oligopleuronectes* being right-eyed and having a lateral process on the eye-side frontal^{109,110}. *Stratigraphy*: See discussion in Harrington et al.¹. *Absolute age estimate*: 29.62 Ma¹. *Prior setting*: lognormal prior, minimum age 29.62 Ma, mean=1.0, S.D.= 0.45, upper 95% CI: 35.3 Ma¹.

xxxi. Node: Stem lineage Bothus, dating the MRCA of *Bothus pantherinus* and *Crossorhombus azureus*. *First occurrence*: *Bothus* sp. from the Middle Tsurevsky Member of the Tsurevsky Formation along the bank of the Psheka River, Caucasus¹¹¹. *Resolution in phylogenetic analyses*: None. *Character states*: A specific affinity to *Bothus* is supported by the presence of robust rectangular haemal spines^{111,112}. *Stratigraphy*: See discussion in Harrington et al.¹. *Absolute age estimate*: 11.056 Ma¹. *Prior setting*: lognormal prior, minimum age 29.62 Ma, mean=1.0, S.D.= 0.84, upper 95% CI: 39.9 Ma¹.

xxxii. Node: Stem lineage Pseudocrenilabrinae, dating the MRCA of *Bathybates minor* and *Amphilophus citrinellus*, which subtends the MRCA of the clade that contains Pseudocrenilabrinae and Cichlinae. *First occurrence*: †*Mahengechromis plethos* from Mahenge, Tanzania¹¹³. *Resolution in phylogenetic analyses*: Several phylogenetic resolutions of †*Mahengechromis* place the taxon as either a crown lineage Cichlidae or crown lineage Pseudocrenilabrinae^{113,114}. We follow Rabosky et al.⁸⁹ in conservatively treating †*Mahengechromis* as a stem-lineage Pseudocrenilabrinae. *Character states*: The identification of †*Mahengechromis* as a cichlid is supported by the morphology of the lower pharyngeal jaw, squamation, and meristics of vertebrae and median fins¹¹³⁻¹¹⁵. *Stratigraphy*: The Mahenge fossil deposits accumulated in a crater formed by intrusion of kimberlite and U-Pb of a zircon crystal dates the formation of the kimberlite at 45.83 +/-0.17 Ma¹¹⁶. Because the lacustrine sediments

predate the kimberlite emplacement it was suggested the age of the fossil deposits are 0.2 to 0.1 Ma younger^{116,117}. We use the conservative date of 45 Ma used in Rabosky et al.⁸⁹. Absolute age estimate: 45.0 Ma. *Prior setting*: lognormal prior, minimum age 45.0 Ma, mean=1.0, S.D.= 1.29, upper 95% CI: 67.3 Ma.

xxxiii. Node: Crown lineage Exocetoidei, dating the MRCA of *Xenentodon cancila* and *Hemiramphus far*, which subtends the MRCA of Belonidae and Hemiramphidae. *First occurrence*: †*Rhamphexocoetus volans* from Pesciara beds of ‘Calcari nummulitici’, Bolca, Italy¹¹⁸. *Resolution in phylogenetic analyses*: None. *Character states*: lower jaw symphysis extended; ventral lobe of caudal fin enlarged relative to dorsal lobe; pectoral fins greatly expanded¹¹⁹⁻¹²¹. *Stratigraphy*: upper Ypresian [NP14]^{64,65}. *Absolute age estimate*: 49.0 Ma³. *Prior setting*: lognormal prior, minimum age 49.0 Ma, mean=1.0, S.D.= 1.49, upper 95% CI: 80.52 Ma³.

xxxiv. Node: Stem lineage Calotomus (Labridae), dating the MRCA of *Calotomus spinidens* and *Sparisoma radians*. *First occurrence*: †*Calotomus preisli* from the Leitha Limestone, St. Margarethen, Austria¹²². *Resolution in phylogenetic analyses*: None. *Character states*: Presence of upper pharyngeal bones bearing 1 to 3 rows of teeth and presence of a lateral canine on the premaxilla are synapomorphies for Scarinae. A conical tooth on the medial face of the premaxilla is a synapomorphy of *Calotomus*¹²². *Stratigraphy*: The Leitha Limestone is constrained by calcareous nannofossils to the standard biozone NN6¹²², which is entirely in the Serravallian stage of the Miocene. The top of NN6 is dated at 11.9 Ma³. *Absolute age estimate*: 11.9 Ma³. *Prior setting*: lognormal prior, minimum age 11.9 Ma, mean=1.0, S.D.= 1.501, upper 95% CI: 43.95 Ma³.

xxxv. Node: Stem lineage Luvaridae, dating the MRCA of *Luvarus imperialis* and *Acanthurus bahianus*, which subtends the MRCA of *Luvarus* and the clade containing *Zanclus cornutus* and Acanthuridae. *First occurrence*: †*Avitoluvarus diana*, †*A. mariannae*, †*Kushlukia permira*, and †*Luvarus necopinatus*. Danatinsk Suite, Uyly-Kushlyuk locality, Turkmenistan¹²³. *Resolution in phylogenetic analyses*: a parsimony analysis of morphological characters resolves a clade that contains †*Avitoluvarus*, †*Kushlukia*, †*Luvarus necopinatus*, and *L. imperialis*, which is sister to a

clade comprising *Zanclus* and Acanthuridae¹²³. *Character states*: median pterygial truss surrounding most of body; two or fewer dorsal-fin spines; no anal-fin spines; distal end of first anal-fin pterygiophore greatly elongated anteriorly; hypurals 1-4 fused; caudal fins broadly overlap hypural(s); pelvic fin rudimentary in adults; teeth absent or greatly reduced¹²³.

Stratigraphy: uppermost Thanetian-lowermost Ypresian⁵⁷. *Absolute age estimate*: 55.8 Ma⁵⁴.

Prior setting: lognormal prior, minimum age 55.8 Ma, mean=1.0, S.D.= 0.661, upper 95% CI: 63.9 Ma⁷.

xxxvi. Node: Stem lineage Acanthurinae, dating the MRCA of *Acanthurus bahianus* and *Naso unicornis*, which subtends the MRCA of Acanthuridae. *First occurrence*: †*Proacanthurus tenius* from the ‘Pesciara beds of ‘Calcari nummulitici’, Bolca, Italy¹²⁴. *Resolution in phylogenetic analyses*: None. *Character states*: caudal peduncle bears folding spine¹²⁴. *Stratigraphy*: upper Ypresian [NP14]⁶⁴. *Absolute age estimate*: 50 Ma⁶⁴. *Prior setting*: lognormal prior, minimum age 50.0 Ma, mean=1.0, S.D.= 0.6, upper 95% CI: 57.3 Ma⁹³.

xxxvii. Node: Stem lineage Siganidae, dating the MRCA of *Siganus spinus* and *Scatophagus argus*. *First occurrence*: †*Siganopygaeus rarus*. Danatinsk Suite, Uylya-Kushlyuk locality, Turkmenistan¹²⁵. *Resolution in phylogenetic analyses*: parsimony analysis of morphological characters resolves four Eocene and Oligocene taxa, including †*Siganopygaeus*, as stem-lineage Siganidae¹²⁵. *Character states*: two pelvic-fin spines; seven or more anal-fin spines; ten or fewer anal-fin rays¹²⁵. *Stratigraphy*: uppermost Thanetian-lowermost Ypresian⁵⁷. *Absolute age estimate*: 55.8 Ma⁵⁴. *Prior setting*: lognormal prior, minimum age 55.8 Ma, mean=1.0, S.D.= 0.661, upper 95% CI: 63.9 Ma⁷.

xxxviii. Node: Stem lineage of Chaetodontidae, dating the MRCA of *Chaetodon kleinii* and *Leiognathus equula*, which subtends the MRCA of the clade that contains Chaetodontidae and Leiognathidae. *First occurrence*: Chaetodontidae cf. *Chaetodon* (tholichthys-stage larvae) from the ‘Fish shales’, Frauenweiler clay pit, Germany^{101,126}. *Resolution in phylogenetic analyses*: None. *Character states*: overlapping, sequential articulation between first dorsal fin pterygiophores, supraneurals, and supraoccipital crest; second infraorbital excluded from orbital margin; two sets of lateral processes on each side of first dorsal fin pterygiophore define a clear

groove; distal head of second supraneural longer than that of first supraneural¹²⁶⁻¹²⁸.

Stratigraphy: The ‘Fish shales’ lie within NP23¹⁰⁹. *Absolute age estimate*: 29.62 Ma³. *Prior setting*: lognormal prior, minimum age 29.62 Ma, mean=1.0, S.D.= 1.498, upper 95% CI: 61.6 Ma³.

xxxix. Node: Stem lineage *Chaetodon*, dating the MRCA of *Chaetodon kleinii* and *Prognathodes marcellae*. *First occurrence*: †*Chaetodon fischeuri* from the Saint-Denis du Sig, Raz-el-Aïn, Les Planteurs, and Eugène, Algeria¹²⁷. *Resolution in phylogenetic analyses*: None. *Character states*: overlapping, sequential articulation between first dorsal fin pterygiophores, supraneurals, and supraoccipital crest; second infraorbital excluded from orbital margin; two sets of lateral processes on each side of first dorsal fin pterygiophore define a clear groove; distal head of second supraneural longer than that of first supraneural^{127,128}. *Stratigraphy*: Messinian¹²⁹⁻¹³¹. *Absolute age estimate*: 7.1 Ma. *Prior setting*: lognormal prior, minimum age 7.1 Ma, mean=0.26, S.D.= 0.2, upper 95% CI: 8.9 Ma⁷.

xl. Node: Stem lineage *Gazza*, dating the MRCA of *Gazza minuta* and *Leiognathus equula*. *First occurrence*: †*Euleiognathus tottori* from the Iwami Formation, Tottori Group, Japan^{132,133}. *Resolution in phylogenetic analyses*: none. *Character states*: long ascending processes of premaxillae; paddle-like expansions of neural and haemal spine of preural centrum 4; single supraneural; serrated anterior margins of fin spines; caniniform teeth¹³⁴. The final character is unique to *Gazza* within leiognathids^{132,135}. The nesting of *Gazza* within the phylogeny of Leiognathidae indicates caniniform teeth are derived within the clade^{134,136,137}. See Gill and Michalski¹³⁸ who are sceptical that †*Euleiognathus* is a leiognathid. *Stratigraphy*: middle Miocene^{132,133}. *Absolute age estimate*: 11.6 Ma¹³⁹. *Prior setting*: lognormal prior, minimum age 11.6 Ma, mean=0.8, S.D.= 1.0, upper 95% CI: 23.1 Ma⁷.

xli. Node: Stem lineage Diodontidae, dating the MRCA of *Diodon liturosus* and *Canthigaster rostrata*, which subtends the MRCA of Diodontidae and Tetraodontidae. *First occurrence*: †*Prodiodon tenuispinus*, †*P. erinaceus*, †*Heptadiodon echinus*, and †*Zignodon fornasieroae* from the Pesciara beds of ‘Calcarei nummulitici’, Bolca, Italy¹⁴⁰. *Resolution in phylogenetic analyses*: parsimony analysis of morphological characters resolves a clade containing

†*Prodiodon tenuispinus*, †*P. erinaceus*, †*Heptadiodon echinus*, †*Zignodon fornasieroae*, *Diodon holocanthus*, and *Chilomycterus schoepfi*¹⁴⁰. *Character states*: premaxillae fused along midline; dentaries fused along midline; jaws massive¹⁴⁰. *Stratigraphy*: upper Ypresian [NP14]⁶⁴. *Absolute age estimate*: 50 Ma⁵⁴. *Prior setting*: lognormal prior, minimum age 50.0 Ma, mean=1.0, S.D.=0.6, upper 95% CI: 57.3 Ma⁷.

xlii. Node: Stem lineage of Balistidae, dating the MRCA of *Balistes capriscus* and *Aluterus monoceros*, which subtends the MRCA of Balistidae and Monacanthidae. *First occurrence*: †*Gornylistes prodigiosus* from the Kuma Horizon, Krasnodar Region, Caucasus¹⁴¹. *Resolution in phylogenetic analyses*: None. *Character states*: ventral shaft of second spine-bearing dorsal pterygiophore absent; supraneural strut present between abdominal neural spine and final spine-bearing dorsal pterygiophore; four anal-fin pterygiophores anterior to the haemal spine of the third caudal vertebra¹⁴⁰. *Stratigraphy*: Bartonian [NP17] Kumian regional stage⁵³. *Absolute age estimate*: 37.2 Ma⁵⁴. *Prior setting*: lognormal prior, minimum age 37.2 Ma, mean=1.0, S.D.=0.42, upper 95% CI: 42.6Ma⁷.

xliii. Node: Stem lineage Antennarioidei, dating the MRCA of *Antennarius striatus* and *Ogcocephalus radiatus*. *First occurrence*: †*Eophryne bartutii* from the Pesciara beds of ‘Calcari nummulitici’, Bolca, Italy¹⁴². *Resolution in phylogenetic analyses*: None. †*Eophryne* was hypothesized to share common ancestry with Antennariidae based on overall morphological similarity¹⁴². The phylogenetic placement used for this calibration is conservatively applied to the more inclusive Antennarioidei. *Character states*: triradiate ectopterygoid; spatulate postmaxillary process of premaxilla¹⁴²⁻¹⁴⁴. *Stratigraphy*: upper Ypresian [NP14]⁶⁴. *Absolute age estimate*: 50 Ma⁵⁴. *Prior setting*: lognormal prior, minimum age 50.0 Ma, mean=1.0, S.D.=0.6, upper 95% CI: 57.3 Ma⁹³.

3. Supplementary results and discussion

a. Phylogenetic analyses

The maximum likelihood analyses of the 702-taxon and 1,084-taxon UCE datasets confidently resolve the phylogenetic relationships of all sampled acanthomorph families. The phylogeny

inferred from the IQ-TREE analysis of the single-partition, concatenated 1,084-taxon dataset is represented in Supplementary Figs. 1–25. The results of the five other phylogenetic analyses are available on Dryad. Bootstrap support values across the entire IQ-TREE phylogeny are high, with most nodes being supported by 100% bootstrap support and only 76 of 1,107 nodes (6.87%) having values $\leq 100\%$. Tree topologies inferred using the different methods described in *Section 1d* are largely consistent according to comparisons conducted in TOPD-FMITS v.4.6²¹ (see Supplementary Table 2). Robinson-Foulds metrics across all comparisons were low (≤ 0.033), as were nodal distances (≤ 1.046). Supplementary Table 2 lists the 19 species that differ in their phylogenetic relationships across the different analyses. Most of these species are found in areas of the tree that have been historically difficult to resolve, such as Anthiadidae (previously Anthiaginae classified in Serranidae), Carangidae and Apogonidae. Tree topologies inferred in IQ-TREE and RAxML using multiple-partition, 700-taxon alignments were identical.

The summary species tree inferred using coalescent methods from individual gene trees (Extended Data Fig. 2) largely corroborates the relationships among the most inclusive lineages of acanthomorphs inferred from the concatenated datasets (Figs. 1,2, Supplementary Figs. 1-25), such as in the resolution of Lampriformes as the sister lineage of a monophyletic Paracanthopterygii and the monophyly of Acanthopterygii. There remain notable topological differences between the concatenated and coalescent approaches. The few nodes in the concatenated dataset phylogenies with moderate bootstrap support are often incongruent with the summary species tree, but discordance also occurs at nodes with 100% BSS. The ASTRAL-III species tree differs from the concatenated-dataset, maximum likelihood phylogeny in the inference of Trachichthyiformes and Beryciformes as a clade that is sister to Percomorpha, the gadiform *Bregmaceros* as the sister lineage of a clade containing *Stylephorus* and all other gadiforms, the placement of *Centrogenys* outside of Labriformes, the position of *Pholidichthys* as the second earliest-diverging blenniform lineage (with Polycentridae sister to Cichlidae), and the non-monophyly of Acropomatiformes (Extended Data Fig. 2). The ASTRAL-III species tree also does not resolve Gerreidae as the sister lineage of all other Acanthuriformes. Further, the phylogenetic placement of major euperuvian clades differ in the summary tree estimated under the multi-species coalescent model.

In contrast to the concatenated-dataset trees, support for the summary species tree is globally low, including for relationships that are classical expectations from pre-phylogenetic

classifications and are resolved in numerous other molecular phylogenetic analyses of acanthomorphs. This pattern is reflective of conflict among gene trees, an expected result given the low phylogenetic informativeness of individual UCE loci¹⁴⁵⁻¹⁴⁷, particularly at deep time scales¹⁴⁸. Bayesian estimation of genome-wide concordance factors through BUCKy allow for the examination of the conflict among gene trees at some focal nodes. For example, BUCKy analyses corroborate the monophyly of a clade containing Beryciformes and Percomorpha (Figs. 1, 3c) despite the resolution of a clade containing Beryciformes and Trachichthyiformes in the ASTRAL-III summary tree. For other relationships such as the sister lineage of Acanthopterygii, the BUCKy concordance factor analyses fail to provide confident gene-tree support for all topologies, even those found in both the coalescent- and concatenated-based analyses (Figs. 1,3b and Extended Data Fig. 2).

Further, for the relationships tested with BUCKy and for the branches that differ between the IQ-TREE (Figs. 1,2 and Supplementary Figs. 1–25) and ASTRAL-III (Extended Data Fig. 2) topologies, IQ-TREE site-concordance factor (sCF) values tend to be similar to or lower than the support for alternate topologies (see relevant file in the Dryad repository). Some important relationships such as the monophyly of Paracanthopterygii, its sister relationship to Lampriformes, the common ancestry of *Polymixia* and Percopsiformes, and the position of *Centrogenys* as sister to Labridae have notably higher gene concordance factor (gCF) estimates than the gene discordance factor (gDF) values despite similarities in site support (sDF) for one or more discordant topologies. The effects of ILS are expected to be greater on the branches of other major relationships where $sCF < 0.33\%$ and $gCF \leq gDF$ or there is a large difference between sDF1 and sDF2²⁶⁰. Examples include the placement of *Acanthistius* as the earliest-diverging perciform lineage (gCF=gDF1=0.11%; sCF=30.61%; sDF1=47.77%; sDF2=21.61%), the sister relationship between Beryciformes and Percomorpha (gCF=4.18%; gDF1=5.2%; sCF=28.63%; sDF1=46.96%; sDF2=24.41%), and the common-ancestry of Scombriformes and Syngnathiformes (gCF=1.42%; gDF1=0.1%; sCF=27.22%; sDF1=49.31%; sDF2=23.46%). Such branches might be indicative of the anomaly zone and require further examination^{260,261}; for these cases, phylogenetic inference using maximum parsimony may be more appropriate than a maximum likelihood or summary species tree approach²⁶¹.

Overall, the strong site support for competing topologies suggests that discordance among gene trees and sites may be partially influenced by ILS, particularly for the branches with

low bootstrap support or those that differ between the ASTRAL-III and IQ-TREE analyses. This result is not unexpected, as incomplete lineage sorting is especially prevalent at deep-time scales in UCE datasets¹⁴⁵ and a number of discrepancies between the presented topologies represent early-diverging relationships. Much of the supposed ILS is likely due to short branches^{260,261} at these deep time scales as the maximum likelihood concordance factors are correlated to branch length with a moderate effect size (see legend of Extended Data Fig. 1). In fact, the average length of the branches with site discordance factor (sDF) estimates higher than the sCF values (as shown in Figs. 1,2) and those with sCF values similar to the sDF estimates (i.e. no greater than 15%) is 0.0026 substitutions per sequence site. In contrast, the average branch length for the entire UCE phylogeny is 0.011 substitutions per site. That said, it would be unwise to disregard the potential effects of other drivers of low gene or site support such as missing data or a lack of strong signal among genes and sites.

b. Classification of Acanthomorpha and a new delimitation of taxonomic orders in Percomorpha

The non-percomorph acanthomorphs are classified into eight taxonomic orders: Lampriformes, Percopsiformes, Polymixiiformes (a single genus, *Polymixia*) Zeiformes, Gadiformes, Stylephoriformes (a single species, *Stylephorus chordatus*), Trachichthyiformes, and Beryciformes (Fig. 1). The new UCE-inferred phylogeny provides an opportunity to reevaluate the classification of Percomorpha to identify inclusive taxonomic groupings that reflect phylogenetic relationships. An initial effort at building classifications based on molecular phylogenies attempted to preserve the ordinal ranks of the clades such as the Pleuronectiformes, Tetraodontiformes, Atheriniformes, and Synbranchiformes¹⁴⁹. This classification proposed a delimitation of 33 taxonomic orders in Percomorpha that each contain an average of only 7.4 families and 492.9 species, and resulted in 10% of all percomorph families unassigned to a taxonomic order¹⁴⁹. In Figs. 1–2 and Supplementary Table 3 we offer an alternative delimitation of 13 clades that we treat as taxonomic orders to accommodate the classification of all 290 percomorph families. In the proposed classification, each taxonomic order comprises an average 2,226.8 species and 18.2 families.

The names of the orders in the proposed percomorph classification are consistent with conventions in ichthyological systematics by establishing a link with one of the constituent

taxonomic families and using the “-iformes” suffix^{150,151}. For example, this delimitation of Blenniiformes includes the Blenniidae and 48 other families (e.g., cichlids, livebearers, and mullets) that were previously identified as a monophyletic group in molecular phylogenetic studies^{3,8,93,152-154}. Previously named Ovalentaria¹⁵⁴, this diverse clade of percomorphs had been divided among seven orders¹⁴⁹, one of which, Mugiliformes, included a single family, Mugilidae (mulletts).

b. Phylogeny of non-percomorph acanthomorphs

i. Monophyly and relationships of Paracanthopterygii

Similar to other phylogenomic studies, this UCE inferred phylogeny resolves a monophyletic Paracanthopterygii that includes *Polymixia* (beardfishes), Percopsiformes, Zeiformes, *Stylephorus chordatus* (Tube-eye), and Gadiformes (Fig. 1, Supplementary Fig. 1)^{3,8,155}. While relationships within Paracanthopterygii differ among phylogenomic studies, the resolution of a clade containing *Polymixia* and Percopsiformes is the best-supported topology in the Bayesian concordance factor analysis, with the 95% credible interval of the two alternative resolutions of *Polymixia* not overlapping with the optimal tree topology (Fig. 3a, Supplementary Fig. 1). Results from the IQ-TREE, maximum likelihood concordance factor analyses also support a sister relationship between *Polymixia* and Percopsiformes (gCF = 15.87%, sCF = 37.78%) as opposed to alternative resolutions (e.g. gDF2 = 6.03, sDF2 = 34.58). There is a relatively low percentage of loci and sites supporting a clade containing *Polymixia* and Percopsiformes, and a chi-squared test comparing the number of genes supporting discordant topologies (gEF_p = 0.27) suggests that incomplete lineage sorting may contribute to discordance along this branch of the acanthomorph phylogeny.

ii. Phylogenetic relationships of Lampriformes

The new UCE phylogeny of Acanthomorpha resolves Lampriformes as the sister lineage of Paracanthopterygii (Fig. 1), which agrees with a previous phylogenetic analysis of UCE loci³. Other studies offer conflicting phylogenetic positions for Lampriformes; a phylogenomic analysis of ~1,000 exons resolve lampriforms as the sister lineage of the Acanthopterygii⁸, while morphological phylogenies place the lampriforms as the sister lineage of all other Acanthomorpha¹⁵⁶. The Bayesian concordance factor analyses result in overlapping 95%

credible intervals for the phylogeny that places lampriforms as sister to Paracanthopterygii and the phylogeny that resolves lampriforms as the sister lineage of all other acanthomorphs (Fig. 3b). The phylogeny that resolves lampriforms and Acanthopterygii as sister lineages scored the lowest Bayesian concordance factors and the 95% credible interval of its concordance factors do not overlap with the credible interval of the phylogeny that resolves Lampriformes as the sister lineage of Paracanthopterygii (Fig. 3b). Results of the maximum likelihood gene- and site-concordance factor analyses are the inference from BUCKy, as support for alternate topologies via discordance factors (e.g. sCF1 = 2.68%, sCF2 = 34.59%) are similar to the percent of genes supporting a sister relationship between Lampriformes and Paracanthopterygii (gCF = 6.08%, sCF = 33.65%).

iii. Phylogenetic relationships of Gadiformes

The new UCE phylogeny of Gadiformes is similar to a recent study that utilized DNA sequences from more than 14,000 portions of protein coding genes¹⁵⁷. Results from the two analyses are congruent in resolving *Bregmaceros* (codlets) as the sister lineage of all other Gadiformes, though this is not the topology most supported by the maximum likelihood concordance factor analyses (gCF = 34.83%, sCF = 40.48%, gDF2 = 37.08%, sDF2 = 43.45%). The two studies differ in three specific relationships. The UCE phylogeny resolves Muraenolepididae (eel cods) and Trachyrincidae (armored grenadiers) as sister lineages, but the exon phylogeny resolves *Melanonus* (pelagic cods) as the sister lineage of Muraenolepididae. The UCE phylogeny places Merlucciidae (merluccid hakes) as the sister lineage of an inclusive clade containing Phycidae (phycid hakes), Lotidae (hakes and burbots), and Gadidae (cods and haddocks), but the exon phylogeny resolves Merlucciidae as the sister lineage of a clade containing *Eulichthys polynemus* (Eucla cod), Muraenolepididae, *Melanonus*, Trachyrincidae, Moridae, *Macruonus* (blue grenadiers), *Lyconus* (Atlantic hakes), Bathygadidae (rattails), *Steindachneria argenta*, and Macrouridae. Lotidae is resolved as monophyletic in the exon phylogeny¹⁵⁷, but this lineage is paraphyletic in the UCE phylogeny with *Lota lota* (Burbot) resolved as the sister lineage of a clade containing *Brosme brosme* (Cusk), *Molva* (lings), and Gadidae (true cods) (Fig. 1, Supplementary Fig. 1).

iv. Phylogenetic relationships of Acanthopterygii and resolution of the sister lineage of the hyper-diverse Percomorpha

Acanthopterygii includes Trachichthyiformes, Beryciformes, and Percomorpha (Fig. 1). The earliest molecular studies identified the sister lineage of percomorphs as either a monophyletic group consisting of Trachichthyiformes and Beryciformes^{7,93} or the beryciform subclade Holocentridae (squirrelfishes)¹⁵². The UCE inferred phylogeny presented in this study and previous phylogenomic analyses resolve Trachichthyiformes as the sister lineage to all other acanthopterygians and Beryciformes, which includes Holocentridae, as the percomorph sister lineage^{3,8,155,158} (Fig. 1, Supplementary Fig. 2). This topology is also the most supported hypothesis in the Bayesian concordance factor analyses (Fig. 3c). The alternative hypotheses, including the phylogeny that places Holocentridae as sister to Percomorpha, produced substantially lower Bayesian concordance factor scores with 95% credible intervals that do not overlap with the scores of the optimal phylogeny (Fig. 3c). The UCE data presented here reject the hypothesis that Holocentridae is the sister lineage of Percomorpha.

c. Phylogenetic relationships of Percomorpha

Percomorphs are classified in an astounding 290 taxonomic families¹⁵⁹, which is more than living birds (252 families) and many more than mammals (167 families), squamates (58 families), amphibians (67 families), and turtles (11 families)¹⁶⁰⁻¹⁶². By the middle of the 20th century the vast majority of percomorph families were delimited and considered monophyletic groups^{150,163}, but relationships among these delimited taxonomic families were woefully unresolved at the start of the 21st century^{164,165}. This lack of phylogenetic resolution among the nearly 300 taxonomic families led to the now famous analogy that Percomorpha was the “bush at the top” of the teleost phylogeny¹⁶⁶. Since the start of the 21st century, however, molecular studies have offered dramatic resolution of percomorph relationships^{3,8,93,152}. The UCE phylogeny inferred in this study resolves the species sampled from 276 taxonomic families into one of twelve taxonomic orders that contain more than one family. All 12 of these inclusive lineages are monophyletic and strongly supported in the UCE phylogeny (Figs. 1,2, Supplementary Figs. 3–25). Relationships are consistent with previous efforts using Sanger sequenced loci and phylogenomic analyses, but no prior analysis included a high fraction (276 of 290) of the percomorph families.

The UCE phylogeny has strong node support along the backbone of Percomorpha including Eupercaria, which is an inclusive clade containing Perciformes, Centrarchiformes, Labriformes, Acropomatiformes, and Acanthuriformes (Fig. 2, Supplementary Figs. 16–25). Previous phylogenetic analyses strongly support monophyly of Eupercaria but provide little resolution and node support for the interrelationships of its constituent lineages^{8,93,152}. The only node in the UCE percomorph phylogeny shared among the delimited 13 taxonomic orders that is not supported with a bootstrap score of 100% is the resolution of Acropomatiformes and Acanthuriformes as a clade, which is supported with a bootstrap score of 99% (Supplementary Fig. 22).

i. The deepest node in the phylogeny of percomorphs: the phylogenetic relationships of Ophidiiformes

Ophidiiformes (cusk eels) is resolved as the sister lineage to all other percomorphs (Fig. 1). Relationships within this species-rich lineage of mostly marine fishes are not well known and the delimitation of taxonomic families is in flux¹⁶⁷. The UCE phylogeny resolves two clades in Ophidiiformes that correspond to the suborders Bythitoidei and Ophidioidei (Fig. 1, Supplementary Fig. 3). Within Bythitoidei, the families Dinematchthyidae (pygmy brotulas) and Bythitidae (livebearing brotulas) are both monophyletic (Supplementary Fig. 3). As discovered in previous studies¹⁶⁷⁻¹⁶⁹, the formerly recognized taxonomic families Parabrotulidae and Aphyonidae are phylogenetically nested in Bythitidae (Supplementary Fig. 3). Historically, Ophidioidei contained Ophidiidae and Carapidae, but the UCE phylogeny (Fig. 1, Supplementary Fig. 3) as well as previous studies using whole mtDNA genome sequences and Sanger sequenced nuclear genes resolve Carapidae as phylogenetically nested within Ophidiidae^{89,93,152,170}, prompting the synonymization of the family Carapidae with Ophidiidae¹⁴⁹.

ii. Phylogenetic relationships of Batrachoididae

There is limited taxon sampling of Batrachoididae in the UCE phylogeny, but the subfamily Batrachoidinae (sampled with *Batrachoides pacifici* and *Opsanus tau*) is paraphyletic (Supplementary Fig. 3). Porichthyinae is paraphyletic in a phylogeny inferred from Sanger sequenced mitochondrial and nuclear genes⁸⁹.

iii. Phylogeny of Gobiiformes

One of the most surprising results from molecular analyses of percomorph phylogeny was the discovery that gobies, cardinalfishes (Apogonidae), and nurseryfishes (Kurtidae) resolve in a strongly supported monophyletic group^{7,171,172}. Subsequent molecular studies resolved two competing hypotheses of relationships among the major lineages of Gobiiformes: 1) *Kurtus* and Apogonidae resolved as a clade, or 2) Apogonidae as the sister lineage of a clade containing *Trichonotus* (sand divers) and Gobiioidei^{3,93,152,172-176}. The UCE phylogeny in this study resolves two major lineages in Gobiiformes: the Apogonoidei that contains *Kurtus* and Apogonidae, and a clade containing *Trichonotus* and Gobiioidei (Fig. 1, Supplementary Figs. 3,4). The relationships of the eight taxonomic families classified in Gobiioidei are identical to phylogenies inferred using Sanger sequenced mtDNA and nuclear genes^{175,176} (Fig. 1, Supplementary Fig. 4).

iv. Phylogenetic relationships of Scombriformes and Syngnathiformes

Scombriformes (e.g., tunas, cutlassfishes and butterfishes) and Syngnathiformes (e.g., seahorses, flying gurnards and dragonets) are resolved as sister lineages in the UCE phylogeny (Fig. 1), a result that is consistent with other molecular phylogenetic analyses^{3,8,93}. This particular result has the surprising implication that relative to all other percomorph teleosts, tunas and seahorses are closely related.

Tunas, barracudas, cutlassfishes and swordfishes were historically classified in Scombroidei. Early phylogenetic analyses of Sanger sequenced mtDNA and nuclear genes resolved species classified in the traditional delimitation of Scombroidei into two distantly related percomorph lineages¹⁷⁷. Xiphiidae (swordfishes), Istiophoridae (billfishes) and Sphyraenidae (barracudas) were resolved in the clade Carangiformes along with flatfishes, jacks and archerfishes (Fig. 1)¹. The remaining lineages of the historical Scombroidei— Scombridae (tunas), Gempylinae (snake mackerels), Trichiurinae (cutlassfishes) and *Pomatomus saltatrix* (Bluefish)—are resolved in the clade Scombriformes that also includes the stromatioids, e.g., Stromateidae (butterfishes) and Chiasmodontidae (swallowers)⁵. Other lineages in Scombriformes include the enigmatic *Icosteus aenigmaticus* (Ragfish) and *Amarsipus carlsbergi* (Bagless Glassfish), both of which are deep-branching, monotypic lineages that long evaded phylogenetic resolution among percomorphs (Fig. 1, Supplementary Fig. 5). The UCE phylogeny resolves *Lepidocybium flavobrunneum* (Escolar) as the sister lineage of a clade

containing Gempylidae and Trichiuridae (Fig. 1, Supplementary Fig. 6). *Lepidocybium flavobrunneum* is traditionally classified in Gempylidae, which is paraphyletic in the UCE phylogeny as the remaining gempylids are more closely related to species of Trichiuridae (Fig. 1, Supplementary Fig. 6). This relationship has previously been resolved in a phylogenetic analysis using morphological data⁹².

Syngnathiformes as consisting of seahorses and pipefishes, flying gurnards, goatfishes, and dragonets was first resolved as a clade in phylogenetic analyses of Sanger sequenced mtDNA and nuclear genes^{152,178}. Prior to the application of molecular phylogenetics, Callionymidae (dragonets) and Draconettidae (draconettids) were classified as closely related to Gobiesocidae (clingfishes)¹⁷⁹⁻¹⁸². As reflected in molecular phylogenies, Pietsch⁶⁸ proposed that Dactylopteridae (helmet gurnards) were closely related to other syngnathiform lineages, but they were classified by others with the sculpins, rockfishes and scorpionfishes in Scorpaeniformes. Mullidae (goatfishes) were long classified in the wastebasket taxon Perciformes^{150,180,183} but thought to be closely related to Haemulidae (grunts) and Sparidae (porgies)¹⁸⁴. The UCE phylogeny resolves two major lineages of Syngnathiformes: 1) a clade we delimit as Mulloidei that contains Pegasidae (seamoths), Dactylopteridae, Mullidae, Callionymidae, and Draconettidae and 2) a lineage we delimit as Syngnathoidei, consisting of Syngnathidae (pipefishes and seahorses), Solenostomidae (ghost pipefishes), Aulostomidae (trumpetfishes), Fistularidae (cornetfishes), Centriscidae (shrimpfishes) and Macroramphosidae (snipefishes) (Fig. 1, Supplementary Figs. 7–9).

v. Relationships among Blenniiformes, Synbranchiformes and Carangiformes

The UCE phylogeny resolves a strongly supported monophyletic group where Blenniiformes (e.g., blennies, cichlids, livebearers, and mullets) is the sister lineage of a clade containing Synbranchiformes (e.g., swamp eels, gouramies, snakeheads, and leaffishes) and Carangiformes (e.g., flatfishes, jacks and pompanos, billfishes, and barracudas). The discovery of this clade is one of the many dramatic results from molecular phylogenetics of percomorphs⁹³, as this large and inclusive group contains more than 7,300 species that are classified into 92 taxonomic families.

vi. Blenniiformes: Phylogenetic relationships of Atherinoidei (Cyprinodontoidea, Belonoidea and Atherinoidea)

The monophyly of Blenniiformes—originally named Ovalentaria—resulted from a phylogenetic analysis of Sanger sequenced nuclear genes¹⁵⁴. In the UCE phylogeny, Blenniiformes is monophyletic and contains two major clades: Atherinoidei (formerly Atherinomorpha) and all other lineages of Blenniiformes. Atherinoidei contains three major lineages: 1) Belonoidea (formerly Beloniformes, which includes needlefishes, medakas, halfbeaks, and flying fishes), 2) Cyprinodontoidea (formerly Cyprinodontiformes, which includes killifishes, rivulines, pupfishes, and livebearers), and 3) Atherinoidea (formerly Atheriniformes, which includes silversides and rainbowfishes). Phylogenomic analysis of our UCE dataset results in a well-resolved phylogeny of Atherinoidei, where every node along the backbone of the atherinoid tree is supported with a 100% bootstrap score (Fig. 1, Supplementary Fig. 10). Morphological phylogenies resolve Atherinoidea as the sister lineage of a clade containing Belonoidea and Cyprinodontoidea^{120,185}, but the UCE phylogeny resolves Atherinoidea and Belonoidea as sister lineages (Fig. 1, Supplementary Fig. 10).

Over the past 15 years, the number of taxonomic families recognized in Cyprinodontoidea (killifishes, rivulines, pupfishes, and livebearers) increased from 10 to 16^{159,164}. The recognition of these six additional families resulted from phylogenetic analyses of Sanger sequenced mtDNA and nuclear genes that overturned the results of morphological studies¹⁸⁶⁻¹⁸⁸ and demonstrated the non-monophyly of Cyprinodontidae (pupfishes) and Poeciliidae (livebearers). The UCE phylogeny (Fig. 1, Supplementary Fig. 10) is consistent with morphological phylogenetic analyses in the resolution of Rivulidae (New World rivulines), Aplocheilidae (Asian rivulines), and Nothobranchiidae (African rivulines) as a monophyletic group, as well as a clade containing Poeciliidae, Anablepidae (four-eyed fishes), *Valencia* (toothcarps), Procatopodidae (African lampeyes), Fundulidae (topminnows), Cyprinodontidae, *Profundulus* (Middle American killifishes), Goodeidae (goodeids), and *Cubanichthys* (Caribbean killifishes)^{189,190}. Morphological and molecular phylogenetic studies show congruence on specific relationships within Cyprinodontoidea. For example, the morphological analysis by Costa¹⁹⁰ identified *Profundulus* and Goodeidae as a clade. This result is supported in the UCE phylogeny as well as studies from Sanger sequenced mtDNA and nuclear genes¹⁸⁶⁻¹⁸⁸. Among the notable differences between molecular and morphological phylogenies of cyprinodontoids is

the resolution of Cyprinodontidae and Fundulidae as sister lineages (Fig. 1, Supplementary Fig. 10).

Belonoidea is monophyletic in the UCE phylogeny, but despite limited taxon sampling the families Zenarchopteridae and Hemiramphidae are found to be paraphyletic (Fig. 1, Supplementary Fig. 10). Five families of Belonoidea are recognized in Eschmeyer's Catalog of Fishes¹⁵⁹. Phylogenies resulting from analyses of morphological characters and Sanger sequenced mtDNA nest Scomberesocidae (sauries) well within Belonidae (needlefishes) and resolve Hemiramphidae (halfbeaks) as paraphyletic relative to Exocoetidae (flyingfishes)^{191,192}. In the UCE phylogeny, the hemiramphid *Oxyporhamphus micropterus* is more closely related to the sampled species of Exocoetidae than the other two sampled hemiramphids (Fig. 1, Supplementary Fig. 10), as previously inferred using morphological data¹⁹³. The new phylogeny also resolves *Zenarchopterus dispar* as more closely related to the sampled belonid species *Xenentodon cancila* than to the other two sampled zenarchopterid species (Fig. 1, Supplementary Fig. 10).

There are 11 taxonomic families of Atherinoidea recognized in Eschmeyer's Catalog of Fishes¹⁵⁹, but Notocheiridae is well nested in Atherinopsidae in phylogenetic analyses of Sanger sequenced mtDNA and nuclear genes^{194,195}. Of the ten other families, eight are sampled in the UCE phylogeny. Missing from the analysis is the monotypic Dentatherinidae (Mercer's tusked silverside) and Telmatherinidae (Celebes rainbowfishes). The UCE phylogeny is consistent with current classifications and previous molecular and morphological phylogenetic analyses in resolving Atherinopsidae (New World silversides) as the sister lineage of all other atherinoids^{93,152,194,196} (Fig. 1, Supplementary Fig. 10). Another area of agreement in the UCE phylogeny and previous molecular analyses is the resolution of a clade containing the monogeneric Atherionidae (pricklenose silversides) and Phallostethidae (priapiumfishes)¹⁹⁵ (Fig. 1, Supplementary Fig. 10).

There are differences in the recognition of taxonomic families of Atherinoidea in Eschmeyer's Catalog of Fishes¹⁵⁹ and Nelson et al.¹⁵¹ that involve lineages associated with Melanotaeniidae (rainbowfishes). Following Dyer and Chernoff¹⁹⁶, Nelson et al.¹⁵¹ treat Bedotiidae (Madagascar rainbowfishes), Pseudomugilidae (blue eyes), and Telmatherinidae as subfamilies of Melanotaeniidae. This delimitation of Melanotaeniidae is not supported in the UCE phylogeny as Bedotiidae is resolved as the sister lineage of Atherinidae (Old World

silversides) (Fig. 1, Supplementary Fig. 10). In previous analyses of Sanger sequenced mtDNA and nuclear genes, Melanotaeniidae is paraphyletic because the species *Cairnsichthys rhombosomoides* is resolved as the sister lineage of a clade containing all sampled species of Telmatherinidae and Pseudomugilidae^{194,195}; however, in the UCE phylogeny Melanotaeniidae—sampled with *Cairnsichthys* and *Iriatherina wernerii*—is monophyletic with strong node support (Fig. 1, Supplementary Fig. 10). The non-monophyly of Melanotaeniidae in previous phylogenetic analyses is likely driven by limited phylogenetic informativeness of Sanger sequenced genes to resolve relationships among Atherinoidea, as evidenced by the low bootstrap and Bayesian posterior node support values associated with these phylogenies^{194,195}.

vii. Blenniiformes: Phylogenetic relationships of Cichlidae, Pholidichthys and Polycentridae

Within Blenniiformes, the UCE phylogeny resolves a clade containing Cichlidae, *Pholidichthys* (engineer gobies) and Polycentridae (leaffishes) (Fig. 1, Supplementary Fig. 11). Before the advent of molecular phylogenetics, the morphology of the pharyngeal jaw apparatus was cited as evidence to group Cichlidae with Labridae (wrasses and parrotfishes), Embiotocidae (surfperches), and Pomacentridae (damsel-fishes) in a group named Labroidei¹⁹⁷⁻²⁰⁰. Phylogenetic analyses of ten Sanger sequenced nuclear genes strongly resolved *Pholidichthys* (engineer gobies) and Cichlidae as sister lineages, but these analyses did not confidently identify a sister lineage of this clade within the Blenniiformes^{93,154}. As recently delimited²⁰¹, Polycentridae contains five species classified among four genera distributed in freshwater habitats in Africa and South America: *Afronandus sheljuzhkoii* (Africa), *Polycentropsis abbreviata* (Africa), *Polycentrus* (two species in South America), and *Monocirrhus polyacanthus* (South America). The resolution of the freshwater Polycentridae as the sister lineage of the clade containing *Pholidichthys*-Cichlidae provides insight into the origin of freshwater blenniiform lineages and the biogeographic relationships of freshwater fishes in South America and Africa^{202,203}.

viii. Blenniiformes: Relationships of Mugilidae, Ambassidae, Pseudochromidae, Congrogadidae and Pomacentridae

The phylogenetic relationships of Mugilidae (mulletts) have long vexed phylogenetic studies of acanthomorphs, leading Stiassny²⁰⁴ to declare in a morphological phylogenetic study that “without mullets our lives would be a lot simpler.” Morphological analysis of branchial

musculature supported a hypothesis that Mugilidae and Atherinoidei (formerly Atherinomorpha) are sister lineages²⁰⁵, but analysis of pelvic girdle morphology supported an affinity with other percomorph lineages²⁰⁴. The heterogeneity of relationships inferred from these two different anatomical systems appears explained in the results of molecular phylogenetic analyses with Mugilidae, Atherinoidei, or other “higher” percomorph lineages sensu Johnson and Patterson¹⁵⁶ resolved in Blenniiformes. In Sanger sequencing efforts, the sister lineage of Mugilidae within Blenniiformes varies between Plesiopidae (longfins) and Embiotocidae (surfperches), always with weak node support^{93,153,154}. However, analysis of the UCE dataset and phylogenomic inferences based on exon data⁸ both resolve Mugilidae and Ambassidae as sister lineages with strong node support (Fig. 1, Supplementary Fig. 11).

In phylogenetic studies of Sanger sequenced mtDNA and nuclear genes, Pseudochromidae (dottybacks) is resolved as paraphyletic relative to Plesiopidae (roundheads) and Pomacentridae (damsel-fishes)^{93,152}. In the UCE phylogeny, Pseudochromidae is paraphyletic because Congrogadidae (eelblennies) is resolved as the sister lineage of a clade containing the remaining species of Pseudochromidae, Plesiopidae, Pomacentridae, Grammatidae (basslets), Opistognathidae (jawfishes), Gobiesocidae (clingfishes), and Blennioidei (blennies) (Fig. 1, Supplementary Fig. 11).

ix. Blenniiformes: Phylogenetic relationships of Grammatidae, Opistognathidae, Gobiesocidae and Blennioidei

The UCE phylogeny is congruent with trees inferred using exon data and Sanger sequenced mtDNA and nuclear genes in resolving a clade containing Grammatidae, Opistognathidae, Gobiesocidae, and Blennioidei^{8,93,152}, but differs in resolving Embiotocidae (surfperches) as the sister lineage of this clade (Fig. 1, Supplementary Fig. 11). Grammatidae and Opistognathidae are successive outgroups to a clade containing Gobiesocidae and Blennioidei (Fig. 1, Supplementary Fig. 11). In the UCE phylogeny, the relationships among the families of Blennioidei—Tripterygiidae (triplefin blennies), Dactyloscopidae (sand stargazers), Blenniidae (combtooth blennies), Clinidae (kelp blennies), Labrisomidae (labrisomid blennies), and Chaenopsidae (tube blennies)—are nearly identical to those inferred from Sanger sequenced mtDNA and nuclear genes^{93,152} (Fig. 1, Supplementary Fig. 11). However, a study with the

largest sampling of blennioid species indicates that Labrisomidae and Chaenopsidae are both paraphyletic²⁰⁶.

x. Phylogenetic relationships of Synbranchiformes

Previous analyses of Sanger sequenced genes and phylogenomic datasets consistently resolve Synbranchioidei (swamp eels, earthworm eels, armored sticklebacks, and freshwater spiny eels) and Anabantoidei (gouramies, snakeheads, and Asian leaffishes) as a clade^{8,93,152-154}.

One of the many surprises to emerge from the molecular phylogenies of percomorphs was the resolution of *Indostomus* (armored sticklebacks) as nested within Synbranchioidei^{93,153,170,207,208}. Traditionally, *Indostomus* was classified with seahorses, shrimpfish, and sticklebacks in the polyphyletic Gasterosteiformes based on the presence of dermal bony plates along the side of the body, a reduced cranial skeleton, and a small mouth size¹⁶⁴. Analysis of developmental ontogeny of several morphological traits led to the conclusion that *Indostomus* is closely related to sticklebacks (Gasterosteidae)²⁰⁹. However, *Indostomus* and sticklebacks are distantly related in all molecular phylogenies and Gasterosteidae is classified here in Perciformes. Aside from the resolution of *Indostomus* as a synbranchoid, specifically as the sister lineage of Synbranchidae (swamp eels), the UCE phylogeny of Synbranchioidei is identical to relationships inferred from morphology where Synbranchidae is resolved as the sister lineage of a clade containing Chaudhuriidae (earthworm eels) and Mastacembelidae (freshwater spiny eels)²¹⁰ (Fig. 1, Supplementary Fig. 12).

Anabantoidei—delimited here as including Nandidae (Asian leaffishes), Badidae (chameleonfishes), Pristolepididae (Malayan leaffishes), Channidae (snakeheads), Helostomatidae (Kissing Gourami), Anabantidae (climbing gouramies), and Osphronemidae (gouramies and fighting fishes)—is monophyletic in the UCE phylogeny and characterized by the unique possession of teeth on the parasphenoid^{201,211:9-12}. The UCE phylogeny resolves a clade containing Pristolepididae, Nandidae, and Badidae (Fig. 1, Supplementary Figs. 12,13), which is supported with a unique morphology of the ventral gill arch musculature where the *rectus ventralis IV* has an additional insertion on the ceratobranchial 5^{201,212}. The clade containing Badidae and Nandidae is supported with two morphological traits: 1) a distally divided haemal spine on the second preural centrum and 2) the restriction of the attachment cells in eggs to the ventral side of the yolk sac^{201: Figs. 2d-f, 4}. Previous classifications grouped

Pristolepididae and Badidae in Nandidae¹⁶⁴. Given that the current delimitation of Nandidae and Pristolepididae each contain a single genus and Badidae includes two genera, future classifications can reduce monogeneric families and limit redundant taxonomic group names by classifying all these lineages in Nandidae.

The UCE phylogeny resolves Channidae, Helostomatidae, Anabantidae, and Osphronemidae as a strongly supported monophyletic group (Fig. 1, Supplementary Figs. 12,13). This phylogeny differs from those inferred using Sanger sequenced nuclear genes in resolving Helostomatidae as the sister lineage of a clade containing Anabantidae and Osphronemidae versus Helostomatidae as the sister lineage of Anabantidae or Osphronemidae^{93,201}.

xi. Phylogenetic relationships of Carangiformes

The UCE phylogeny is broadly congruent with other studies using UCEs¹, but differs in the relationships of *Lates*, *Centropomus* (snooks), and *Sphyraena* (barracudas) (Fig. 1, Supplementary Fig. 14). Analyses of Sanger sequenced nuclear genes consistently supported the monophyly of Carangiformes^{93,152,213,214}, but did not strongly support the relationships among the major carangiform clades. The UCE phylogeny includes a clade containing Centropomidae (sampled with *Lates* and *Centropomus*), *Lactarius lactarius* (False Trevally), and *Sphyraena*. Previous analyses using UCEs also resolved Centropomidae as monophyletic¹, but placed *Sphyraena* as the sister lineage of all other Carangiformes. A phylogenetic analysis of Carangiformes based on a dataset that combines a smaller number of UCE loci with discretely coded morphological characters resolves Centropomidae as paraphyletic with *Lates* and *Psammoperca*, forming a clade that is sister to a lineage containing *Centropomus*, *Lactarius* and *Sphyraena*²¹⁵.

The UCE phylogeny resolves three major lineages of Carangiformes: 1) an unnamed clade (discussed above) containing Centropomidae, *Lactarius*, and *Sphyraena*, 2) an unnamed clade containing Polynemidae (threadfins) and Pleuronectoidei (flatfishes), and 3) a clade delimited here as Carangoidei that contains *Leptobrama* (beachsalmons), *Toxotes* (archerfishes), *Nematistius pectoralis* (roosterfish), *Mene maculata* (moonfish), *Xiphias gladius* (swordfish), Istiophoridae (billfishes), and Carangoidea (Fig. 1, Supplementary Figs. 14,15).

As resolved in several analyses using Sanger sequenced loci and UCE-based phylogenomic analyses^{1,89,93,152,216}, the traditional delimitation of Carangidae (jacks and pompanos) is paraphyletic. Carangidae, limited to the subfamilies Naucratinae and Caranginae, is the sister lineage of a clade containing the former carangid subfamilies Scomberoidinae and Trachinotinae, Echeneidae (remoras), *Rachycentron canadum* (cobia), and *Coryphaena* (dolphinfishes) (Fig. 1, Supplementary Fig. 15).

xii. Eupercaria: relationships among Perciformes, Centrarchiformes, Labriformes, Acropomatiformes and Acanthuriformes

Phylogenetic analyses of Sanger sequenced loci led to the resolution of Eupercaria, an inclusive clade that contains more than 37% of species and 53% of all taxonomic families in Percomorpha¹⁴⁹. While earlier studies resolved a clade containing Perciformes, Centrarchiformes, Labriformes, Acropomatiformes, and Acanthuriformes, phylogenies inferred from Sanger sequenced genes provided little resolution for the relationships among the major lineages of Eupercaria^{93,152}. Analysis of the UCE dataset results in a phylogeny where Eupercaria is resolved as a clade with strong support for the relationships among the major lineages; Perciformes, Centrarchiformes, and Labriformes are found to be successive outgroups to a clade containing Acropomatiformes and Acanthuriformes. All of the nodes along the backbone of the eupercarian phylogeny are supported with bootstrap values of 100% except the clade containing Acropomatiformes and Acanthuriformes (BSS = 99%) (Fig. 2, Supplementary Fig. 22). The phylogenomic analyses of the UCE loci resolve this substantial issue of the teleost phylogeny, which was once identified as the new bush on the top of the percomorph phylogeny¹⁵².

xiii. Phylogenetic relationships of Perciformes

Prior to the application of molecular data to investigate the phylogenetic relationships of teleosts, the vast majority of percomorphs were classified in the catchall taxon Perciformes. In addition to perciforms, percomorphs included morphologically unique and disparate lineages such as Pleuronectiformes (flatfishes), Tetraodontiformes (pufferfishes), and Gasterosteiformes (sticklebacks and seahorses). Any lineage of percomorph that was not as morphologically distinctive as a flatfish or seahorse was classified in Perciformes. At the end of the 20th century Perciformes contained more than 10,000 species and 160 taxonomic families¹⁶⁴. Phylogenetic

analyses of molecular datasets revealed that the perciform wastebasket contained lineages that spanned much of the backbone of the Percomorpha phylogeny. The UCE phylogeny offers a confirmation for the disassembly of Perciformes that involves the migration of more than 100 taxonomic families into nearly all other major lineages of Percomorpha.

An entirely different concept and delimitation of Perciformes emerged from molecular phylogenetic studies^{93,152,153,165,171,217-221}. No longer a taxonomic wastebasket, Perciformes (as delimited here) contains more than 3,200 species that are classified among at least 53 taxonomic families and comprises a diverse array of lineages that not only were previously classified as perciforms, but also as scorpaeniforms and gasterosteiforms^{6,151}. In addition to the namesake Percidae (perches, walleyes, and darters), the newer concept of Perciformes resulting from molecular phylogenetic analyses includes seabasses, scorpionfishes, rockfishes, sculpins, searobins, weaverfishes, notothenioids, eelpouts, sticklebacks, flatheads, and many others (Supplementary Table 3).

Molecular analyses consistently resolve the traditional delimitation of Serranidae (sea basses), which contains more than 60 genera and 450 species, as non-monophyletic in Perciformes^{93,165,221}. In the UCE phylogeny, taxa comprising the traditional Serranidae resolve in four or five different lineages (Supplementary Fig. 16). Epinephelidae (groupers) and Anthiadidae (basslets and anthians) are resolved as successive sister lineages or as a monophyletic group that is the sister lineage of all other Perciformes. The less inclusive delimitation of Serranidae is strongly resolved as the sister lineage of Bembropidae (duckbills). *Acanthistius* is resolved as either the sister lineage of Anthiadidae, where it is traditionally classified, or as the sister lineage of all other perciforms except Epinephelidae and Anthiadidae. The enigmatic *Niphon spinosus*, which has long avoided a confident phylogenetic or taxonomic placement^{222,223}, strongly resolves as the sister lineage of Percidae (Fig. 2, Supplementary Fig. 16).

In addition to the non-monophyly of the traditional Serranidae, the molecular phylogeny of Perciformes provides several strongly supported relationships that were not anticipated from inferences using morphological characters^{156,183,224}. The UCE phylogeny is congruent with earlier analyses using Sanger sequenced loci but provides greater resolution and node support than obtained in earlier efforts. The commercially and scientifically important freshwater lineage Percidae is resolved in a clade that contains the marine *Niphon spinosus* and Trachinidae

(weaverfishes), a lineage we refer to as Percoidei (Fig. 2, Supplementary Fig. 16, Supplementary Table 3). Notothenioidei includes the well-known Antarctic adaptive radiation as well as *Percophis brasiliensis* (Brazilian Flathead), which is distributed in the Atlantic Ocean from the coast of southern Brazil to central Argentina²²⁵. Notothenioidei is strongly resolved as the sister lineage of a new delimitation of Scorpaenoidei that includes almost all the lineages traditionally classified in Scorpaeniformes such as Platycephalidae (flatheads), Scorpaenidae (scorpionfishes and rockfishes), Triglidae (searobins), Bembridae (deepwater flatheads), Platycephalidae (flatheads), Hoplichthyidae (ghost flatheads), Hexagrammidae (greenlings), Trichodontidae (sandfishes), Cyclopteridae (lumpfishes), Liparidae (snailfishes), and Cottidae (sculpins). In addition to these classic scorpaeniform lineages the new delimitation of Scorpaenoidei includes Zoarcoidea (eelpouts, ronquils, and wolffishes) and Gasterosteioidea (sand eel, tubesnouts, and sticklebacks) (Fig. 2, Supplementary Figs. 17, 18).

The UCE phylogeny of Scorpaenoidei is quite different from trees inferred using a dataset of morphological characters and Sanger sequenced mtDNA and nuclear genes²²⁶. For example, Smith et al.²²⁶ resolved Platycephalidae as the sister lineage of Triglidae, but the UCE phylogeny places Platycephalidae as the sister lineage of all other scorpaenoids (Fig. 2, Supplementary Fig. 17). In the UCE tree there are three major clades of Scorpaenoidei that contain multiple taxonomic families, but several families resolve along the backbone of the scorpaenoid phylogeny. Scorpaenoidea is here delimited as a strongly supported clade that includes *Normanichthys crockeri* (Mote Sculpin), Neosebastidae (gurnard scorpionfishes), Congiopodidae (horsefishes), Synanceiidae (stonefishes), and Scorpaenidae (Fig. 2, Supplementary Fig. 17). Bembridae, Triglidae, and Anoplopomatidae (sablefishes) resolve as successive sister lineages to a large clade containing all the lineages classified in Cottoidea (sculpins), Gasterosteioidea, and Zoarcoidea (Fig. 2, Supplementary Figs. 18, 19, Supplementary Table 3).

Gasterosteioidea and Zoarcoidea resolve as sister lineages with strong node support, which is a result supported in earlier phylogenetic analyses of Sanger sequenced mtDNA and nuclear genes^{93,152}. Within Zoarcoidea the Bathymasteridae (ronquils) are resolved as the sister lineage of all other zoarcoids. In an earlier study using Sanger sequenced loci, Bathymasteridae was resolved as paraphyletic⁹³, but the UCE phylogenetic analyses sample all three bathymasterid genera and strongly support the lineage as a monophyletic group (Supplementary

Fig. 18). *Scytalina cerdale* (Graveldiver) is nested well within Stichaeidae (Supplementary Fig. 18) while *Gymnoclinus cristulatus* (Trident Prickleback) is distantly related to other stichaeids (Supplementary Fig. 19), resolving as the sister lineage of Neozoarcidae. Previous phylogenetic analyses of morphology and Sanger sequenced mtDNA and nuclear genes resolve Stichaeidae as paraphyletic²²⁷⁻²²⁹. The zoarcoid lineages *Cryptacanthodes* (wrymouths), Lumpenidae (pricklebacks), *Zaprora silenus* (Prowfish), Opisthocentridae (ocellated blennies), *Ptilichthys goodei* (Quillfish), Pholidae (gunnels), *Gymnoclinus*, Neozoarcidae, Anarhichadidae (wolffishes), and Zoarcidae (eelpouts) resolve as a strongly supported clade that is the sister lineage of the paraphyletic Stichaeidae (Fig. 2, Supplementary Figs. 18,19).

xiii. Phylogenetic relationships of Centrarchiformes

Phylogenetic analyses of Sanger sequenced mtDNA and nuclear genes led to the discovery of Centrarchiformes, a clade of approximately 300 species classified in at least 16 taxonomic families^{93,152,214,230,231}. Consistent with these earlier phylogenetic studies^{93,152,230,231}, the UCE phylogeny resolves *Percalates* as the sister lineage of all other Centrarchiformes (Fig. 2, Supplementary Fig. 20). Terapontoidei includes Girellidae (nibblers), Scorpididae (halfmoons), *Dichistius*, Microcanthidae, *Oplegnathus* (knifejaws), Kyphosidae (sea chubs), *Kuhlia* (flagtails), and Terapontidae (grunters) (Supplementary Fig. 20). Centrarchoidei is delimited here as a clade that includes *Enoplosus armatus* (Oldwife) and Percichthyidae (temperate perches), Centrarchoidea which includes Centrarchidae (sunfishes, blackbasses, and pygmy sunfishes) and Siniperceidae (Chinese perches), and Cirrhitoida which includes Cirrhitidae (hawkfishes), Latridae (trumpeters), *Chironemus* (kelpfishes), *Cheilodactylus*, and *Aplodactylus* (marblefishes) (Fig. 2, Supplementary Fig. 20, Supplementary Table 3).

The classification of Centrarchiformes is dynamic and unsettled, reflected in part by a high proportion of families that contain a single genus. Molecular phylogenies consistently resolve two sets of traditionally delimited centrarchiform families as non-monophyletic. First, the two species of *Percalates* were traditionally classified as Percichthyidae²²⁴, but resolve as the sister lineage of all other centrarchiforms^{93,149,152,214,230}. There is no described taxonomic family to accommodate the classification of *Percalates*. Second, the classification of families within Cirrhitoida was dramatically realigned as a result of molecular phylogenetic analyses. Traditionally, Cheilodactylidae (morwongs) contained three to five genera and approximately 20

species^{180,232}. Previous phylogenetic analyses of mtDNA genes, morphological characters, and UCE data resolved Cheilodactylidae as polyphyletic, with all but two of the species traditionally classified as cheilodactylids nested within a paraphyletic Latridae²³³⁻²³⁵. The findings of these phylogenetic analyses resulted in a transfer of these species to Latridae from Cheilodactylidae. The new UCE phylogeny is consistent with these previous results, but differs from the phylogeny presented in Ludt et al.²³⁵ in resolving *Aplodactylus* rather than *Chironemus* as the sister lineage of *Cheilodactylus* (Fig. 2, Supplementary Fig. 20).

xiv. Phylogenetic relationships of Labriformes

The UCE phylogeny strongly resolves a clade we delimit as Labriformes which contains two major lineages: Uranoscoipoidei and Labroidei (Supplementary Fig. 21). As resolved in previous phylogenies inferred from Sanger sequenced nuclear genes¹⁷⁶, Uranoscoipoidei contains Uranoscopidae (stargazers), Ammodytidae (sandlances), and Pinguipedidae (sandperches) as successive sister lineages to a clade containing the enigmatic *Cheimarrichthys fosteri* (Torrentfish) and Leptoscopidae (southern sandfishes) (Fig. 2, Supplementary Fig. 21). Morphological studies place *Cheimarrichthys* as closely related to Pinguipedidae or as the sister lineage of all “trachinoids,” which include all the lineages delimited here as Uranoscoipoidei²³⁶⁻²³⁸. The hypothesis that *Cheimarrichthys* and Pinguipedidae share common ancestry was rejected through the discovery that *Cheimarrichthys* shares more derived morphological character states with Leptoscopidae than any other “trachinoid” or uranoscopoid lineage²³⁹. Reflective of their shared common ancestry, *Cheimarrichthys* and Leptoscopidae have a similar geographic distribution; *Cheimarrichthys* is an anadromous species widely distributed among the rivers of New Zealand and leptoscopids are distributed along the Pacific and Indian coasts of Australia and New Zealand^{240,241}.

Labroidei includes the sister lineages *Centrogenys vaigiensis* (False Scorpionfish) and Labridae (wrasses and parrotfishes) (Fig. 2, Supplementary Fig. 21). As discussed above regarding Blennioformes, the species rich marine Labridae and the freshwater Cichlidae were hypothesized as closely related based on the morphology of the modified “labroid” pharyngeal jaw apparatus¹⁹⁷⁻¹⁹⁹, which is now known to have originated multiple times in Percomorpha¹⁵⁴. Previous molecular phylogenetic analyses using Sanger sequenced nuclear genes demonstrated that labrids and cichlids are not closely related despite both having modified “labroid”

pharyngeal jaws, but these early molecular studies resulted in an ambiguous and poorly supported resolution of the species rich Labridae^{93,154}. The resolution of Labridae and *Centrogenys vaigiensis* as sister lineages in the UCE phylogeny is interesting as both lineages have all three components of the modified labroid pharyngeal jaw apparatus¹⁵⁴.

xv. Phylogenetic relationships of Acropomatiformes

The discovery of Acropomatiformes resulted entirely from phylogenetic analyses of Sanger sequenced mtDNA and nuclear and genes^{93,176,214,225} and was never intimated through the study of morphology^{183,224}. The lineage is an odd assortment of deep sea and near shore percomorph lineages that were previously classified in the wastebasket version of Perciformes and the demonstrably polyphyletic Trachinoidei^{93,176,225}. While molecular studies consistently resolve Acropomatiformes as a clade, its monophyly is not strongly supported with Bayesian posteriors or bootstrap values and relationships within the clade differ dramatically across studies^{93,176,214,225,242}.

The UCE phylogeny resolves Acropomatiformes as monophyletic with 100% bootstrap support (Fig. 2, Supplementary Fig. 22). All but two nodes within Acropomatiformes are present in 100% of the bootstrap replicates. First, the clade containing *Bathyclupea* (deepsea herrings), *Champsodon* (gapers), Creediidae (sandburrowers), and Hemerocoetidae (signalfishes) is supported with a bootstrap score of 97%. Second, the clade containing *Scombrops* (gnomefishes), Symphysanodontidae (slopefishes), Epigonidae (deepwater cardinalfishes), and Howellidae (oceanic basslets) is supported with a 99% bootstrap score (Fig. 2, Supplementary Fig. 22). The relationships among acropomatiforms in the UCE tree are quite different from any previous study and include the non-monophyly of Polyprionidae (wreckfishes) as *Polyprion* is resolved as the sister lineage of a clade containing *Glaucosoma* (pearl perches), Pempheridae (sweepers), and *Lateolabrax* (Asian seaperches) while *Stereolepis* is the sister lineage of a clade containing *Banjos* (banjofishes) and Pentacerotidae (armorheads). The resolution of Howellidae and Epigonidae as sister lineages in the UCE phylogeny is interesting in the context of four osteological traits shared between these two lineages and the possibility of additional shared traits in Howellidae and other acropomatiform lineages²⁴³. Future phylogenetic studies will round out the sampling of Acropomatiformes by including *Dinolestes lewini* (Long-finned Pike),

Malakichthyidae (temperate ocean-basses), and Synagropidae (splitfin ocean-basses) to take advantage of the strong phylogenetic resolution provided by the UCE loci for this clade.

xvi. Phylogenetic relationships of Acanthuriformes

The first wave of molecular phylogenetic analyses of percomorphs was based on whole mitochondrial genomes and small sets of Sanger sequenced mitochondrial and nuclear genes. The major lineages of percomorphs and their composition began to emerge because of these molecular phylogenetic analyses. The monophyly of the major percomorph lineages and their relationships to one another are well resolved in the UCE phylogeny and we delimit these inclusive clades as taxonomic orders (e.g., Gobiiformes, Scombriformes, and Perciformes). Hampering these earliest molecular phylogenetic studies of percomorphs was a lack of phylogenetic resolution for relationships within and between major lineages of Eupercaria which include Perciformes, Centrarchiformes, Acropomatiformes, and what Smith et al.²¹⁶ delimit as Acanthuriformes. The lack of phylogenetic resolution was particularly acute in Acanthuriformes, a lineage that includes more than 2,320 species classified in 56 taxonomic families. The phylogenies resulting from earlier molecular studies resolved taxonomic families within Acanthuriformes as monophyletic with high bootstrap support [e.g., Chaetodontidae (butterflyfishes), Acanthuridae (surgeonfishes), and Sparidae (porgies)], but had very poor support for relationships among these lineages^{93,152,216}.

Acanthuriformes is monophyletic in the UCE phylogeny with strong bootstrap node support; however, six nodes along the backbone of the acanthuriform phylogeny have bootstrap scores ranging from 70% to 94% (Fig. 2, Supplementary Figs. 22–24). Despite this lower support for a small portion of the acanthuriform phylogeny, the UCE tree provides insight into several issues not resolved in earlier molecular studies of percomorph phylogenetics. First, Gerreidae (morjarras), which long evaded phylogenetic resolution, is the sister lineage of all other Acanthuriformes (Fig. 2, Supplementary Fig. 22). Second, Moronidae (temperate basses) and Sillaginidae (whitings) are resolved here as sister lineages (Fig. 2, Supplementary Fig. 22). Though they were resolved as a closely related in earlier molecular studies⁹³, Lutjanidae and Haemulidae are distantly related in the UCE phylogeny (Fig. 2, Supplementary Figs. 22,23). Finally, ten lineages identified as *incertae sedis* within Eupercaria by Betancur-R et al.¹⁴⁹ are

phylogenetically resolved with moderate to high bootstrap support in Acanthuriformes (Fig. 2, Supplementary Figs. 22–24).

One of the most surprising findings from molecular studies of the teleost phylogeny was the resolution of Lophioidei (anglerfishes, formerly Lophiiformes) and Tetraodontoidei (puffers and molas, formerly Tetraodontiformes) as sister lineages^{3,7,8,93,152,170,219}. An analogous rearrangement within Mammalia in terms of divergence times might be recognition of a clade of marsupials as the sister lineage of primates. In morphology-based classifications, the lophioids were placed in Paracanthopterygii^{164,244}, phylogenetically distant from other percomorph lineages. This migration of lophioids as paracanthopterygians into a derived clade of percomorphs is among the most significant changes in 21st century vertebrate phylogenetics. While the discovery that Lophioidei and Tetraodontoidei are closely related was based on phylogenetic analyses of molecular data, subsequent investigation of their morphology identified several soft tissue characters that are likely synapomorphies of a lophioid-tetraodontoid clade²⁴⁵. It has also been discovered that the larvae of these two lineages exhibit unique morphology and pigmentation²⁴⁶. Congruent with earlier studies, the UCE tree resolves an inclusive lineage containing *Siganus* (rabbitfishes), Scatophagidae (scats), Priacanthidae (bigeyes), Cepolidae (bandfishes), and Caproidae (boarfishes) as the sister lineage of the Lophioidei-Tetraodontoidei clade. These nodes in the UCE phylogeny are all characterized by high bootstrap support values (Fig. 2, Supplementary Figs. 24,25).

xvii. Acanthuriformes: phylogenetic relationships of Tetraodontoidei

Some of the earliest phylogenetic analyses of ray-finned fishes focused on relationships within Tetraodontoidei, resulting in numerous phylogenetic analyses based on morphological and molecular datasets^{140,152,247-254}. While there are important differences among nearly all the phylogenies of tetraodontoids, most analyses consistently resolve three to four sets of sister lineages that include Triacanthodidae (spikefishes)-Triacanthidae (triplespines), Diodontidae (porcupinefishes)-Tetraodontidae (puffers), Balistidae (triggerfishes)-Monacanthidae (filefishes), and Aracaniidae (deepwater boxfishes)-Ostraciidae (boxfishes)^{93,140,152,247,254}, but all these phylogenies differ in how these lineages relate to one another. They are also incongruent regarding the relationships of *Triodon macropterus* (Threetooth Puffer) and Molidae (molas and ocean sunfishes). The UCE phylogeny and most of the earlier molecular phylogenies do not

resolve the subclade formerly named Tetraodontoidei, which contained Triodontidae, Molidae, Diodontidae, and Tetraodontidae^{93,152,249-252}. The monophyly of this group was inferred, in part, based on the beak-like teeth in the upper and lower jaws and on a non-protractile upper jaw¹⁴⁰.

The relationships of Tetraodontoidei in the UCE phylogeny are strongly supported with high bootstrap values at every node (Fig. 2, Supplementary Fig. 24), but differ from all previous topologies inferred using morphology, molecules, or combined morphological and molecular datasets. The UCE phylogeny resolves the relationships of *Triodon* and Molidae and contains three major lineages: 1) a clade containing *Triodon*, Aracanidae, and Ostraciidae, 2) a clade containing Triacanthodidae, Triacanthidae, Balistidae, and Monacanthidae, and 3) a clade containing Molidae, Diodontidae, and Tetraodontidae (Fig. 2, Supplementary Fig. 24).

xviii. Acanthuriformes: phylogenetic relationships of Lophioidei

The UCE phylogeny includes 16 of 18 recognized taxonomic families of Lophioidei; the monotypic Centrophrynidae and Lophichthyidae are not sampled. Phylogenies of Lophioidei inferred from morphological characters, whole mtDNA genome sequences, and Sanger sequenced mtDNA and nuclear genes all differ from one another^{93,152,255,256}. Congruent with all other phylogenetic analyses, the UCE phylogeny resolves the Lophiidae (goosefishes) as the sister lineage of all other Lophioidei (Fig. 2, Supplementary Fig. 25). It is also congruent with a previous phylogenetic analysis of lophioids in resolving Ogocephalidae (batfishes) as the sister lineage of a clade previously named Antennarioidei that contains Antennariidae (frogfishes), Tetrabrachiidae (tetrabranchid frogfishes), and Brachionichthyidae (handfishes)²⁵⁷. All nodes along the backbone of the UCE lophioid phylogeny have high bootstrap support (Fig. 2, Supplementary Fig. 25).

The UCE phylogeny is congruent with previous molecular phylogenetic analyses in resolving Chaunacidae (coffinfishes) as the sister lineage of the eleven taxonomic families that comprise the deepsea anglerfishes^{93,152,255}, delimited here as Ceratioidea (Fig. 2, Supplementary Fig. 25, Supplementary Table 3). The UCE phylogeny and previous molecular analyses using whole mitochondrial genomes resolve Thaumathichthyidae (wolftrap anglers) as paraphyletic with *Lasiognathus* nested within Oneirodidae (dreamers)²⁵⁵. Within the ceratioids, the UCE phylogeny resolves *Neoceratias spinifer* (Toothed Seadevil), Linophrynidae (leftvents), and Ceratiidae (seadevils) as a monophyletic group (Fig. 2, Supplementary Fig. 25). These three

lineages all exhibit male obligate sexual parasitism and dramatically altered their immune systems through losing the capacity for somatic diversification of antigen receptor genes²⁵⁸. All previous morphological and molecular phylogenetic analyses of ceratioids resulted in the non-monophyly of the lineages exhibiting obligate male sexual parasitism, implying multiple origins of this unique reproductive mode^{255,258,259}. In contrast, the UCE phylogeny implies a single evolutionary origin of this unique trait (Fig. 2, Supplementary Fig. 25).

e. Divergence-time estimates

For both the 702- and 1,084-taxon phylogenies, our relaxed-clock molecular dating analyses estimated similar stem lineage ages across the multiple subsamples of UCE loci, with overlapping 95% highest posterior densities for most nodes (Supplementary Table 4). There were also no observable differences in the median node heights reported in Maximum Clade Credibility trees built using post-burn-in trees that were randomly sampled (as in the tree represented in Figs. 1,2), or using post-burn-in trees that were systematically sampled after a certain number of MCMC iterations (Supplementary Table 4).

Our age estimates are largely in agreement with those presented in previous phylogenomic analyses of ~1,000 UCE loci³ and ~1,100 exons⁸ (Extended Data Fig. 3). For most major clades, we infer slightly older stem ages, but with 95% highest posterior density credible intervals that overlap with the dates reported in these previous studies (Extended Data Fig. 3). However, our analyses inferred comparably younger stem lineage ages for *Polymixia*, Percopsiformes, and clades within Eupercaria^{3,8}. Our stem lineage age estimates are significantly older for Gobiiformes and the Syngnathiformes-Scombriformes clade³. Perhaps as a result of incongruent phylogenetic topologies, our analyses inferred younger stem age estimates for Acanthuriformes than estimated in the phylogenomic analysis of exon data⁸.

We similarly estimate crown lineage ages for major clades with 95% highest posterior densities that largely overlap with previous phylogenomic analyses^{3,8}. Exceptions include the crown age estimates of Acanthuriformes, Syngnathiformes and Scombriformes, Trachichthyiformes, Beryciformes, Gobiiformes, Syngnathiformes and Blenniiformes. Many of the discrepancies in crown ages likely result from differences among inferred phylogenetic trees (especially within Eupercaria), or from the relatively sparse taxon sampling in previous phylogenomic studies^{3,8}.

f. Diversification rate analyses

Our results do not support a significant effect of the K-Pg on acanthomorph lineage diversification rates. TESS-CoMET results indicate constant tree-wide diversification rates through most of the history of Acanthomorpha, with no evidence of a mass extinction (Extended Data Fig. 5). Although Extended Data Fig. 5e suggest a brief increase in the global net-diversification (speciation minus extinction) rate at approximately 50 mya (followed by a decline), we observe very low Bayesian support for these rate shifts (Extended Data Fig. 5b,d). Parameter estimates for speciation and extinction rates converged in all TESS-CoMET runs (ESS values > 200 and Geweke statistics within the 95% confidence intervals for all time points). Convergence results for the CoMET run visualized in Extended Data Fig. 5 are available in Supplementary Fig. 26. All replicate analyses produced diversification plots that were virtually indistinguishable from one another. The results of the Gelman-Rubin test, which calculates the ratio of within-sample variance to between-sample variance, ensured that rate parameters and shift time parameters converged across the independent, replicate analyses (Rubin-Gelman statistic < 1.05) (Supplementary Fig. 27).

The CoMET results do report moderately supported shifts ($2 \leq 2\ln \text{ Bayes Factors} \leq 6$) in speciation and extinction rates in the last 10 million years (Extended Data Fig. 5a–e). We strongly suspect, however, that these shifts are an artefact of the CoMET model, perhaps due to how it accounts for incomplete taxon sampling. This suspicion is supported by diversification patterns reported in numerous other studies²⁶²⁻²⁶⁵, which all demonstrate (often dramatic) rate shifts close to the present-day. It remains unclear how these recent patterns may affect the inference of older rate shifts. May et al.²⁶⁶ describe that more recent mass extinction events may cause a “shadow effect” that diminishes the signal of earlier mass extinctions. As it stands, we have no evidence that the rate shift we observe in the mid- to late-Neogene could be overshadowing or weakening a signal for an earlier shift in diversification rates.

Indeed, our tests of relative model fit in TESS corroborate CoMET’s estimate of constant diversification rates (Extended Data Fig. 6). Pairwise comparisons of marginal likelihoods using Bayes Factors suggested that a constant branching-process model best represents the pattern of diversification in Acanthomorpha. In general, this test of relative model fit strongly favored models assuming uniform sampling methods over diversified methods. Therefore, after

the model assuming a constant birth-death process and uniform sampling, the next most-favored branching process models were an episodic model that accounted for a rate shift 50 mya (in accordance with the blip in net-diversification rates from the CoMET analysis) and a model with speciation rates that decreased through time, both of which assumed uniform sampling. The predictive distributions of the gamma statistic, number of taxa, and lineage-through-time (LTT) plots for the three most-favored branching process models are reported in Supplementary Fig. 28. The models assuming a tree-wide rate shift at 50 my or a decreasing speciation rate produce posterior-predictive distributions that are in accordance with the empirical estimates from the time-calibrated acanthomorph phylogeny (Supplementary Fig. 28b,c,e,f,h,i). However, the distribution under a simpler, constant rate model is also in agreement and appears to produce the most similar LTT plots to the empirical data (Supplementary Fig. 28a,d,g).

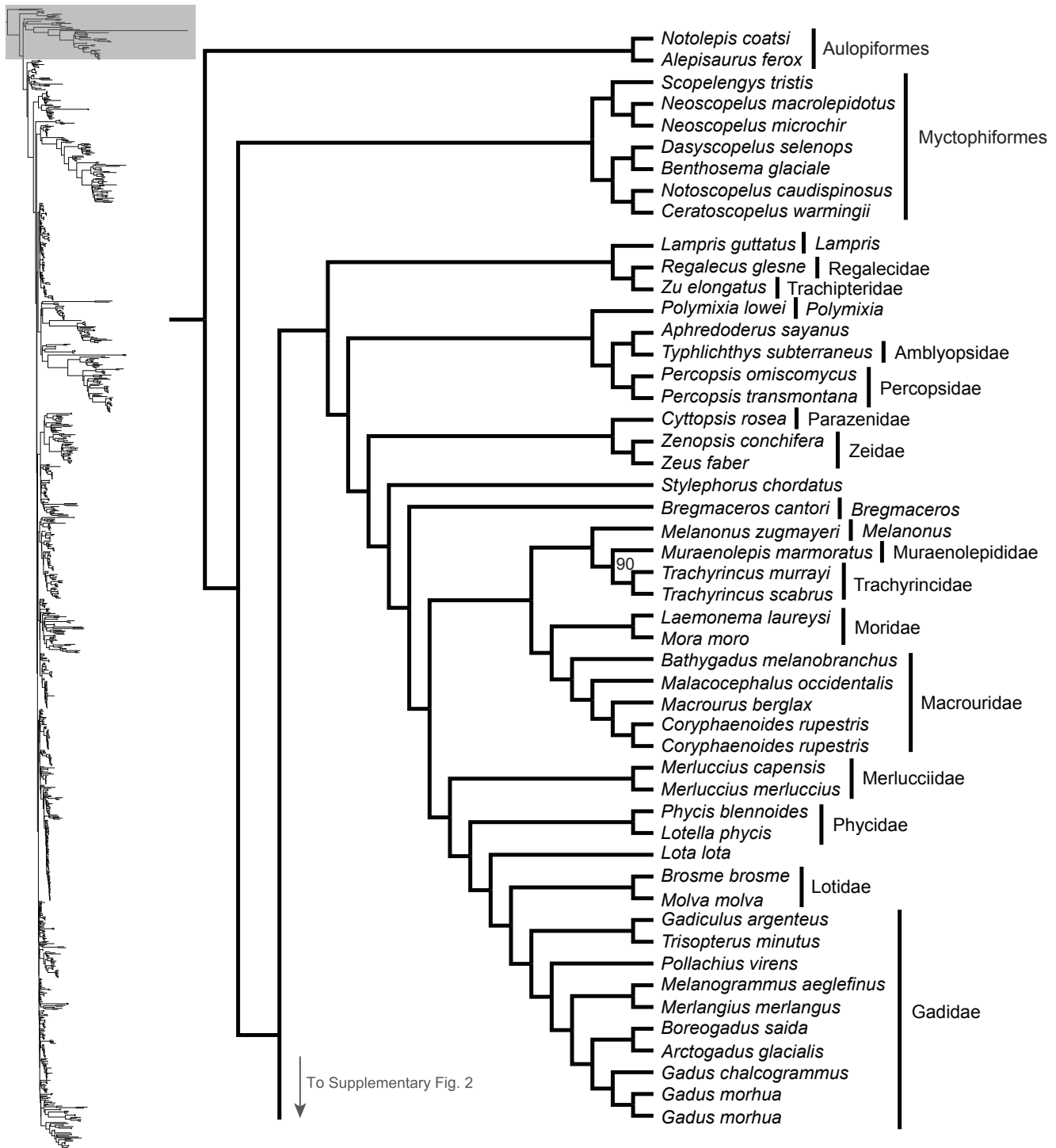
There is controversy surrounding the popular macroevolutionary modeling program BAMM^{267,268}, so indications of lineage diversification rate heterogeneity in the time-calibrated acanthomorph phylogeny are viewed with a degree of skepticism. Since the size of the phylogeny is so large, in every analysis BAMM estimated multiple shift configurations that were relatively equiprobable. We therefore chose not to examine configurations with the maximum a posteriori probability. Rather, for each analysis we chose to interrogate the maximum shift credibility (MSC) configuration, which considers only configurations sampled in the reversible-jump MCMC simulations and maximizes the product of the marginal branch-specific shift probabilities. In the 23 BAMM analyses that were conducted using the time-calibrated 1,084-taxon phylogeny, MSC configurations inferred anywhere between 22 and 33 well-supported rate shifts (Supplementary Fig. 29). The regression line in Supplementary Fig. 29, calculated using base R, demonstrates that the prior number of shifts specified in BAMM does not dramatically affect the estimated number of rate shifts (slope = 0.105) and only weakly predicts the posterior variation ($y = 0.149x + 25.063$; $R^2 = 0.217$). The average number of rate shifts among the MSC configurations was approximately 28. Bayes factor comparisons for each analysis, however, supported models with a number of diversification rate shifts in the upper 30s or low 40s, depending on the specified priors. This was true even for analyses with prior models that expected one rate shift in the phylogeny.

In Extended Data Fig. 7, we present the MSC configuration resulting from an analysis with a prior model that expected 15 rate shifts and ran a 2-chain MCMC simulation with a deltaT

value of 0.5. Log-likelihood values across all analyses were similar, but the analyses with prior models assuming 15 or 40 expected shifts displayed the highest effective sample sizes (ESS) for their log-likelihoods and for the number of shift events. Since the estimated number and positions of the rate shifts were similar across analyses with different priors, we take note of the 19 clades with leading branches that were estimated to have undergone rate shifts by at least 16 ($\geq 70\%$) of the 23 BAMM analyses. The 19 shared clades, several of which (e.g. zoarcoids, darters, notothenioids, labrids, cichlids and gobies) have previously been described as having undergone radiations, are labeled with blue numbers in Extended Data Fig. 7. They include: 1) Dinematchthyidae, 2) Apogoninae (Apogonidae to the exclusion of *Pseudamia*), 3) Gobiidae and Oxudercidae, 4) Mastacembelidae, 5) the clade defined by Scopthalmidae and Soleidae, 6) Carangidae (to the exclusion of *Seriola*), 7) Pseudocrenilabrinae (in Cichlidae), 8) Poeciliidae, 9) Labridae, 10) Sciaenidae, 11) Chaetodontidae, 12) Acanthuridae (to the exclusion of *Naso*), 13) Anthiadae and Epinephelidae, 14.) darters (Etheostomatinae), 15) the clade defined by “Nototheniidae” and Channichthyidae (see Supplementary Fig. 17 for clarification), 16) *Sebastes*, 17) the clade defined by Trichodontidae and Psychrolutidae, 18) Lycodinae (in Zoarcidae), and 19) the clade defined by Stichaeidae and Zoarcidae. We chose to present the configuration in Extended Data Fig. 7 because the analysis assuming 40 rate shifts had more rate shifts beyond these 19 clades than the analysis assuming 15 expected rate shifts. Still, the MSC configuration presented in Extended Data Fig. 7 highlights eight additional rate shifts that are labelled with black numbers and are not present in this list of 19. Furthermore, while the MSC configuration in Extended Data Fig. 7 identifies rate shifts occurring within Acanthuridae and Zoarcidae, these shifts occur along a different-yet-nearby internal branch than in most of the other configurations. Specifically, the configuration in Extended Data Fig. 7 flags one rate shift in the branch leading to Acanthuridae to the exclusion of *Naso* and *Prionurus*, and another in the lineage defined by *Bothrocara* and *Lycodes concolor* (within Zoarcidae).

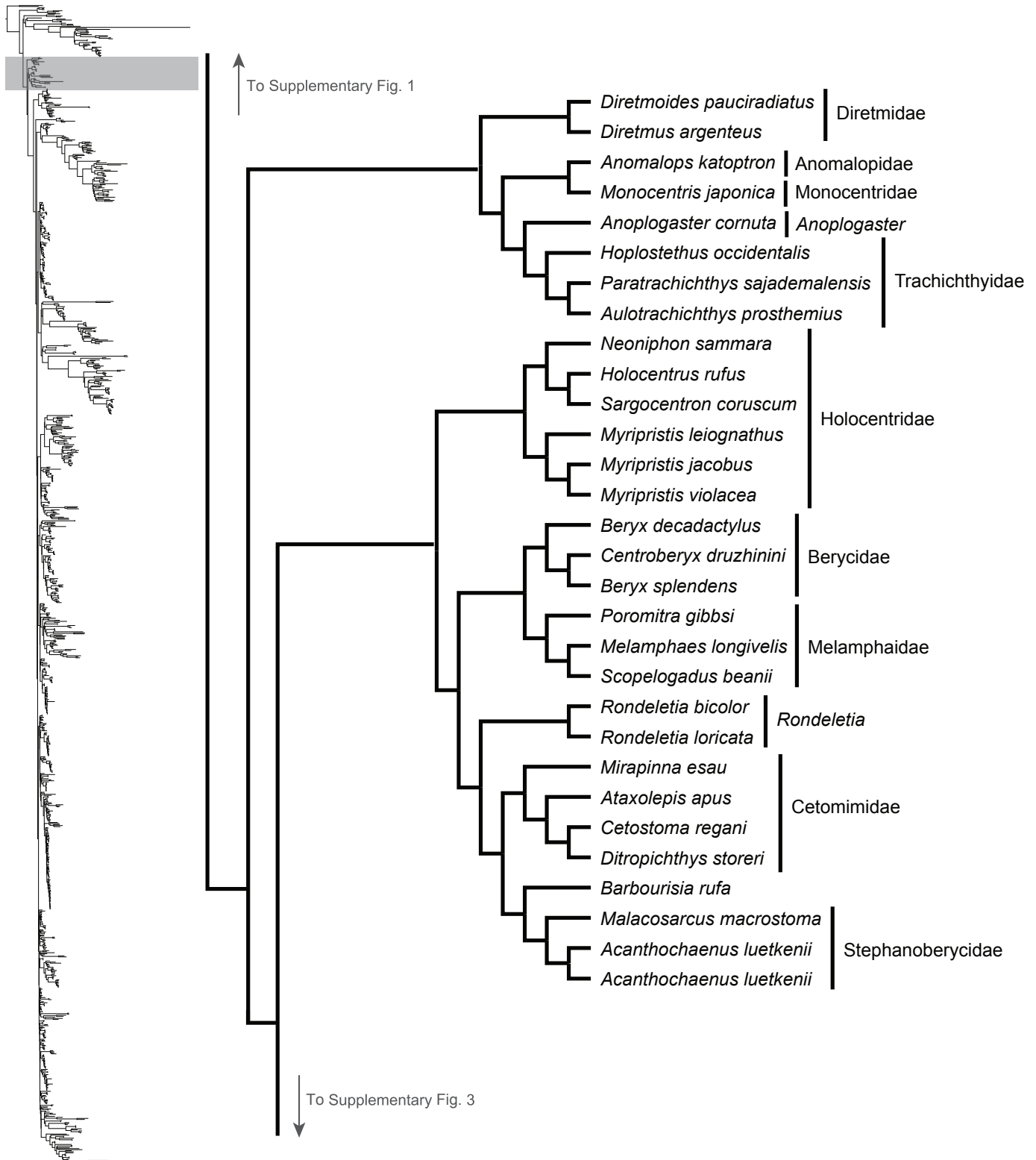
The fact that many of the rate shifts identified by BAMM occur along tipwards branches may indicate that the species richness of Acanthomorpha is driven by relatively recent, more phylogenetically or geographically localized radiations instead of a burst of diversification after the K-Pg. This pattern does not seem to be unique to acanthomorphs; numerous radiations have shown to have a similar pattern of constant diversification across the K-Pg boundary despite bursts in the origin of disparity in morphological and ecological traits²⁶⁹. Nevertheless, there is a

chance that this pattern is the by-product of analytical corrections for incomplete sampling. Such corrections may reduce the statistical power to infer shifts in diversification rates and increase the probability of Type II error when rate variation is present²⁷⁰. It is also known that Bayesian methods of diversification rate estimation, including BAMM and TESS, penalize parameter-rich diversification models and favor less-complex models even under liberal priors. Given the infinite number of possible diversification scenarios that could result in the observed phylogeny²⁷¹, it is therefore possible that TESS estimated a constant-rate model to best fit our data because of its simplicity rather than its accuracy.



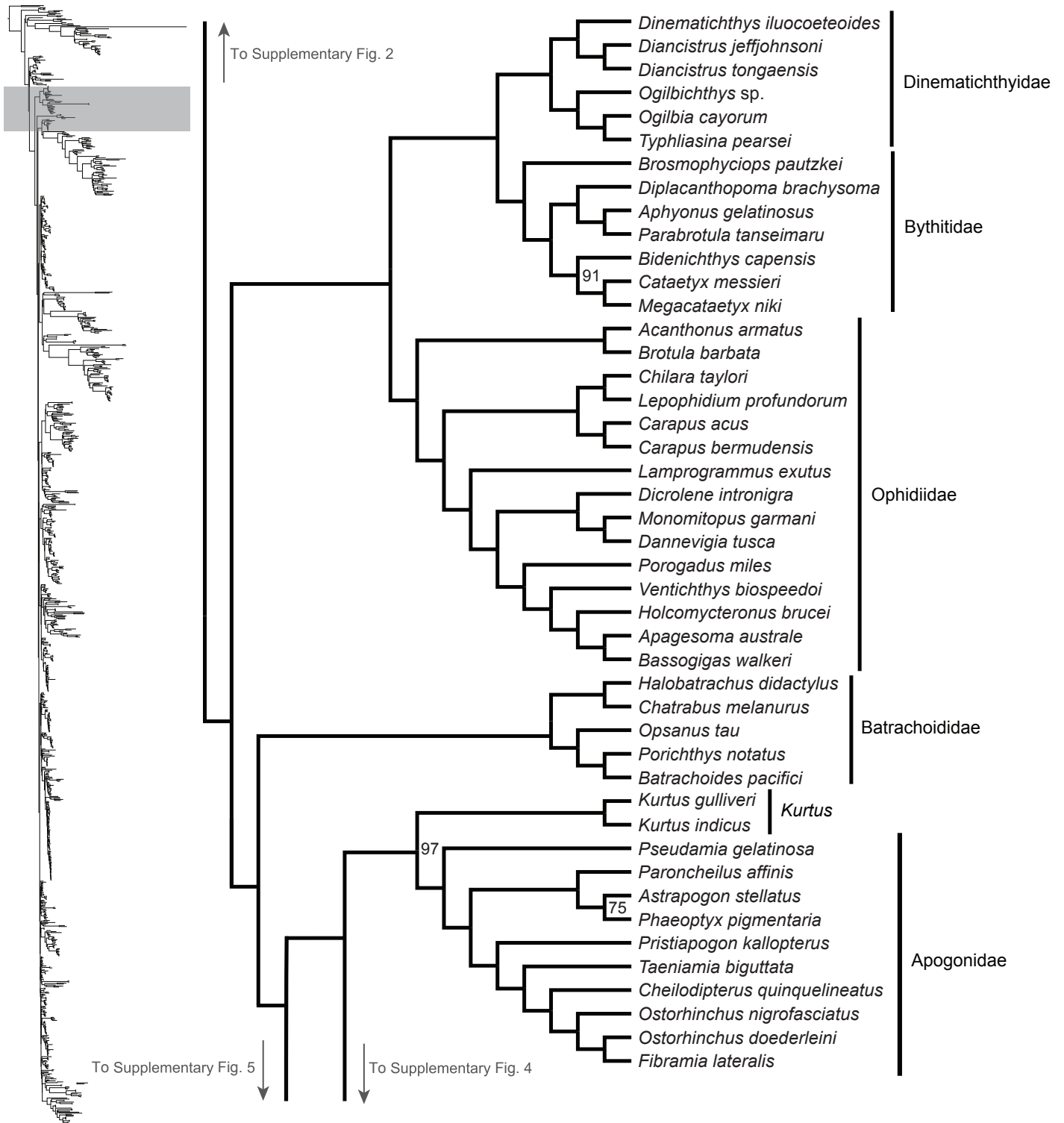
Supplementary Fig. 1: Maximum likelihood phylogeny inferred in IQ-TREE.

A guide tree on the left marks (with a gray rectangle), the region of the acanthomorph tree represented in the figure. Numbers at nodes reflect bootstrap support values. All nodes without a numerical annotation have 100% bootstrap support. Orders, families or genera for taxa are listed to the right of the vertical black bars. Any tips left unassigned to a higher taxon are monospecific or monogeneric taxa.



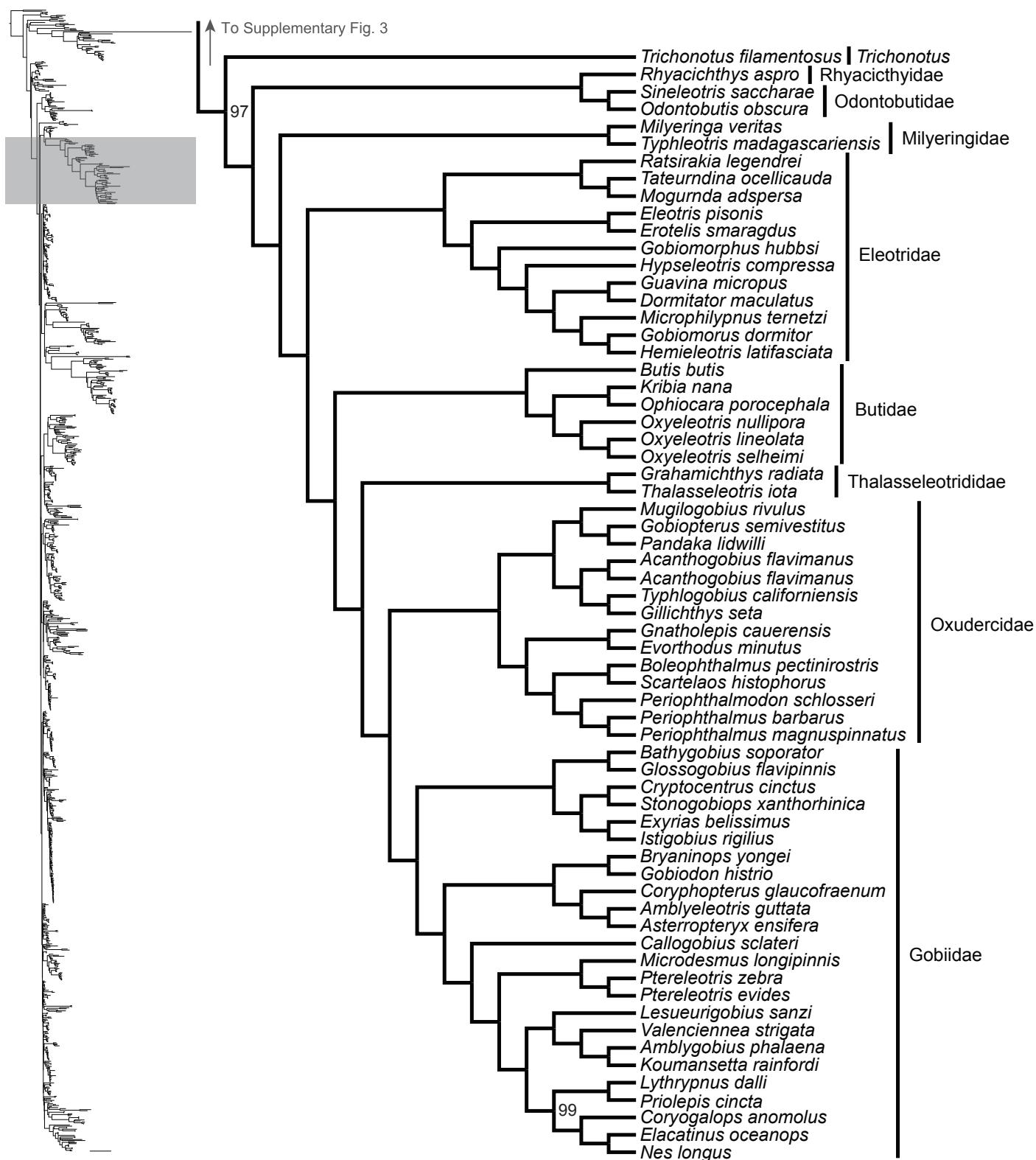
Supplementary Fig. 2: Maximum likelihood phylogeny inferred in IQ-TREE.

A guide tree on the left marks (with a gray rectangle), the region of the acanthomorph tree represented in the figure. All nodes have 100% bootstrap support. Orders, families or genera for taxa are listed to the right of the vertical black bars. Any tips left unassigned to a higher taxon are monospecific or monogeneric taxa.



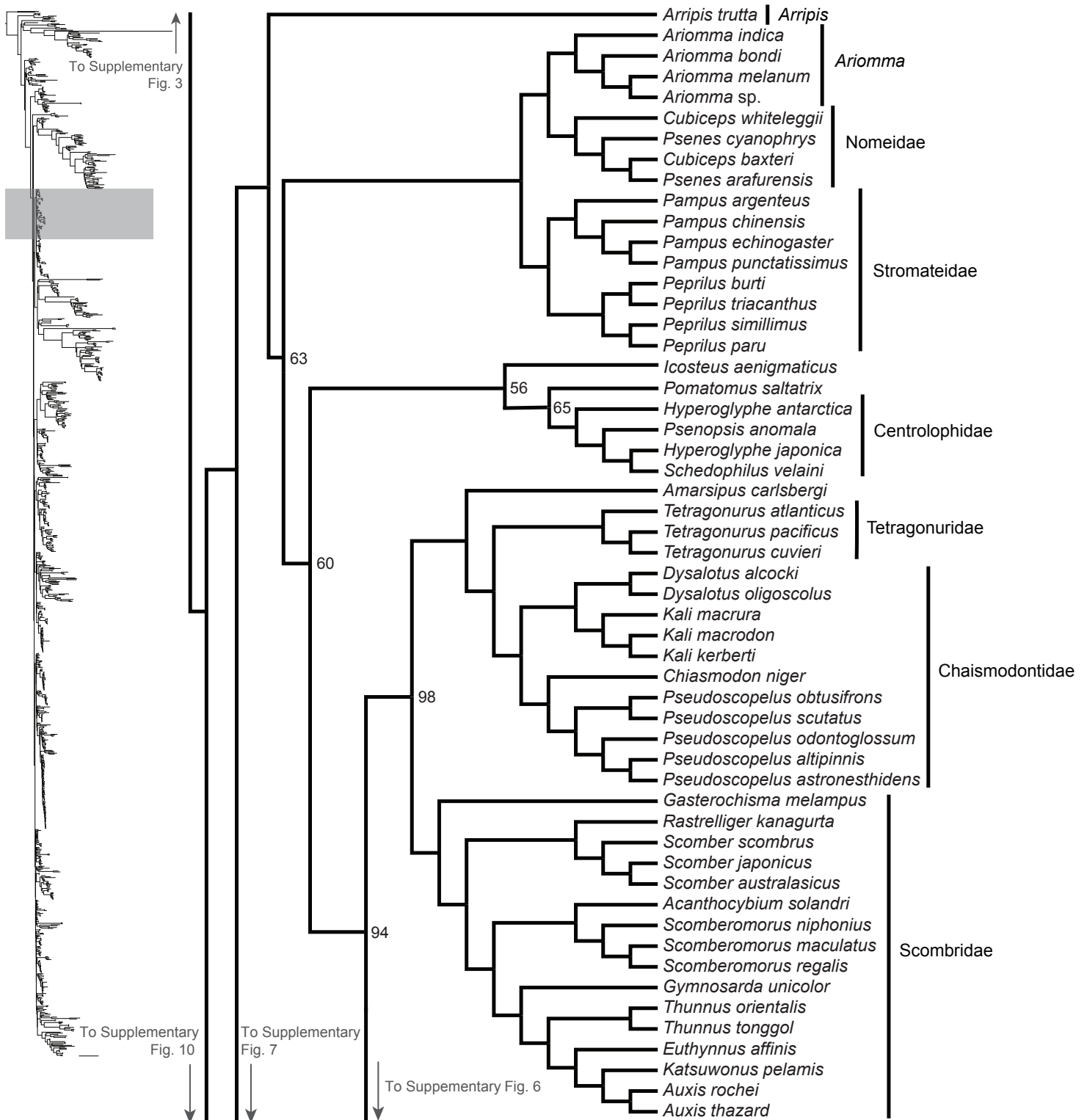
Supplementary Fig. 3: Maximum likelihood phylogeny inferred in IQ-TREE.

A guide tree on the left marks (with a gray rectangle), the region of the acanthomorph tree represented in the figure. Numbers at nodes reflect bootstrap support values. All nodes without a numerical annotation have 100% bootstrap support. Orders, families or genera for taxa are listed to the right of the vertical black bars.



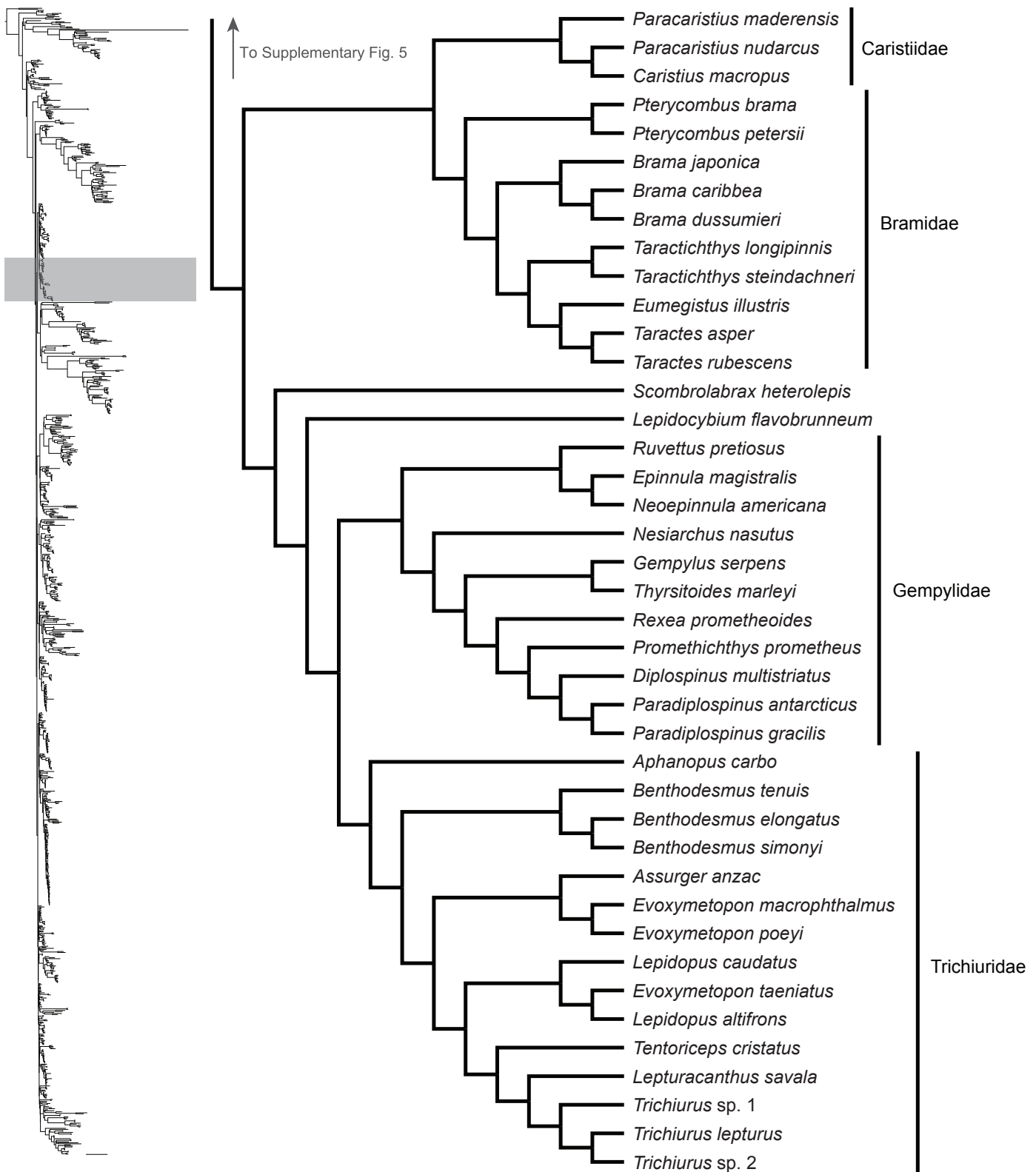
Supplementary Fig. 4: Maximum likelihood phylogeny inferred in IQ-TREE.

A guide tree on the left marks (with a gray rectangle), the region of the acanthomorph tree represented in the figure. Numbers at nodes reflect bootstrap support values. All nodes without a numerical annotation have 100% bootstrap support. Orders, families or genera for taxa are listed to the right of the vertical black bars.



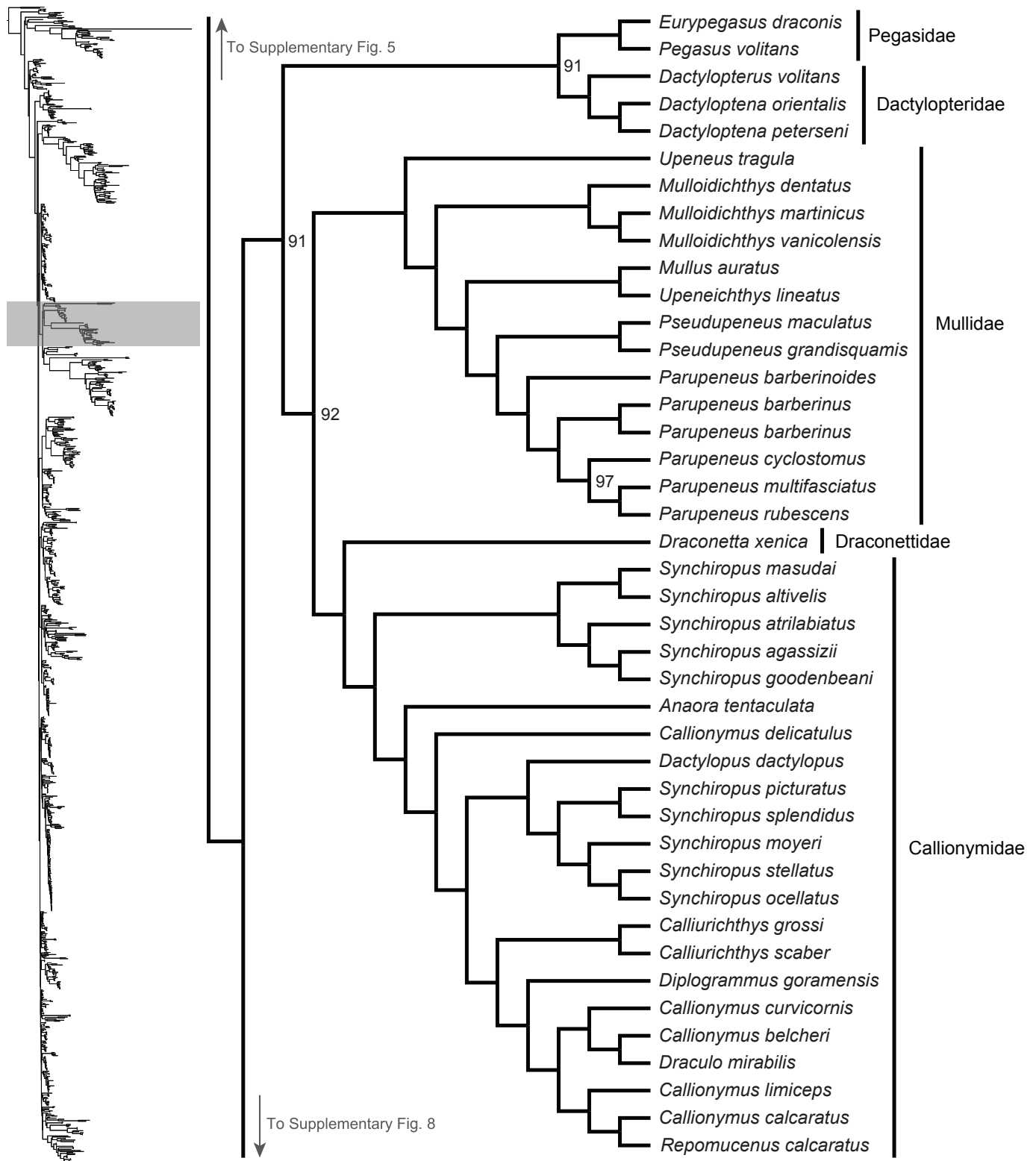
Supplementary Fig. 5: Maximum likelihood phylogeny inferred in IQ-TREE.

A guide tree on the left marks (with a gray rectangle), the region of the acanthomorph tree represented in the figure. Numbers at nodes reflect bootstrap support values. All nodes without a numerical annotation have 100% bootstrap support. Orders, families or genera for taxa are listed to the right of the vertical black bars. Any tips left unassigned to a higher taxon are monospecific or monogeneric taxa.



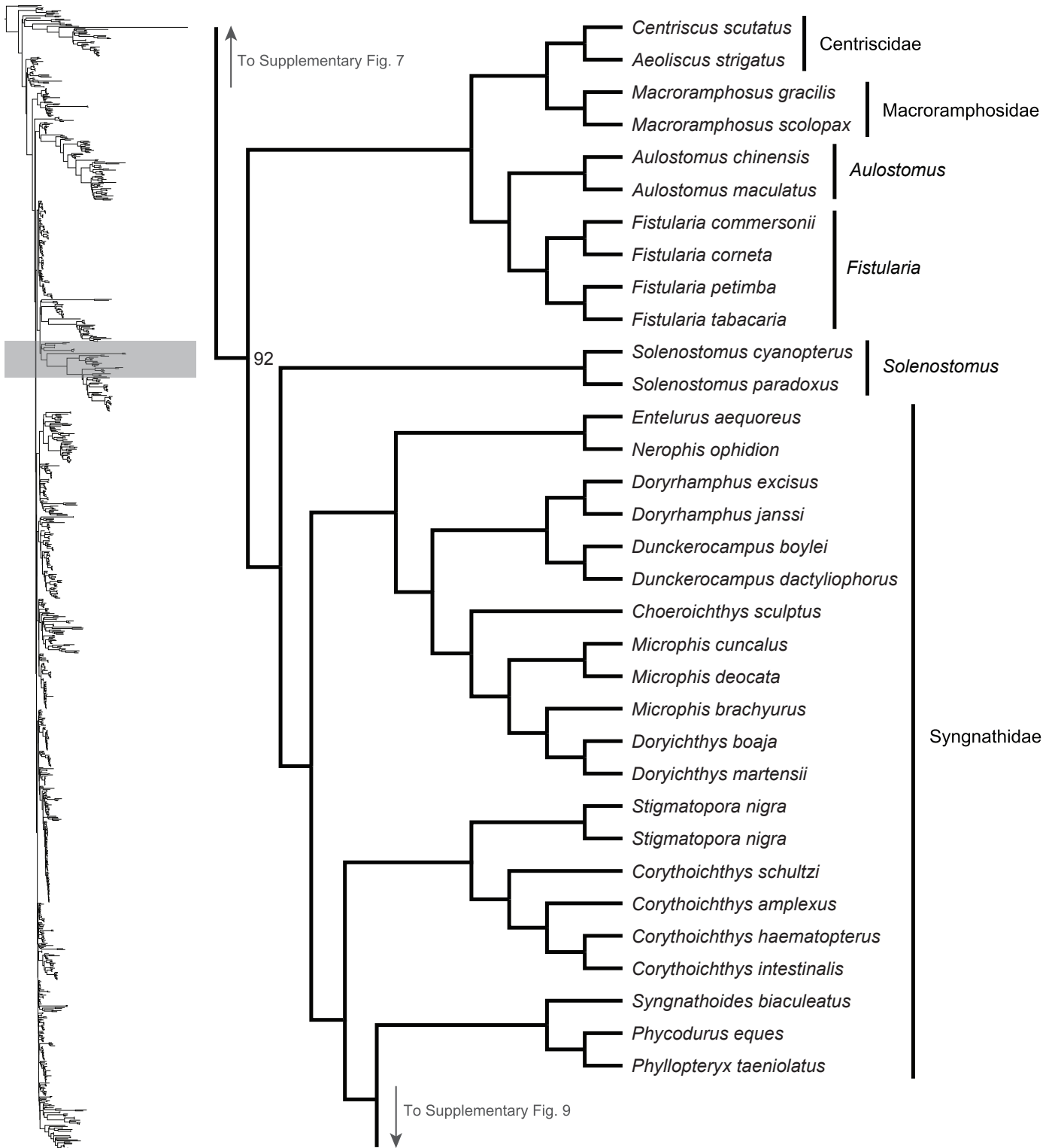
Supplementary Fig. 6: Maximum likelihood phylogeny inferred in IQ-TREE.

A guide tree on the left marks (with a gray rectangle), the region of the acanthomorph tree represented in the figure. All nodes have 100% bootstrap support. Orders, families or genera for taxa are listed to the right of the vertical black bars. Any tips left unassigned to a higher taxon are monospecific or monogeneric taxa.



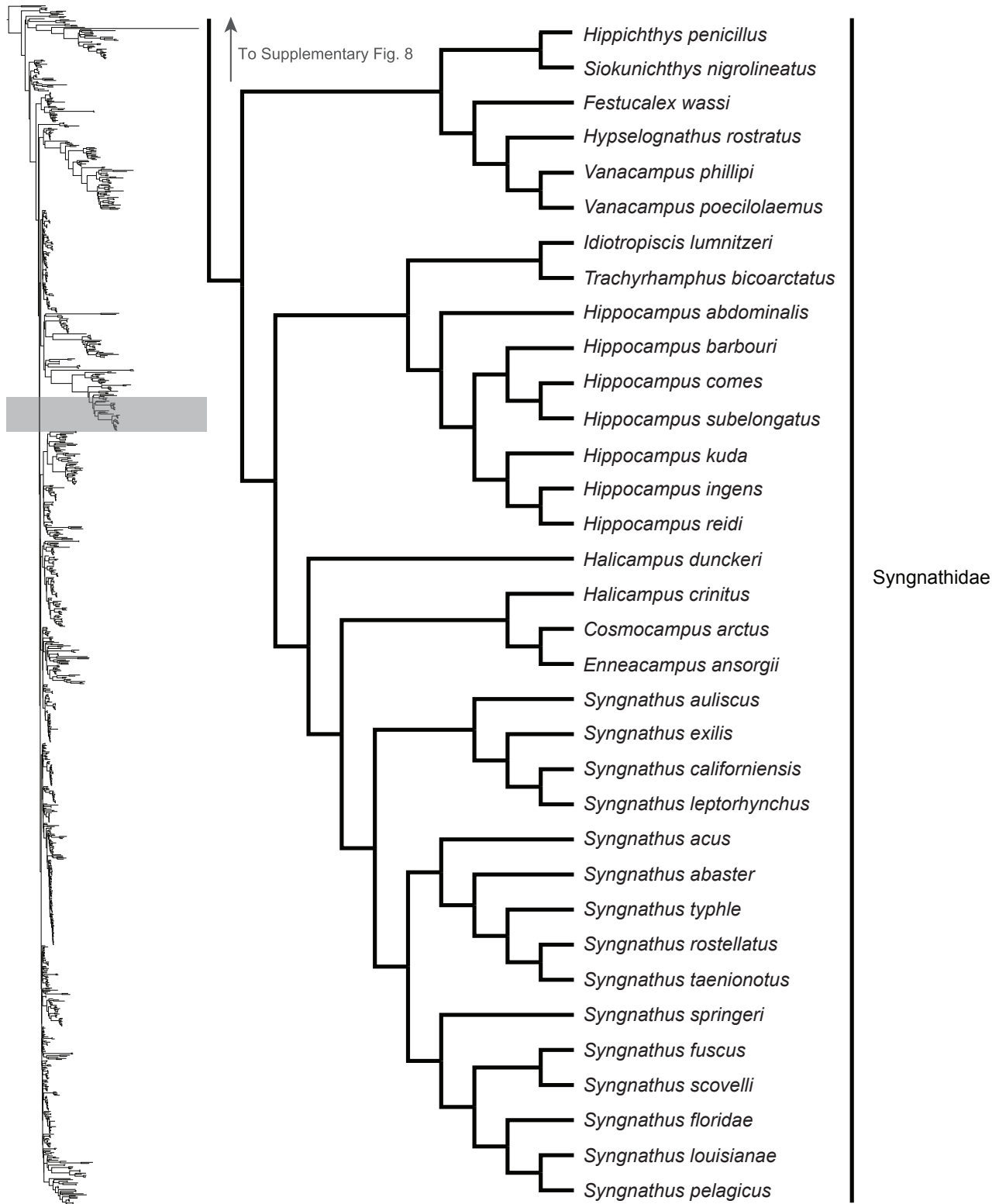
Supplementary Fig. 7: Maximum likelihood phylogeny inferred in IQ-TREE.

A guide tree on the left marks (with a gray rectangle), the region of the acanthomorph tree represented in the figure. Numbers at nodes reflect bootstrap support values. All nodes without a numerical annotation have 100% bootstrap support. Orders, families or genera for taxa are listed to the right of the vertical black bars.



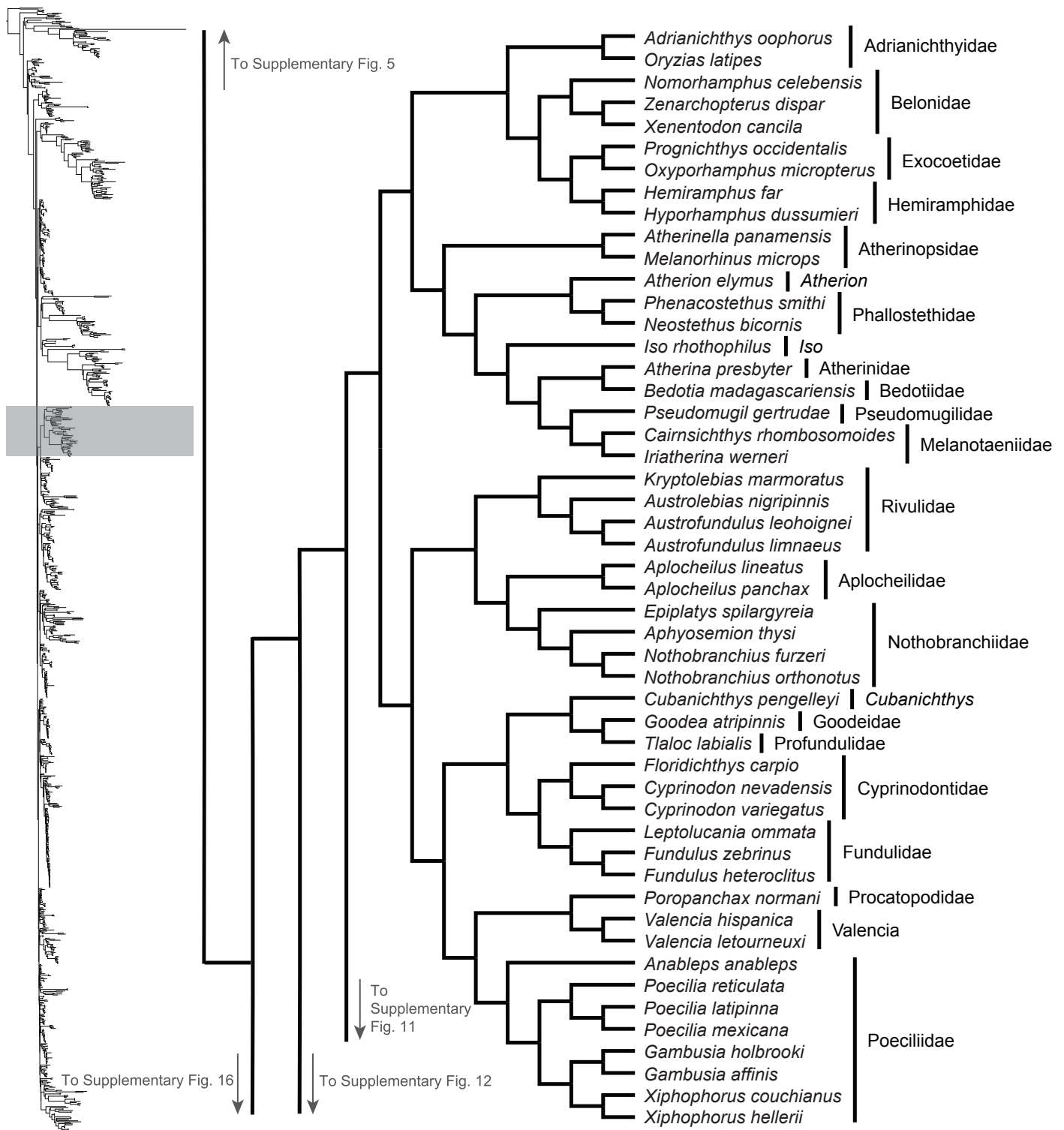
Supplementary Fig. 8: Maximum likelihood phylogeny inferred in IQ-TREE.

A guide tree on the left marks (with a gray rectangle), the region of the acanthomorph tree represented in the figure. Numbers at nodes reflect bootstrap support values. All nodes without a numerical annotation have 100% bootstrap support. Orders, families or genera for taxa are listed to the right of the vertical black bars.



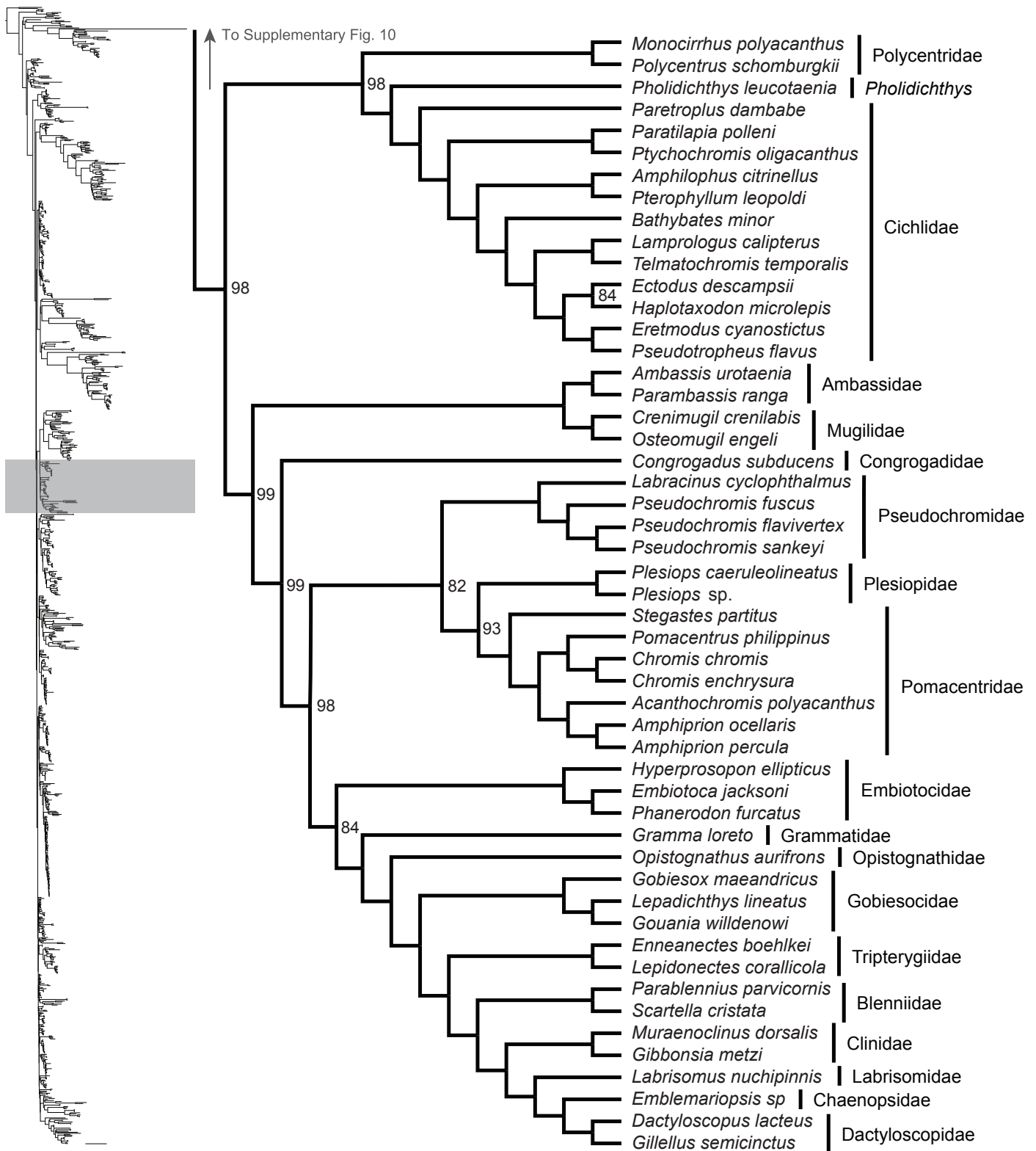
Supplementary Fig. 9: Maximum likelihood phylogeny inferred in IQ-TREE.

A guide tree on the left marks (with a gray rectangle), the region of the acanthomorph tree represented in the figure. All nodes have 100% bootstrap support. Orders, families or genera for taxa are listed to the right of the vertical black bars.



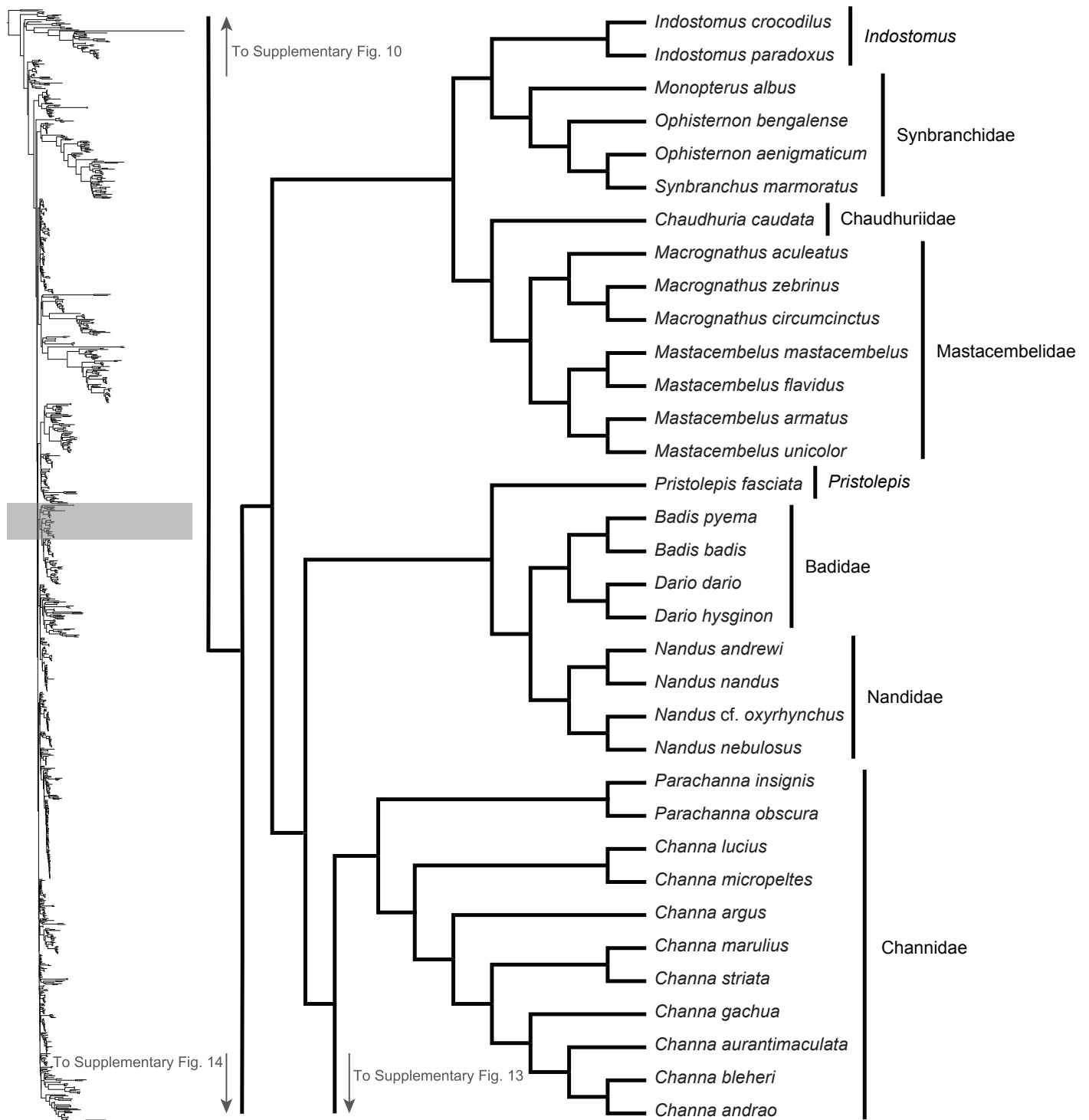
Supplementary Fig. 10: Maximum likelihood phylogeny inferred in IQ-TREE.

A guide tree on the left marks (with a gray rectangle), the region of the acanthomorph tree represented in the figure. All nodes have 100% bootstrap support. Orders, families or genera for taxa are listed to the right of the vertical black bars.



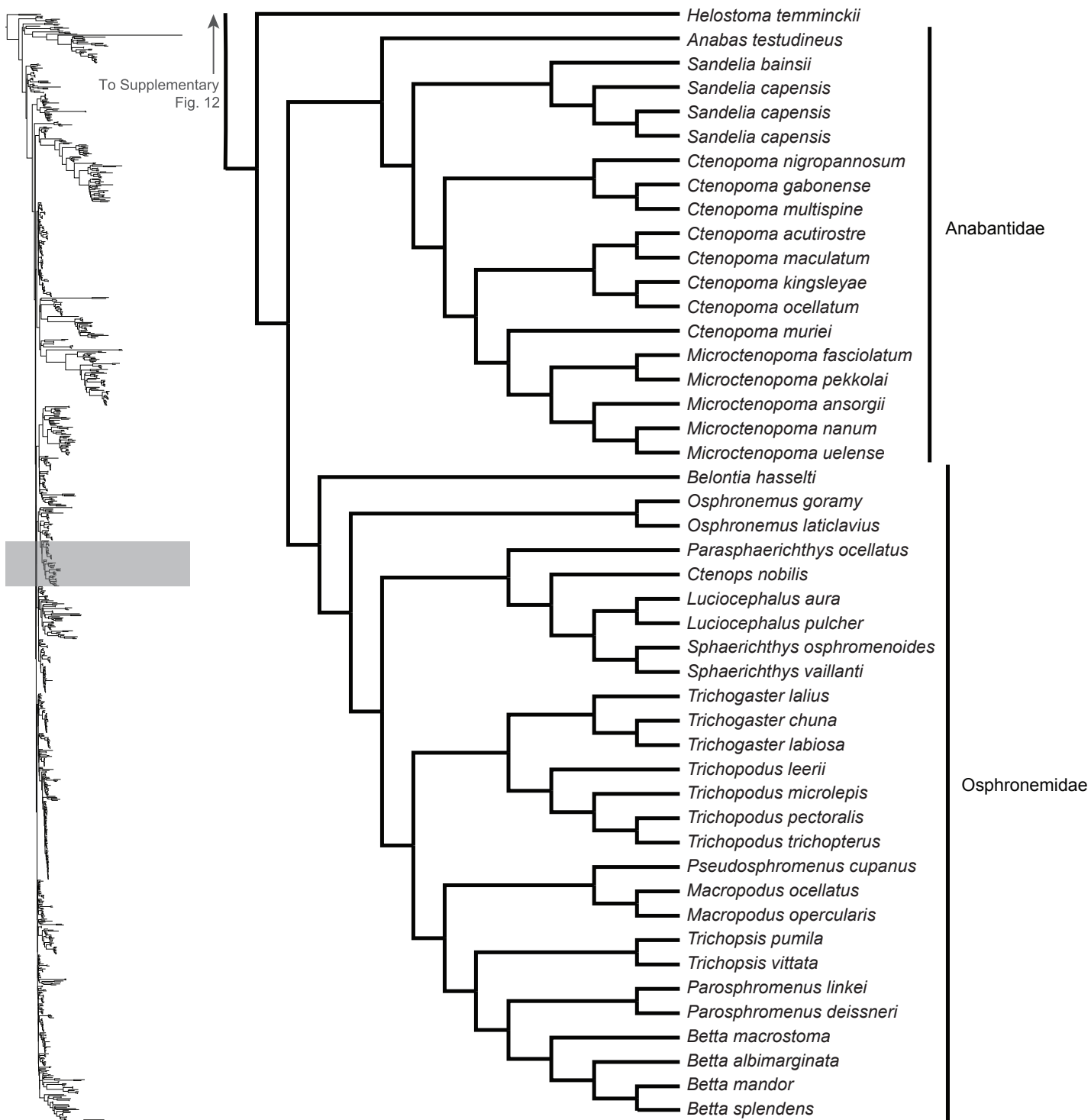
Supplementary Fig. 11: Maximum likelihood phylogeny inferred in IQ-TREE.

A guide tree on the left marks (with a gray rectangle), the region of the acanthomorph tree represented in the figure. Numbers at nodes reflect bootstrap support values. All nodes without a numerical annotation have 100% bootstrap support. Orders, families or genera for taxa are listed to the right of the vertical black bars.



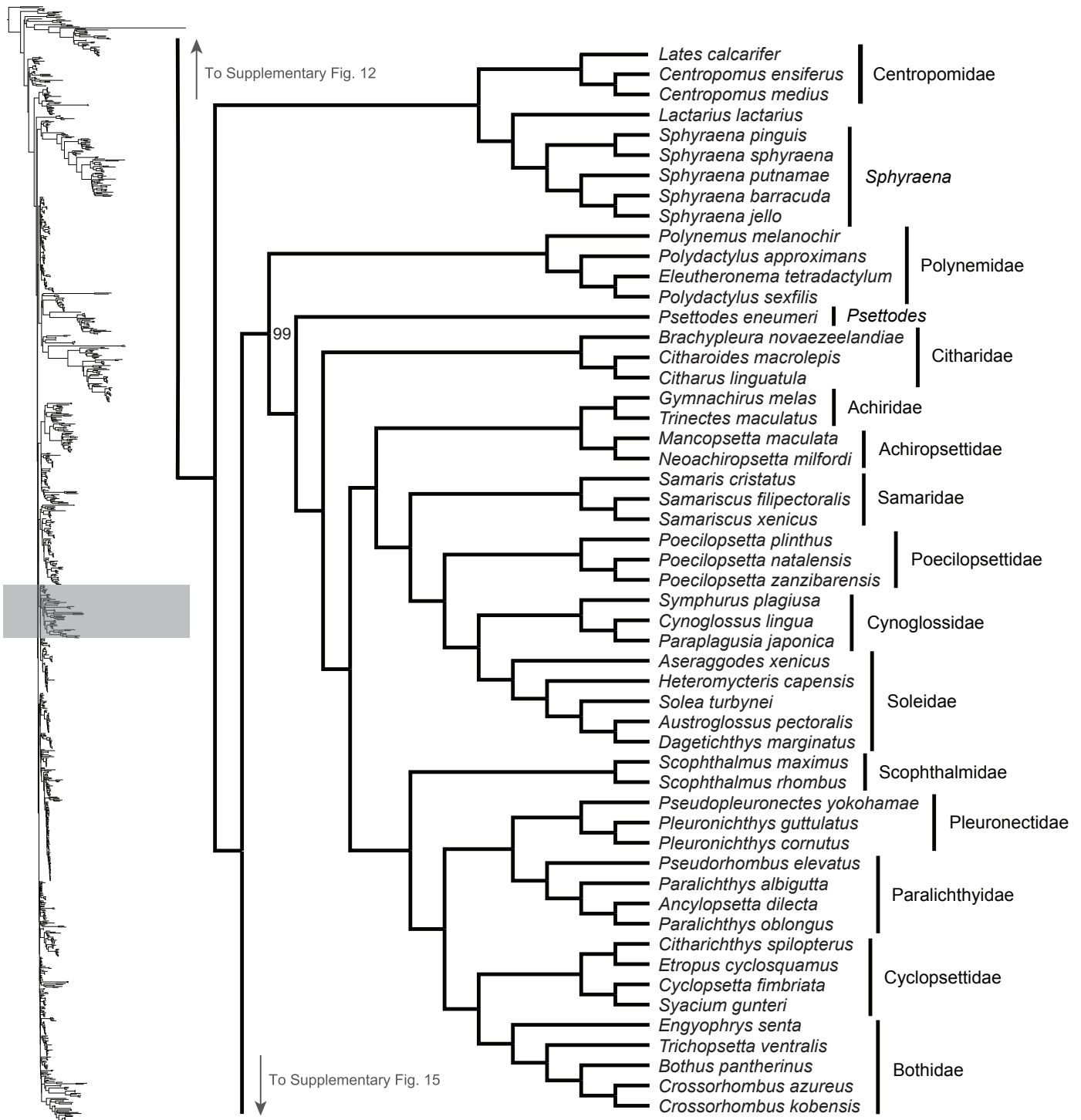
Supplementary Fig. 12: Maximum likelihood phylogeny inferred in IQ-TREE.

A guide tree on the left marks (with a gray rectangle), the region of the acanthomorph tree represented in the figure. All nodes have 100% bootstrap support. Orders, families or genera for taxa are listed to the right of the vertical black bars.



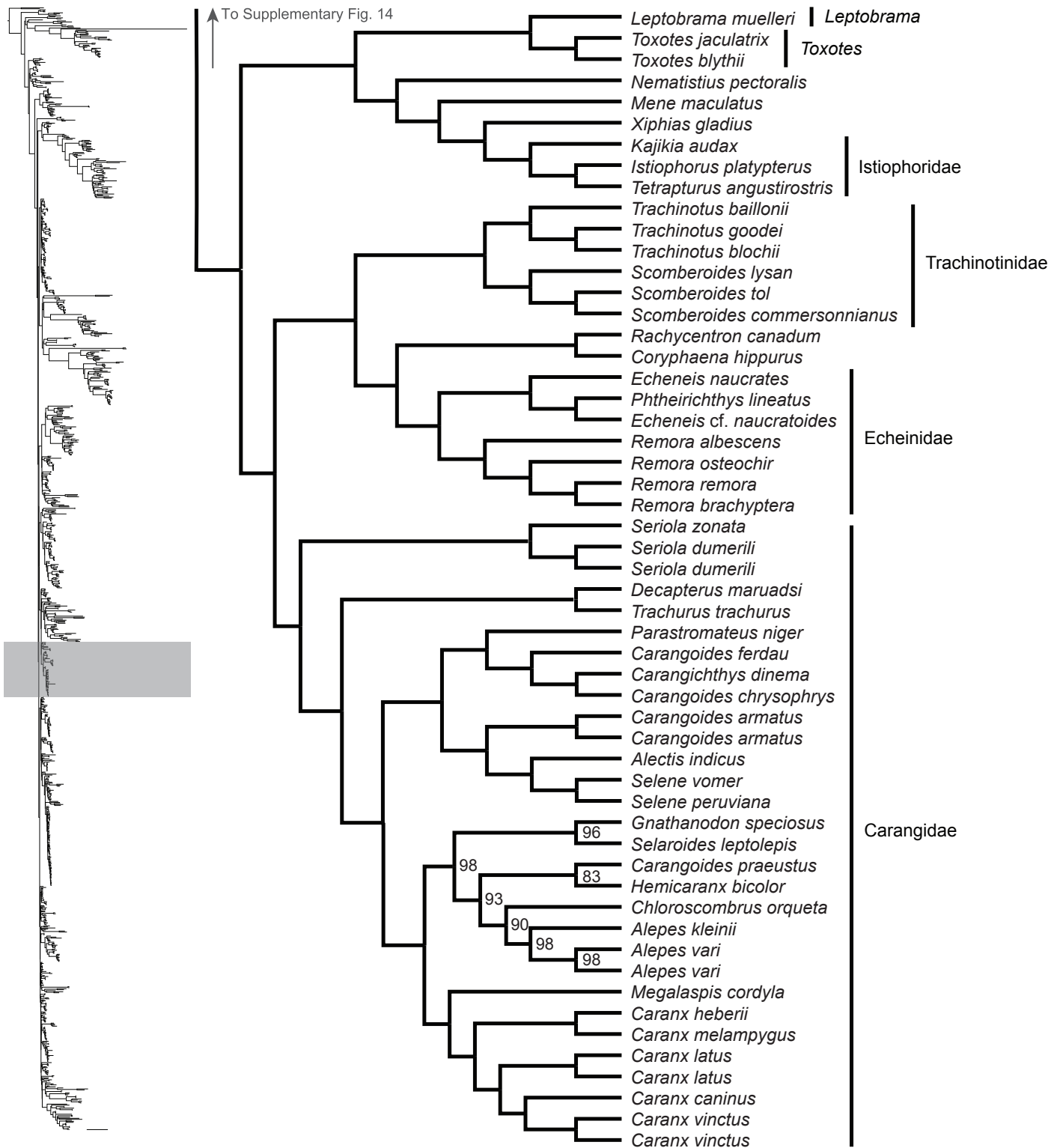
Supplementary Fig. 13: Maximum likelihood phylogeny inferred in IQ-TREE.

A guide tree on the left marks (with a gray rectangle), the region of the acanthomorph tree represented in the figure. All nodes have 100% bootstrap support. Orders, families or genera for taxa are listed to the right of the vertical black bars. Any tips left unassigned to a higher taxon are monospecific or monogeneric taxa.



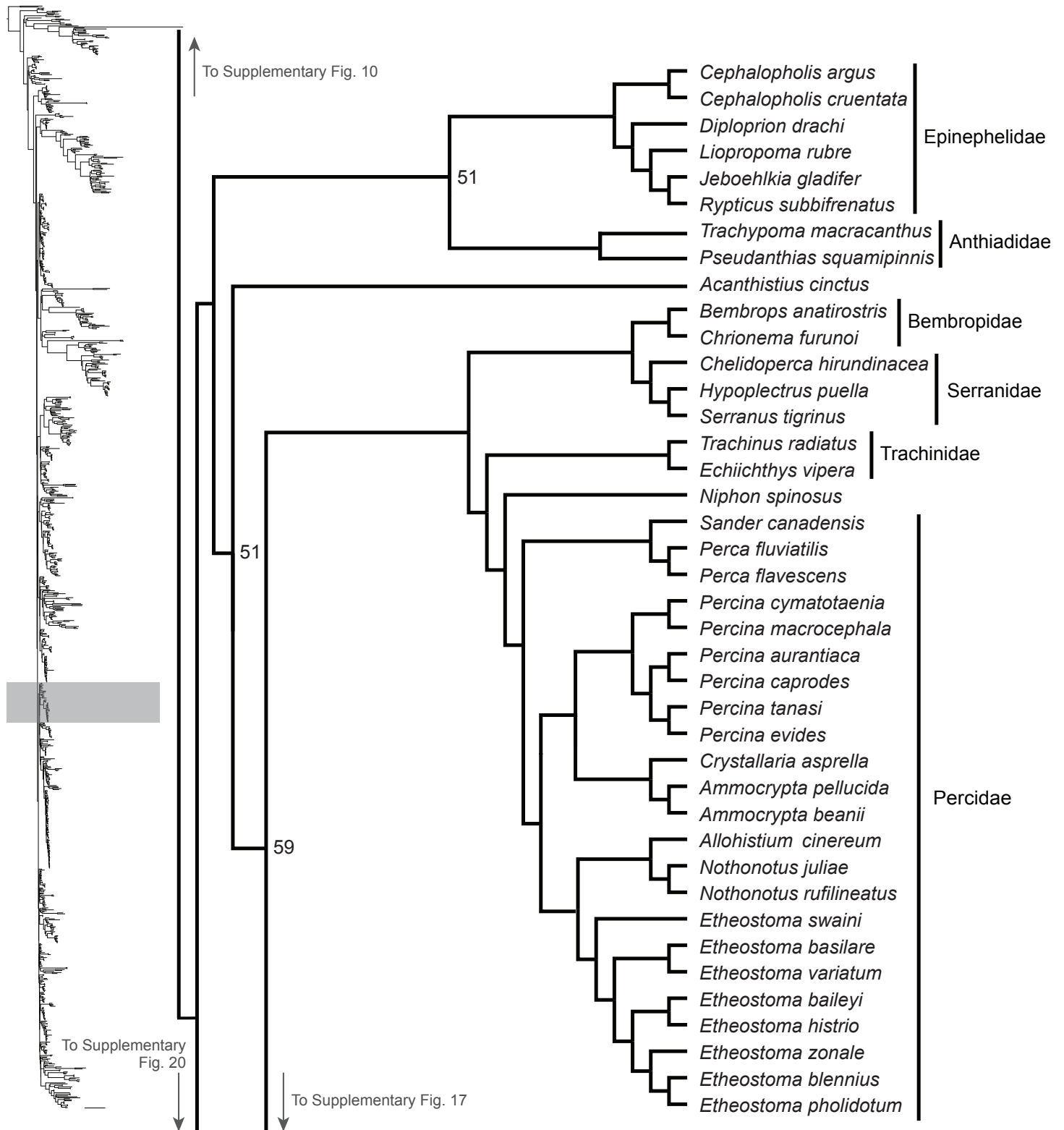
Supplementary Fig. 14: Maximum likelihood phylogeny inferred in IQ-TREE.

A guide tree on the left marks (with a gray rectangle), the region of the acanthomorph tree represented in the figure. Numbers at nodes reflect bootstrap support values. All nodes without a numerical annotation have 100% bootstrap support. Orders, families or genera for taxa are listed to the right of the vertical black bars. Any tips left unassigned to a higher taxon are monospecific or monogeneric taxa.



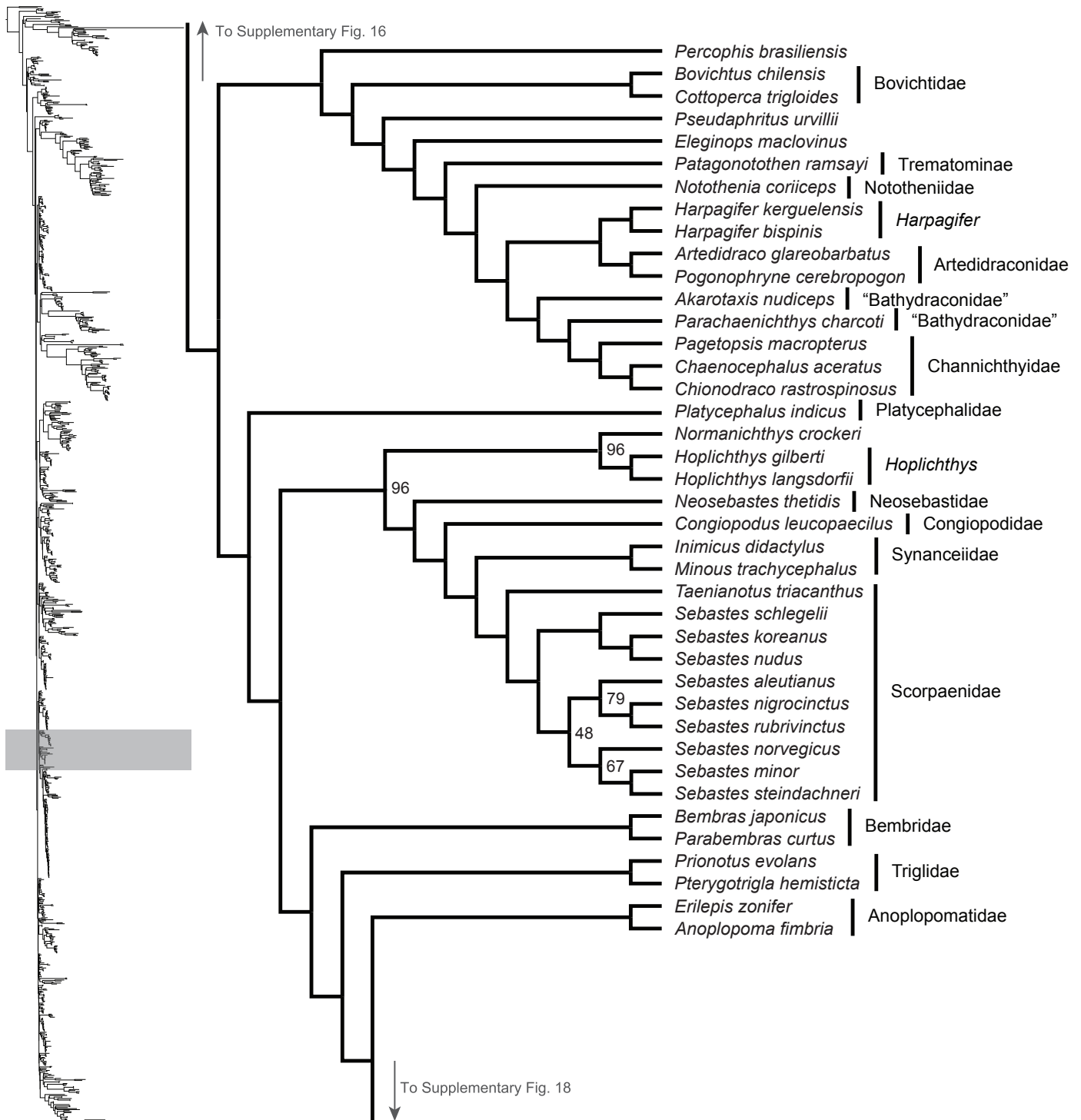
Supplementary Fig. 15: Maximum likelihood phylogeny inferred in IQ-TREE

A guide tree on the left marks (with a gray rectangle), the region of the acanthomorph tree represented in the figure. Numbers at nodes reflect bootstrap support values. All nodes without a numerical annotation have 100% bootstrap support. Orders, families or genera for taxa are listed to the right of the vertical black bars. Any tips left unassigned to a higher taxon are monospecific or monogeneric taxa.



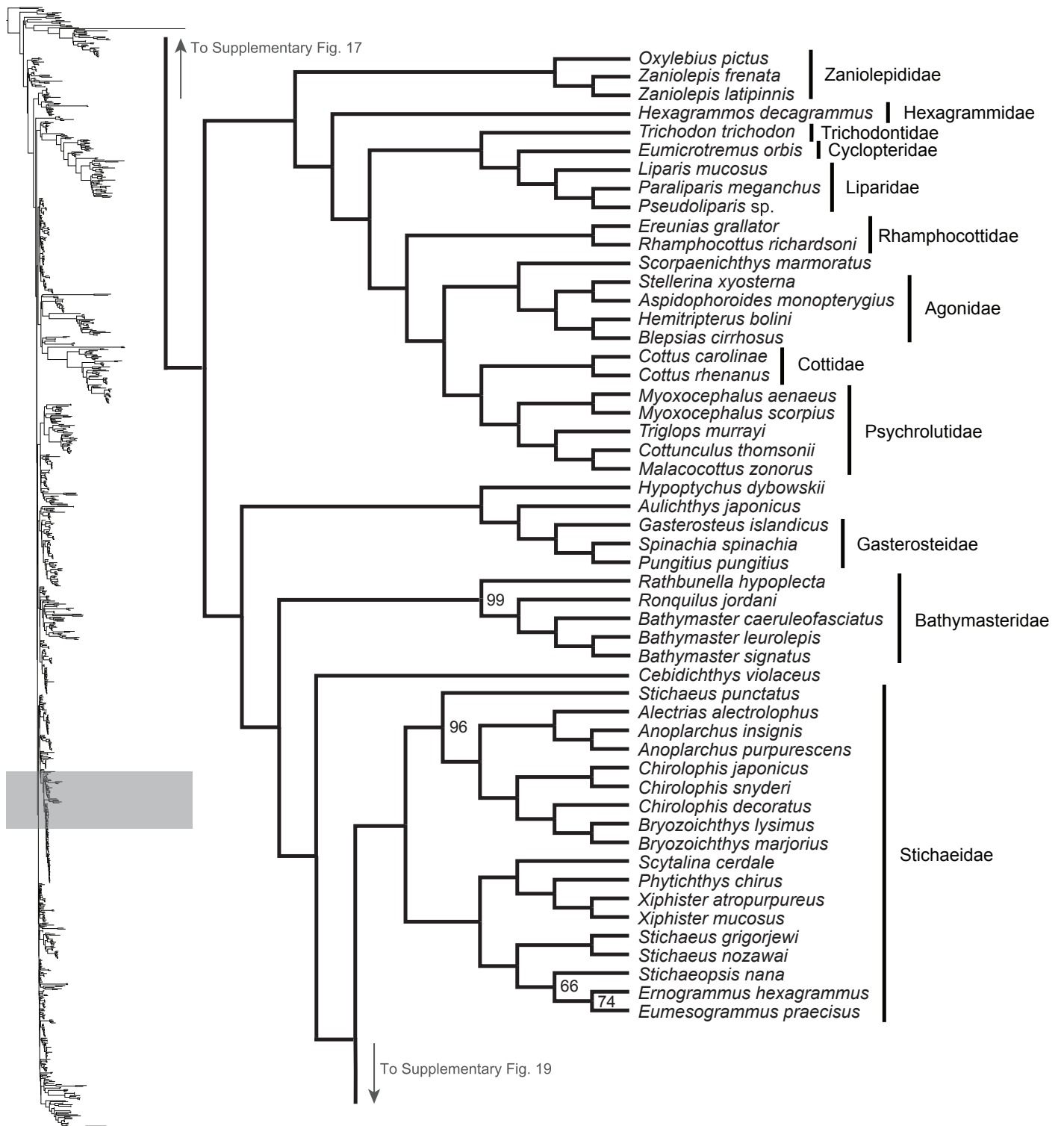
Supplementary Fig. 16: Maximum likelihood phylogeny inferred in IQ-TREE.

A guide tree on the left marks (with a gray rectangle), the region of the acanthomorph tree represented in the figure. Numbers at nodes reflect bootstrap support values. All nodes without a numerical annotation have 100% bootstrap support. Orders, families or genera for taxa are listed to the right of the vertical black bars. Any tips left unassigned to a higher taxon are monospecific or monogeneric taxa.



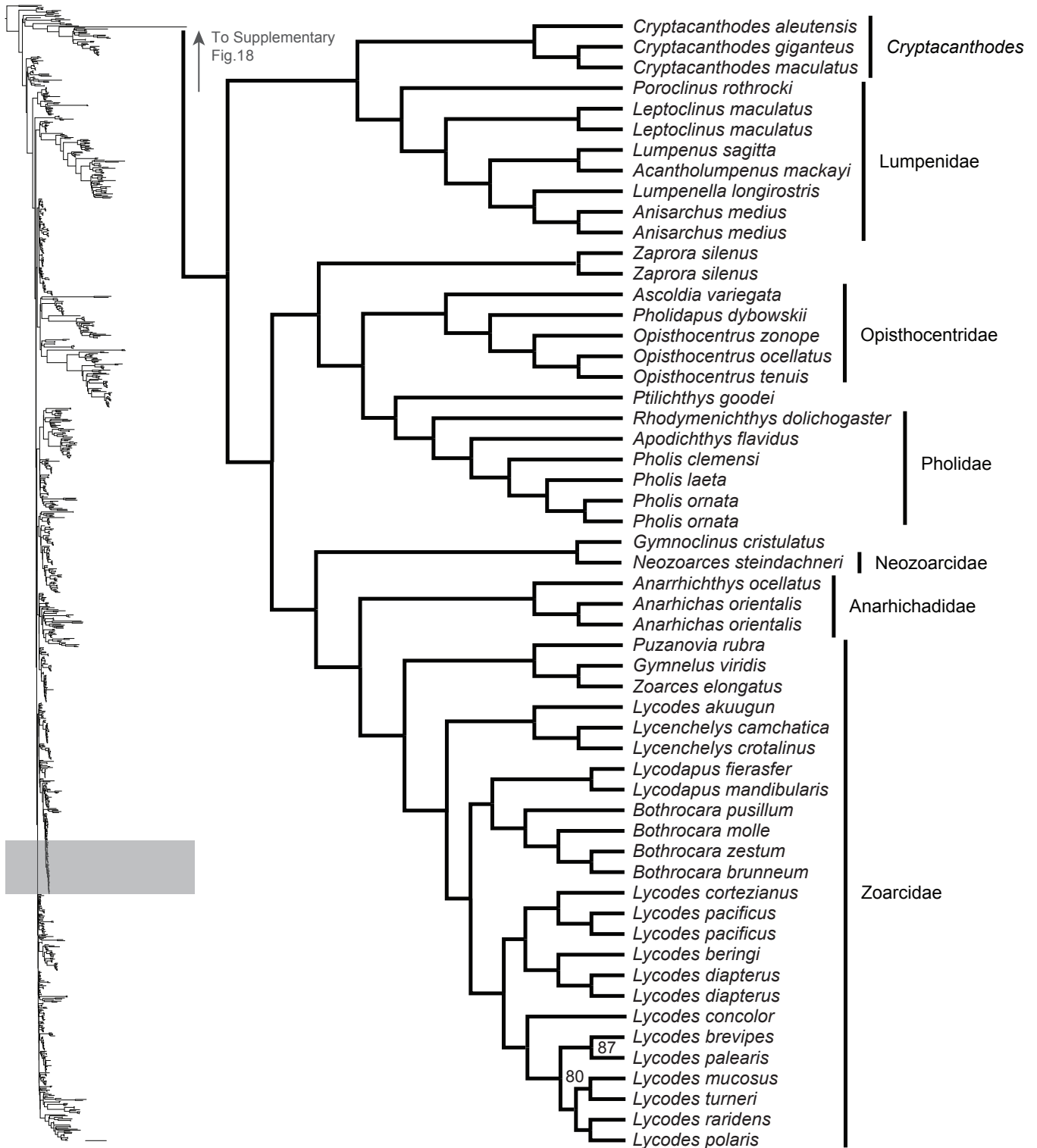
Supplementary Fig. 17: Maximum likelihood phylogeny inferred in IQ-TREE.

A guide tree on the left marks (with a gray rectangle), the region of the acanthomorph tree represented in the figure. Numbers at nodes reflect bootstrap support values. All nodes without a numerical annotation have 100% bootstrap support. Orders, families or genera for taxa are listed to the right of the vertical black bars. Any tips left unassigned to a higher taxon are monospecific or monogeneric taxa.



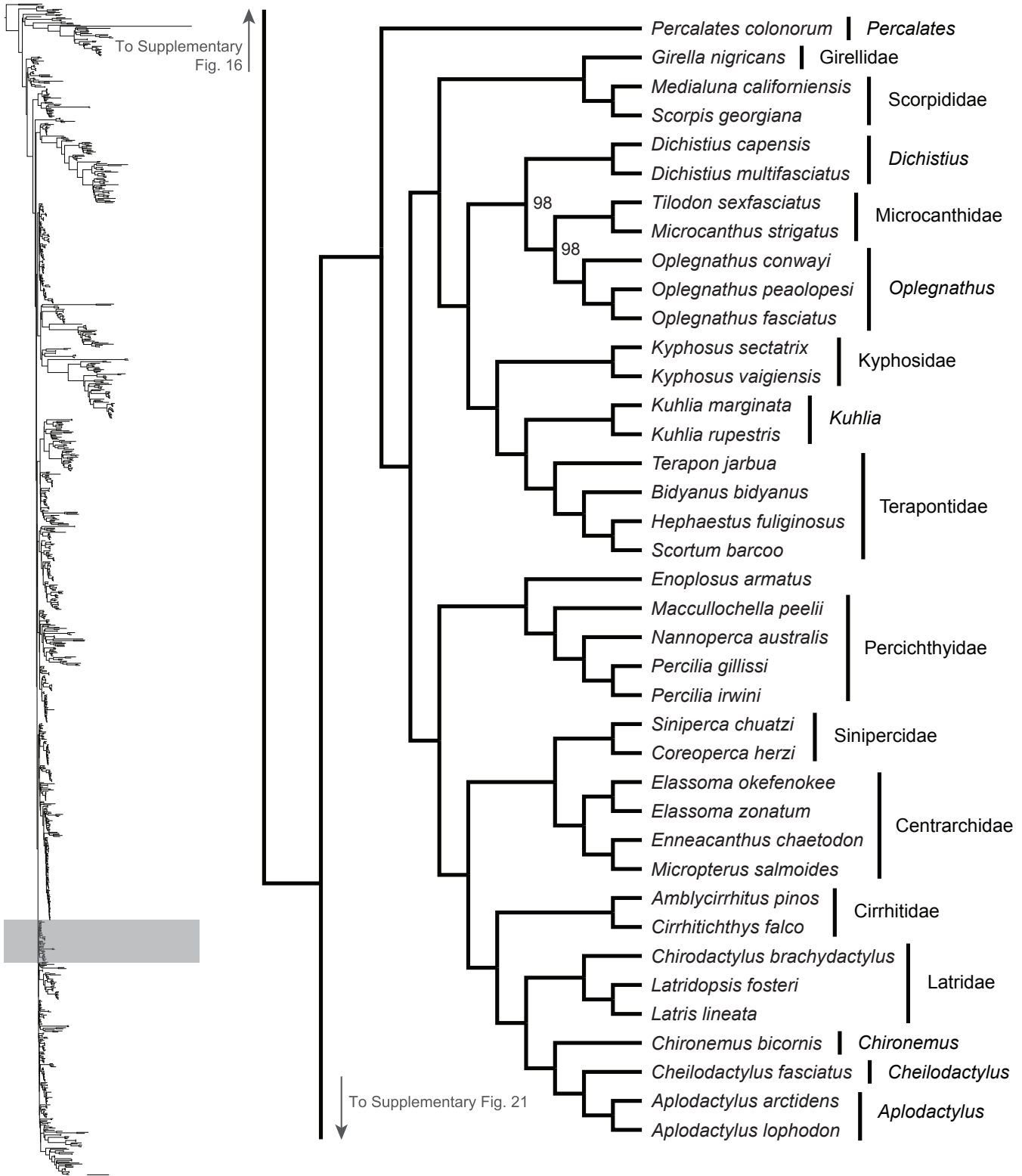
Supplementary Fig. 18: Maximum likelihood phylogeny inferred in IQ-TREE.

A guide tree on the left marks (with a gray rectangle), the region of the acanthomorph tree represented in the figure. Numbers at nodes reflect bootstrap support values. All nodes without a numerical annotation have 100% bootstrap support. Orders, families or genera for taxa are listed to the right of the vertical black bars. Any tips left unassigned to a higher taxon are monospecific or monogeneric taxa.



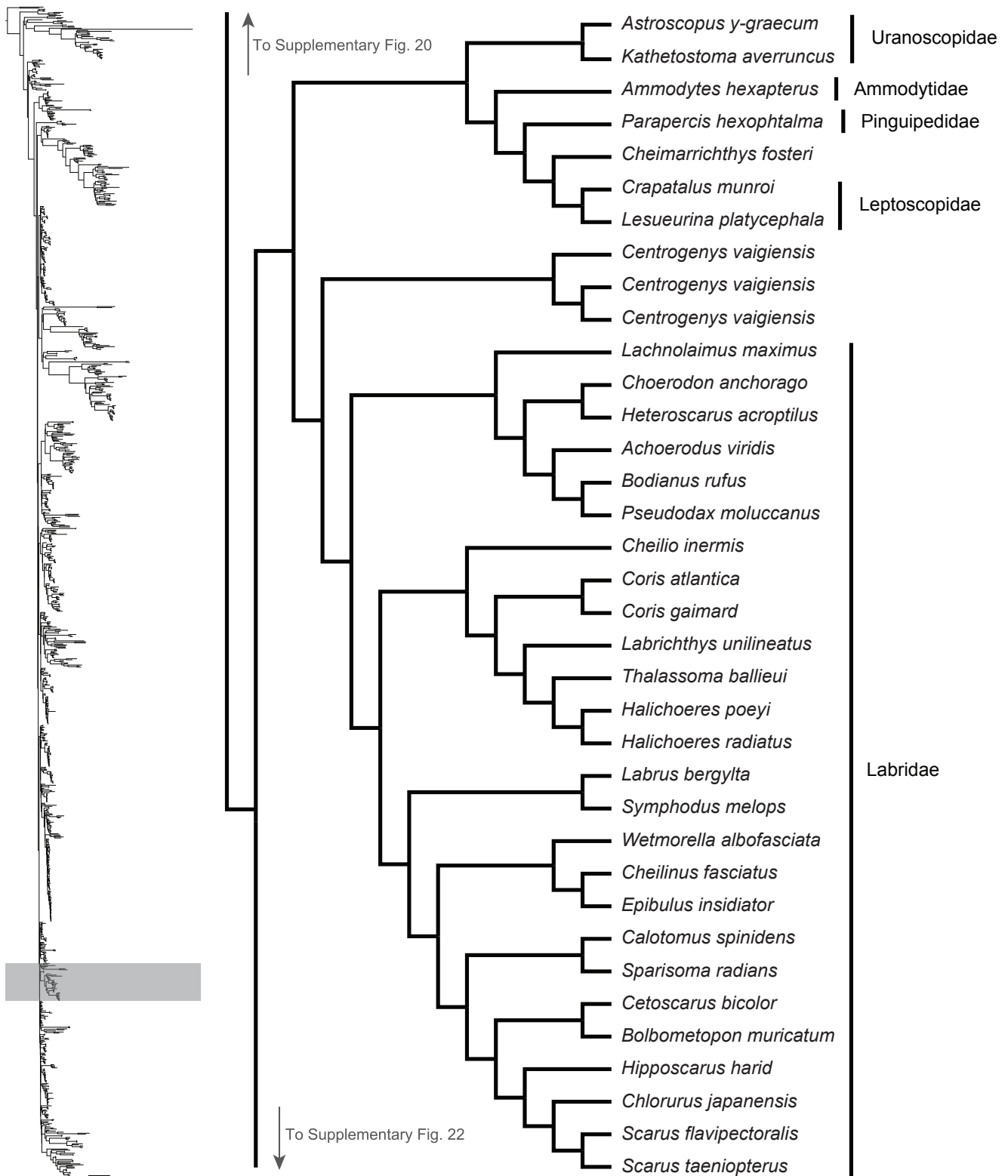
Supplementary Fig. 19: Maximum likelihood phylogeny inferred in IQ-TREE.

A guide tree on the left marks (with a gray rectangle), the region of the acanthomorph tree represented in the figure. Numbers at nodes reflect bootstrap support values. All nodes without a numerical annotation have 100% bootstrap support. Orders, families or genera for taxa are listed to the right of the vertical black bars. Any tips left unassigned to a higher taxon are monospecific or monogeneric taxa.



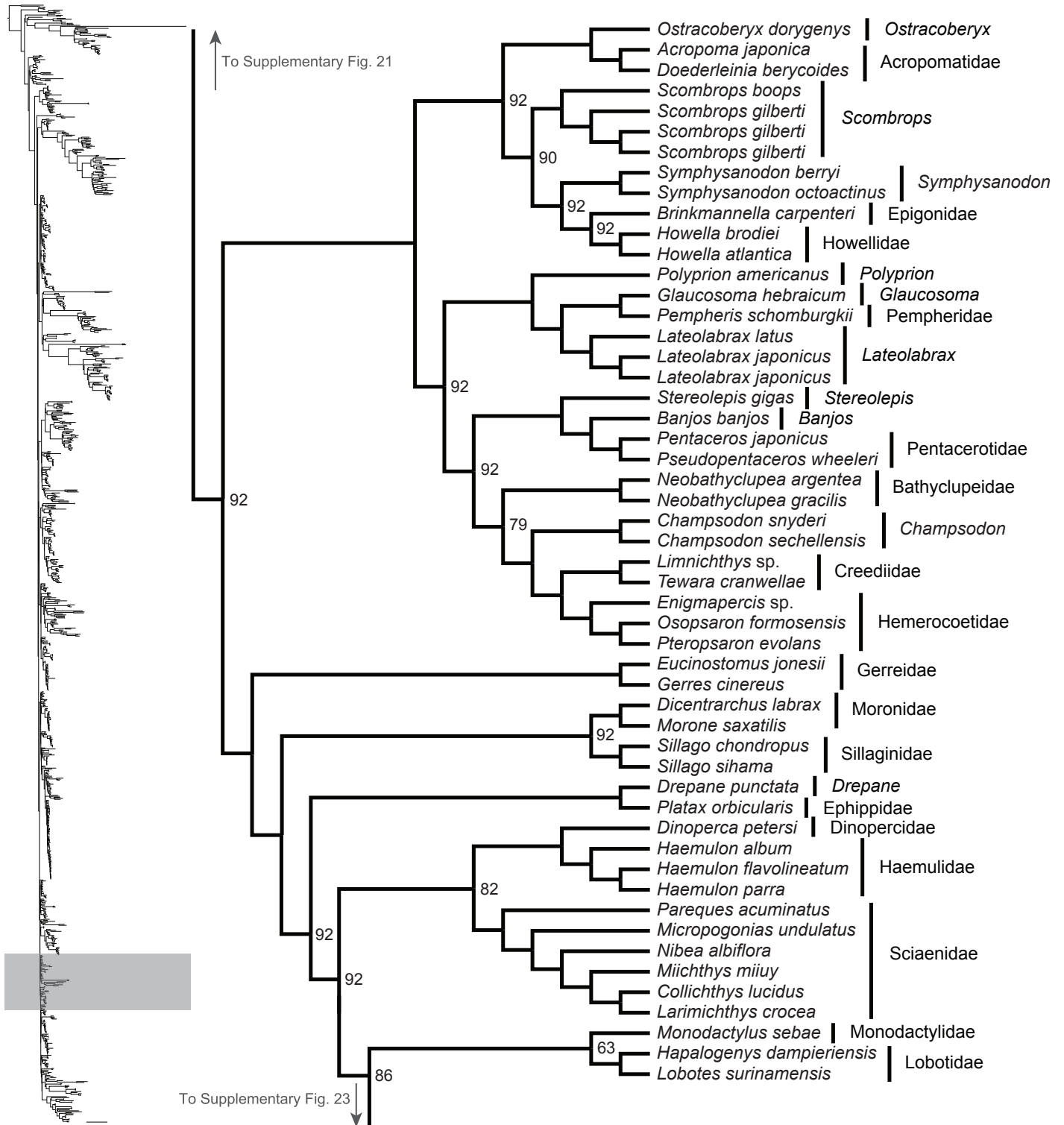
Supplementary Fig. 20: Maximum likelihood phylogeny inferred in IQ-TREE.

A guide tree on the left marks (with a gray rectangle), the region of the acanthomorph tree represented in the figure. Numbers at nodes reflect bootstrap support values. All nodes without a numerical annotation have 100% bootstrap support. Orders, families or genera for taxa are listed to the right of the vertical black bars. Any tips left unassigned to a higher taxon are monospecific or monogeneric taxa.



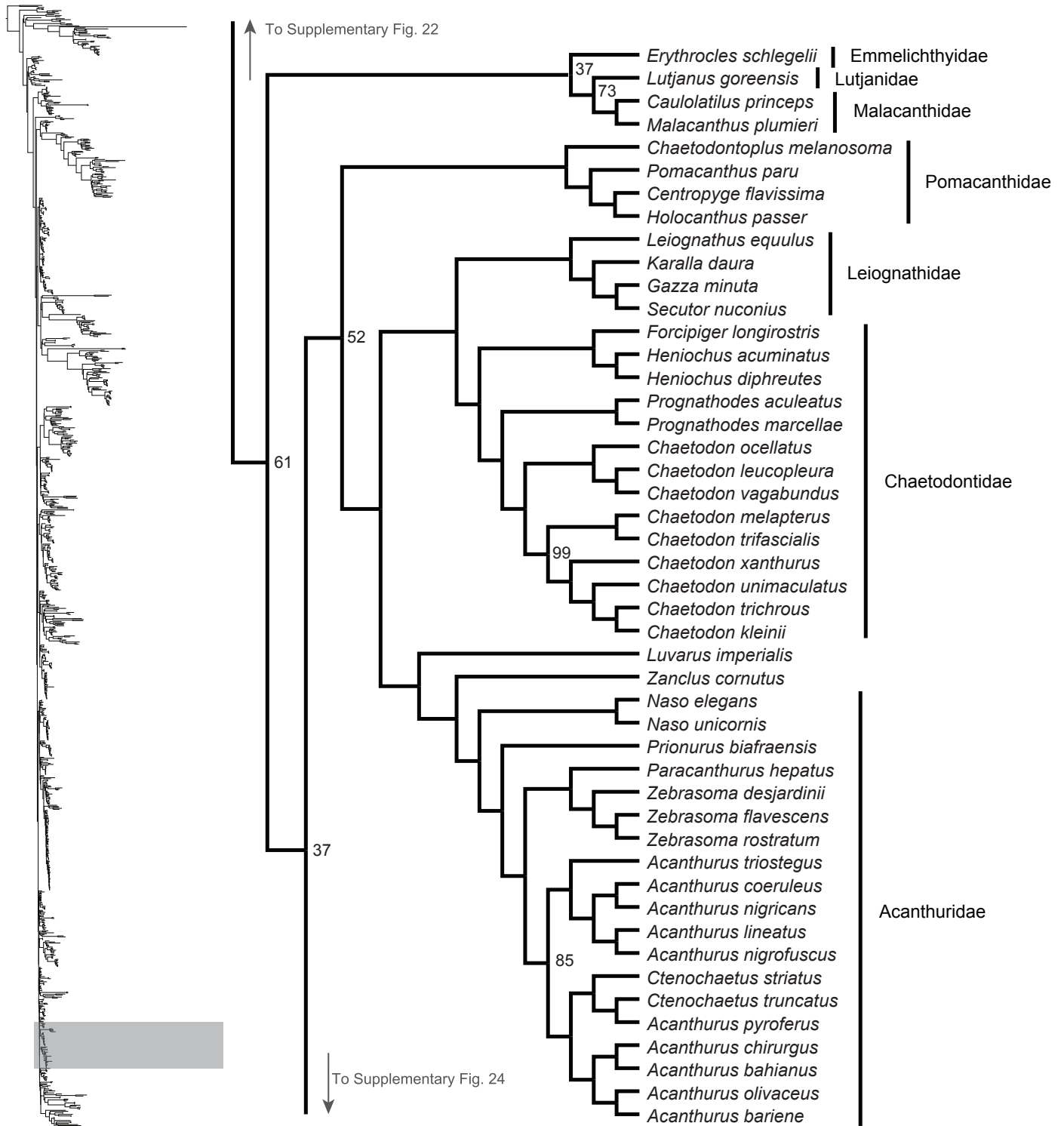
Supplementary Fig. 21: Maximum likelihood phylogeny inferred in IQ-TREE.

A guide tree on the left marks (with a gray rectangle), the region of the acanthomorph tree represented in the figure. All nodes have 100% bootstrap support. Orders, families or genera for taxa are listed to the right of the vertical black bars. Any tips left unassigned to a higher taxon are monospecific or monogeneric taxa.



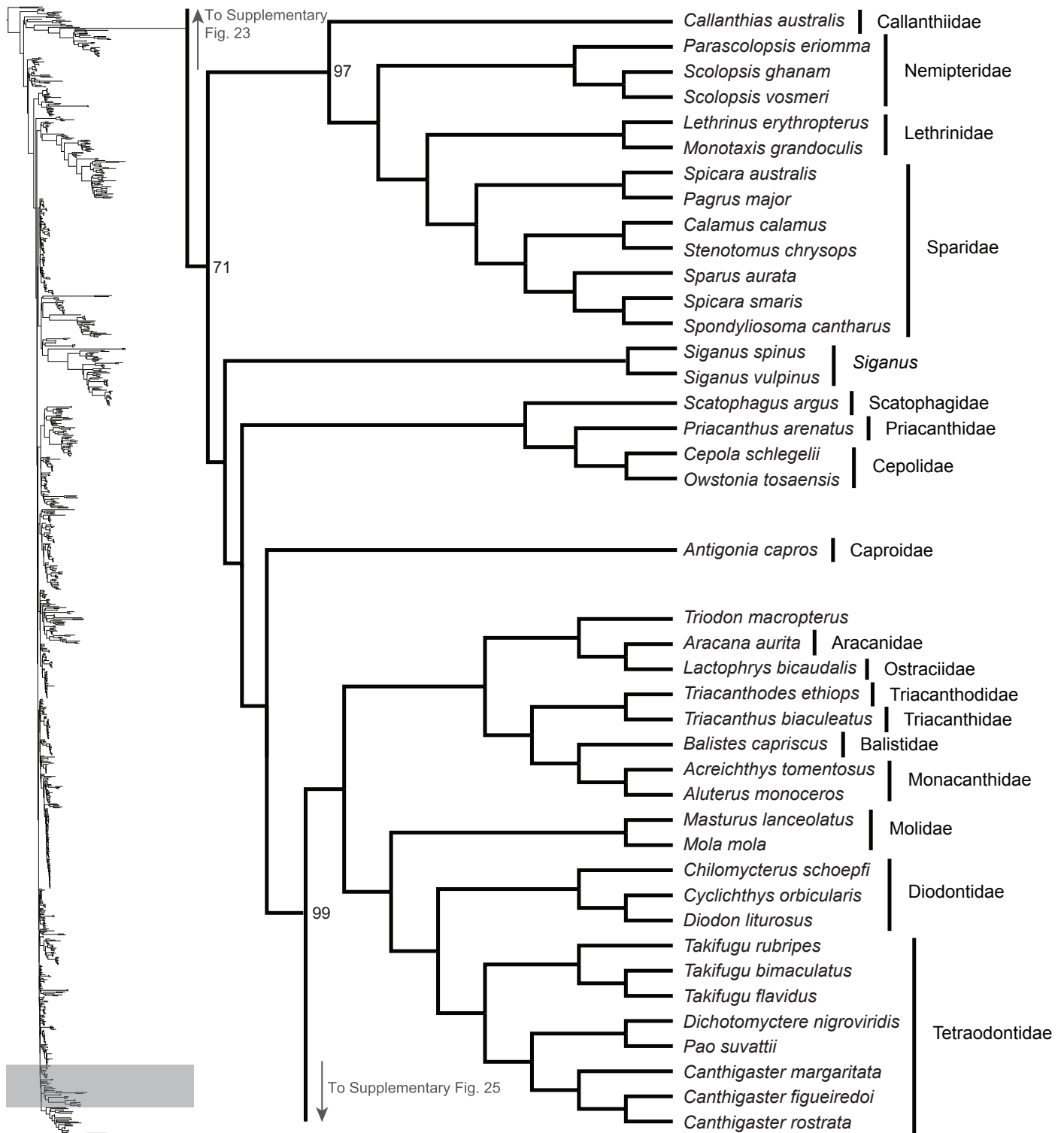
Supplementary Fig. 22: Maximum likelihood phylogeny inferred in IQ-TREE.

A guide tree on the left marks (with a gray rectangle), the region of the acanthomorph tree represented in the figure. Numbers at nodes reflect bootstrap support values. All nodes without a numerical annotation have 100% bootstrap support. Orders, families or genera for taxa are listed to the right of the vertical black bars.



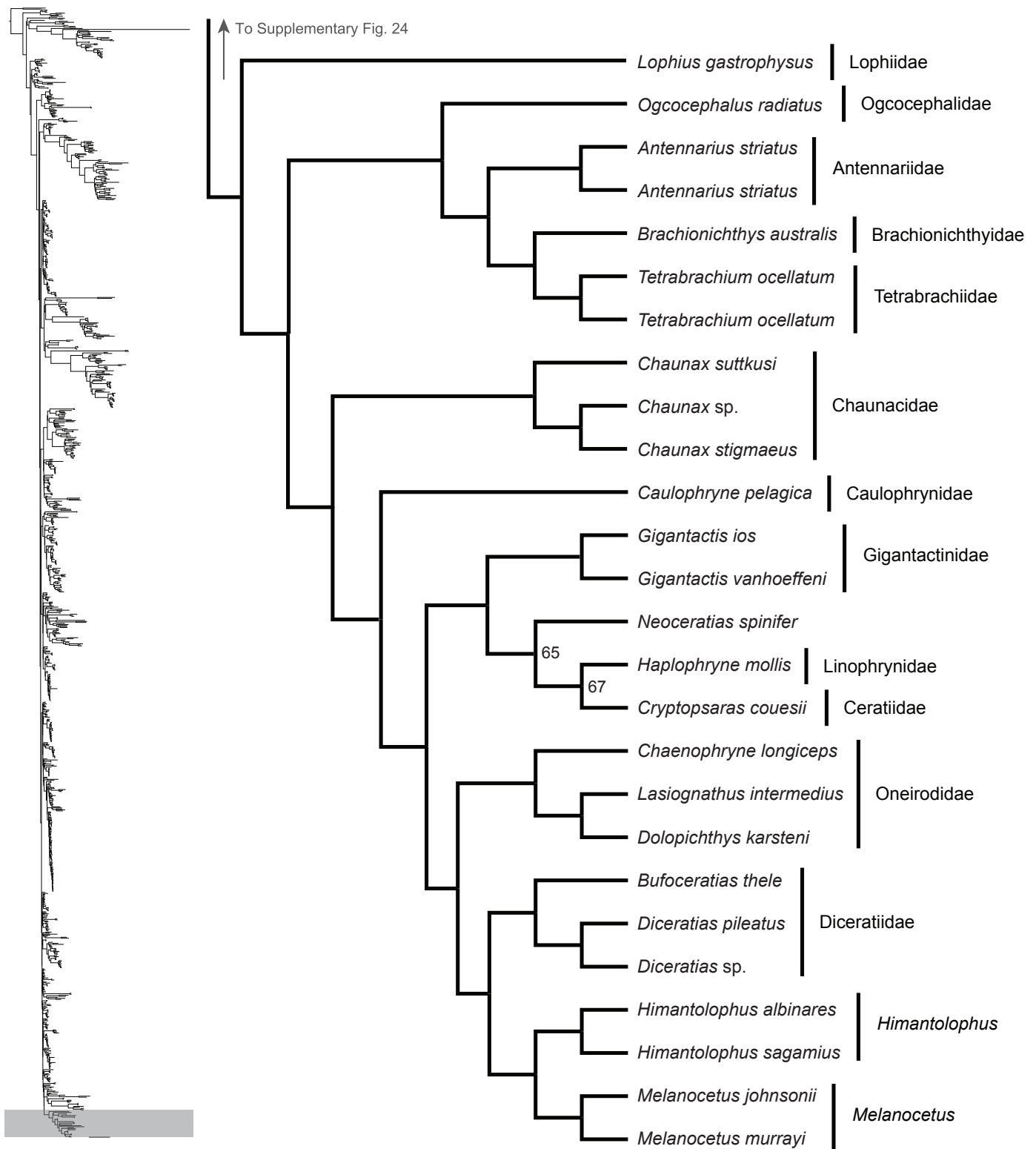
Supplementary Fig. 23: Maximum likelihood phylogeny inferred in IQ-TREE.

A guide tree on the left marks (with a gray rectangle), the region of the acanthomorph tree represented in the figure. Numbers at nodes reflect bootstrap support values. All nodes without a numerical annotation have 100% bootstrap support. Orders, families or genera for taxa are listed to the right of the vertical black bars. Any tips left unassigned to a higher taxon are monospecific or monogeneric taxa.



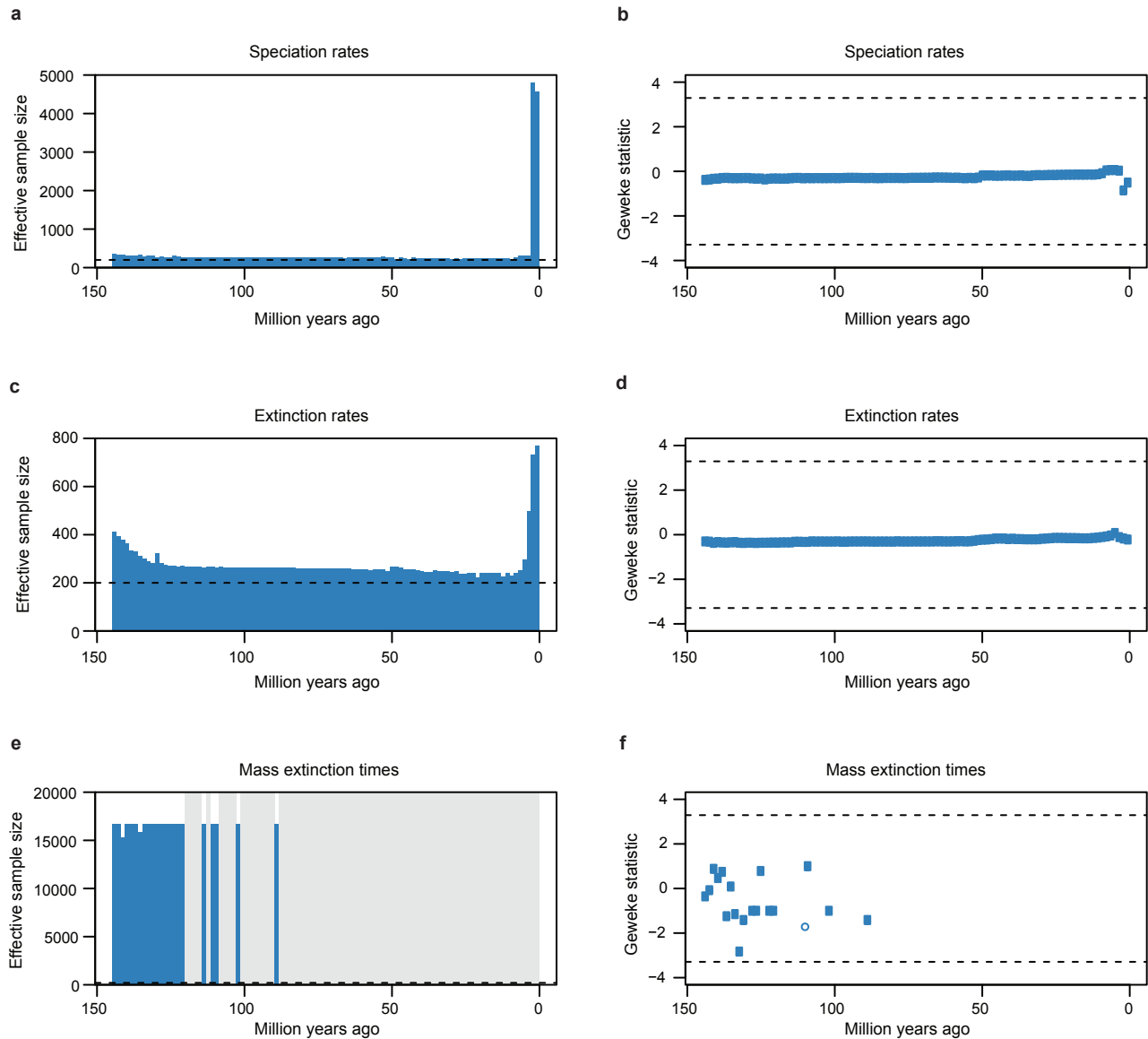
Supplementary Fig. 24: Maximum likelihood phylogeny inferred in IQ-TREE.

A guide tree on the left marks (with a gray rectangle), the region of the acanthomorph tree represented in the figure. Numbers at nodes reflect bootstrap support values. All nodes without a numerical annotation have 100% bootstrap support. Orders, families or genera for taxa are listed to the right of the vertical black bars. Any tips left unassigned to a higher taxon are monospecific taxa.



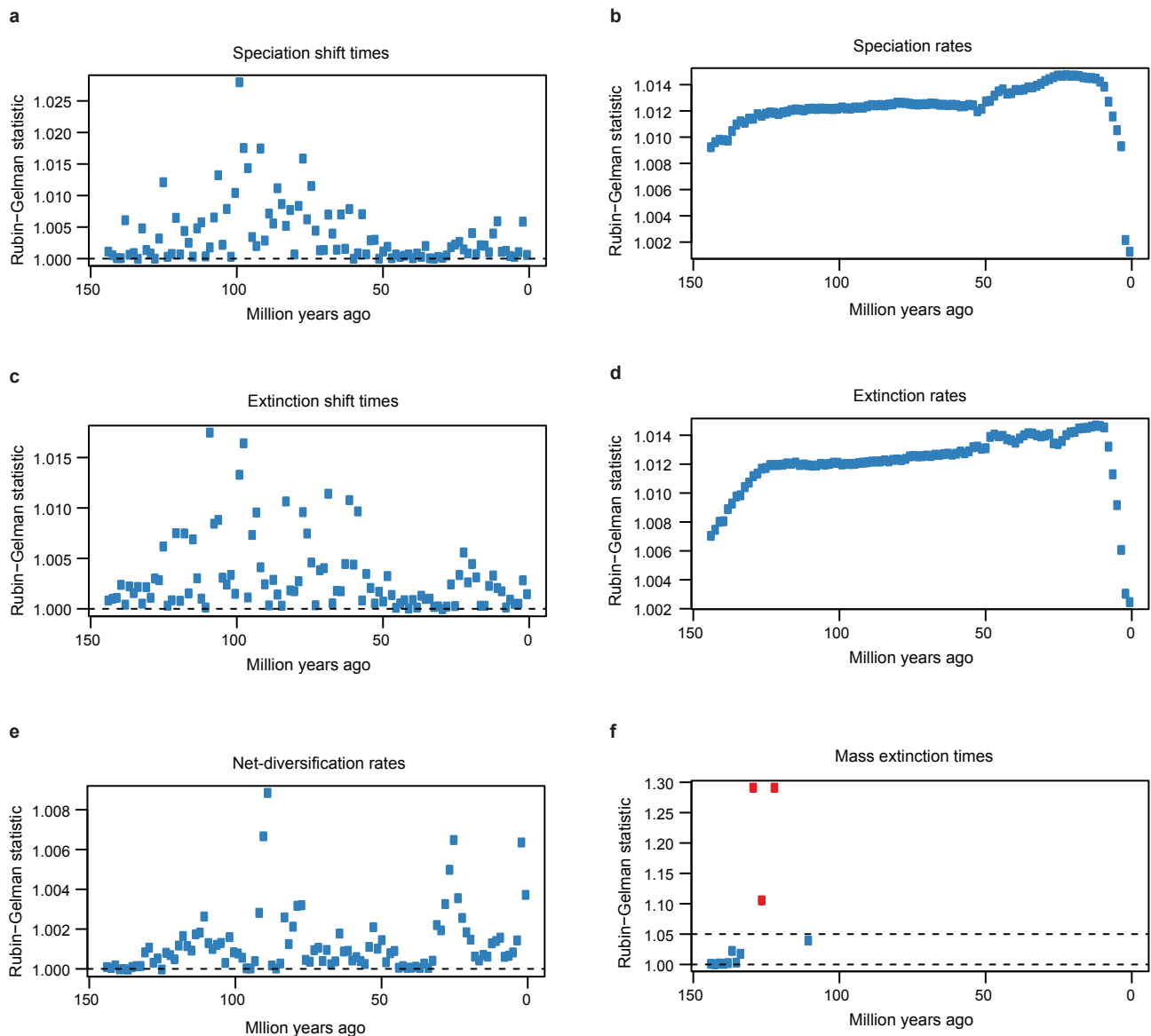
Supplementary Fig. 25: Maximum likelihood phylogeny inferred in IQ-TREE.

A guide tree on the left marks (with a gray rectangle), the region of the acanthomorph tree represented in the figure. Numbers at nodes reflect bootstrap support values. All nodes without a numerical annotation have 100% bootstrap support. Orders, families or genera for taxa are listed to the right of the vertical black bars. Any tips left unassigned to a higher taxon are monospecific or monogeneric taxa.

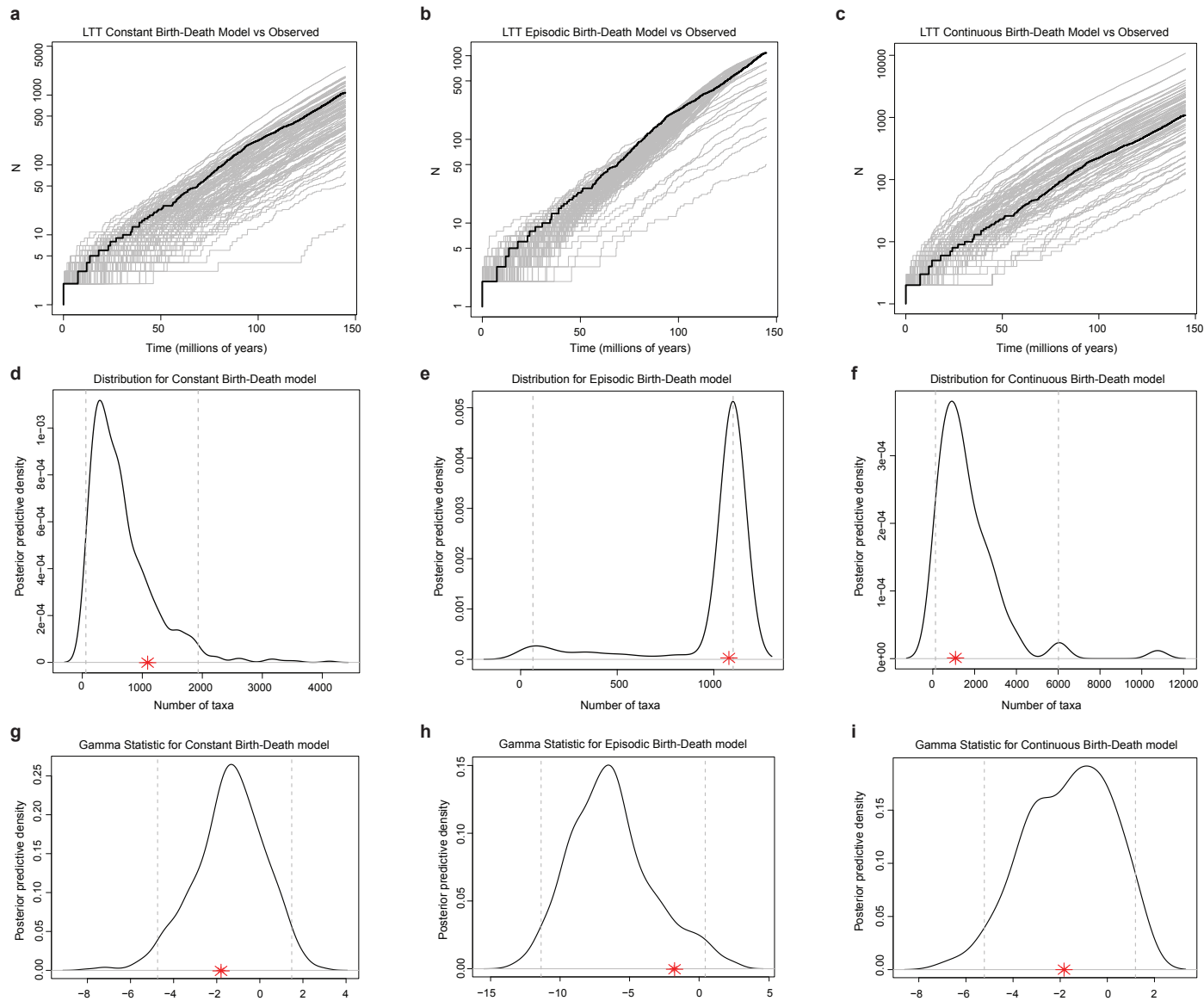


Supplementary Fig. 26: Effective sample sizes (ESS) of parameters and Geweke diagnostics reflect within-chain convergence in the TESS-CoMET analysis depicted in Extended Data Fig. 1.

Blue bars and dots reflect that the run successfully converged for the parameter at a given time interval. Horizontal dashed lines reflect canonical, acceptable threshold values or 95% confidence intervals for the two diagnostics (ESS ≥ 200 for **a**, **c**, and **e**; $P > 0.05$ for **b**, **d**, and **f**). **a**, Effective sample size for speciation rate estimates. **b**, Geweke statistic for post-burn-in speciation rate estimates. **c**, Effective sample size for extinction rate estimates. **d**, Geweke statistic for post-burn-in extinction rate estimates. **e**, Effective sample size for mass extinction times. **f**, Geweke statistic for post-burn-in mass extinction times.

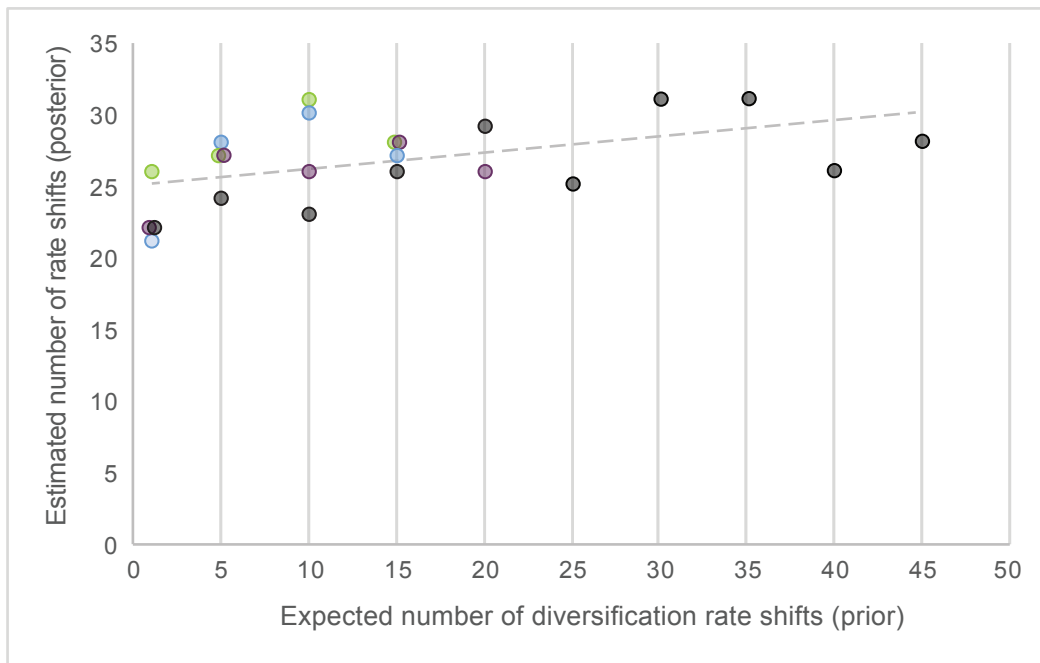


Supplementary Fig. 27: Results of the Gelman-Rubin test show convergence of three independent replicates of the TESS-CoMET analysis represented in Extended Data Fig. 1. Blue dots indicate that the ratio of within-chain variance to between-chain variance is <1.05 , suggesting the independent MCMC simulations have converged on the same distribution of parameter values. Red dots indicate failed convergence of runs for those time interval-specific parameter estimates. Horizontal dashed lines represent the ideal value (1.00) for the diagnostic. **a**, Rubin-Gelman statistic for speciation shift times. **b**, Rubin-Gelman statistic for speciation rates. **c**, Rubin-Gelman statistic for extinction shift times. **d**, Rubin-Gelman statistic for extinction rates. **e**, Rubin-Gelman statistic for net-diversification rates. **f**, Rubin-Gelman statistic for mass extinction time estimates. A second horizontal dashed line marks the critical value (1.05) above which the test is considered to have failed for that estimate.



Supplementary Fig. 28: Assessment of the absolute fit of three candidate birth-death (BD) models to the time-calibrated phylogeny of Acanthomorpha.

Figures **a-c** compare lineage-through-time (LTT) curves for simulated trees under a given model (grey lines) to the LTT curve observed for the acanthomorph phylogeny (black line). Figures **d-e** plot the posterior-predictive distributions for the total number of species estimated to exist in the tree under each model. Dashed lines represent the 95% credible interval for the distribution and red asterisks indicate the total number of acanthomorph species (1,075) in the empirical dataset. Figures **g-i** plot the posterior-predictive distributions for the gamma statistic. Dashed lines represent the 95% credible interval for the distribution and red asterisks indicate the value of the gamma statistic empirically calculated for the acanthomorph phylogeny. Candidate models include: 1.) a constant rate birth-death model, 2.) an episodic birth-death model with a rate shift 50 Mya and 3.) a birth-death model with decreasing speciation rates through time. All three candidate models assume uniform (random) incomplete taxon sampling.



Supplementary Fig. 29: The posterior number of shifts in speciation rates inferred in BAMM is weakly predicted by the prior.

Our BAMM analyses used varying numbers of expected speciation rate shifts, and so the resulting maximum shift credibility (MSC) configurations displayed different numbers of estimated rate shifts, shown here as a scatterplot. The slope of the dashed, regression line (0.1049) suggests that changing the inputted prior parameter does not greatly affect the posterior prediction ($y = 0.1049x + 25.063$; R-squared= 0.217). The standard error of the prior coefficient is 0.0436 and of the intercept is 0.8393. This correlation analysis was performed using base R functions. Colors of data points correspond to the settings used when running Markov Chain Monte Carlo (MCMC) simulations in BAMM: black corresponds to 4 MCMC chains in the analysis with a deltaT of 0.05, purple corresponds to 4 MCMC chains in the analysis with a deltaT of 0.1, blue corresponds to 2 MCMC chains in the analysis with a deltaT of 0.05, and green corresponds to 2 MCMC chains in the analysis with a deltaT of 0.1.

Supplementary Table 1: Binomial names and higher taxonomic classification of species included in the phylogeny, institutional voucher information for specimens (if applicable), and NCBI SRA BioSample accession numbers. The sixth column (‘Morphology Analyses’) denotes whether species were included in the body shape analyses, and the seventh column (‘Concordance Analyses’) denotes if samples were included in the BUCKy concordance factor analyses. NCBI BioSample numbers denoted with an asterisk (*) indicate samples for which UCE data were extracted from whole genome sequence data.

Order	Higher Taxa (Family or Genus)	Species Name	Voucher ID	NCBI BioSample	Morphology Analyses	Concordance Analyses
Aulopiformes	Alepisauridae	<i>Alepisaurus ferox</i>	YPM ICH 25657	SAMN05915027	✓	
Aulopiformes	Paralepididae	<i>Notolepis coatsi</i>	YPM ICH 022576	SAMN22936233	✓	
Myctophiformes	Myctophidae	<i>Benthoosema glaciale</i>	See NCBI SRA	SAMEA4028768*	✓	
Myctophiformes	Myctophidae	<i>Ceratoscopelus warmingii</i>	SIO 0510-09-28	SAMN05915048	✓	
Myctophiformes	Myctophidae	<i>Dasyscopelus selenops</i>	YPM ICH 25697	SAMN22936213	✓	✓
Myctophiformes	Myctophidae	<i>Notoscopelus caudispinosus</i>	YPM ICH 028430	SAMN22936234	✓	
Myctophiformes	Neoscopelidae	<i>Neoscopelus macrolepidotus</i>	ASIZP 0913636	SAMN22936223	✓	
Myctophiformes	Neoscopelidae	<i>Neoscopelus microchir</i>	ASIZO 0910701	SAMN22936223	✓	✓
Myctophiformes	Neoscopelidae	<i>Scopelengys tristis</i>	UW 115136	SAMN22936364	✓	
Lampriformes	<i>Lampris</i>	<i>Lampris guttatus</i>	SIO 04-195	SAMN05915079	✓	✓
Lampriformes	Regalecidae	<i>Regalecus glesne</i>	YPM ICH 26237	SAMN05915116		
Lampriformes	Trachipteridae	<i>Zu elongatus</i>	NMNZ P.042029/TS3	SAMN05915140	✓	✓
Polymixiiformes	<i>Polymixia</i>	<i>Polymixia lowei</i>	YPM ICH 025498	SAMN05915104	✓	✓
Percopsiformes		<i>Aphredoderus sayanus</i>	YPM ICH 25183	SAMN05915031	✓	✓
Percopsiformes	Amblyopsidae	<i>Typhlichthys subterraneus</i>	See NCBI SRA	SAMEA4028771*	✓	
Percopsiformes	Percopsidae	<i>Percopsis omiscomycus</i>	YPM ICH 017307	SAMN05915097		✓
Percopsiformes	Percopsidae	<i>Percopsis transmontana</i>	See NCBI SRA	SAMEA4028770*		
Zeiformes	Parazenidae	<i>Cyttopsis rosea</i>	See NCBI SRA KUIT 2929, MCZ 155779	SAMEA4028773*	✓	✓
Zeiformes	Zeidae	<i>Zenopsis conchifera</i>		SAMN05915138	✓	
Zeiformes	Zeidae	<i>Zeus faber</i>	NSMT 62233	SAMN05915139	✓	✓
Stylephoriformes		<i>Stylephorus chordatus</i>	YPM ICH 25672	SAMN05915127	✓	✓
Gadiformes	<i>Bregmaceros</i>	<i>Bregmaceros cantori</i>	See NCBI SRA	SAMEA4028775*	✓	✓
Gadiformes	<i>Melanonus</i>	<i>Melanonus zugmayeri</i>	See NCBI SRA	SAMEA4028779*	✓	
Gadiformes	Muraenolepididae	<i>Muraenolepis marmoratus</i>	See NCBI SRA	SAMEA4028780*		
Gadiformes	Trachyrincidae	<i>Trachyrincus murrayi</i>	See NCBI SRA	SAMEA4028782*		
Gadiformes	Trachyrincidae	<i>Trachyrincus scabrurus</i>	See NCBI SRA	SAMEA4028781*		
Gadiformes	Moridae	<i>Laemonema laureysi</i>	See NCBI SRA	SAMEA4028784*	✓	
Gadiformes	Moridae	<i>Mora moro</i>	See NCBI SRA	SAMEA4028783*	✓	
Gadiformes	Macrouridae	<i>Bathygadus melanobranchus</i>	See NCBI SRA	SAMEA4028785*	✓	
Gadiformes	Macrouridae	<i>Coryphaenoides rupestris</i>	YPM ICH 025367	SAMN05915057	✓	

Gadiformes	Macrouridae	<i>Coryphaenoides rupestris</i>	See NCBI SRA	SAMN08010939*	
Gadiformes	Macrouridae	<i>Macrourus berglax</i>	See NCBI SRA	SAMEA4028786*	✓
Gadiformes	Macrouridae	<i>Malacocephalus occidentalis</i>	See NCBI SRA	SAMEA4028787*	✓
Gadiformes	Merlucciidae	<i>Merluccius capensis</i>	See NCBI SRA	SAMEA4028778*	
Gadiformes	Merlucciidae	<i>Merluccius merluccius</i>	See NCBI SRA	SAMEA4028777*	✓
Gadiformes	Phycidae	<i>Lotella phycis</i>	See NCBI SRA	SAMEA4028789*	
Gadiformes	Phycidae	<i>Phycis blennoides</i>	See NCBI SRA	SAMEA4028788*	✓
Gadiformes		<i>Lota lota</i>	See NCBI SRA	SAMEA4028790*	✓
Gadiformes	Lotidae	<i>Brosme brosme</i>	See NCBI SRA	SAMEA4028792*	✓
Gadiformes	Lotidae	<i>Molva molva</i>	See NCBI SRA	SAMEA4028791*	✓
Gadiformes	Gadidae	<i>Arctogadus glacialis</i>	See NCBI SRA	SAMEA4028798*	
Gadiformes	Gadidae	<i>Boreogadus saida</i>	See NCBI SRA	SAMEA4028799*	✓
Gadiformes	Gadidae	<i>Gadiculus argenteus</i>	See NCBI SRA	SAMEA4028794*	✓
Gadiformes	Gadidae	<i>Gadus chalcogrammus</i>	See NCBI SRA	SAMEA4028800*	
Gadiformes	Gadidae	<i>Gadus morhua</i>	YPM ICH 020859	SAMN05915065	✓ ✓
Gadiformes	Gadidae	<i>Gadus morhua</i>	See NCBI SRA	SAMEA4028801*	
Gadiformes	Gadidae	<i>Melanogrammus aeglefinus</i>	See NCBI SRA	SAMEA104602249*	✓
Gadiformes	Gadidae	<i>Merlangius merlangus</i>	See NCBI SRA	SAMEA4028797*	✓
Gadiformes	Gadidae	<i>Pollachius virens</i>	See NCBI SRA	SAMEA4028795*	✓
Gadiformes	Gadidae	<i>Trisopterus minutus</i>	See NCBI SRA	SAMEA4028793*	✓
Trachichthyiformes	Diretmidae	<i>Diretmoides pauciradiatus</i>	YPM ICH 028266 Pers. Coll.: N. Merrett, "JMS"	SAMN22936030	✓
Trachichthyiformes	Diretmidae	<i>Diretmus argenteus</i>		SAMN22936031	✓
Trachichthyiformes	Anomalopidae	<i>Anomalops katoptron</i>	YPM ICH 020676	SAMN22935859	
Trachichthyiformes	Monocentridae	<i>Monocentris japonica</i>	YFTC 13715	SAMN22936203	✓
Trachichthyiformes	<i>Anoplogaster</i>	<i>Anoplogaster cornuta</i>	YPM ICH 025640	SAMN05915028	✓ ✓
Trachichthyiformes	Trachichthyidae	<i>Aulotrachichthys prosthemiis</i>	ASIZD 0910678	SAMN22935879	
Trachichthyiformes	Trachichthyidae	<i>Hoplostethus occidentalis</i>	YFTC 14563, n.v.	SAMN22936107	✓
Trachichthyiformes	Trachichthyidae	<i>Paratrachichthys sajademalensis</i>	YFTC 14534, n.v.	SAMN22935880	
Beryciformes	Holocentridae	<i>Holocentrus rufus</i>	See NCBI SRA	SAMEA4028806*	✓ ✓
Beryciformes	Holocentridae	<i>Myripristis jacobus</i>	See NCBI SRA	SAMEA4028805*	✓
Beryciformes	Holocentridae	<i>Myripristis leiognathus</i>	Pers. Coll.: M.Alfaro, Alfaro 875	SAMN05915086	✓
Beryciformes	Holocentridae	<i>Myripristis violacea</i>	Pers. Coll.: P.Wainwright, PW2260B	SAMN05915087	✓ ✓
Beryciformes	Holocentridae	<i>Neoniphon sammara</i>	See NCBI SRA	SAMEA4028807*	✓
Beryciformes	Holocentridae	<i>Sargocentron coruscum</i>	YPM ICH 23957	SAMN05915119	✓
Beryciformes	Berycidae	<i>Beryx decadactylus</i>	YFTC 13731, n.v.	SAMN22935898	✓
Beryciformes	Berycidae	<i>Beryx splendens</i>	See NCBI SRA	SAMEA4028808*	✓
Beryciformes	Berycidae	<i>Centroberyx druzhinini</i>	ASIZD 0911026	SAMN22935940	✓
Beryciformes	Melamphaidae	<i>Melamphaes longivelis</i>	YPM ICH 028501	SAMN22936191	✓
Beryciformes	Melamphaidae	<i>Poromitra gibbsi</i>	YPM ICH 028486	SAMN22936312	✓

Beryciformes	Melamphaidae	<i>Scopelogadus beanii</i>	YPM ICH 028434	SAMN22936365	✓
Beryciformes	<i>Rondeletia</i>	<i>Rondeletia bicolor</i>	YPM ICH 027515	SAMN22936342	✓
Beryciformes	<i>Rondeletia</i>	<i>Rondeletia loricata</i>	YPM ICH 25674	SAMN05915117	✓
Beryciformes	Cetomimidae	<i>Ataxolepis apus</i>	YPM ICH 025531	SAMN22935874	
Beryciformes	Cetomimidae	<i>Cetostoma regani</i>	YPM ICH 028287	SAMN22935948	✓
Beryciformes	Cetomimidae	<i>Ditropichthys storeri</i>	YPM ICH 028280	SAMN22936032	✓
Beryciformes	Cetomimidae	<i>Mirapinna esau</i>	YFTC 26026, n.v.	SAMN22936319	
Beryciformes		<i>Barbourisia rufa</i>	YPM ICH 010068	SAMN22935887	✓ ✓
Beryciformes	Stephanoberycidae	<i>Acanthochaenus luetkenii</i>	YFTC 24122, n.v.	SAMN22935827	✓
Beryciformes	Stephanoberycidae	<i>Acanthochaenus luetkenii</i>	YFTC 24124, n.v.	SAMN22935828	
Beryciformes	Stephanoberycidae	<i>Malacosarcus macrostoma</i>	USNM 400019	SAMN22936184	
Ophidiiformes	Dinematichthyidae	<i>Diancistrus jeffjohnsoni</i>	YFTC 32439, n.v. KUIT 674, USNM	SAMN22936017	✓
Ophidiiformes	Dinematichthyidae	<i>Dinematichthys iluocoeteoides</i>	334123 KUIT 676, USNM	SAMN22936025	✓
Ophidiiformes	Dinematichthyidae	<i>Diancistrus tongaensis</i>	374200	SAMN22936018	✓
Ophidiiformes	Dinematichthyidae	<i>Ogilbia cayorum</i>	ZMUC P771463 KUIT 168, USNM	SAMN22936237	
Ophidiiformes	Dinematichthyidae	<i>Ogilbichthys</i> sp.	349073	SAMN22936238	
Ophidiiformes	Dinematichthyidae	<i>Typhliasina pearsei</i>	ZMUC P771455	SAMN22936435	
Ophidiiformes	Bythitidae	<i>Aphyonus gelatinosus</i>	ZMUB/MAR 3880	SAMN22935862	
Ophidiiformes	Bythitidae	<i>Bidenichthys capensis</i>	KUIT 6466, n.v. KUIT 3292, SAIAB	SAMN22935903	
Ophidiiformes	Bythitidae	<i>Brosmophyciops pautzkei</i>	86260	SAMN22935916	
Ophidiiformes	Bythitidae	<i>Cataetyx messieri</i>	ZMUC P771617 KUIT 3292, MCZ	SAMN22935935	✓
Ophidiiformes	Bythitidae	<i>Diplacanthopoma brachysoma</i>	155341	SAMN22936028	
Ophidiiformes	Bythitidae	<i>Megacataetyx niki</i>	NMNZ P.41257	SAMN22935936	
Ophidiiformes	Bythitidae	<i>Parabrotula tanseimaru</i>	CBM 10557	SAMN18716611*	
Ophidiiformes	Ophidiidae	<i>Acanthonus armatus</i>	MNHN 2004-1311	SAMN22935831	
Ophidiiformes	Ophidiidae	<i>Apagesoma australe</i>	ZMUC P771525	SAMN22935861	
Ophidiiformes	Ophidiidae	<i>Bassogigas walkeri</i>	SIO 08-109	SAMN22935888	✓
Ophidiiformes	Ophidiidae	<i>Brotula barbata</i>	See NCBI SRA	SAMEA4028811*	✓
Ophidiiformes	Ophidiidae	<i>Carapus acus</i>	See NCBI SRA	SAMEA4028813*	
Ophidiiformes	Ophidiidae	<i>Carapus bermudensis</i>	KUIT 1172, KUI 27038	SAMN05915045	
Ophidiiformes	Ophidiidae	<i>Chilara taylori</i>	KUIT 2201, KUI 28277	SAMN22935972	✓
Ophidiiformes	Ophidiidae	<i>Dannevigia tusca</i>	YFTC 32428, n.v. KUIT 3677, MCZ	SAMN22936013	
Ophidiiformes	Ophidiidae	<i>Dicrolene intronigra</i>	158834	SAMN22936024	✓
Ophidiiformes	Ophidiidae	<i>Holcomycteronus brucei</i>	ZMUC P771528	SAMN22936103	
Ophidiiformes	Ophidiidae	<i>Lamprogrammus exutus</i>	See NCBI SRA	SAMEA4028812*	✓
Ophidiiformes	Ophidiidae	<i>Lepophidium profundorum</i>	KUIT 1571, KUI 27197	SAMN22936140	✓
Ophidiiformes	Ophidiidae	<i>Monomitopus garmani</i>	ZMUC P771573	SAMN22936206	
Ophidiiformes	Ophidiidae	<i>Porogadus miles</i>	ZMUB/MAR 2661	SAMN22936311	

Ophidiiformes	Ophidiidae	<i>Ventichthys biospeedoi</i>	MNHN 2004-2038	SAMN22936438		
Batrachoidiformes	Batrachoididae	<i>Batrachoides pacifici</i>	See NCBI SRA	SAMN05915038		
Batrachoidiformes	Batrachoididae	<i>Chatrabus melanurus</i>	See NCBI SRA	SAMEA4028814*	✓	
Batrachoidiformes	Batrachoididae	<i>Halobatrachus didactylus</i>	YFTC 17238, n.v.	SAMN22936085	✓	✓
Batrachoidiformes	Batrachoididae	<i>Opsanus tau</i>	YPM ICH 24156 Pers. Coll.: P.Wainwright, PW267:	SAMN22936248	✓	✓
Batrachoidiformes	Batrachoididae	<i>Porichthys notatus</i>	B50	SAMN22936309	✓	
Gobiiformes	<i>Kurtus</i>	<i>Kurtus gulliveri</i>	TMB 09-2	SAMN05915077	✓	✓
Gobiiformes	<i>Kurtus</i>	<i>Kurtus indicus</i>	AMNH 251591	SAMN22936124		
Gobiiformes	Apogonidae	<i>Astrapogon stellatus</i>	YPM ICH 021834 Pers. Coll.:	SAMN22935872	✓	
Gobiiformes	Apogonidae	<i>Cheilodipterus quinquelineatus</i>	P.Wainwright, PW1704B Pers. Coll.:	SAMN22935969	✓	
Gobiiformes	Apogonidae	<i>Fibramia lateralis</i>	P.Wainwright, PW2294B	SAMN05915032		
Gobiiformes	Apogonidae	<i>Ostorhinchus doederleini</i>	LACM 000974	SAMN22568987		✓
Gobiiformes	Apogonidae	<i>Ostorhinchus nigrofasciatus</i>	LACM-T 000970 Pers. Coll: M. Alfaro, MEA	SAMN05915092	✓	
Gobiiformes	Apogonidae	<i>Paroncheilus affinis</i>	LACM-T 000493	SAMN05915099	✓	
Gobiiformes	Apogonidae	<i>Phaeoptyx pigmentaria</i>	YPM ICH 026618	SAMN22936317	✓	
Gobiiformes	Apogonidae	<i>Pseudamia gelatinosa</i>	n.v.	SAMN22569001	✓	✓
Gobiiformes	Apogonidae	<i>Taeniamia biguttata</i>	LACM 000975	SAMN22568902		
Gobiiformes	<i>Trichonotus</i>	<i>Trichonotus filamentosus</i>	LSUMZ 14120	SAMN22936425	✓	✓
Gobiiformes	Rhyacichthyidae	<i>Rhyacichthys aspro</i>	NSMT-P 97135	SAMN22936341		
Gobiiformes	Odontobutidae	<i>Odontobutis obscura</i>	See NCBI SRA	SAMN05915089	✓	✓
Gobiiformes	Odontobutidae	<i>Sineleotris saccharae</i>	LACM-T, n.v.	SAMN22569008		
Gobiiformes	Milyeringidae	<i>Milyeringa veritas</i>	SAMA, n.v.	SAMN22568978		
Gobiiformes	Milyeringidae	<i>Typhleotris madagascariensis</i>	FMNH 116498	SAMN22569011		
Gobiiformes	Eleotridae	<i>Dormitator maculatus</i>	LACM 000017	SAMN22568918	✓	
Gobiiformes	Eleotridae	<i>Eleotris pisonis</i>	LACM 000019	SAMN22568924	✓	
Gobiiformes	Eleotridae	<i>Erotelis smaragdus</i>	LACM-T 000042	SAMN05915063	✓	
Gobiiformes	Eleotridae	<i>Gobiomorphus hubbsi</i>	LACM-T, n.v.	SAMN15908306	✓	
Gobiiformes	Eleotridae	<i>Gobiomorus dormitor</i>	NCSM 068278	SAMN22568929	✓	
Gobiiformes	Eleotridae	<i>Guavina micropus</i>	Pers. Coll.: VanTass/Rob	SAMN22568932	✓	
Gobiiformes	Eleotridae	<i>Hemieleotris latifasciata</i>	LACM 000018	SAMN22568933	✓	
Gobiiformes	Eleotridae	<i>Hypseleotris compressa</i>	LACM 000104	SAMN15908312	✓	
Gobiiformes	Eleotridae	<i>Microphilypnus ternetzi</i>	ANSP 180643	SAMN22568977		
Gobiiformes	Eleotridae	<i>Mogurnda adspersa</i>	LACM-T 000069	SAMN05915085	✓	
Gobiiformes	Eleotridae	<i>Ratsirakia legendrei</i>	LACM 000007	SAMN22569003		
Gobiiformes	Eleotridae	<i>Tateurndina ocellicauda</i>	LACM 000066	SAMN22569010	✓	
Gobiiformes	Butidae	<i>Butis butis</i>	LACM 000045	SAMN22568909		
Gobiiformes	Butidae	<i>Kribia nana</i>	LACM 000077	SAMN22568971	✓	

Gobiiformes	Butidae	<i>Ophiocara porocephala</i>	LACM-T 000001	SAMN05915091	
Gobiiformes	Butidae	<i>Oxyeleotris lineolata</i>	LACM-T 000021	SAMN22936255	✓
Gobiiformes	Butidae	<i>Oxyeleotris nullipora</i>	LACM-T 000596	SAMN22568992	
Gobiiformes	Butidae	<i>Oxyeleotris selheimi</i>	LACM-T 000006	SAMN22568993	✓
Gobiiformes	Thalasseleotrididae	<i>Grahamichthys radiata</i>	YPM ICH 26585	SAMN22936082	✓
Gobiiformes	Thalasseleotrididae	<i>Thalasseleotris iota</i>	YPM ICH 26584	SAMN22936412	
Gobiiformes	Oxudercidae	<i>Acanthogobius flavimanus</i>	LACM-T 000295	SAMN22568897	✓
Gobiiformes	Oxudercidae	<i>Boleophthalmus pectinirostris</i>	See NCBI SRA	SAMN03201692*	✓
Gobiiformes	Oxudercidae	<i>Evorthodus minutus</i>	LACM-T 000265	SAMN05915064	✓
Gobiiformes	Oxudercidae	<i>Gillichthys seta</i>	LACM-T 000281	SAMN05915066	✓
Gobiiformes	Oxudercidae	<i>Gnatholepis cauerensis</i>	LACM 001122	SAMN22568926	✓
Gobiiformes	Oxudercidae	<i>Gobiopterus semivestitus</i>	LACM 000090	SAMN22568930	
Gobiiformes	Oxudercidae	<i>Mugilogobius rivulus</i>	LACM 000262	SAMN22568983	✓
Gobiiformes	Oxudercidae	<i>Pandaka lidwilli</i>	LACM 000254	SAMN22568994	
Gobiiformes	Oxudercidae	<i>Periophthalmodon schlosseri</i>	See NCBI SRA	SAMN03201695*	
Gobiiformes	Oxudercidae	<i>Periophthalmus barbarus</i>	LACM-T 000273	SAMN05915098	✓
Gobiiformes	Oxudercidae	<i>Periophthalmus magnuspinnatus</i>	See NCBI SRA	SAMN03201694*	
Gobiiformes	Oxudercidae	<i>Scartelaos histophorus</i>	See NCBI SRA	SAMN03201693*	✓
Gobiiformes	Oxudercidae	<i>Typhlogobius californiensis</i>	LACM 000025	SAMN22569012	✓
Gobiiformes	Gobiidae	<i>Amblyeleotris guttata</i>	LACM 001025	SAMN22568899	✓
Gobiiformes	Gobiidae	<i>Amblygobius phalaena</i>	LACM 000195	SAMN22568900	✓
Gobiiformes	Gobiidae	<i>Asterropteryx ensifera</i>	LACM 001050	SAMN22568903	✓
Gobiiformes	Gobiidae	<i>Bathygobius soporator</i>	LACM-T 000511	SAMN05915037	✓
Gobiiformes	Gobiidae	<i>Bryaninops yongei</i>	LACM 000164	SAMN22568907	✓
Gobiiformes	Gobiidae	<i>Callogobius sclateri</i>	LACM 000172	SAMN22568911	✓
Gobiiformes	Gobiidae	<i>Coryogalops anomolus</i>	LACM 000243	SAMN22568914	
Gobiiformes	Gobiidae	<i>Coryphopterus glaucofraenum</i>	LACM 000578	SAMN22568915	✓
Gobiiformes	Gobiidae	<i>Cryptocentrus cinctus</i>	LACM 001086	SAMN22568916	✓
Gobiiformes	Gobiidae	<i>Elacatinus oceanops</i>	LACM 000230	SAMN22568931	✓
Gobiiformes	Gobiidae	<i>Exyrias belissimus</i>	LACM 000168	SAMN22568924	✓
Gobiiformes	Gobiidae	<i>Glossogobius flavipinnis</i>	LACM 000311	SAMN22568925	✓
Gobiiformes	Gobiidae	<i>Gobiodon histrio</i>	LACM 000239	SAMN22568927	✓
Gobiiformes	Gobiidae	<i>Istigobius rigilius</i>	LACM 001078	SAMN22568968	✓
Gobiiformes	Gobiidae	<i>Koumansetta rainfordi</i>	n.v.	SAMN22568969	
Gobiiformes	Gobiidae	<i>Lesueurigobius sanzi</i>	See NCBI SRA	SAMEA4028816*	✓
Gobiiformes	Gobiidae	<i>Lythrypnus dalli</i>	LACM 000190	SAMN22568974	✓
Gobiiformes	Gobiidae	<i>Microdesmus longipinnis</i>	LACM 000617	SAMN22568975	
Gobiiformes	Gobiidae	<i>Nes longus</i>	LACM 000222	SAMN22568985	✓
Gobiiformes	Gobiidae	<i>Priolepis cincta</i>	LACM 000904	SAMN22568999	✓

Gobiiformes	Gobiidae	<i>Ptereleotris evides</i>	Pers. Coll.: P.Wainwright, PW2064B	SAMN05915113	✓	✓
Gobiiformes	Gobiidae	<i>Ptereleotris zebra</i>	LACM 000594	SAMN22569002	✓	
Gobiiformes	Gobiidae	<i>Stonogobiops xanthorhinica</i>	LACM 001049	SAMN22569009		
Gobiiformes	Gobiidae	<i>Valenciennea strigata</i>	LACM-T 000898	SAMN05915136	✓	
Scombriformes	<i>Arripis</i>	<i>Arripis trutta</i>	FAKU 82391	SAMN13222433	✓	✓
Scombriformes	<i>Ariomma</i>	<i>Ariomma bondi</i>	YPM ICH 025637	SAMN13222429	✓	
Scombriformes	<i>Ariomma</i>	<i>Ariomma indica</i>	NSMT 64808 KUIT 5304, MCZ	SAMN13222430	✓	
Scombriformes	<i>Ariomma</i>	<i>Ariomma melana</i>	161902	SAMN13222431	✓	
Scombriformes	<i>Ariomma</i>	<i>Ariomma</i> sp.	YPM ICH 027642	SAMN13222432		
Scombriformes	Nomeidae	<i>Cubiceps whiteleggii</i>	SNFR 14797	SAMN13222449	✓	
Scombriformes	Nomeidae	<i>Cubiceps baxteri</i>	SIO 98-26	SAMN13222448	✓	
Scombriformes	Nomeidae	<i>Psenes cyanophrys</i>	YPM ICH 025740	SAMN13222496	✓	
Scombriformes	Nomeidae	<i>Psenes arafurensis</i>	SNFR 14835	SAMN13222495	✓	
Scombriformes	Stromateidae	<i>Pampus argenteus</i>	LSUMZ 5282	SAMN13222483	✓	
Scombriformes	Stromateidae	<i>Pampus chinensis</i>	LSUMZ 5300	SAMN13222484		
Scombriformes	Stromateidae	<i>Pampus echinogaster</i>	KAUM 64926	SAMN13222485		
Scombriformes	Stromateidae	<i>Pampus punctatissimus</i>	CBM 12672	SAMN13222531		
Scombriformes	Stromateidae	<i>Peprilus burti</i>	KUIT 5086, KUI 30083	SAMN13222490	✓	
Scombriformes	Stromateidae	<i>Peprilus paru</i>	KUIT 5169, KUI 30096	SAMN13222489	✓	
Scombriformes	Stromateidae	<i>Peprilus simillimus</i>	KUIT 9394, KUI 23694	SAMN13222491	✓	
Scombriformes	Stromateidae	<i>Peprilus triacanthus</i>	YPM ICH 024677	SAMN13222492		
Scombriformes		<i>Pomatomus saltatrix</i>	Pers. Coll.: P.Wainwright, PW1568	SAMN05915106	✓	
Scombriformes	Centrolophidae	<i>Hyperoglyphe antarctica</i>	SNFR 16241	SAMN13222465	✓	
Scombriformes	Centrolophidae	<i>Hyperoglyphe japonica</i>	CBM 13628	SAMN13222466	✓	
Scombriformes	Centrolophidae	<i>Psenopsis anomala</i>	Miya-11-231	SAMN05915108	✓	
Scombriformes	Centrolophidae	<i>Schedophilus velaini</i>	SNFR 16403	SAMN13222508	✓	
Scombriformes	Icosteidae	<i>Icosteus aenigmaticus</i>	SIO 99-95	SAMN13222467	✓	
Scombriformes		<i>Amarsipus carlsbergi</i>	CBM 17750	SAMN10081044 *	✓	
Scombriformes	Tetragonuridae	<i>Tetragonurus atlanticus</i>	YPM ICH 027663	SAMN13222521	✓	
Scombriformes	Tetragonuridae	<i>Tetragonurus cuvieri</i>	NSMT 65749	SAMN13222522		
Scombriformes	Tetragonuridae	<i>Tetragonurus pacificus</i>	SNFR 15336	SAMN13222523		
Scombriformes	Chiasmodontidae	<i>Chiasmodon niger</i>	YPM ICH 25663	SAMN05915052	✓	
Scombriformes	Chiasmodontidae	<i>Dysalotus alcocki</i>	YPM ICH 025665	SAMN13222451	✓	
Scombriformes	Chiasmodontidae	<i>Dysalotus oligoscolus</i>	YPM ICH 025654	SAMN13222452		
Scombriformes	Chiasmodontidae	<i>Kali kerberti</i>	UW 115135	SAMN05915076	✓	
Scombriformes	Chiasmodontidae	<i>Kali macrodon</i>	YPM ICH 027772 KUIT 8140, MCZ	SAMN13222468	✓	
Scombriformes	Chiasmodontidae	<i>Kali macrura</i>	165931	SAMN13222469		
Scombriformes	Chiasmodontidae	<i>Pseudoscopelus altipinnis</i>	YPM ICH 027632	SAMN13222498		
Scombriformes	Chiasmodontidae	<i>Pseudoscopelus astronesthicens</i>	KUIT 6518, MCZ 164170	SAMN13222499		

Scombriformes	Chiasmodontidae	<i>Pseudoscopelus obtusifrons</i>	YPM ICH 027787	SAMN13222501	
Scombriformes	Chiasmodontidae	<i>Pseudoscopelus odontoglossum</i>	YPM ICH 027854	SAMN13222500	
Scombriformes	Chiasmodontidae	<i>Pseudoscopelus scutatus</i>	YPM ICH 025805	SAMN13222503	
Scombriformes	Scombridae	<i>Acanthocybium solandri</i>	KUIT 5425	SAMN13222425	✓
Scombriformes	Scombridae	<i>Auxis rochei</i>	CBM 14077	SAMN13222436	✓
Scombriformes	Scombridae	<i>Auxis thazard</i>	CBM 12877	SAMN13222437	
Scombriformes	Scombridae	<i>Euthynnus affinis</i>	CBM 12671	SAMN13222455	✓
Scombriformes	Scombridae	<i>Gasterochisma melampus</i>	NSMT 93197	SAMN13222462	
Scombriformes	Scombridae	<i>Gymnosarda unicolor</i>	NSMT 62530	SAMN13222464	✓
Scombriformes	Scombridae	<i>Katsuwonus pelamis</i>	CBM 12672	SAMN13222471	✓
Scombriformes	Scombridae	<i>Rastrelliger kanagurta</i>	NSMT 76071	SAMN13222505	✓
Scombriformes	Scombridae	<i>Scomber australasicus</i>	CBM 12636	SAMN22936357	✓
Scombriformes	Scombridae	<i>Scomber japonicus</i>	CBM 12641	SAMN13222509	✓
Scombriformes	Scombridae	<i>Scomber scombrus</i>	YPM ICH 020681	SAMN05915123	✓
Scombriformes	Scombridae	<i>Scomberomorus maculatus</i>	Pers. Coll.: P. Wainwright, PW1207	SAMN05915124	✓
Scombriformes	Scombridae	<i>Scomberomorus niphonius</i>	CBM 14469	SAMN13222512	
Scombriformes	Scombridae	<i>Scomberomorus regalis</i>	KUIT 5159, KUI 30178	SAMN13222513	✓
Scombriformes	Scombridae	<i>Thunnus orientalis</i>	NSMT-P 93077	SAMN13222524	✓
Scombriformes	Scombridae	<i>Thunnus tonggol</i>	SNFR 16558	SAMN13222525	
Scombriformes	Caristiidae	<i>Caristius macropus</i>	UW 113533	SAMN13222445	
Scombriformes	Caristiidae	<i>Paracaristius maderensis</i>	YPM ICH 027617	SAMN13222486	
Scombriformes	Caristiidae	<i>Paracaristius nudarcus</i>	YPM ICH 25618	SAMN22936261	
Scombriformes	Bramidae	<i>Brama caribbea</i>	YPM ICH 025808	SAMN13222442	✓
Scombriformes	Bramidae	<i>Brama dussumieri</i>	CBM 15373	SAMN13222443	✓
Scombriformes	Bramidae	<i>Brama japonica</i>	SIO 01-183	SAMN05915040	✓
Scombriformes	Bramidae	<i>Eumegistus illustris</i>	n.v. tissue only KUIT 8137, MCZ	SAMN13222454	
Scombriformes	Bramidae	<i>Pterycombus brama</i>	165918	SAMN13222504	✓
Scombriformes	Bramidae	<i>Pterycombus petersii</i>	OCF-P 20071225	SAMN13222532	✓
Scombriformes	Bramidae	<i>Taractes asper</i>	SIO 00-165	SAMN05915132	
Scombriformes	Bramidae	<i>Taractes rubescens</i>	CBM 14224	SAMN13222517	
Scombriformes	Bramidae	<i>Taractichthys longipinnis</i>	KUIT 5403	SAMN13222518	
Scombriformes	Bramidae	<i>Taractichthys steindachneri</i>	CBM 14163	SAMN13222519	✓
Scombriformes		<i>Scombrolabrax heterolepis</i>	NMNZ 40456	SAMN13222514	
Scombriformes		<i>Lepidocybium flavobrunneum</i>	CBM 12751	SAMN13222474	
Scombriformes	Gempylidae	<i>Diplospinus multistriatus</i>	YPM ICH 025671	SAMN13222450	✓
Scombriformes	Gempylidae	<i>Epinnula magistralis</i>	NSMT 62524	SAMN13222453	
Scombriformes	Gempylidae	<i>Gempylus serpens</i>	NSMT 62526 KUIT 3543, MCZ	SAMN13222463	✓
Scombriformes	Gempylidae	<i>Neopinnula americana</i>	158587	SAMN13222480	✓
Scombriformes	Gempylidae	<i>Nesiarchus nasutus</i>	NSMT 75668	SAMN13222481	✓

Scombriformes	Gempylidae	<i>Paradiplospinus antarcticus</i>	KUIT 925, MCZ 131300	SAMN13222487	✓
Scombriformes	Gempylidae	<i>Paradiplospinus gracilis</i>	YPM ICH 022377	SAMN13222488	
Scombriformes	Gempylidae	<i>Promethichthys prometheus</i>	CBM 13627	SAMN13222494	✓
Scombriformes	Gempylidae	<i>Rexea prometheoides</i>	OCF-P 20140707-2	SAMN13222506	
Scombriformes	Gempylidae	<i>Ruvettus pretiosus</i>	SIO 06-116	SAMN05915118	✓
Scombriformes	Gempylidae	<i>Thyrsitoides marleyi</i>	NSMT 73382	SAMN13222526	
Scombriformes	Trichiuridae	<i>Aphanopus carbo</i>	HUMZ 220745	SAMN13222427	✓
Scombriformes	Trichiuridae	<i>Assurger anzac</i>	SIO 18126	SAMN05915034	
Scombriformes	Trichiuridae	<i>Benthodesmus elongatus</i>	YPM ICH 025649 KUIT 3542, MCZ	SAMN13222438	✓
Scombriformes	Trichiuridae	<i>Benthodesmus simonyi</i>	158586	SAMN13222439	✓
Scombriformes	Trichiuridae	<i>Benthodesmus tenuis</i>	HUMZ 220516	SAMN13222440	
Scombriformes	Trichiuridae	<i>Evoxymetopon macrophthalmus</i>	SNFR 14546	SAMN13222456	
Scombriformes	Trichiuridae	<i>Evoxymetopon poeyi</i>	NSMT 77666 KUIT 5249, MCZ	SAMN13222457	
Scombriformes	Trichiuridae	<i>Evoxymetopon taeniatus</i>	160934 KUIT 3546, MCZ	SAMN13222458	✓
Scombriformes	Trichiuridae	<i>Lepidopus altifrons</i>	158590	SAMN13222475	✓
Scombriformes	Trichiuridae	<i>Lepidopus caudatus</i>	KUIT 8084, n.v.	SAMN13222476	✓
Scombriformes	Trichiuridae	<i>Lepturacanthus savala</i>	LSUMZ 78	SAMN13222477	✓
Scombriformes	Trichiuridae	<i>Tentoriceps cristatus</i>	SNFR 17729	SAMN13222520	✓
Scombriformes	Trichiuridae	<i>Trichiurus lepturus</i>	CBM 12994	SAMN13222527	✓
Scombriformes	Trichiuridae	<i>Trichiurus</i> sp. 1	SNFR 17528	SAMN13222528	
Scombriformes	Trichiuridae	<i>Trichiurus</i> sp. 2	SNFR 17533	SAMN13222529	
Sygnathiformes	Pegasidae	<i>Eurypegus draconis</i>	See NCBI SRA	SAMN06563069	
Sygnathiformes	Pegasidae	<i>Pegasus volitans</i>	See NCBI SRA	SAMN06563109	✓
Sygnathiformes	Dactylopteridae	<i>Dactyloptena orientalis</i>	See NCBI SRA	SAMN06563054	✓
Sygnathiformes	Dactylopteridae	<i>Dactyloptena peterseni</i>	See NCBI SRA	SAMN06563055	✓
Sygnathiformes	Dactylopteridae	<i>Dactylopterus volitans</i>	See NCBI SRA	SAMN06563056	✓
Sygnathiformes	Mullidae	<i>Mulloidichthys dentatus</i>	See NCBI SRA	SAMN06563097	
Sygnathiformes	Mullidae	<i>Mulloidichthys martinicus</i>	See NCBI SRA	SAMN06563098	✓
Sygnathiformes	Mullidae	<i>Mulloidichthys vanicolensis</i>	See NCBI SRA	SAMN06563099	✓
Sygnathiformes	Mullidae	<i>Mullus auratus</i>	See NCBI SRA	SAMN22936211	✓
Sygnathiformes	Mullidae	<i>Parupeneus barberinoides</i>	See NCBI SRA	SAMN06563103	✓
Sygnathiformes	Mullidae	<i>Parupeneus barberinus</i>	See NCBI SRA	SAMN22936275	✓
Sygnathiformes	Mullidae	<i>Parupeneus barberinus</i>	See NCBI SRA	SAMN06563108	
Sygnathiformes	Mullidae	<i>Parupeneus cyclostomus</i>	See NCBI SRA	SAMN06563105	✓
Sygnathiformes	Mullidae	<i>Parupeneus multifasciatus</i>	See NCBI SRA	SAMN06563106	✓
Sygnathiformes	Mullidae	<i>Parupeneus rubescens</i>	See NCBI SRA	SAMN06563107	
Sygnathiformes	Mullidae	<i>Pseudupeneus grandisquamis</i>	See NCBI SRA	SAMN06563113	✓
Sygnathiformes	Mullidae	<i>Pseudupeneus maculatus</i>	See NCBI SRA	SAMN06563112	✓
Sygnathiformes	Mullidae	<i>Upeneichthys lineatus</i>	See NCBI SRA	SAMN06563144	✓

Sygnathiformes	Mullidae	<i>Upeneus tragula</i>	See NCBI SRA YFTC 25957; Pers. Coll.: Eri Katayama	SAMN06563145	✓	
Sygnathiformes	Draconettidae	<i>Draconetta xenica</i>		SAMN22936035		
Sygnathiformes	Callionymidae	<i>Anaora tentaculata</i>	See NCBI SRA	SAMN06563036		
Sygnathiformes	Callionymidae	<i>Callionymus belcheri</i>	See NCBI SRA	SAMN06563039	✓	✓
Sygnathiformes	Callionymidae	<i>Callionymus calcaratus</i>	See NCBI SRA	SAMN06563114		
Sygnathiformes	Callionymidae	<i>Callionymus curvicornis</i>	See NCBI SRA	SAMN06563040	✓	
Sygnathiformes	Callionymidae	<i>Callionymus delicatulus</i>	See NCBI SRA	SAMN06563041	✓	
Sygnathiformes	Callionymidae	<i>Callionymus limiceps</i>	See NCBI SRA	SAMN06563042	✓	
Sygnathiformes	Callionymidae	<i>Calliurichthys grossi</i>	See NCBI SRA	SAMN06563043		
Sygnathiformes	Callionymidae	<i>Calliurichthys scaber</i>	See NCBI SRA	SAMN06563044		
Sygnathiformes	Callionymidae	<i>Dactylopus dactylopus</i>	See NCBI SRA	SAMN06563057	✓	
Sygnathiformes	Callionymidae	<i>Diplogrammus goramensis</i>	See NCBI SRA	SAMN06563058	✓	
Sygnathiformes	Callionymidae	<i>Draculo mirabilis</i>	See NCBI SRA	SAMN06563066		
Sygnathiformes	Callionymidae	<i>Repomucenus calcaratus</i>	See NCBI SRA	SAMN22936338		
Sygnathiformes	Callionymidae	<i>Synchiropus agassizii</i>	See NCBI SRA	SAMN06563075		
Sygnathiformes	Callionymidae	<i>Synchiropus ativelis</i>	See NCBI SRA	SAMN06563120		
Sygnathiformes	Callionymidae	<i>Synchiropus atrilabiatus</i>	See NCBI SRA	SAMN06563121	✓	
Sygnathiformes	Callionymidae	<i>Synchiropus goodenbeani</i>	See NCBI SRA	SAMN22936067		
Sygnathiformes	Callionymidae	<i>Synchiropus masudai</i>	See NCBI SRA	SAMN06563077		
Sygnathiformes	Callionymidae	<i>Synchiropus moyeri</i>	See NCBI SRA	SAMN06563122		
Sygnathiformes	Callionymidae	<i>Synchiropus ocellatus</i>	See NCBI SRA	SAMN06563123		
Sygnathiformes	Callionymidae	<i>Synchiropus picturatus</i>	See NCBI SRA	SAMN06563124	✓	
Sygnathiformes	Callionymidae	<i>Synchiropus splendidus</i>	See NCBI SRA	SAMN06563125	✓	
Sygnathiformes	Callionymidae	<i>Synchiropus stellatus</i>	See NCBI SRA	SAMN06563101	✓	
Sygnathiformes	Centriscidae	<i>Aeoliscus strigatus</i>	See NCBI SRA	SAMN06563035	✓	
Sygnathiformes	Centriscidae	<i>Centriscus scutatus</i>	See NCBI SRA	SAMN06563045		✓
Sygnathiformes	Centriscidae	<i>Macroramphosus gracilis</i>	See NCBI SRA	SAMN06563091	✓	
Sygnathiformes	Centriscidae	<i>Macroramphosus scolopax</i>	See NCBI SRA KUIT 6839, SAIAB 77945	SAMN06563092	✓	
Sygnathiformes	<i>Aulostomus</i>	<i>Aulostomus chinensis</i>		SAMN13222435	✓	
Sygnathiformes	<i>Aulostomus</i>	<i>Aulostomus maculatus</i>	See NCBI SRA	SAMN06563038	✓	
Sygnathiformes	<i>Fistularia</i>	<i>Fistularia commersonii</i>	See NCBI SRA	SAMN06563071	✓	
Sygnathiformes	<i>Fistularia</i>	<i>Fistularia corneta</i>	See NCBI SRA	SAMN06563072	✓	
Sygnathiformes	<i>Fistularia</i>	<i>Fistularia petimba</i>	See NCBI SRA	SAMN06563073	✓	
Sygnathiformes	<i>Fistularia</i>	<i>Fistularia tabacaria</i>	See NCBI SRA	SAMN06563074		
Sygnathiformes	<i>Solenostomus</i>	<i>Solenostomus cyanopterus</i>	See NCBI SRA	SAMN06563117		
Sygnathiformes	<i>Solenostomus</i>	<i>Solenostomus paradoxus</i>	See NCBI SRA	SAMN06563118		
Sygnathiformes	Syngnathidae	<i>Choeroichthys sculptus</i>	See NCBI SRA	SAMN06563046		
Sygnathiformes	Syngnathidae	<i>Corythoichthys amplexus</i>	See NCBI SRA	SAMN06563047	✓	
Sygnathiformes	Syngnathidae	<i>Corythoichthys haematopterus</i>	See NCBI SRA	SAMN06563049	✓	

Sygnathiformes	Syngnathidae	<i>Corythoichthys intestinalis</i>	See NCBI SRA	SAMN06563050	✓
Sygnathiformes	Syngnathidae	<i>Corythoichthys schultzi</i>	See NCBI SRA	SAMN06563051	✓
Sygnathiformes	Syngnathidae	<i>Cosmocampus arctus</i>	See NCBI SRA	SAMN06563052	✓
Sygnathiformes	Syngnathidae	<i>Doryichthys boaja</i>	See NCBI SRA	SAMN06563059	
Sygnathiformes	Syngnathidae	<i>Doryichthys martensii</i>	See NCBI SRA	SAMN06563060	
Sygnathiformes	Syngnathidae	<i>Doryrhamphus excisus</i>	See NCBI SRA	SAMN06563061	✓
Sygnathiformes	Syngnathidae	<i>Doryrhamphus janssi</i>	See NCBI SRA	SAMN06563062	
Sygnathiformes	Syngnathidae	<i>Dunckerocampus boylei</i>	See NCBI SRA	SAMN06563064	
Sygnathiformes	Syngnathidae	<i>Dunckerocampus dactyliophorus</i>	See NCBI SRA	SAMN22936037	
Sygnathiformes	Syngnathidae	<i>Enneacampus ansorgii</i>	See NCBI SRA	SAMN06563067	
Sygnathiformes	Syngnathidae	<i>Entelurus aequoreus</i>	See NCBI SRA	SAMN06563068	✓
Sygnathiformes	Syngnathidae	<i>Festucalex wassi</i>	See NCBI SRA	SAMN06563070	
Sygnathiformes	Syngnathidae	<i>Halicampus crinitus</i>	See NCBI SRA	SAMN06563093	✓
Sygnathiformes	Syngnathidae	<i>Halicampus dunckeri</i>	See NCBI SRA	SAMN06563078	✓
Sygnathiformes	Syngnathidae	<i>Hippichthys penicillus</i>	See NCBI SRA	SAMN06563079	✓
Sygnathiformes	Syngnathidae	<i>Hippocampus abdominalis</i>	See NCBI SRA	SAMN06563080	✓
Sygnathiformes	Syngnathidae	<i>Hippocampus barbouri</i>	See NCBI SRA	SAMN22936099	✓
Sygnathiformes	Syngnathidae	<i>Hippocampus comes</i>	See NCBI SRA	SAMN06563082	✓ ✓
Sygnathiformes	Syngnathidae	<i>Hippocampus ingens</i>	See NCBI SRA	SAMN22936100	✓
Sygnathiformes	Syngnathidae	<i>Hippocampus kuda</i>	See NCBI SRA	SAMN22936101	✓
Sygnathiformes	Syngnathidae	<i>Hippocampus reidi</i>	See NCBI SRA	SAMN06563087	✓
Sygnathiformes	Syngnathidae	<i>Hippocampus subelongatus</i>	See NCBI SRA	SAMN06563088	
Sygnathiformes	Syngnathidae	<i>Hypselognathus rostratus</i>	See NCBI SRA	SAMN06563089	
Sygnathiformes	Syngnathidae	<i>Idiotropiscis lumnitzeri</i>	See NCBI SRA	SAMN06563090	
Sygnathiformes	Syngnathidae	<i>Microphis brachyurus</i>	See NCBI SRA	SAMN06563094	✓
Sygnathiformes	Syngnathidae	<i>Microphis cuncalus</i>	See NCBI SRA	SAMN06563095	
Sygnathiformes	Syngnathidae	<i>Microphis deocata</i>	See NCBI SRA	SAMN06563096	
Sygnathiformes	Syngnathidae	<i>Nerophis ophidion</i>	See NCBI SRA	SAMN06563102	✓
Sygnathiformes	Syngnathidae	<i>Phycodurus eques</i>	See NCBI SRA	SAMN06563110	
Sygnathiformes	Syngnathidae	<i>Phyllopteryx taeniolatus</i>	See NCBI SRA	SAMN06563111	
Sygnathiformes	Syngnathidae	<i>Siokunichthys nigrolineatus</i>	See NCBI SRA	SAMN06563116	
Sygnathiformes	Syngnathidae	<i>Stigmatopora nigra</i>	See NCBI SRA	SAMN06563119	
Sygnathiformes	Syngnathidae	<i>Stigmatopora nigra</i>	See NCBI SRA	SAMN22936400	
Sygnathiformes	Syngnathidae	<i>Syngnathoides biaculeatus</i>	See NCBI SRA	SAMN06563126	✓
Sygnathiformes	Syngnathidae	<i>Syngnathus abaster</i>	See NCBI SRA	SAMN06563127	✓
Sygnathiformes	Syngnathidae	<i>Syngnathus acus</i>	See NCBI SRA	SAMN06563128	
Sygnathiformes	Syngnathidae	<i>Syngnathus auliscus</i>	See NCBI SRA	SAMN06563129	
Sygnathiformes	Syngnathidae	<i>Syngnathus californiensis</i>	See NCBI SRA	SAMN06563130	✓
Sygnathiformes	Syngnathidae	<i>Syngnathus exilis</i>	See NCBI SRA	SAMN06563131	
Sygnathiformes	Syngnathidae	<i>Syngnathus floridae</i>	See NCBI SRA	SAMN06563132	✓

Sygnathiformes	Syngnathidae	<i>Syngnathus fuscus</i>	See NCBI SRA	SAMN06563133	✓
Sygnathiformes	Syngnathidae	<i>Syngnathus leptorhynchus</i>	see Longo <i>et al.</i> 2017	SAMN22936406	✓
Sygnathiformes	Syngnathidae	<i>Syngnathus louisianae</i>	See NCBI SRA	SAMN06563135	
Sygnathiformes	Syngnathidae	<i>Syngnathus pelagicus</i>	see Longo <i>et al.</i> 2017	SAMN22936407	✓
Sygnathiformes	Syngnathidae	<i>Syngnathus rostellatus</i>	See NCBI SRA	SAMN06563137	✓
Sygnathiformes	Syngnathidae	<i>Syngnathus scovelli</i>	See NCBI SRA	SAMN06563138	✓
Sygnathiformes	Syngnathidae	<i>Syngnathus springeri</i>	See NCBI SRA	SAMN06563139	
Sygnathiformes	Syngnathidae	<i>Syngnathus taenionotus</i>	See NCBI SRA	SAMN06563140	
Sygnathiformes	Syngnathidae	<i>Syngnathus typhle</i>	See NCBI SRA	SAMN06563141	✓
Sygnathiformes	Syngnathidae	<i>Trachyrhamphus bicoarctatus</i>	See NCBI SRA	SAMN06563143	✓
Sygnathiformes	Syngnathidae	<i>Vanacampus phillipi</i>	See NCBI SRA	SAMN06563146	✓
Sygnathiformes	Syngnathidae	<i>Vanacampus poecilolaemus</i>	See NCBI SRA	SAMN06563147	
Blenniiformes	Adrianichthyidae	<i>Adrianichthys oophorus</i>	USNM 38982	SAMN22935841	✓
Blenniiformes	Adrianichthyidae	<i>Oryzias latipes</i>	YFTC 32445, n.v.	SAMN22936249	✓ ✓
Blenniiformes	Belonidae	<i>Nomorhamphus celebensis</i>	YPM ICH 021568 Pers. Coll.: M.Alfaro,	SAMN22936229	
Blenniiformes	Belonidae	<i>Xenentodon cancila</i>	Alfaro 586 KUIT 4504, CAS	SAMN05915137	✓
Blenniiformes	Belonidae	<i>Zenarchopterus dispar</i>	222403	SAMN22936451	
Blenniiformes	Exocoetidae	<i>Prognichthys occidentalis</i>	KUIT 5173, KUI 30212	SAMN22935970	✓
Blenniiformes	Exocoetidae	<i>Oxyporhamphus micropterus</i>	LACM 46125.003	SAMN22936257	✓ ✓
Blenniiformes	Hemiramphidae	<i>Hyporhamphus dussumieri</i>	KUIT 4269, KUI 37091 KUIT 6756, SAIAB	SAMN22936112	✓
Blenniiformes	Hemiramphidae	<i>Hemiramphus far</i>	77898	SAMN22936092	✓
Blenniiformes	Atherinopsidae	<i>Atherinella panamensis</i>	YFTC 16681, n.v.	SAMN22935876	✓
Blenniiformes	Atherinopsidae	<i>Melanorhinus microps</i>	LACM T-000545	SAMN22936194	
Blenniiformes	<i>Atherion</i>	<i>Atherion elymus</i>	YFTC 16683, n.v.	SAMN22935877	
Blenniiformes	Phallostethidae	<i>Neostethus bicornis</i>	YFTC 16684, n.v. KUIT 2700, USNM	SAMN22936226	✓
Blenniiformes	Phallostethidae	<i>Phenacostethus smithi</i>	329346	SAMN22936290	
Blenniiformes	<i>Iso</i>	<i>Iso rhothophilus</i>	YFTC 16682, n.v.	SAMN22936117	✓
Blenniiformes	Atherinidae	<i>Atherina presbyter</i>	KUIT 8637	SAMN22935875	
Blenniiformes	Bedotiidae	<i>Bedotia madagascariensis</i>	YFTC 21585, n.v.	SAMN22935894	✓
Blenniiformes	Pseudomugilidae	<i>Pseudomugil gertrudae</i>	KUIT 1696, KUI 29882	SAMN22936323	✓
Blenniiformes	Melanotaeniidae	<i>Cairnsichthys rhombosomoides</i>	YFTC 16675, n.v.	SAMN22935920	
Blenniiformes	Melanotaeniidae	<i>Iriatherina wernerii</i>	YPM ICH 025213 Pers. Coll.: Reznick Lab	SAMN22936116	✓
Blenniiformes	Rivulidae	<i>Austrofundulus lehoignei</i>	UCRiverside	SAMN22935881	✓
Blenniiformes	Rivulidae	<i>Austrofundulus limnaeus</i>	See NCBI SRA Pers. Coll.: Reznick Lab	SAMN03490872*	✓
Blenniiformes	Rivulidae	<i>Austrolebias nigripinnis</i>	UCRiverside	SAMN22935883	
Blenniiformes	Rivulidae	<i>Kryptolebias marmoratus</i>	See NCBI SRA	SAMN04622665*	✓
Blenniiformes	Aplocheilidae	<i>Aplocheilus lineatus</i>	YPM ICH 025213	SAMN22935864	✓
Blenniiformes	Aplocheilidae	<i>Aplocheilus panchax</i>	YPM ICH 025220	SAMN22935865	✓

Blenniiformes	Nothobranchiidae	<i>Aphyosemion thysi</i>	AMNH 258919	SAMN22935863	✓	
Blenniiformes	Nothobranchiidae	<i>Epiplatys spilargyreia</i>	AMNH 257025	SAMN22936049	✓	✓
Blenniiformes	Nothobranchiidae	<i>Nothobranchius furzeri</i>	See NCBI SRA	SAMEA2698544*		
Blenniiformes	Nothobranchiidae	<i>Nothobranchius orthonotus</i>	See NCBI SRA	SAMEA2698544*		
Blenniiformes	<i>Cubanichthys</i>	<i>Cubanichthys pengelleyi</i>	YFTC 16678, n.v.	SAMN22936009		
Blenniiformes	Goodeidae	<i>Goodea atripinnis</i>	SLU 6644	SAMN22936081	✓	
Blenniiformes	Profundulidae	<i>Tlaloc labialis</i>	SLU 8114	SAMN22936320		
Blenniiformes	Cyprinodontidae	<i>Cyprinodon nevadensis</i>	See NCBI SRA	SAMN03072616*	✓	
Blenniiformes	Cyprinodontidae	<i>Cyprinodon variegatus</i>	See NCBI SRA	SAMN02736898*	✓	
Blenniiformes	Cyprinodontidae	<i>Floridichthys carpio</i>	KUIT 6534, KUI 35360	SAMN22936066	✓	
Blenniiformes	Fundulidae	<i>Fundulus heteroclitus</i>	See NCBI SRA	SAMN03277211*		
Blenniiformes	Fundulidae	<i>Fundulus zebrinus</i>	YFTC 16686, n.v.	SAMN22936068	✓	✓
Blenniiformes	Fundulidae	<i>Leptolucania ommata</i>	YFTC 23708, n.v.	SAMN22936142		
Blenniiformes	Procatopodidae	<i>Poropanchax normani</i>	YPM ICH 025212	SAMN22936313		
Blenniiformes	<i>Valencia</i>	<i>Valencia hispanica</i>	MNCN/ADN 63424	SAMN22936436	✓	
Blenniiformes	<i>Valencia</i>	<i>Valencia letourneuxi</i>	YFTC 25747, n.v.	SAMN22936437		
Blenniiformes	Poeciliidae	<i>Anableps anableps</i>	YPM ICH 024513	SAMN22935853	✓	
Blenniiformes	Poeciliidae	<i>Gambusia affinis</i>	See NCBI SRA	SAMN07157452*	✓	✓
Blenniiformes	Poeciliidae	<i>Gambusia holbrooki</i>	MNCN/ADN 59090	SAMN22936069	✓	
Blenniiformes	Poeciliidae	<i>Poecilia latipinna</i>	See NCBI SRA	SAMN02048973*	✓	
Blenniiformes	Poeciliidae	<i>Poecilia mexicana</i>	See NCBI SRA	SAMN02048972*	✓	
Blenniiformes	Poeciliidae	<i>Poecilia reticulata</i>	See NCBI SRA	SAMN02404645*	✓	
Blenniiformes	Poeciliidae	<i>Xiphophorus couchianus</i>	See NCBI SRA	SAMN03922721*	✓	
Blenniiformes	Poeciliidae	<i>Xiphophorus hellerii</i>	See NCBI SRA	SAMN09545741*	✓	
Blenniiformes	Polycentridae	<i>Monocirrhus polyacanthus</i>	P.Wainwright, PW1656 Pers. Coll.:	SAMN22936204	✓	✓
Blenniiformes	Polycentridae	<i>Polycentrus schomburgkii</i>	P.Wainwright, PW1659 Pers. Coll.:	SAMN22936304		
Blenniiformes	<i>Pholidichthys</i>	<i>Pholidichthys leucotaenia</i>	P.Wainwright, PW1329	SAMN05915100	✓	✓
Blenniiformes	Cichlidae	<i>Amphilophus citrinellus</i>	See NCBI SRA	SAMEA2698536*	✓	
Blenniiformes	Cichlidae	<i>Bathybates minor</i>	See NCBI SRA	SAMN04011497	✓	
Blenniiformes	Cichlidae	<i>Ectodus descampsi</i>	See NCBI SRA	SAMN04011500		
Blenniiformes	Cichlidae	<i>Eretmodus cyanostictus</i>	See NCBI SRA	SAMN04011501	✓	
Blenniiformes	Cichlidae	<i>Haplotaxodon microlepis</i>	See NCBI SRA	SAMN04011503		
Blenniiformes	Cichlidae	<i>Lamprologus calipterus</i>	See NCBI SRA	SAMN04011505	✓	
Blenniiformes	Cichlidae	<i>Paratilapia polleni</i>	YPM ICH 023179	SAMN22936271		
Blenniiformes	Cichlidae	<i>Paretroplus dambabe</i>	YPM ICH 023180	SAMN22936272	✓	✓
Blenniiformes	Cichlidae	<i>Pseudotropheus flavus</i>	See NCBI SRA	SAMN04011494		
Blenniiformes	Cichlidae	<i>Pterophyllum leopoldi</i>	YPM ICH 023150	SAMN05915114		✓
Blenniiformes	Cichlidae	<i>Ptychochromis oligacanthus</i>	YPM ICH 023177	SAMN22936331	✓	
Blenniiformes	Cichlidae	<i>Telmatochromis temporalis</i>	See NCBI SRA	SAMN04011535	✓	

Blenniiformes	Ambassidae	<i>Ambassis urotaenia</i>	YPM ICH 020542	SAMN22935847	✓	
Blenniiformes	Ambassidae	<i>Parambassis ranga</i>	YFTC 1064, n.v.	SAMN22935953	✓	✓
Blenniiformes	Mugilidae	<i>Crenimugil crenilabis</i>	YPM ICH 026701	SAMN22935994		
Blenniiformes	Mugilidae	<i>Osteomugil engeli</i>	YFTC 23617, n.v.	SAMN22936209		
Blenniiformes	Congrogadidae	<i>Congrogadus subducens</i>	YPM ICH 25208	SAMN22935986		
Blenniiformes	Plesiopidae	<i>Plesiops caeruleolineatus</i>	YPM ICH 026606	SAMN22936299		
Blenniiformes	Plesiopidae	<i>Plesiops</i> sp.	Pers. Coll.: M.Alfaro, Alfaro 13MS4	SAMN05915101		
Blenniiformes	Pseudochromidae	<i>Labracinus cyclophthalmus</i>	Pers. Coll.: P.Wainwright, PW1689	SAMN22936127		✓
Blenniiformes	Pseudochromidae	<i>Pseudochromis flavivertex</i>	CAS LR151	SAMN05915110	✓	
Blenniiformes	Pseudochromidae	<i>Pseudochromis fuscus</i>	See NCBI SRA	SAMEA4028829*	✓	
Blenniiformes	Pseudochromidae	<i>Pseudochromis sankeyi</i>	CAS LR117	SAMN05915111	✓	
Blenniiformes	Pomacentridae	<i>Acanthochromis polyacanthus</i>	See NCBI SRA	SAMN06347167*	✓	✓
Blenniiformes	Pomacentridae	<i>Amphiprion ocellaris</i>	See NCBI SRA	SAMN07982614*	✓	
Blenniiformes	Pomacentridae	<i>Amphiprion percula</i>	See NCBI SRA	SAMN08615572*	✓	
Blenniiformes	Pomacentridae	<i>Chromis chromis</i>	See NCBI SRA	SAMEA4028828*	✓	
Blenniiformes	Pomacentridae	<i>Chromis enchrysur</i>	CAS CEN01	SAMN05915054	✓	
Blenniiformes	Pomacentridae	<i>Pomacentrus philippinus</i>	YPM ICH 026633	SAMN22936308	✓	
Blenniiformes	Pomacentridae	<i>Stegastes partitus</i>	YPM ICH 24711	SAMN22936392	✓	
Blenniiformes	Embiotocidae	<i>Embiotoca jacksoni</i>	Pers. Coll.: P.Wainwright, PW227: B09	SAMN22936043	✓	✓
Blenniiformes	Embiotocidae	<i>Hyperprosopon ellipticus</i>	INHS 45420	SAMN22936110	✓	
Blenniiformes	Embiotocidae	<i>Phanerodon furcatus</i>	Pers. Coll.: P.Wainwright, PW269: B52	SAMN22936289	✓	
Blenniiformes	Grammatidae	<i>Gramma loreto</i>	CAS GLO01	SAMN05915067	✓	
Blenniiformes	Opistognathidae	<i>Opistognathus aurifrons</i>	YPM ICH 025216	SAMN22936245	✓	
Blenniiformes	Gobiesocidae	<i>Gobiesox maeandricus</i>	Pers. Coll.: P.Wainwright, PW2497	SAMN22936080	✓	✓
Blenniiformes	Gobiesocidae	<i>Gouania willdenowi</i>	See NCBI SRA	SAMEA104026382*	✓	
Blenniiformes	Gobiesocidae	<i>Lepadichthys lineatus</i>	KUIT 4109, CAS 224422	SAMN22936138		
Blenniiformes	Tripterygiidae	<i>Enneanectes boehlkei</i>	KUIT 166, USNM 327602	SAMN22936047		
Blenniiformes	Tripterygiidae	<i>Lepidonectes corallicola</i>	SIO 02-82	SAMN22936139		
Blenniiformes	Blenniidae	<i>Parablennius parvicornis</i>	See NCBI SRA	SAMEA4028827*	✓	✓
Blenniiformes	Blenniidae	<i>Scartella cristata</i>	CAS SCR01	SAMN05915120	✓	
Blenniiformes	Clinidae	<i>Gibbonsia metzi</i>	Pers. Coll.: P.Wainwright, PW221: B03	SAMN22936073	✓	
Blenniiformes	Clinidae	<i>Muraenoclinus dorsalis</i>	KUIT 6488	SAMN22936212		
Blenniiformes	Labrisomidae	<i>Labrisomus nuchipinnis</i>	CAS LNU08	SAMN05915078		
Blenniiformes	Chaenopsidae	<i>Emblemariopsis</i> sp.	CAS EMB01	SAMN05915061		
Blenniiformes	Dactyloscopidae	<i>Dactyloscopus lacteus</i>	SIO 02-88-1	SAMN22936012		
Blenniiformes	Dactyloscopidae	<i>Gillellus semicinctus</i>	SIO 01-167	SAMN22936076	✓	

Synbranchiformes	<i>Indostomus</i>	<i>Indostomus crocodilus</i>	YPM ICH 23894	SAMN22936113		
Synbranchiformes	<i>Indostomus</i>	<i>Indostomus paradoxus</i>	n.v. tissue whole	SAMN22936114	✓	✓
Synbranchiformes	Synbranchidae	<i>Monopterus albus</i>	Per. Coll.: W.L.Smith 22	SAMN22936207	✓	
Synbranchiformes	Synbranchidae	<i>Ophisternon aenigmaticum</i>	LSUMZ 16237	SAMN22936239		
Synbranchiformes	Synbranchidae	<i>Ophisternon bengalense</i>	UF 235970	SAMN22936240		
Synbranchiformes	Synbranchidae	<i>Synbranchus marmoratus</i>	KUIT 10406, KUI 41318	SAMN22936405		
Synbranchiformes	Chaudhuriidae	<i>Chaudhuria caudata</i>	UF 173154	SAMN22935963		
Synbranchiformes	Mastacembelidae	<i>Macrogathus aculeatus</i>	UF 161615	SAMN22936177		
Synbranchiformes	Mastacembelidae	<i>Macrogathus circumcinctus</i>	UF 170247	SAMN22936178		
Synbranchiformes	Mastacembelidae	<i>Macrogathus zebrinus</i>	Pers. Coll.: J.Day	SAMN22936179	✓	
Synbranchiformes	Mastacembelidae	<i>Mastacembelus armatus</i>	Pers. Coll.: J.Day	SAMN22936185	✓	
Synbranchiformes	Mastacembelidae	<i>Mastacembelus flavidus</i>	SAIAB 79915	SAMN22936186		
Synbranchiformes	Mastacembelidae	<i>Mastacembelus mastacembelus</i>	Pers. Coll.: J.Day JF1390	SAMN22936187		
Synbranchiformes	Mastacembelidae	<i>Mastacembelus unicolor</i>	UF 166011	SAMN22936188		✓
Synbranchiformes	<i>Pristolepis</i>	<i>Pristolepis fasciata</i>	UF 162364	SAMN22936318	✓	
Synbranchiformes	Badidae	<i>Badis badis</i>	Pers. Coll.: J.Day	SAMN22935884	✓	
Synbranchiformes	Badidae	<i>Badis pyema</i>	YFTC 18189, n.v.	SAMN22935885	✓	
Synbranchiformes	Badidae	<i>Dario dario</i>	YFTC 18190, n.v.	SAMN22936014		
Synbranchiformes	Badidae	<i>Dario hysginon</i>	YFTC 20196, n.v.	SAMN22936015	✓	
Synbranchiformes	Nandidae	<i>Nandus andrewi</i>	Pers. Coll.: P.Wainwright, PW1657	SAMN22936215		
Synbranchiformes	Nandidae	<i>Nandus nandus</i>	Pers. Coll.: P.Wainwright, PW1663	SAMN22936217	✓	
Synbranchiformes	Nandidae	<i>Nandus nebulosus</i>	Pers. Coll.: P.Wainwright, PW1660	SAMN22936218	✓	
Synbranchiformes	Nandidae	<i>Nandus cf. oxyrhynchus</i>	Pers. Coll.: W.L.Smith 488	SAMN22936216	✓	
Synbranchiformes	Channidae	<i>Channa andrao</i>	Pers. Coll.: J.Day	SAMN22935954		
Synbranchiformes	Channidae	<i>Channa argus</i>	CBM 12593	SAMN22935955		
Synbranchiformes	Channidae	<i>Channa aurantimaculata</i>	Pers. Coll.: J.Day	SAMN22935956		
Synbranchiformes	Channidae	<i>Channa bleheri</i>	Pers. Coll.: J.Day	SAMN22935957		
Synbranchiformes	Channidae	<i>Channa gachua</i>	Pers. Coll.: J.Day	SAMN22935958	✓	
Synbranchiformes	Channidae	<i>Channa lucius</i>	UF 236121	SAMN22935959		
Synbranchiformes	Channidae	<i>Channa marulius</i>	UF 237264	SAMN22935960	✓	
Synbranchiformes	Channidae	<i>Channa micropeltes</i>	Pers. Coll.: W.L.Smith 355	SAMN22935961	✓	
Synbranchiformes	Channidae	<i>Channa striata</i>	UF 173357	SAMN22935962	✓	
Synbranchiformes	Channidae	<i>Parachanna insignis</i>	CUMV 96133	SAMN22936263		
Synbranchiformes	Channidae	<i>Parachanna obscura</i>	CUMV 96491	SAMN22936264		
Synbranchiformes		<i>Helostoma temminckii</i>	Pers. Coll.: W.L.Smith 36	SAMN22936090	✓	
Synbranchiformes	Anabantidae	<i>Anabas testudineus</i>	UF 237404	SAMN22935852	✓	
Synbranchiformes	Anabantidae	<i>Ctenopoma acutirostre</i>	CUMV 93049	SAMN22936000	✓	
Synbranchiformes	Anabantidae	<i>Ctenopoma gabonense</i>	CUMV 87803	SAMN22936001		

Synbranchiformes	Anabantidae	<i>Ctenopoma kingsleyae</i>	CUMV 91505	SAMN22936002	✓
Synbranchiformes	Anabantidae	<i>Ctenopoma maculatum</i>	CUMV 92275	SAMN22936003	
Synbranchiformes	Anabantidae	<i>Ctenopoma multispine</i>	CUMV 91229	SAMN22936004	
Synbranchiformes	Anabantidae	<i>Ctenopoma muriei</i>	CUMV 94531	SAMN22936005	✓
Synbranchiformes	Anabantidae	<i>Ctenopoma nigropannosum</i>	CUMV 96662 Pers. Coll.: W.L.Smith	SAMN22936006	✓
Synbranchiformes	Anabantidae	<i>Ctenopoma ocellatum</i>	279	SAMN22936007	
Synbranchiformes	Anabantidae	<i>Microctenopoma ansorgii</i>	YPM ICH 025197	SAMN22936196	✓
Synbranchiformes	Anabantidae	<i>Microctenopoma fasciolatum</i>	YPM ICH 32030	SAMN22936197	
Synbranchiformes	Anabantidae	<i>Microctenopoma nanum</i>	CUMV 93021	SAMN22936198	✓
Synbranchiformes	Anabantidae	<i>Microctenopoma pekkolai</i>	CUMV 94529	SAMN22936199	
Synbranchiformes	Anabantidae	<i>Microctenopoma uelense</i>	CUMV 91502	SAMN22936200	
Synbranchiformes	Anabantidae	<i>Sandelia bainsii</i>	SAIAB 199798	SAMN22936347	
Synbranchiformes	Anabantidae	<i>Sandelia capensis</i>	SAIAB 186085	SAMN22936349	✓
Synbranchiformes	Anabantidae	<i>Sandelia capensis</i>	SAIAB 186114	SAMN22936349	
Synbranchiformes	Anabantidae	<i>Sandelia capensis</i>	SAIAB 186029	SAMN22936348	
Synbranchiformes	Osphronemidae	<i>Belontia hasselti</i>	UF 165962	SAMN22935895	✓
Synbranchiformes	Osphronemidae	<i>Betta albimarginata</i>	Pers. Coll.: J.Day	SAMN22935899	
Synbranchiformes	Osphronemidae	<i>Betta macrostoma</i>	Pers. Coll.: J.Day	SAMN22935900	✓
Synbranchiformes	Osphronemidae	<i>Betta mandor</i>	YPM ICH 34720	SAMN22935901	
Synbranchiformes	Osphronemidae	<i>Betta splendens</i>	Pers. Coll.: J.Day	SAMN22935902	✓
Synbranchiformes	Osphronemidae	<i>Ctenops nobilis</i>	YPM ICH 33735	SAMN22936008	✓
Synbranchiformes	Osphronemidae	<i>Luciocephalus aura</i>	UF 167012 Pers. Coll.: W.L.Smith	SAMN22936150	
Synbranchiformes	Osphronemidae	<i>Luciocephalus pulcher</i>	718	SAMN22936151	
Synbranchiformes	Osphronemidae	<i>Macropodus ocellatus</i>	CBM 12607	SAMN22936180	
Synbranchiformes	Osphronemidae	<i>Macropodus opercularis</i>	Pers. Coll.: J.Day Pers. Coll.: W.L.Smith	SAMN22936181	✓
Synbranchiformes	Osphronemidae	<i>Osphronemus goramy</i>	536	SAMN22936251	✓
Synbranchiformes	Osphronemidae	<i>Osphronemus latyclavius</i>	YFTC 20201, n.v.	SAMN22936252	
Synbranchiformes	Osphronemidae	<i>Parasphaerichthys ocellatus</i>	YPM ICH 32028	SAMN22936269	✓
Synbranchiformes	Osphronemidae	<i>Parosphromenus deissneri</i>	Pers. Coll.: J.Day	SAMN22936273	✓
Synbranchiformes	Osphronemidae	<i>Parosphromenus linkei</i>	YFTC 20193, n.v.	SAMN22936274	
Synbranchiformes	Osphronemidae	<i>Pseudosphromenus cupanus</i>	YPM ICH 33699 Pers. Coll.: W.L.Smith	SAMN22936327	
Synbranchiformes	Osphronemidae	<i>Sphaerichthys osphromenoides</i>	308	SAMN22936384	✓
Synbranchiformes	Osphronemidae	<i>Sphaerichthys vaillanti</i>	Pers. Coll.: J.Day	SAMN22936385	
Synbranchiformes	Osphronemidae	<i>Trichogaster chuna</i>	Pers. Coll.: J.Day	SAMN22936422	
Synbranchiformes	Osphronemidae	<i>Trichogaster labiosa</i>	YPM ICH 32029	SAMN22936423	✓
Synbranchiformes	Osphronemidae	<i>Trichogaster lalius</i>	Pers. Coll.: J.Day	SAMN22936424	✓
Synbranchiformes	Osphronemidae	<i>Trichopodus leerii</i>	Pers. Coll.: J.Day	SAMN22936426	✓
Synbranchiformes	Osphronemidae	<i>Trichopodus microlepis</i>	Pers. Coll.: J.Day	SAMN22936427	
Synbranchiformes	Osphronemidae	<i>Trichopodus pectoralis</i>	YPM ICH 021566	SAMN22936428	✓

Synbranchiformes	Osphronemidae	<i>Trichopodus trichopterus</i>	LSUMZ 13914	SAMN22936429	✓
Synbranchiformes	Osphronemidae	<i>Trichopsis pumila</i>	n.v.	SAMN22936431	✓
Synbranchiformes	Osphronemidae	<i>Trichopsis vittata</i>	UF 162202	SAMN22936432	✓
Carangiformes	Centropomidae	<i>Lates calcarifer</i>	NTM 92	SAMN05785344	✓
Carangiformes	Centropomidae	<i>Centropomus ensiferus</i>	LSUMZ 16022	SAMN22935943	✓
Carangiformes	Centropomidae	<i>Centropomus medius</i>	KUIT 8498, KUI 40301	SAMN05915046	✓
Carangiformes		<i>Lactarius lactarius</i>	NSMT-P 91244	SAMN22936130	
Carangiformes	<i>Sphyraena</i>	<i>Sphyraena barracuda</i>	LSUMZ 15881	SAMN22936386	✓
Carangiformes	<i>Sphyraena</i>	<i>Sphyraena jello</i>	LSUMZ 17037	SAMN22936387	✓
Carangiformes	<i>Sphyraena</i>	<i>Sphyraena pinguis</i>	LSUMZ 17074	SAMN22936388	✓
Carangiformes	<i>Sphyraena</i>	<i>Sphyraena putnamae</i>	KUIT 6785, photo voucher	SAMN05915126	✓
Carangiformes	<i>Sphyraena</i>	<i>Sphyraena sphyraena</i>	Pers. Coll.: W.L.Smith 499	SAMN05785363	
Carangiformes	Polynemidae	<i>Eleutheronema tetradactylum</i>	Pers. Coll.: H.Larson	SAMN05785336	✓
Carangiformes	Polynemidae	<i>Polydactylus approximans</i>	LSUMZ 17875	SAMN22936305	✓
Carangiformes	Polynemidae	<i>Polydactylus sexfilis</i>	KUIT 6829, SAIAB 77939	SAMN05915103	
Carangiformes	Polynemidae	<i>Polynemus melanochir</i>	LSUMZ 14165	SAMN22936306	
Carangiformes	<i>Psettodes</i>	<i>Psettodes eneumeri</i>	LSUMZ 5295	SAMN05785354	✓
Carangiformes	Citharidae	<i>Brachypleura novaezeelandiae</i>	LSUMZ 13790	SAMN22935914	
Carangiformes	Citharidae	<i>Citharus linguatula</i>	Pers. Coll.: W.L.Smith 596	SAMN05785330	
Carangiformes	Citharidae	<i>Citharoides macrolepis</i>	KUIT 2468, KUI 27264	SAMN05915055	✓
Carangiformes	Achiridae	<i>Gymnachirus melas</i>	KUIT 5187, KUI 30098	SAMN05785338	✓
Carangiformes	Achiridae	<i>Trinectes maculatus</i>	KUIT 1501, KUI 27162	SAMN05785371	✓
Carangiformes	Achiropsettidae	<i>Mancopsetta maculata</i>	Pers. Coll.: W.L.Smith 714	SAMN05785346	
Carangiformes	Achiropsettidae	<i>Neoachiropsetta milfordi</i>	Pers. Coll.: W.L.Smith 715	SAMN05785350	
Carangiformes	Samaridae	<i>Samaris cristatus</i>	SAIAB 82287	SAMN22936345	✓
Carangiformes	Samaridae	<i>Samariscus filipectoralis</i>	LSUMZ 13484	SAMN22936346	
Carangiformes	Samaridae	<i>Samariscus xenicus</i>	KUIT 2484, KUI 27266	SAMN05785357	✓
Carangiformes	Poecilopsettidae	<i>Poecilopsetta natalensis</i>	SAIAB 81888	SAMN22936301	
Carangiformes	Poecilopsettidae	<i>Poecilopsetta plinthus</i>	KUIT 2473, KUI 27256	SAMN05915102	✓
Carangiformes	Poecilopsettidae	<i>Poecilopsetta zanzibarensis</i>	SAIAB 82402	SAMN22936302	
Carangiformes	Cynoglossidae	<i>Cynoglossus lingua</i>	LSUMZ 17034	SAMN22936011	✓
Carangiformes	Cynoglossidae	<i>Paraplagusia japonica</i>	LSUMZ 17060	SAMN22936267	
Carangiformes	Cynoglossidae	<i>Symphurus plagiusa</i>	AMNH 474	SAMN05785364	
Carangiformes	Soleidae	<i>Aseraggodes xenicus</i>	KUIT 5719, KUI 32536	SAMN05915093	✓
Carangiformes	Soleidae	<i>Austroglossus pectoralis</i>	SAIAB 200601	SAMN22935882	
Carangiformes	Soleidae	<i>Dagetichthys marginatus</i>	SAIAB 200744	SAMN22936404	
Carangiformes	Soleidae	<i>Heteromycteris capensis</i>	SAIAB 191581	SAMN22936095	
Carangiformes	Soleidae	<i>Solea turbynei</i>	SAIAB 82350	SAMN22936382	✓

Carangiformes	Scophthalmidae	<i>Scophthalmus maximus</i>	See NCBI SRA	SAMN08049846*	✓
Carangiformes	Scophthalmidae	<i>Scophthalmus rhombus</i>	KUIT 5416, n.v.	SAMN05785360	✓
Carangiformes	Pleuronectidae	<i>Pleuronichthys cornutus</i>	LSUMZ 17067	SAMN22936300	✓
Carangiformes	Pleuronectidae	<i>Pleuronichthys guttulatus</i>	SIO 01-179	SAMN05785340	
Carangiformes	Pleuronectidae	<i>Pseudopleuronectes yokohamae</i>	LSUMZ 17053	SAMN22936325	✓
Carangiformes	Paralichthyidae	<i>Ancylosetta dilecta</i>	LSUMZ 15797	SAMN22935857	
Carangiformes	Paralichthyidae	<i>Paralichthys albigutta</i>	AMNH Uncat E172	SAMN05785351	✓
Carangiformes	Paralichthyidae	<i>Paralichthys oblongus</i>	KUIT 1493, KUI 27158	SAMN05915073	✓
Carangiformes	Paralichthyidae	<i>Pseudorhombus elevatus</i>	LSUMZ 16603	SAMN22936326	✓
Carangiformes	Cyclopsettidae	<i>Citharichthys spilopterus</i>	LSUMZ 15927	SAMN22935984	
Carangiformes	Cyclopsettidae	<i>Cyclopsetta fimbriata</i>	KUIT 3985, KUI 29710	SAMN05785333	✓
Carangiformes	Cyclopsettidae	<i>Etropus cyclosquamus</i>	KUIT 5241, KUI 30193	SAMN05785337	✓
Carangiformes	Cyclopsettidae	<i>Syacium gunteri</i>	LSUMZ 15543	SAMN22936401	✓
Carangiformes	Bothidae	<i>Bothus pantherinus</i>	KUIT 5642, SAIAB 86150	SAMN05915039	✓
Carangiformes	Bothidae	<i>Crossorhombus azureus</i>	LSUMZ 14148	SAMN22935995	✓
Carangiformes	Bothidae	<i>Crossorhombus kobensis</i>	KUIT 2485, KUI 27267	SAMN05785332	
Carangiformes	Bothidae	<i>Engyophrys senta</i>	LSUMZ 15538	SAMN22936044	
Carangiformes	Bothidae	<i>Trichopsetta ventralis</i>	LSUMZ 15806	SAMN22936430	
Carangiformes	<i>Leptobrama</i>	<i>Leptobrama muelleri</i>	FMNH 119722	SAMN05785345	✓
Carangiformes	<i>Toxotes</i>	<i>Toxotes blythii</i>	YPM ICH 32036	SAMN22936414	✓
Carangiformes	<i>Toxotes</i>	<i>Toxotes jaculatrix</i>	YPM ICH 020543	SAMN05915135	✓
Carangiformes		<i>Nematistius pectoralis</i>	LSUMZ 18084	SAMN22936221	
Carangiformes		<i>Mene maculatus</i>	Pers. Coll.: W.L.Smith 370	SAMN05915082	✓
Carangiformes		<i>Xiphias gladius</i>	Pers. Coll.: W.L.Smith 787	SAMN05785372	✓
Carangiformes	Istiophoridae	<i>Istiophorus platypterus</i>	KUIT 5428	SAMN05915075	
Carangiformes	Istiophoridae	<i>Kajikia audax</i>	SIO 06-38	SAMN22936119	
Carangiformes	Istiophoridae	<i>Tetrapturus angustirostris</i>	SIO 05-31	SAMN05785366	
Carangiformes	Trachinotinae	<i>Scomberoides commersonianus</i>	KUIT 8988, photo voucher	SAMN05785359	✓
Carangiformes	Trachinotinae	<i>Scomberoides lysan</i>	LSUMZ 14159	SAMN22936358	✓
Carangiformes	Trachinotinae	<i>Scomberoides tol</i>	SAIAB AV-2010-091	SAMN22936359	✓
Carangiformes	Trachinotinae	<i>Trachinotus baillonii</i>	SAIAB RB-09-160	SAMN22936415	✓
Carangiformes	Trachinotinae	<i>Trachinotus blochii</i>	KUIT 6793, SAIAB 77903	SAMN05785368	
Carangiformes	Trachinotinae	<i>Trachinotus goodei</i>	YFTC 1994, n.v. KUIT 3521, MCZ	SAMN22936416	✓
Carangiformes		<i>Rachycentron canadum</i>	157656 KUIT 7212, SAIAB	SAMN05915115	
Carangiformes		<i>Coryphaena hippurus</i>	77983	SAMN05915056	✓
Carangiformes	Echeneidae	<i>Echeneis naucrates</i>	SAIAB HM07-581	SAMN22936038	✓
Carangiformes	Echeneidae	<i>Echeneis neucratoides</i>	KUIT 1201, KUI 27104	SAMN05785335	
Carangiformes	Echeneidae	<i>Phtheichthys lineatus</i>	SAIAB ACEP-09-224	SAMN22936295	✓

Carangiformes	Echeneidae	<i>Remora albescens</i>	SIO 05-37	SAMN22936334	✓	
Carangiformes	Echeneidae	<i>Remora brachyptera</i>	SIO 07-91	SAMN22936335	✓	
Carangiformes	Echeneidae	<i>Remora osteochir</i>	SIO 11-34	SAMN22936336	✓	
Carangiformes	Echeneidae	<i>Remora remora</i>	SAIAB ACEP-08-1660	SAMN22936337	✓	
Carangiformes	Carangidae	<i>Alectis indicus</i>	KUIT 8966, photo voucher	SAMN05915025	✓	
Carangiformes	Carangidae	<i>Alepes kleinii</i>	KUIT 8986, photo voucher	SAMN05915026		
Carangiformes	Carangidae	<i>Alepes vari</i>	QM A01251	SAMN22935844		
Carangiformes	Carangidae	<i>Alepes vari</i>	QM I39515	SAMN22935845		
Carangiformes	Carangidae	<i>Carangichthys dinema</i>	FRLM 48738	SAMN22935924		
Carangiformes	Carangidae	<i>Carangoides armatus</i>	LSUMZ 16745	SAMN22935925		
Carangiformes	Carangidae	<i>Carangoides armatus</i>	LSUMZ 16745	SAMN22935925		
Carangiformes	Carangidae	<i>Carangoides chrysocephalus</i>	SAIAB Event Number: AV/2010-04; n.v.	SAMN22935926	✓	
Carangiformes	Carangidae	<i>Carangoides ferdau</i>	SAIAB Event Number: PCH 2005-27; n.v.	SAMN22935927	✓	
Carangiformes	Carangidae	<i>Carangoides praeustus</i>	FRLM 51405	SAMN22935928		
Carangiformes	Carangidae	<i>Caranx caninus</i>	LSUMZ 17829	SAMN22935929	✓	
Carangiformes	Carangidae	<i>Caranx heberii</i>	SAIAB Event Number JRG-PDO-15-215; n.v.	SAMN22935930		
Carangiformes	Carangidae	<i>Caranx latus</i>	UF 180908	SAMN22935931	✓	✓
Carangiformes	Carangidae	<i>Caranx latus</i>	UF 183512	SAMN22935932		
Carangiformes	Carangidae	<i>Caranx melampygus</i>	KUIT 5657, SAIAB 86154	SAMN05915044	✓	
Carangiformes	Carangidae	<i>Caranx vinctus</i>	LSUMZ 14570	SAMN22935933		
Carangiformes	Carangidae	<i>Caranx vinctus</i>	LSUMZ 14585	SAMN22935934		
Carangiformes	Carangidae	<i>Chloroscombrus orqueta</i>	KUIT 8495, KUI 40296 KUIT 8984, photo voucher	SAMN05915053	✓	
Carangiformes	Carangidae	<i>Decapterus maruadsi</i>	LSUMZ 17993	SAMN05785334	✓	
Carangiformes	Carangidae	<i>Gnathanodon speciosus</i>	LSUMZ 17993	SAMN22936079	✓	
Carangiformes	Carangidae	<i>Hemicaranx bicolor</i>	MNHN 1913-0110	SAMN22936091	✓	
Carangiformes	Carangidae	<i>Megalaspis cordyla</i>	KUIT 4705	SAMN05785347	✓	
Carangiformes	Carangidae	<i>Parastromateus niger</i>	LSUMZ 17039	SAMN22936270	✓	
Carangiformes	Carangidae	<i>Selaroides leptolepis</i>	LSUMZ 14065	SAMN22936371	✓	
Carangiformes	Carangidae	<i>Selene peruviana</i>	SIO 07-88L	SAMN22936372		
Carangiformes	Carangidae	<i>Selene vomer</i>	LSUMZ 14271	SAMN22936373	✓	
Carangiformes	Carangidae	<i>Seriola dumerili</i>	Pers. Coll.: P.Wainwright, PW2629	SAMN22936374	✓	
Carangiformes	Carangidae	<i>Seriola dumerili</i>	SAIAB ACEP-09-314	SAMN22936375		
Carangiformes	Carangidae	<i>Seriola zonata</i>	KUIT 1188, KUI 27046	SAMN05915125	✓	
Carangiformes	Carangidae	<i>Trachurus trachurus</i>	KUIT 8077, n.v.	SAMN05785370	✓	
Perciformes	Epinephelidae	<i>Cephalopholis argus</i>	CAS CAG01	SAMN05915047	✓	✓
Perciformes	Epinephelidae	<i>Cephalopholis cruentata</i>	YPM ICH 24718	SAMN22935945	✓	
Perciformes	Epinephelidae	<i>Diploprion drachi</i>	Pers. Coll.: G. Bernardi	SAMN22936029	✓	
Perciformes	Epinephelidae	<i>Jeboehlkia gladifer</i>	AMNH CUR13192	SAMN22936118		✓

Perciformes	Epinephelidae	<i>Liopropoma rubre</i>	YPM ICH 24752	SAMN22936146	✓	
Perciformes	Epinephelidae	<i>Rypticus subbfrenatus</i>	YPM ICH 24697	SAMN22936344	✓	
Perciformes	Anthiidae	<i>Acanthistius cinctus</i>	Pers. Coll.: L.Liggins, KER-427	SAMN22935826	✓	✓
Perciformes	Anthiidae	<i>Pseudanthias squamipinnis</i>	Pers. Coll.: M.Alfaro, Alfaro-969	SAMN05915109	✓	✓
Perciformes	Anthiidae	<i>Trachypoma macracanthus</i>	Pers. Coll.: L.Liggins, KER-433	SAMN22936418		
Perciformes	Bembropidae	<i>Bembrops anatirostris</i>	YFTC 14558, n.v.	SAMN22935897	✓	
Perciformes	Bembropidae	<i>Chrionema furunoi</i>	NSMT-P 78494	SAMN22935982		
Perciformes	Serranidae	<i>Chelidoperca hirundinacea</i>	NSMT-P115036	SAMN22935971		
Perciformes	Serranidae	<i>Hypoplectrus puella</i>	Pers. Coll.: M.Alfaro, Alfaro-1010.1	SAMN05915074	✓	
Perciformes	Serranidae	<i>Serranus tigrinus</i>	Pers. Coll.: P.Wainwright, PW1343: mea207	SAMN22936376	✓	✓
Perciformes	Trachinidae	<i>Echiichthys vipera</i>	YFTC 24258, n.v.	SAMN22936039		
Perciformes	Trachinidae	<i>Trachinus radiatus</i>	n.v.	SAMN22936417	✓	
Perciformes		<i>Nippon spinosus</i>	SIO 00-174	SAMN22936228	✓	✓
Perciformes	Percidae	<i>Allohistium cinereum</i>	UT 91.7531	SAMN22936057	✓	
Perciformes	Percidae	<i>Ammocrypta beanii</i>	INHS 38611	SAMN22935849	✓	
Perciformes	Percidae	<i>Ammocrypta pellucida</i>	YPM ICH 017573	SAMN22935850	✓	
Perciformes	Percidae	<i>Crystallaria asprella</i>	YFTC 686, n.v.	SAMN22935997	✓	
Perciformes	Percidae	<i>Etheostoma baileyi</i>	UT 91.7240	SAMN22936054	✓	
Perciformes	Percidae	<i>Etheostoma basilare</i>	n.v.	SAMN22936055	✓	
Perciformes	Percidae	<i>Etheostoma blennioides</i>	YPM ICH 024144	SAMN22936056		
Perciformes	Percidae	<i>Etheostoma histrio</i>	YPM ICH 016102	SAMN22936058	✓	
Perciformes	Percidae	<i>Etheostoma pholidotum</i>	YPM ICH 015608	SAMN22936059		
Perciformes	Percidae	<i>Etheostoma swaini</i>	YPM ICH 027128	SAMN22936060		
Perciformes	Percidae	<i>Etheostoma variatum</i>	YPM ICH 23724	SAMN22936061	✓	
Perciformes	Percidae	<i>Etheostoma zonale</i>	UT 91.6631	SAMN22936062	✓	
Perciformes	Percidae	<i>Nothonotus juliae</i>	INHS 38559	SAMN22936231		
Perciformes	Percidae	<i>Nothonotus rufilineatus</i>	UT 91.7011	SAMN22936232		
Perciformes	Percidae	<i>Perca flavescens</i>	YPM ICH 027384	SAMN22936278	✓	
Perciformes	Percidae	<i>Perca fluviatilis</i>	See NCBI SRA	SAMN08954933*	✓	
Perciformes	Percidae	<i>Percina aurantiaca</i>	INHS 64349	SAMN22936282	✓	
Perciformes	Percidae	<i>Percina caprodes</i>	YPM ICH 27964	SAMN22936283	✓	✓
Perciformes	Percidae	<i>Percina cymatotaenia</i>	YPM ICH 018551	SAMN22936284	✓	
Perciformes	Percidae	<i>Percina evides</i>	YPM ICH 023560	SAMN22936285	✓	
Perciformes	Percidae	<i>Percina macrocephala</i>	YPM ICH 024352; ex UT 91.7318	SAMN22936286	✓	
Perciformes	Percidae	<i>Percina tanasi</i>	YFTC 25474, n.v.	SAMN22936287	✓	
Perciformes	Percidae	<i>Sander canadensis</i>	n.v.	SAMN22936351	✓	
Perciformes		<i>Percophis brasiliensis</i>	LBP 8654 T35304	SAMN22936288	✓	
Perciformes	Bovichtidae	<i>Bovichtus chilensis</i>	YPM ICH 027476	SAMN22935912	✓	

Perciformes	Bovichtidae	<i>Cottoperca trigloides</i>	YFTC 3925, n.v.	SAMN22935990	✓
Perciformes		<i>Pseudaphritus urvillii</i>	YFTC 16619, n.v.	SAMN22936321	✓
Perciformes		<i>Eleginops maclovinus</i>	YPM ICH 016549	SAMN22936042	✓
Perciformes	"Nototheniidae"	<i>Notothenia coriiceps</i>	YPM ICH 016542	SAMN22936235	✓
Perciformes	"Nototheniidae"	<i>Patagonotothen ramsayi</i>	YFTC 24090, n.v.	SAMN22936276	✓
Perciformes	<i>Harpagifer</i>	<i>Harpagifer bispinis</i>	YFTC 21691, n.v.	SAMN22936088	✓
Perciformes	<i>Harpagifer</i>	<i>Harpagifer kerguelensis</i>	YFTC 4830, n.v.	SAMN22936089	
Perciformes	Artedidraconidae	<i>Artedidraco glareobarbatus</i>	YFTC 14511, n.v.	SAMN22935869	✓
Perciformes	Artedidraconidae	<i>Pogonophryne cerebropogon</i>	YFTC 24233, n.v.	SAMN22936303	✓
Perciformes	"Bathdraconidae"	<i>Akarotaxis nudiceps</i>	YPM ICH 024118	SAMN22935842	✓
Perciformes	"Bathdraconidae"	<i>Parachaenichthys charcoti</i>	YPM ICH 022368	SAMN22936262	
Perciformes	Channichthyidae	<i>Chaenocephalus aceratus</i>	See NCBI SRA	SAMEA4028820*	✓
Perciformes	Channichthyidae	<i>Chionodraco rastrospinosus</i>	YPM ICH 016672	SAMN22935974	✓
Perciformes	Channichthyidae	<i>Pagetopsis macropterus</i>	NZNM 043556	SAMN22936258	
Perciformes	Platycephalidae	<i>Platycephalus indicus</i>	ASIZ 10910261 Pers. Coll.: Leonardo Castro	SAMN22936298	✓
Perciformes		<i>Normanichthys crockeri</i>		SAMN22936230	✓
Perciformes	<i>Hoplichthys</i>	<i>Hoplichthys gilberti</i>	ASIZP 9010790	SAMN22936105	✓
Perciformes	<i>Hoplichthys</i>	<i>Hoplichthys langsdorfi</i>	ASIZP 0913594	SAMN22936106	✓
Perciformes	Neosebastidae	<i>Neosebastes thetidis</i>	NMV A 22113	SAMN22936225	✓
Perciformes	Congiopodidae	<i>Congiopodus leucopaecilus</i>	NMNZ P.044580 Pers. Coll.: P.Wainwright, PCW 3785	SAMN22935985	✓
Perciformes	Synanceiidae	<i>Inimicus didactylus</i>		SAMN22936115	✓
Perciformes	Synanceiidae	<i>Minous trachycephalus</i>	NMV A 29712-004	SAMN22936201	✓
Perciformes	Scorpaenidae	<i>Sebastes aleutianus</i>	See NCBI SRA	SAMN03964772*	✓
Perciformes	Scorpaenidae	<i>Sebastes koreanus</i>	See NCBI SRA	SAMN10490951*	
Perciformes	Scorpaenidae	<i>Sebastes minor</i>	See NCBI SRA	SAMN03354192*	
Perciformes	Scorpaenidae	<i>Sebastes nigrocinctus</i>	See NCBI SRA	SAMN02981553*	✓
Perciformes	Scorpaenidae	<i>Sebastes norvegicus</i>	See NCBI SRA	SAMEA4028819*	✓
Perciformes	Scorpaenidae	<i>Sebastes nudus</i>	See NCBI SRA	SAMN10490952*	
Perciformes	Scorpaenidae	<i>Sebastes rubrivinctus</i>	See NCBI SRA	SAMN02981552*	
Perciformes	Scorpaenidae	<i>Sebastes schlegelii</i>	See NCBI SRA	SAMN10490953*	✓
Perciformes	Scorpaenidae	<i>Sebastes steindachneri</i>	See NCBI SRA	SAMN03579458*	✓
Perciformes	Scorpaenidae	<i>Taenianotus triacanthus</i>	Pers. Coll.: M.Alfaro, Alfaro-889	SAMN05915130	✓
Perciformes	Bembridae	<i>Bembras japonicus</i>	ASIZPO 910626	SAMN22935896	
Perciformes	Bembridae	<i>Parabembras curtus</i>	ASIZPO 910628	SAMN22936259	
Perciformes	Triglidae	<i>Prionotus evolans</i>	YPM ICH 017358	SAMN22936315	✓
Perciformes	Triglidae	<i>Pterygotrigla hemisticta</i>	ASIZP 091046	SAMN22936329	
Perciformes	Anoplopomatidae	<i>Anoplopoma fimbria</i>	See NCBI SRA	SAMN02144194*	✓
Perciformes	Anoplopomatidae	<i>Erilepis zonifer</i>	YPM ICH 026411	SAMN22936051	

Perciformes	Zaniolepididae	<i>Oxylebius pictus</i>	UW 113229	SAMN22936256	✓
Perciformes	Zaniolepididae	<i>Zaniolepis frenata</i>	UW 119888	SAMN22936444	✓
Perciformes	Zaniolepididae	<i>Zaniolepis latipinnis</i>	FMNH 121496	SAMN22936445	✓
Perciformes	Hexagrammidae	<i>Hexagrammos decagrammus</i>	INHS 45417	SAMN22936096	✓
Perciformes	Trichodontidae	<i>Trichodon trichodon</i>	UW 117635	SAMN22936421	✓
Perciformes	Cyclopteridae	<i>Eumicrotremus orbis</i>	Pers. Coll.: P.Wainwright, PW2499	SAMN22936065	✓
Perciformes	Liparidae	<i>Liparis mucosus</i>	n.v.	SAMN22936147	✓
Perciformes	Liparidae	<i>Paraliparis meganchus</i>	YPM ICH 022466	SAMN22936265	✓
Perciformes	Liparidae	<i>Pseudoliparis</i> sp.	See NCBI SRA	SAMN10662039*	
Perciformes	Rhamphocottidae	<i>Ereunias grallator</i>	Pers. Coll.: M.Miya 01-054	SAMN22936050	
Perciformes	Rhamphocottidae	<i>Rhamphocottus richardsoni</i>	Pers. Coll.: P.Wainwright, PW2440	SAMN22936339	
Perciformes		<i>Scorpaenichthys marmoratus</i>	Pers. Coll.: P.Wainwright, PW222: B04	SAMN22936366	✓
Perciformes	Agonidae	<i>Aspidophoroides monopterygius</i>	YPM ICH 020685	SAMN22935871	✓
Perciformes	Agonidae	<i>Blepsias cirrhosus</i>	Pers. Coll.: P.Wainwright, PW2441	SAMN22935905	✓
Perciformes	Agonidae	<i>Hemitripteris bolini</i>	UW 151146	SAMN22936093	✓
Perciformes	Agonidae	<i>Stellerina xyosterna</i>	n.v.	SAMN22936393	✓
Perciformes	Cottidae	<i>Cottus carolinae</i>	YPM ICH 021076	SAMN22935992	✓
Perciformes	Cottidae	<i>Cottus rhenanus</i>	See NCBI SRA KUIT 3570, MCZ	SAMN04145896*	
Perciformes	Psychrolutidae	<i>Cottunculus thomsonii</i>	159183	SAMN22935991	✓
Perciformes	Psychrolutidae	<i>Malacocottus zonorus</i>	KUIT 2319, KUI 28057	SAMN22936183	✓
Perciformes	Psychrolutidae	<i>Myoxocephalus aenaeus</i>	YPM ICH 021194	SAMN22936214	✓
Perciformes	Psychrolutidae	<i>Myoxocephalus scorpius</i>	See NCBI SRA	SAMEA4028818*	✓
Perciformes	Psychrolutidae	<i>Triglops murrayi</i>	YPM ICH 020694	SAMN22936433	✓
Perciformes		<i>Hypoptychus dybowskii</i>	NSMT-P72827	SAMN22936111	
Perciformes		<i>Aulichthys japonicus</i>	NSMT-P72829	SAMN22935878	✓
Perciformes	Gasterosteidae	<i>Gasterosteus islandicus</i>	YFTC 16641, n.v.	SAMN22936070	✓
Perciformes	Gasterosteidae	<i>Pungitius pungitius</i>	See NCBI SRA	SAMN05210078*	✓
Perciformes	Gasterosteidae	<i>Spinachia spinachia</i>	YFTC 16669, n.v.	SAMN22936391	✓
Perciformes	Bathymasteridae	<i>Bathymaster caeruleofasciatus</i>	UW 150110	SAMN22935891	✓
Perciformes	Bathymasteridae	<i>Bathymaster leurolepis</i>	UW 48567	SAMN22935892	✓
Perciformes	Bathymasteridae	<i>Bathymaster signatus</i>	UW 119600	SAMN22935893	✓
Perciformes	Bathymasteridae	<i>Rathbunella hypoplecta</i>	n.v.	SAMN22936333	
Perciformes	Bathymasteridae	<i>Ronquilus jordani</i>	UW 116967	SAMN22936343	✓
Perciformes		<i>Cebidichthys violaceus</i>	INHS 45421	SAMN22935939	✓
Perciformes	Stichaeidae	<i>Alectrias alectrolophus</i>	UW 47876	SAMN22935843	✓
Perciformes	Stichaeidae	<i>Anoplarchus insignis</i>	UW 47871	SAMN22935860	✓
Perciformes	Stichaeidae	<i>Anoplarchus purpurescens</i>	UW 151344	SAMN22936442	✓

Perciformes	Stichaeidae	<i>Bryozoichthys lysimus</i>	UW 150624	SAMN22935917	✓
Perciformes	Stichaeidae	<i>Bryozoichthys marjorius</i>	UW 150104	SAMN22935918	✓
Perciformes	Stichaeidae	<i>Chirolophis decoratus</i>	UW 119212	SAMN22935976	✓
Perciformes	Stichaeidae	<i>Chirolophis japonicus</i>	UW 47908	SAMN22935977	
Perciformes	Stichaeidae	<i>Chirolophis snyderi</i>	UW 150723	SAMN22935978	
Perciformes	Stichaeidae	<i>Ernogrammus hexagrammus</i>	UW 47891	SAMN22936052	✓
Perciformes	Stichaeidae	<i>Eumesogrammus praecisus</i>	UW 150174	SAMN22936064	✓
Perciformes	Stichaeidae	<i>Phytichthys chirus</i>	UW 151660	SAMN22936296	
Perciformes	Stichaeidae	<i>Scytalina cerdale</i>	YPM ICH 026410	SAMN22936369	
Perciformes	Stichaeidae	<i>Stichaeopsis nana</i>	UW 47889	SAMN22936396	
Perciformes	Stichaeidae	<i>Stichaeus grigorjewi</i>	UW 47895	SAMN22936397	✓
Perciformes	Stichaeidae	<i>Stichaeus nozawai</i>	UW 47894	SAMN22936398	✓
Perciformes	Stichaeidae	<i>Stichaeus punctatus</i>	UW 150124	SAMN22936399	✓
Perciformes	Stichaeidae	<i>Xiphister atropurpureus</i>	UW 151673	SAMN22936440	
Perciformes	Stichaeidae	<i>Xiphister mucosus</i>	UW 151678	SAMN22936441	✓
Perciformes	<i>Cryptacanthodes</i>	<i>Cryptacanthodes aleutensis</i>	UW 48737	SAMN22935996	
Perciformes	<i>Cryptacanthodes</i>	<i>Cryptacanthodes giganteus</i>	UW 48792	SAMN22936016	
Perciformes	<i>Cryptacanthodes</i>	<i>Cryptacanthodes maculatus</i>	YPM ICH 020687	SAMN22935996	✓
Perciformes	Lumpenidae	<i>Acantholumpenus mackayi</i>	UW 150276	SAMN22935830	✓
Perciformes	Lumpenidae	<i>Anisarchus medius</i>	UW 49373	SAMN22935858	✓
Perciformes	Lumpenidae	<i>Anisarchus medius</i>	UW 152055	SAMN22936154	
Perciformes	Lumpenidae	<i>Leptoclinus maculatus</i>	UW 49369	SAMN22936141	✓
Perciformes	Lumpenidae	<i>Leptoclinus maculatus</i>	UW 151205	SAMN22936153	✓
Perciformes	Lumpenidae	<i>Lumpenella longirostris</i>	UW 151000	SAMN22936152	✓
Perciformes	Lumpenidae	<i>Lumpenus sagitta</i>	UW 150616	SAMN22936155	✓
Perciformes	Lumpenidae	<i>Poroclinus rothrocki</i>	UW 150577	SAMN22936310	✓
Perciformes		<i>Zaprora silenus</i>	UW 152655	SAMN22936446	✓
Perciformes		<i>Zaprora silenus</i>	UW 150107	SAMN22936447	
Perciformes	Opisthocentridae	<i>Askoldia variegata</i>	UW 44508	SAMN22935870	
Perciformes	Opisthocentridae	<i>Opisthocentrus ocellatus</i>	UW 44935	SAMN22936242	✓
Perciformes	Opisthocentridae	<i>Opisthocentrus tenuis</i>	UW 47877	SAMN22936243	✓
Perciformes	Opisthocentridae	<i>Opisthocentrus zonope</i>	UW 47885	SAMN22936244	✓
Perciformes	Opisthocentridae	<i>Pholidapus dybowskii</i>	UW 47882	SAMN22936241	
Perciformes		<i>Ptilichthys goodiei</i>	Pers. Coll.: P.Wainwright, PCW 2416	SAMN22936330	✓
Perciformes	Pholidae	<i>Apodichthys flavidus</i>	UW 151663	SAMN22935867	✓
Perciformes	Pholidae	<i>Pholis clemensi</i>	UW 47872	SAMN22936291	
Perciformes	Pholidae	<i>Pholis laeta</i>	UW 43793	SAMN22936292	
Perciformes	Pholidae	<i>Pholis ornata</i>	Pers. Coll.: P.Wainwright, PW244: B27	SAMN22936293	✓

Perciformes	Pholidae	<i>Pholis ornata</i>	UW 151676	SAMN22936294	
Perciformes	Pholidae	<i>Rhodymenichthys dolichogaster</i>	UW 44516	SAMN22936340	✓
Perciformes		<i>Gymnoclinus cristulatus</i>	UW 44509	SAMN22936084	
Perciformes	Neozoarcidae	<i>Neozoarces steindachneri</i>	UW 47875	SAMN22936227	
Perciformes	Anarhichadidae	<i>Anarhichas orientalis</i>	UW 150194	SAMN22935855	✓
Perciformes	Anarhichadidae	<i>Anarhichas orientalis</i>	UW 111905	SAMN22935854	
Perciformes	Anarhichadidae	<i>Anarrhichthys ocellatus</i>	UW 49014	SAMN22935856	
Perciformes	Zoarcidae	<i>Bothrocara brunneum</i>	UW 150525	SAMN22935908	✓
Perciformes	Zoarcidae	<i>Bothrocara molle</i>	UW 111363	SAMN22935909	✓
Perciformes	Zoarcidae	<i>Bothrocara pusillum</i>	UW 151315	SAMN22935910	✓
Perciformes	Zoarcidae	<i>Bothrocara zestum</i>	UW 150975	SAMN22935911	
Perciformes	Zoarcidae	<i>Gymnelus viridis</i>	UW 150119	SAMN22936083	✓
Perciformes	Zoarcidae	<i>Lycenchelys camchatica</i>	UW 119335	SAMN22936157	✓
Perciformes	Zoarcidae	<i>Lycenchelys crotalinus</i>	UW 118611	SAMN22936158	✓
Perciformes	Zoarcidae	<i>Lycodapus fierasfer</i>	UW 115137	SAMN22936159	✓
Perciformes	Zoarcidae	<i>Lycodapus mandibularis</i>	UW 152155	SAMN22936160	✓
Perciformes	Zoarcidae	<i>Lycodes akuugun</i>	UW 117198	SAMN22936161	
Perciformes	Zoarcidae	<i>Lycodes beringi</i>	UW 150976	SAMN22936162	✓
Perciformes	Zoarcidae	<i>Lycodes brevipes</i>	UW 151235	SAMN22936163	✓
Perciformes	Zoarcidae	<i>Lycodes concolor</i>	UW 150529	SAMN22936164	✓
Perciformes	Zoarcidae	<i>Lycodes cortezianus</i>	UW 115164	SAMN22936165	✓
Perciformes	Zoarcidae	<i>Lycodes diapterus</i>	YFTC 13952, n.v.	SAMN22936166	✓
Perciformes	Zoarcidae	<i>Lycodes diapterus</i>	UW 119963	SAMN22936167	
Perciformes	Zoarcidae	<i>Lycodes mucosus</i>	UW 152426	SAMN22936168	
Perciformes	Zoarcidae	<i>Lycodes pacificus</i>	UW 119472	SAMN22936170	✓
Perciformes	Zoarcidae	<i>Lycodes pacificus</i>	UW 113585	SAMN22936169	
Perciformes	Zoarcidae	<i>Lycodes palearis</i>	UW 152045	SAMN22936171	✓
Perciformes	Zoarcidae	<i>Lycodes polaris</i>	UW 152421	SAMN22936172	✓
Perciformes	Zoarcidae	<i>Lycodes raridens</i>	UW 152485	SAMN22936173	✓
Perciformes	Zoarcidae	<i>Lycodes turneri</i>	UW 150133	SAMN22936174	✓
Perciformes	Zoarcidae	<i>Puzanovia rubra</i>	UW 150349	SAMN22936332	
Perciformes	Zoarcidae	<i>Zoarces elongatus</i>	UW 44917	SAMN22936452	✓
Centrarchiformes	<i>Percalates</i>	<i>Percalates colonorum</i>	Pers. Coll.: Peter Unmack	SAMN22936279	✓
Centrarchiformes	Girellidae	<i>Girella nigricans</i>	Pers. Coll.: Giacomo Bernardi	SAMN22936077	✓ ✓
Centrarchiformes	Scorpididae	<i>Medialuna californiensis</i>	YFTC 21006, n.v.	SAMN22936190	✓
Centrarchiformes	Scorpididae	<i>Scorpis georgiana</i>	Pers. Coll.: JP Hobbs	SAMN22936367	✓
Centrarchiformes	<i>Dichistius</i>	<i>Dichistius capensis</i>	SAIAB 87252	SAMN22936022	
Centrarchiformes	<i>Dichistius</i>	<i>Dichistius multifasciatus</i>	SAIAB 86789	SAMN22936023	
Centrarchiformes	Microcanthidae	<i>Microcanthus strigatus</i>	Pers. Coll.: JP Hobbs	SAMN22936195	

Centrarchiformes	Microcanthidae	<i>Tilodon sexfasciatus</i>	Pers. Coll.: JP Hobbs	SAMN22936413	
Centrarchiformes	<i>Oplegnathus</i>	<i>Oplegnathus conwayi</i>	SIO 05-48	SAMN22936246	
Centrarchiformes	<i>Oplegnathus</i>	<i>Oplegnathus fasciatus</i>	See NCBI SRA	SAMN07331350*	✓
Centrarchiformes	<i>Oplegnathus</i>	<i>Oplegnathus peaolopesi</i>	SAIAB 86857	SAMN22936247	
Centrarchiformes	Kyphosidae	<i>Kyphosus sectatrix</i>	YPM ICH 024907	SAMN22936125	✓
Centrarchiformes	Kyphosidae	<i>Kyphosus vaigiensis</i>	NMND 403373	SAMN22936126	✓
Centrarchiformes	<i>Kuhlia</i>	<i>Kuhlia marginata</i>	UF 162616	SAMN22936122	✓
Centrarchiformes	<i>Kuhlia</i>	<i>Kuhlia rupestris</i>	KUIT 5666, SAIAB 86171	SAMN22936123	✓
Centrarchiformes	Terapontidae	<i>Bidyanus bidyanus</i>	Pers. Coll.: Peter Unmack	SAMN22935904	✓
Centrarchiformes	Terapontidae	<i>Hephaestus fuliginosus</i>	Pers. Coll.: Peter Unmack	SAMN22936094	✓
Centrarchiformes	Terapontidae	<i>Scortum barcoo</i>	Pers. Coll.: Peter Unmack	SAMN22936368	
Centrarchiformes	Terapontidae	<i>Terapon jarbua</i>	Pers. Coll.: Peter Unmack	SAMN22936408	✓
Centrarchiformes		<i>Enoplosus armatus</i>	Pers. Coll.: P. Wainwright, PW 3119	SAMN22936048	✓
Centrarchiformes	Percichthyidae	<i>Maccullochella peelii</i>	Pers. Coll.: P. Wainwright, PW 1633	SAMN22936176	✓
Centrarchiformes	Percichthyidae	<i>Nannoperca australis</i>	Pers. Coll.: Peter Unmack	SAMN22936219	
Centrarchiformes	Percichthyidae	<i>Percilia gillissi</i>	Pers. Coll.: Peter Unmack	SAMN22936280	
Centrarchiformes	Percichthyidae	<i>Percilia irwini</i>	Pers. Coll.: Peter Unmack	SAMN22936281	
Centrarchiformes	Sinipercidae	<i>Coreoperca herzi</i>	YPM ICH 026803	SAMN22935987	✓
Centrarchiformes	Sinipercidae	<i>Siniperca chuatzii</i>	YPM ICH 023856	SAMN22936381	✓
Centrarchiformes	Centrarchidae	<i>Elassoma okefenokee</i>	Pers. Coll.: P. Wainwright, PW667: FL18	SAMN22936040	✓
Centrarchiformes	Centrarchidae	<i>Elassoma zonatum</i>	YPM ICH 021245	SAMN22936041	✓
Centrarchiformes	Centrarchidae	<i>Enneacanthus chaetodon</i>	UF 236219	SAMN22936046	✓
Centrarchiformes	Centrarchidae	<i>Micropterus salmoides</i>	YPM ICH 023651	SAMN05915084	✓
Centrarchiformes	Cirrhitidae	<i>Amblycirrhitis pinos</i>	KUIT 224, USNM 349043	SAMN22935848	✓
Centrarchiformes	Cirrhitidae	<i>Cirrhitichthys falco</i>	KUIT 684, USNM 334280	SAMN22935983	✓
Centrarchiformes	Latridae	<i>Chirodactylus brachydactylus</i>	KUIT 6471	SAMN22935975	✓
Centrarchiformes	Latridae	<i>Latridopsis fosteri</i>	YFTC 24241, n.v.	SAMN22936135	
Centrarchiformes	Latridae	<i>Latris lineata</i>	SAMA ABTC 102988	SAMN22936136	
Centrarchiformes	<i>Chironemus</i>	<i>Chironemus bicornis</i>	FMNH 107336	SAMN22935979	✓
Centrarchiformes	<i>Cheilodactylus</i>	<i>Cheilodactylus fasciatus</i>	Pers. Coll.: Chris Burridge	SRX5100538	✓
Centrarchiformes	<i>Aplodactylus</i>	<i>Aplodactylus arctidens</i>	NMV A 24857	SAMN22935866	✓
Centrarchiformes	<i>Aplodactylus</i>	<i>Aplodactylus lophodon</i>	Pers. Coll.: Chris Burridge	SRR8285884	✓
Labriformes	Uranoscopidae	<i>Astroscoptes y graecum</i>	KUIT 16, KUI 22957	SAMN22935873	✓
Labriformes	Uranoscopidae	<i>Kathetostoma averruncus</i>	KUIT 464, KUI 28152	SAMN22936121	✓
Labriformes	Ammodytidae	<i>Ammodytes hexapterus</i>	Pers. Coll.: P. Wainwright, PW2451	SAMN22935851	✓

Labriformes	Pinguipedidae	<i>Parapercis hexophtalma</i>	KUIT 6766, SAIAB 77885	SAMN22936266	✓	✓
Labriformes		<i>Cheimarrichthys fosteri</i>	See NCBI SRA	SAMN05915051	✓	
Labriformes	Leptoscopidae	<i>Crapatalus munroi</i>	CSIRO H 7106-01	SAMN22935993		
Labriformes	Leptoscopidae	<i>Lesueurina platycephala</i>	CSIRO H 7106-03	SAMN22936143		
Labriformes		<i>Centrogenys vaigiensis</i>	LSUMZ 16511	SAMN22935941	✓	
Labriformes		<i>Centrogenys vaigiensis</i>	LSUMZ 16559	SAMN22935942		✓
Labriformes		<i>Centrogenys vaigiensis</i>	LSUMZ 16559	SAMN22935942		
Labriformes	Labridae	<i>Achoerodus viridis</i>	Pers. Coll.: D.Bellwood M507, n.v.	SAMN22935838		
Labriformes	Labridae	<i>Bodianus rufus</i>	Pers. Coll.: D.Bellwood M383, n.v.	SAMN22935906		
Labriformes	Labridae	<i>Bolbometopon muricatum</i>	Pers. Coll.: D.Bellwood Choat_SIO1, n.v.	SAMN22935907	✓	
Labriformes	Labridae	<i>Calotomus spinidens</i>	Pers. Coll.: H.Choat G2118, n.v.	SAMN22935923	✓	
Labriformes	Labridae	<i>Cetoscarus bicolor</i>	Pers. Coll.: H.Choat G113, n.v.	SAMN22935947	✓	
Labriformes	Labridae	<i>Cheilinus fasciatus</i>	Pers. Coll.: D.Bellwood M215, n.v.	SAMN22935967	✓	
Labriformes	Labridae	<i>Cheilio inermis</i>	Pers. Coll.: D.Bellwood M1187, n.v.	SAMN22935968	✓	
Labriformes	Labridae	<i>Chlorurus japanensis</i>	Pers. Coll.: H.Choat PFC5870, n.v.	SAMN22935980	✓	
Labriformes	Labridae	<i>Choerodon anchorago</i>	Pers. Coll.: D.Bellwood M12, n.v.	SAMN22935981	✓	
Labriformes	Labridae	<i>Coris atlantica</i>	Pers. Coll.: D.Bellwood M1692, n.v.	SAMN22935988		
Labriformes	Labridae	<i>Coris gaimard</i>	Pers. Coll.: D.Bellwood M1359, n.v.	SAMN22935989	✓	
Labriformes	Labridae	<i>Epibulus insidiator</i>	Pers. Coll.: P.Wainwright, PW1897B	SAMN05915062	✓	
Labriformes	Labridae	<i>Halichoeres poeyi</i>	Pers. Coll.: P.Wainwright, PW46	SAMN05915071	✓	
Labriformes	Labridae	<i>Halichoeres radiatus</i>	CAS HRA01	SAMN05915072	✓	
Labriformes	Labridae	<i>Heteroscarus acroptilus</i>	Pers. Coll.: D.Bellwood M492, n.v.	SAMN22936236		
Labriformes	Labridae	<i>Hipposcarus harid</i>	Pers. Coll.: H.Choat PFC6379, n.v.	SAMN22936102	✓	
Labriformes	Labridae	<i>Labrichthys unilineatus</i>	Pers. Coll.: D.Bellwood M254, n.v.	SAMN22936128	✓	
Labriformes	Labridae	<i>Labrus bergylta</i>	See NCBI SRA	SAMEA3939555*	✓	
Labriformes	Labridae	<i>Lachnolaimus maximus</i>	Pers. Coll.: D.Bellwood M397, n.v.	SAMN22936129	✓	✓
Labriformes	Labridae	<i>Pseudodax moluccanus</i>	Pers. Coll.: D.Bellwood M62, n.v.	SAMN22936322	✓	
Labriformes	Labridae	<i>Scarus flavipectoralis</i>	Pers. Coll.: H.Choat G228, n.v.	SAMN22936352	✓	
Labriformes	Labridae	<i>Scarus taeniopterus</i>	Pers. Coll.: H.Choat G754, n.v.	SAMN22936353	✓	✓
Labriformes	Labridae	<i>Sparisoma radians</i>	Pers. Coll.: H.Choat A10, n.v.	SAMN22936383	✓	
Labriformes	Labridae	<i>Symphodus melops</i>	See NCBI SRA	SAMEA4028821*	✓	
Labriformes	Labridae	<i>Thalassoma ballieui</i>	CAS TBA-04	SAMN05915134	✓	
Labriformes	Labridae	<i>Wetmorella albofasciata</i>	Pers. Coll.: D.Bellwood M288, n.v.	SAMN22936439	✓	

Acropomatiformes	<i>Ostracoberyx</i>	<i>Ostracoberyx dorygenys</i>	ASIZPO 911526	SAMN22936253	
Acropomatiformes	Acropomatidae	<i>Acropoma japonica</i>	YPM ICH 010066	SAMN22935840	✓
Acropomatiformes	Acropomatidae	<i>Doederleinia berycoides</i>	NMV Z 6813	SAMN22936033	
Acropomatiformes	<i>Scombrops</i>	<i>Scombrops boops</i>	YFTC 24186, n.v.	SAMN22936360	
Acropomatiformes	<i>Scombrops</i>	<i>Scombrops gilberti</i>	YFTC 24191, n.v.	SAMN22936361	
Acropomatiformes	<i>Scombrops</i>	<i>Scombrops gilberti</i>	YFTC 24192, n.v.	SAMN22936362	
Acropomatiformes	<i>Scombrops</i>	<i>Scombrops gilberti</i>	YFTC 24193, n.v.	SAMN22936363	
Acropomatiformes	<i>Symphysanodon</i>	<i>Symphysanodon berryi</i>	YPM ICH 028303	SAMN22936402	✓
Acropomatiformes	<i>Symphysanodon</i>	<i>Symphysanodon octoactinus</i>	USNM 406214	SAMN22936403	✓
Acropomatiformes	Epigonidae	<i>Brinkmannella carpenteri</i>	YPM ICH 028297	SAMN22935915	
Acropomatiformes	Howellidae	<i>Howella atlantica</i>	YPM ICH 028408	SAMN22936108	
Acropomatiformes	Howellidae	<i>Howella brodiei</i>	YPM ICH 027798	SAMN22936109	
Acropomatiformes	<i>Polyprion</i>	<i>Polyprion americanus</i>	AMS I.42844-002	SAMN22936307	✓
Acropomatiformes	<i>Glaucosoma</i>	<i>Glaucosoma hebraicum</i>	YFTC 18186, n.v.	SAMN22936078	
Acropomatiformes	Pempheridae	<i>Pempheris schomburgkii</i>	YPM ICH 24903	SAMN05915096	✓
Acropomatiformes	<i>Lateolabrax</i>	<i>Lateolabrax japonicus</i>	YFTC 25777, n.v.	SAMN22936133	✓
Acropomatiformes	<i>Lateolabrax</i>	<i>Lateolabrax japonicus</i>	See NCBI SRA	SAMN07680090*	
Acropomatiformes	<i>Lateolabrax</i>	<i>Lateolabrax latus</i>	KAUM 51068	SAMN22936134	
Acropomatiformes	<i>Stereolepis</i>	<i>Stereolepis gigas</i>	SIO 03-74	SAMN22936395	✓
Acropomatiformes	<i>Banjos</i>	<i>Banjos banjos</i>	ASIZPO 801399	SAMN22935886	✓
Acropomatiformes	Pentacerotidae	<i>Pentaceros japonicus</i>	ASIZD 0800699	SAMN22936277	
Acropomatiformes	Pentacerotidae	<i>Pseudopentaceros wheeleri</i>	UW 116954	SAMN22936324	
Acropomatiformes	Bathyclupeidae	<i>Neobathyclupea argentea</i>	YPM ICH 028270	SAMN22935889	
Acropomatiformes	Bathyclupeidae	<i>Neobathyclupea gracilis</i>	NMV A 25118-003	SAMN22935890	
Acropomatiformes	<i>Champsodon</i>	<i>Champsodon sechellensis</i>	SAIAB 84026	SAMN22935951	
Acropomatiformes	<i>Champsodon</i>	<i>Champsodon snyderi</i>	ASIZPO 910951	SAMN22935952	
Acropomatiformes	Creediidae	<i>Limnichthys</i> sp.	KUIT 782	SAMN22936145	
Acropomatiformes	Creediidae	<i>Tewara cranwellae</i>	NMNZ P.044479/TS1	SAMN22936411	
Acropomatiformes	Hemerocoetidae	<i>Enigmapercis</i> sp.	NSMT-P 114722	SAMN22936045	✓
Acropomatiformes	Hemerocoetidae	<i>Osopsaron formosensis</i>	NSMT-P 77318	SAMN22936250	✓
Acropomatiformes	Hemerocoetidae	<i>Pteropsaron evolans</i>	NSMT-P 77317	SAMN22936328	
Euperciformes	Gerreidae	<i>Eucinostomus jonesii</i>	YPM ICH 24864	SAMN22936063	✓ ✓
Euperciformes	Gerreidae	<i>Gerres cinereus</i>	YPM ICH 24843	SAMN22936072	✓
Euperciformes	Moronidae	<i>Dicentrarchus labrax</i>	Pers. Coll.: F.J. Sanchez Vazques, U. of Murica	SAMN22936019	✓
Euperciformes	Moronidae	<i>Morone saxatilis</i>	YPM ICH 018448	SAMN22936210	✓
Euperciformes	Sillaginidae	<i>Sillago chondropus</i>	Pers. Coll.: W.L.Smith KUIT 6745, SAIAB	SAMN22936379	
Euperciformes	Sillaginidae	<i>Sillago sihama</i>	77085	SAMN22936380	✓
Euperciformes	<i>Drepane</i>	<i>Drepane punctata</i>	ROM 69918 KUIT 7072, SAIAB	SAMN22936036	✓
Euperciformes	Ehippididae	<i>Platax orbicularis</i>	77666	SAMN22936297	✓

Euperciformes	Dinopercidae	<i>Dinoperca petersi</i>	SAIAB 81789	SAMN22936026	✓	
Euperciformes	Haemulidae	<i>Haemulon album</i>	CAS HAL01	SAMN05915068	✓	
Euperciformes	Haemulidae	<i>Haemulon flavolineatum</i>	CAS HFG04	SAMN05915069	✓	
Euperciformes	Haemulidae	<i>Haemulon parra</i>	CAS HPA01	SAMN05915070	✓	
Euperciformes	Sciaenidae	<i>Collichthys lucidus</i>	See NCBI SRA	SAMN10225518*	✓	
Euperciformes	Sciaenidae	<i>Larimichthys crocea</i>	See NCBI SRA	SAMN10434301*	✓	
Euperciformes	Sciaenidae	<i>Micropogonias undulatus</i>	YPM ICH 023546	SAMN05915083	✓	
Euperciformes	Sciaenidae	<i>Miichthys miuy</i>	See NCBI SRA	SAMN02486174*	✓	
Euperciformes	Sciaenidae	<i>Nibea albiflora</i>	See NCBI SRA	SAMEA1067819*	✓	
Euperciformes	Sciaenidae	<i>Pareques acuminatus</i>	CAS PAC20	SAMN05915094	✓	
Euperciformes	Monodactylidae	<i>Monodactylus sebae</i>	YPM ICH 020540	SAMN22936205	✓	
Euperciformes	Lobotidae	<i>Hapalogenys dampieriensis</i>	NMV Z 6535	SAMN22936086	✓	
Euperciformes	Lobotidae	<i>Lobotes surinamensis</i>	Pers. Coll.: P.Wainwright, PW2610 KUIT 7270, SAIAB 99238	SAMN22936148	✓	
Euperciformes	Emmelichthyidae	<i>Erythrocles schlegelii</i>	CAS LGO01	SAMN22936053	✓	
Euperciformes	Lutjanidae	<i>Lutjanus goreensis</i>	CAS LGO01	SAMN05915081	✓	
Euperciformes	Malacanthidae	<i>Caulolatilus princeps</i>	SIO 08-66	SAMN22935937	✓	
Euperciformes	Malacanthidae	<i>Malacanthus plumieri</i>	Pers. Coll.: P.Wainwright, PW1198	SAMN22936182	✓	
Euperciformes	Pomacanthidae	<i>Centropyge flavissima</i>	YPM ICH 026532	SAMN22935944	✓	
Euperciformes	Pomacanthidae	<i>Chaetodontoplus melanosoma</i>	Pers. Coll.: P.Wainwright, PW643 Pers. Coll.:	SAMN22935950	✓	✓
Euperciformes	Pomacanthidae	<i>Holacanthus passer</i>	P.Wainwright, PW642	SAMN22936104	✓	✓
Euperciformes	Pomacanthidae	<i>Pomacanthus paru</i>	CAS PPA01	SAMN05915105	✓	
Euperciformes	Leiognathidae	<i>Gazza minuta</i>	YFTC 18187, n.v.	SAMN22936071	✓	✓
Euperciformes	Leiognathidae	<i>Karalla daura</i>	LSUMZ 8791	SAMN22936120	✓	
Euperciformes	Leiognathidae	<i>Leiognathus equula</i>	LSUMZ 8683	SAMN22936137	✓	✓
Euperciformes	Leiognathidae	<i>Secutor nuconius</i>	LSUMZ 8682	SAMN22936370	✓	
Euperciformes	Chaetodontidae	<i>Chaetodon kleinii</i>	Pers. Coll.: P.Wainwright, PW2291B	SAMN05915049	✓	
Euperciformes	Chaetodontidae	<i>Chaetodon leucopleura</i>	See NCBI SRA	SAMN09765312	✓	
Euperciformes	Chaetodontidae	<i>Chaetodon melapterus</i>	See NCBI SRA	SAMN09765325	✓	
Euperciformes	Chaetodontidae	<i>Chaetodon ocellatus</i>	CAS CAC01	SAMN05915050	✓	
Euperciformes	Chaetodontidae	<i>Chaetodon trichrous</i>	See NCBI SRA	SAMN09765350	✓	✓
Euperciformes	Chaetodontidae	<i>Chaetodon trifascialis</i>	See NCBI SRA	SAMN09765353	✓	
Euperciformes	Chaetodontidae	<i>Chaetodon unimaculatus</i>	See NCBI SRA	SAMN09765358	✓	
Euperciformes	Chaetodontidae	<i>Chaetodon vagabundus</i>	See NCBI SRA	SAMN09765361	✓	
Euperciformes	Chaetodontidae	<i>Chaetodon xanthurus</i>	See NCBI SRA	SAMN09765364	✓	
Euperciformes	Chaetodontidae	<i>Forcipiger longirostris</i>	See NCBI SRA	SAMN09765373	✓	✓
Euperciformes	Chaetodontidae	<i>Heniochus acuminatus</i>	See NCBI SRA	SAMN09765375	✓	
Euperciformes	Chaetodontidae	<i>Heniochus diphreutes</i>	See NCBI SRA	SAMN09765376	✓	
Euperciformes	Chaetodontidae	<i>Prognathodes aculeatus</i>	See NCBI SRA	SAMN09765385	✓	✓

Euperciformes	Chaetodontidae	<i>Prognathodes marcellae</i>	See NCBI SRA KUIT 3882, MCZ	SAMN09765386	✓
Euperciformes		<i>Luvarus imperialis</i>	159566	SAMN22936156	✓
Euperciformes		<i>Zanclus cornutus</i>	Pers. Coll.: P.Wainwright, PW1782B	SAMN22936443	✓
Euperciformes	Acanthuridae	<i>Acanthurus bahianus</i>	ANSP 191513	SAMN05915021	✓
Euperciformes	Acanthuridae	<i>Acanthurus bariene</i>	Pers. Coll.: M.Alfaro, Alfaro-909	SAMN05915022	
Euperciformes	Acanthuridae	<i>Acanthurus chirurgus</i>	Pers. Coll.: D.Bellwood M1523, n.v.	SAMN22935832	✓
Euperciformes	Acanthuridae	<i>Acanthurus coeruleus</i>	Pers. Coll.: D.Bellwood M284, n.v.	SAMN22935833	✓
Euperciformes	Acanthuridae	<i>Acanthurus lineatus</i>	Pers. Coll.: D.Bellwood M579, n.v.	SAMN22935834	✓
Euperciformes	Acanthuridae	<i>Acanthurus nigricans</i>	Pers. Coll.: D.Bellwood M309, n.v.	SAMN22935835	✓
Euperciformes	Acanthuridae	<i>Acanthurus nigrofuscus</i>	Pers. Coll.: D.Bellwood M1452, n.v.	SAMN22935836	✓
Euperciformes	Acanthuridae	<i>Acanthurus olivaceus</i>	Pers. Coll.: M.Alfaro, Alfaro-878	SAMN05915023	✓
Euperciformes	Acanthuridae	<i>Acanthurus pyroferus</i>	Pers. Coll.: M.Alfaro, Alfaro-907	SAMN05915024	✓
Euperciformes	Acanthuridae	<i>Acanthurus triostegus</i>	Pers. Coll.: D.Bellwood M677, n.v.	SAMN22935837	✓
Euperciformes	Acanthuridae	<i>Ctenochaetus striatus</i>	Pers. Coll.: D.Bellwood M747, n.v.	SAMN22935998	✓
Euperciformes	Acanthuridae	<i>Ctenochaetus truncatus</i>	Pers. Coll.: D.Bellwood M310, n.v.	SAMN22935999	
Euperciformes	Acanthuridae	<i>Naso elegans</i>	Pers. Coll.: D.Bellwood M1206, n.v.	SAMN22936220	
Euperciformes	Acanthuridae	<i>Naso unicornis</i>	Pers. Coll.: M.Alfaro, Alfaro-mv010.12	SAMN05915088	✓
Euperciformes	Acanthuridae	<i>Paracanthurus hepatus</i>	Pers. Coll.: D.Bellwood M1432, n.v.	SAMN22936260	✓
Euperciformes	Acanthuridae	<i>Prionurus biafraensis</i>	Pers. Coll.: D.Bellwood M1695, n.v.	SAMN22936316	✓
Euperciformes	Acanthuridae	<i>Zebrasoma desjardini</i>	Pers. Coll.: D.Bellwood M1454, n.v.	SAMN22936448	
Euperciformes	Acanthuridae	<i>Zebrasoma flavescens</i>	Pers. Coll.: D.Bellwood M2031, n.v.	SAMN22936449	✓
Euperciformes	Acanthuridae	<i>Zebrasoma rostratum</i>	Pers. Coll.: D.Bellwood M2030, n.v.	SAMN22936450	
Euperciformes	Callanthiidae	<i>Callanthias australis</i>	NMNZ P.052282/TS2	SAMN22935922	
Euperciformes	Nemipteridae	<i>Parascalopsis eriomma</i>	SAIAB 80609	SAMN22936268	✓
Euperciformes	Nemipteridae	<i>Scolopsis ghanam</i>	SAIAB 80378	SAMN22936355	
Euperciformes	Nemipteridae	<i>Scolopsis vosmeri</i>	SAIAB 80713	SAMN22936356	✓
Euperciformes	Lethrinidae	<i>Lethrinus erythropterus</i>	Pers. Coll.: P.Wainwright, PW2049B	SAMN22936144	✓
Euperciformes	Lethrinidae	<i>Monotaxis grandoculis</i>	Pers. Coll.: P.Wainwright, PW2159B	SAMN22936208	✓
Euperciformes	Sparidae	<i>Calamus calamus</i>	Pers. Coll.: P.Wainwright, PW102: 960	SAMN22935921	✓
Euperciformes	Sparidae	<i>Pagrus major</i>	See NCBI SRA	SAMD00076252*	✓
Euperciformes	Sparidae	<i>Sparus aurata</i>	See NCBI SRA	SAMN09603368*	✓
Euperciformes	Sparidae	<i>Spicara australis</i>	SAIAB 81795	SAMN22936389	
Euperciformes	Sparidae	<i>Spicara smaris</i>	SAIAB 81064	SAMN22936390	✓

Euperciformes	Sparidae	<i>Spondyllosoma cantharus</i>	See NCBI SRA	SAMEA4028822*	✓
Euperciformes	Sparidae	<i>Stenotomus chrysops</i>	YPM ICH 017360	SAMN22936394	
Euperciformes	<i>Siganus</i>	<i>Siganus spinus</i>	KUIT 4159 Pers. Coll.:	SAMN22936377	✓
Euperciformes	<i>Siganus</i>	<i>Siganus vulpinus</i>	P.Wainwright, PW1601	SAMN22936378	✓
Euperciformes	Scatophagidae	<i>Scatophagus argus</i>	YPM ICH 020538	SAMN22936354	✓
Euperciformes	Priacanthidae	<i>Priacanthus arenatus</i>	KUIT 1132, KUI 27012	SAMN22936314	✓
Euperciformes	Cepolidae	<i>Cepola schlegelii</i>	ASIZPO 800615	SAMN22935946	✓
Euperciformes	Cepolidae	<i>Owstonia tosaensis</i>	ASIZPO 801455	SAMN22936254	
Euperciformes	Caproidae	<i>Antigonia capros</i>	YPM ICH 25915	SAMN05915030	✓
Tetraodontiformes		<i>Triodon macropterus</i>	Pers. Coll.: W.L. Smith Pers. Coll.:	SAMN22936434	
Tetraodontiformes	Aracnidae	<i>Aracana aurita</i>	P.Wainwright, PW1285	SAMN22935868	✓
Tetraodontiformes	Ostraciidae	<i>Lactophrys bicaudalis</i>	YPM ICH 24800	SAMN22936131	✓
Tetraodontiformes	Triacanthodidae	<i>Triacanthodes ethiops</i>	SAIAB 82125	SAMN22936419	✓
Tetraodontiformes	Triacanthidae	<i>Triacanthus biaculeatus</i>	NSMT 59287 Pers. Coll.:	SAMN22936420	✓
Tetraodontiformes	Balistidae	<i>Balistes capriscus</i>	P.Wainwright, PW2623 Pers. Coll.:	SAMN05915036	✓
Tetraodontiformes	Monacanthidae	<i>Acreichthys tomentosus</i>	P.Wainwright, PW1740B	SAMN22935839	
Tetraodontiformes	Monacanthidae	<i>Aluterus monoceros</i>	YPM ICH 027566	SAMN22935846	✓
Tetraodontiformes	Molidae	<i>Masturus lanceolatus</i>	KUIT 5252, n.v.	SAMN22936189	
Tetraodontiformes	Molidae	<i>Mola mola</i>	YFTC 13718 Pers. Coll.:	SAMN22936202	
Tetraodontiformes	Diodontidae	<i>Chilomycterus schoepfi</i>	P.Wainwright, PW1225	SAMN22935973	✓
Tetraodontiformes	Diodontidae	<i>Cylichthys orbicularis</i>	SAIAB 190092	SAMN22936010	
Tetraodontiformes	Diodontidae	<i>Diodon liturosus</i>	KUIT 7189, SAIAB 78248 Pers. Coll.: M.Alfaro,	SAMN22936027	✓ ✓
Tetraodontiformes	Tetraodontidae	<i>Canthigaster figueiredoi</i>	Alfaro-491	SAMN05915041	✓
Tetraodontiformes	Tetraodontidae	<i>Canthigaster margaritata</i>	CAS LR03	SAMN05915042	
Tetraodontiformes	Tetraodontidae	<i>Canthigaster rostrata</i>	CAS CRO42	SAMN05915043	✓
Tetraodontiformes	Tetraodontidae	<i>Dichotomyctere nigroviridis</i>	See NCBI SRA Pers. Coll.: M.Alfaro,	SAMEA3138311*	
Tetraodontiformes	Tetraodontidae	<i>Pao suvattii</i>	Alfaro-666	SAMN05915133	
Tetraodontiformes	Tetraodontidae	<i>Takifugu bimaculatus</i>	See NCBI SRA	SAMN10524747*	✓
Tetraodontiformes	Tetraodontidae	<i>Takifugu flavidus</i>	See NCBI SRA	SAMN10077091*	
Tetraodontiformes	Tetraodontidae	<i>Takifugu rubripes</i>	See NCBI SRA Pers. Coll.: J.Moore,	SAMEA3138310*	✓
Lophiiformes	Lophiidae	<i>Lophius gastrophysus</i>	JAM99-109 Pers. Coll.: M.Alfaro,	SAMN22936149	✓
Lophiiformes	Ogcocephalidae	<i>Ogcocephalus radiatus</i>	Alfaro-1152 Pers. Coll.: M.Alfaro,	SAMN05915090	✓
Lophiiformes	Antennariidae	<i>Antennarius striatus</i>	Alfaro-961	SAMN05915029	✓
Lophiiformes	Antennariidae	<i>Antennarius striatus</i>	See NCBI SRA	SAMEA4028823*	
Lophiiformes	Brachionichthyidae	<i>Brachionichthys australis</i>	CSIRO H 4465-01	SAMN22935913	
Lophiiformes	Tetrabrachiidae	<i>Tetrabrachium ocellatum</i>	UW A50	SAMN22936409	✓
Lophiiformes	Tetrabrachiidae	<i>Tetrabrachium ocellatum</i>	UW A67	SAMN22936410	

Lophiiformes	Chaunacidae	<i>Chaunax stigmaeus</i>	KUIT 8225, MCZ 166061	SAMN22935965	
Lophiiformes	Chaunacidae	<i>Chaunax suttkusi</i>	KUIT 8159, MCZ 166070	SAMN22935966	✓
Lophiiformes	Chaunacidae	<i>Chaunax</i> sp.	UW 25870	SAMN22935964	
Lophiiformes	Caulophrynidae	<i>Caulophryne pelagica</i>	NMNZ P.043296/TS3	SAMN22935938	
Lophiiformes	Gigantactinidae	<i>Gigantactis ios</i>	MCZ 163303	SAMN22936074	
Lophiiformes	Gigantactinidae	<i>Gigantactis vanhoeffeni</i>	YPM ICH 027791	SAMN22936075	
Lophiiformes		<i>Neoceratias spinifer</i>	UW D17	SAMN22936222	
Lophiiformes	Linophrynidae	<i>Haplophryne mollis</i>	NMNZ P.041209/TS3	SAMN22936087	
Lophiiformes	Ceratiidae	<i>Cryptopsaras couesii</i>	YPM ICH 25702	SAMN05915058	✓
Lophiiformes	Oneirodidae	<i>Chaenophryne longiceps</i>	YPM ICH 25647	SAMN22935949	
Lophiiformes	Oneirodidae	<i>Dolopichthys karsteni</i>	KUIT 5926, MCZ 165969	SAMN22936034	
Lophiiformes	Oneirodidae	<i>Lasiognathus intermedius</i>	YPM ICH 25927	SAMN22936132	
Lophiiformes	Diceratiidae	<i>Bufoeratias thele</i>	UW D6	SAMN22935919	
Lophiiformes	Diceratiidae	<i>Diceratias pileatus</i>	UW D7	SAMN22936020	
Lophiiformes	Diceratiidae	<i>Diceratias</i> sp.	UW D27	SAMN22936021	
Lophiiformes	Himantolophidae	<i>Himantolophus albinares</i>	KUIT 5264, MCZ 161521	SAMN22936097	
Lophiiformes	Himantolophidae	<i>Himantolophus sagamius</i>	SIO 02-2	SAMN22936098	
Lophiiformes	Melanocetidae	<i>Melanocetus johnsonii</i>	UW 115879	SAMN22936192	✓
Lophiiformes	Melanocetidae	<i>Melanocetus murrayi</i>	YPM ICH 027583	SAMN22936193	✓

Institutional Abbreviations: AMNH, American Museum of Natural History, New York; AMS, Australian Museum, Sydney; ANSP, Academy of Natural Sciences, Philadelphia; ASIZ, Academia Sinica, Biodiversity Research Museum, Taipei; CAS, California Academy of Sciences, San Francisco; CBM, Natural History Museum and Institute, Chiba; CSIRO, Commonwealth Scientific and Industrial Research Organisation, Division of Marine and Atmospheric Research, Australian National Fish Collection, Hobart; CUMV, Cornell University Museum of Vertebrates, Ithaca; FAKU, Kyoto University Museum, Kyoto University, Yoshida, Sakyo; FMNH, Field Museum of Natural History, Chicago; FRLM, Fish Collection of the Fisheries Research Laboratory, Mie University, Wagu, Shima; HUMZ, The Hokkaido University Museum, Sapporo; INHS, Illinois Natural History Survey, Champaign; KAUM, Kagoshima University Museum, Korimoto; KUI, University of Kansas Biodiversity Institute, Lawrence; KUIT University of Kansas Biodiversity Institute Ichthyology Tissue Collection, Lawrence; LACM, Natural History Museum of Los Angeles County, Los Angeles; LBP, Laboratório de Biologia e Genética de Peixes, Departamento de Morfologia, Universidade Estadual Paulista “Júlio de Mesquita Filho”, Campus de Rio Claro, São Paulo; LSUMZ, Louisiana Museum of Natural History, Baton Rouge; MCZ, Museum of Comparative Zoology, Harvard University, Cambridge, Massachusetts; MNCN, Museo Nacional de Ciencias Naturales (CSIC), Madrid; MNHN, Museo Nacional de Historia Natural,

Zoología, Santiago; NCSM, North Carolina Museum of Natural Sciences, Raleigh; NMND, National Museum of Natural History, New Delhi; NMNZ, Museum of New Zealand Te Papa Tongarewa, Wellington; NMV, Museum Victoria, Melbourne; NSMT, National Museum of Nature and Science, Ueno Park, Tokyo; NTM, Museums and Art Galleries of the Northern Territory, Darwin; OCF-P, Okinawa Churashima Foundation, Japan; ORIUT, University of Tokyo, Ocean Research Institute, Tokyo; QM, Queensland Museum, Centre for Biodiversity, Brisbane; ROM, Royal Ontario Museum, Department of Natural History, Toronto; SAIAB, South African Institute for Aquatic Biodiversity, Grahamstown; SAMA, South Australian Museum, Adelaide; SIO, Scripps Institution of Oceanography, Marine Vertebrate Collection, University of California, San Diego, La Jolla; SLU, Southeastern Louisiana University, Museum of Biology, Hammond; SNFR, Seikai National Fisheries Research Institute, Nagasaki; UF, University of Florida, Florida Museum of Natural History, Gainesville; USNM, National Museum of Natural History, Smithsonian Institution, Department of Vertebrate Zoology, Washington, D.C.; UT, University of Tennessee, Department of Ecology and Evolutionary Biology, David A. Etnier Ichthyological Collection, Knoxville; UW, University of Washington, Burke Museum of Natural History and Culture, Seattle; YFTC, Yale Fish Tissue Collection, Department of Ecology and Evolutionary Biology, Yale University, New Haven; YPM, Yale University, Peabody Museum of Natural History, New Haven; ZMUB, Universitetsmuseet i Bergen, Bergen, Hordaland; ZMUC, Zoological Museum, University of Copenhagen, Copenhagen.

Supplementary Table 2: Summary of TOPD pairwise comparisons of tree topologies inferred using different methods.

	702-taxon trees		1,084-taxon trees	
Multiple-partition vs IQ-TREEsingle*	IQ-TREEsingle* vs IQ-TREEmulti†	IQ-TREEsingle* vs RAxML	IQ-TREEmulti† vs RAxML	
<i>Acanthistius cinctus</i>	<i>Acanthistius cinctus</i>	<i>Acanthistius cinctus</i>	<i>Apogon affinis</i>	
<i>Arripis trutta</i>	<i>Acanthurus triostegus</i>	<i>Acanthurus triostegus</i>	<i>Astrapogon stellatus</i>	
<i>Chloroscombrus orqueta</i>	<i>Icosteus aenigmaticus</i>	<i>Apogon affinis</i>	<i>Cryptopsaras couesii</i>	
<i>Icosteus aenigmaticus</i>		<i>Astrapogon stellatus</i>	<i>Ectodus descampsii</i>	
<i>Lycodes concolor</i>		<i>Cryptopsaras couesii</i>	<i>Haplotaxodon microlepis</i>	
<i>Pomatomus saltatrix</i>		<i>Ectodus descampsii</i>	<i>Nomorhamphus celebensis</i>	
<i>Pseudanthias squamipinnis</i>		<i>Haplotaxodon microlepis</i>	<i>Phaeoptyx pigmentaria</i>	
<i>Selaroides leptolepis</i>		<i>Icosteus aenigmaticus</i>	<i>Xenentodon cancila</i>	
<i>Sillago sihama</i>		<i>Nomorhamphus celebensis</i>	<i>Zenarchopterus dispar</i>	
		<i>Phaeoptyx pigmentaria</i>		
		<i>Xenentodon cancila</i>		
		<i>Zenarchopterus dispar</i>		
Robinson-Foulds split distances	0.033	0.006	0.012	0.007
# Disagreeing Splits / Total	46 / 1398	14 / 2212	26 / 2212	16 / 2212
Nodal distance	1.05	0.49	0.61	0.51

*IQ-TREEsingle = tree resulting from an IQ-TREE analysis using an unpartitioned alignment

† “IQ-TREEmulti = tree resulting from an IQ-TREE analysis using the ModelFinder Plus option

Columns list taxa with different phylogenetic positions among the compared trees. Robinson-Foulds split distances, the number of disagreeing splits, and nodal distances are provided at the bottom of each column. All RAxML-ng analyses were performed on multiple-partition alignments that were partitioned with PartionFinder2. The topologies of the 702-taxon trees inferred using multiple-partition alignments in IQ-TREE and RAxML-ng were identical.

Supplementary Table 3: Classification of Acanthomorpha. The number of species in each taxonomic order is offered in the second column. Though every family is classified in an order, not every family is classified in a suborder or superfamily.

Order	Number of species	Suborder-Superfamily	Family
Polymixiiformes	10		Polymixiidae
Percopsiformes	12		Amblyopsidae Aphredoderidae Percopsidae
Zeiformes	33		Cyttidae Grammicolepididae Oreosomatidae Parazenidae Zeidae Zeniontidae
Stylephoriformes	1		Stylephoridae
Gadiformes	615		Bathygadidae Bregmacerotidae Eulichthyidae Gadidae Gaidropsaridae Lotidae Lyonidae Macrouridae Macruronidae Melanonidae Merlucciidae Moridae Muraenolepididae Phycidae Ranicipitidae Steindachneriidae Trachyrincidae
Lampriformes	29		

			Lampridae
			Lophotidae
			Radiicephalidae
			Regalecidae
			Trachipteridae
			Veliferidae
Trachichthyiformes	66		
			Anomalopidae
			Anoplogasteridae
			Diretmidae
			Monocentridae
			Trachichthyidae
Beryciformes	211		
			Holocentridae
			Rondeletiidae
			Stephanoberycidae
			Barbourisiidae
			Cetomimidae
			Berycidae
			Melamphaidae
			Gibberichthyidae
			Hispidoberycidae
Ophidiiformes	545		
			Bythitidae
			Dinematichthyidae
			Ophidiidae
Batrachoidiformes	84		
			Batrachoididae
Gobiiformes (=Gobiaria)	2,638		
		Gobioidei	Rhyacichthyidae
		Gobioidei	Odontobutidae
		Gobioidei	Butidae
		Gobioidei	Eleotridae
		Gobioidei	Milyeringidae
		Gobioidei	Thalasseleotrididae
		Gobioidei	Oxudercidae
		Gobioidei	Gobiidae

Scombriformes
(=Pelagiaria)

285

Trichonotidae
Kurtidae
Apogonidae

Amarsipidae
Ariommatidae
Arripidae
Bramidae
Caristiidae
Centrolophidae
Chiasmodontidae
Gempylidae
Icosteidae
Lepidocybidae
Nomeidae
Pomatomidae
Scombridae
Scombrolabracidae
Stromateidae
Tetragonuridae
Trichiuridae

Syngnathiformes
(=Syngnatharia)

674

Syngnathoidei
Syngnathoidei
Syngnathoidei
Syngnathoidei
Syngnathoidei
Syngnathoidei
Callionymoidei
Callionymoidei

Aulostomidae
Centriscidae
Macroramphosidae
Fistularidae
Solenostomidae
Syngnathidae
Callionymidae
Draconettidae
Mullidae
Pegasidae
Dactylopteridae

Blenniiformes
(=Ovalentaria)

5,865

Blennioidei	Blenniidae
Blennioidei	Chaenopsidae
Blennioidei	Clinidae
Blennioidei	Dactyloscopidae
Blennioidei	Gobiesocidae
Blennioidei	Labrisomidae
Blennioidei	Tripterygiidae
Atherinoidei-Belonoidea	Adrianichthyidae
Atherinoidei-Belonoidea	Belonidae
Atherinoidei-Belonoidea	Exocoetidae
Atherinoidei-Belonoidea	Hemiramphidae
Atherinoidei-Cyprinodontoidea	Anablepidae
Atherinoidei-Cyprinodontoidea	Aphaniidae
Atherinoidei-Cyprinodontoidea	Aplocheilidae
Atherinoidei-Cyprinodontoidea	Rivulidae
Atherinoidei-Cyprinodontoidea	Cyprinodontidae
Atherinoidei-Cyprinodontoidea	Fluviphylacidae
Atherinoidei-Cyprinodontoidea	Fundulidae
Atherinoidei-Cyprinodontoidea	Goodeidae
Atherinoidei-Cyprinodontoidea	Nothobranchiidae
Atherinoidei-Cyprinodontoidea	Pantanodontidae
Atherinoidei-Cyprinodontoidea	Poeciliidae
Atherinoidei-Cyprinodontoidea	Profundulidae
Atherinoidei-Cyprinodontoidea	Procatopodidae
Atherinoidei-Cyprinodontoidea	Valenciidae
Atherinoidei-Atherinoidea	Atherinidae
Atherinoidei-Atherinoidea	Atherinopsidae
Atherinoidei-Atherinoidea	Atherionidae
Atherinoidei-Atherinoidea	Bedotiidae
Atherinoidei-Atherinoidea	Dentatherinidae
Atherinoidei-Atherinoidea	Isonidae
Atherinoidei-Atherinoidea	Melanotaeniidae
Atherinoidei-Atherinoidea	Phallostethidae
Atherinoidei-Atherinoidea	Pseudomugilidae
Atherinoidei-Atherinoidea	Telmatherinidae
Cichloidei	Cichlidae

		Cichloidei	Pholidichthyidae
			Ambassidae
			Embiotocidae
			Grammatidae
			Mugilidae
			Opistognathidae
			Plesiopidae
			Polycentridae
			Pomacentridae
			Pseudochromidae
			Congrogadidae
			Plesiopidae
Synbranchiformes	400		
(=Anabantaria)			
		Synbranchoidei	Indostomidae
		Synbranchoidei	Synbranchidae
		Synbranchoidei	Chaudhuriidae
		Synbranchoidei	Mastacembelidae
		Anabantoidei	Anabantidae
		Anabantoidei	Helostomatidae
		Anabantoidei	Osphronemidae
		Anabantoidei	Channidae
		Anabantoidei	Badidae
		Anabantoidei	Nandidae
		Anabantoidei	Pristolepididae
Carangiformes	1,100		
(=Carangaria)			
		Carangoidei-Carangoidea	Carangidae
		Carangoidei-Carangoidea	Trachinotidae
		Carangoidei-Carangoidea	Coryphaenidae
		Carangoidei-Carangoidea	Echeneidae
		Carangoidei-Carangoidea	Rachycentridae
		Carangoidei-Xiphoidea	Istiophoridae
		Carangoidei-Xiphoidea	Xiphiidae
		Carangoidei	Leptobramidae
		Carangoidei	Menidae
		Carangoidei	Nemastiidae

Carangoidei	Toxotidae
Pleuronectoidei	Psettodidae
Pleuronectoidei-Pleuronectoidea	Achiridae
Pleuronectoidei-Pleuronectoidea	Achiropsettidae
Pleuronectoidei-Pleuronectoidea	Bothidae
Pleuronectoidei-Pleuronectoidea	Citharidae
Pleuronectoidei-Pleuronectoidea	Cyclosettidae
Pleuronectoidei-Pleuronectoidea	Cynoglossidae
Pleuronectoidei-Pleuronectoidea	Oncopteridae
Pleuronectoidei-Pleuronectoidea	Paralichthyidae
Pleuronectoidei-Pleuronectoidea	Paralichthodidae
Pleuronectoidei-Pleuronectoidea	Pleuronectidae
Pleuronectoidei-Pleuronectoidea	Poecilopsettidae
Pleuronectoidei-Pleuronectoidea	Rhombosoleidae
Pleuronectoidei-Pleuronectoidea	Samaridae
Pleuronectoidei-Pleuronectoidea	Scophthalmidae
Pleuronectoidei-Pleuronectoidea	Soleidae
	Centropomidae
	Lactariidae
	Polynemidae
	Sphyraenidae

Perciformes

3,192

Percoidei	Percidae
Percoidei	Trachinidae
Percoidei	Nipponidae
	Epinephelidae
	Grammistidae
	Liopropomatidae
	Serranidae
	Anthiadidae
	Bembropidae
	Percophidae
Notothenioidei	Bovichtidae
Notothenioidei	Pseudaphritidae
Notothenioidei	Eleginopsidae
Notothenioidei	Artedidraconidae
Notothenioidei	Bathydraconidae
Notothenioidei	Channichthyidae

Notothenioidei	Harpagiferidae
Notothenioidei	Nototheniidae
Scorpaenoidei	Platycephalidae
Scorpaenoidei	Bembridae
Scorpaenoidei	Congiopodidae
Scorpaenoidei	Neosebastidae
Scorpaenoidei	Hoplichthyidae
Scorpaenoidei	Normanichthyidae
Scorpaenoidei	Synanceiidae
Scorpaenoidei	Triglidae
Scorpaenoidei	Scorpaenidae
Scorpaenoidei	Anoplopomatidae
Scorpaenoidei	Hexagrammidae
Scorpaenoidei	Zaniolepididae
Scorpaenoidei	Trichodontidae
Scorpaenoidei	Cyclopteridae
Scorpaenoidei	Liparidae
Scorpaenoidei	Scorpaenichthyidae
Scorpaenoidei	Agonidae
Scorpaenoidei	Cottidae
Scorpaenoidei	Psychrolutidae
Scorpaenoidei	Rhamphocottidae
Scorpaenoidei	Anarhichadidae
Scorpaenoidei	Bathymasteridae
Scorpaenoidei	Cryptacanthodidae
Scorpaenoidei	Pholidae
Scorpaenoidei	Ptilichthyidae
Scorpaenoidei	Scytalinidae
Scorpaenoidei	Stichaeidae
Scorpaenoidei	Zaproridae
Scorpaenoidei	Eulophiidae
Scorpaenoidei	Opisthocentridae
Scorpaenoidei	Lumpenidae
Scorpaenoidei	Neozoarcidae
Scorpaenoidei	Zoarcidae
Scorpaenoidei	Aulorhynchidae
Scorpaenoidei	Gasterosteidae
Scorpaenoidei	Hypoptychidae

Centrarchiformes

299

Aplodactylidae
Centrarchidae
Cheilodactylidae
Chironemidae
Cirrhitidae
Dichistiidae
Enoplosidae
Girellidae
Kuhliidae
Kyphosidae
Microcanthidae
Scorpididae
Latridae
Oplegnathidae
Percichthyidae
Sinipercidae
Terapontidae

Labriformes

757

Labroidei
Labroidei
Uranoscopoidei
Uranoscopoidei
Uranoscopoidei
Uranoscopoidei
Uranoscopoidei

Labridae
Centrogenyidae
Uranoscopidae
Cheimarrichthyidae
Pinguipedidae
Ammodytidae
Leptoscopidae

Acropomatiformes

308

Acropomatidae
Banjosidae
Bathyclupeidae
Champsodontidae
Creediidae
Dinolestidae
Epigonidae
Glaucosomatidae
Hemerocoetidae
Howellidae
Lateolabracidae

Leptoscopidae
Malakichthyidae
Ostracoberycidae
Pempheridae
Pentacerotidae
Polyprionidae
Stereolepidae
Scombropidae
Synagropidae
Symphysanodontidae

Acanthuriformes

2,350

Acanthuroidei
Acanthuroidei
Acanthuroidei

Acanthuridae
Zanclidae
Luvaridae
Gerreidae
Moronidae
Sillaginidae
Drepaneidae
Ephippidae
Dinopercidae
Haemulidae
Sciaenidae
Monodactylidae
Lobotidae
Emmelichthyidae
Lutjanidae
Malacanthidae
Pomacanthidae
Leiognathidae
Chaetodontidae
Callanthiidae
Lethrinidae
Nemipteridae
Sparidae
Siganidae
Scatophagidae
Priacanthidae
Cepolidae

	Caproidae
Lophioidei	Antennariidae
Lophioidei	Brachionichthyidae
Lophioidei	Caulophrynidae
Lophioidei	Centrophrynidae
Lophioidei	Ceratiidae
Lophioidei	Chaunacidae
Lophioidei	Diceratiidae
Lophioidei	Gigantactinidae
Lophioidei	Himantolophidae
Lophioidei	Linophrynidae
Lophioidei	Lophichthyidae
Lophioidei	Lophiidae
Lophioidei	Melanocetidae
Lophioidei	Neoceratiidae
Lophioidei	Ogcocephalidae
Lophioidei	Oneirodidae
Lophioidei	Tetrabrachiidae
Tetraodontoidei	Aracanidae
Tetraodontoidei	Balistidae
Tetraodontoidei	Diodontidae
Tetraodontoidei	Molidae
Tetraodontoidei	Monacanthidae
Tetraodontoidei	Ostraciidae
Tetraodontoidei	Tetraodontidae
Tetraodontoidei	Triacanthidae
Tetraodontoidei	Triacanthodidae
Tetraodontoidei	Triodontidae

Supplementary Table 4: Divergence date estimates in millions of years (Mya) and 95% Highest Posterior Density (HPD) credible intervals for major acanthomorph clades, generated using six alignments of 30 UCE loci in BEAST. Estimates from the 702-taxon and 1,084-taxon time trees are both represented. All stem and crown ages are calculated from median node heights.

Clade	# of Taxa	Loci Set	Stem Age (Mya)	Stem 95% HPD (Mya)	Crown Age (Mya)	Crown 95% HPD (Mya)
Lampriformes	1,084	30 loci set A	131.28	[112.28, 145.67]	58.09	[55.84, 69.71]
		30 loci set B	134.87	[117.46, 147.27]	57.83	[55.82, 67.74]
		30 loci set C	133.75	[116.00, 146.56]	58.15	[55.82, 72.19]
	702	30 loci set D	133.07	[115.53, 145.96]	57.90	[55.83, 69.38]
		30 loci set E	137.30	[123.25, 147.73]	57.99	[55.81, 69.90]
		30 loci set F	137.28	[119.55, 152.47]	57.90	[55.81, 69.26]
Polymixia	1,084	30 loci set A	96.79	[93.96, 108.22]		
		30 loci set B	98.33	[93.99, 120.28]		
		30 loci set C	97.52	[93.96, 112.48]		
	702	30 loci set D	97.16	[93.94, 111.95]		
		30 loci set E	96.69	[93.92, 108.91]		
		30 loci set F	96.77	[93.93, 109.90]		
Percopsiformes	1,084	30 loci set A	96.79	[93.96, 108.22]	53.54	[40.12, 72.36]
		30 loci set B	98.33	[93.99, 120.28]	53.04	[38.36, 71.85]
		30 loci set C	97.52	[93.96, 112.48]	54.02	[39.34, 75.18]
	702	30 loci set D	97.16	[93.94, 111.95]	36.57	[34.12, 51.86]
		30 loci set E	96.69	[93.92, 108.91]	36.34	[34.12, 46.72]
		30 loci set F	96.77	[93.93, 109.90]	36.40	[34.12, 47.56]
Zeiformes	1,084	30 loci set A	105.92	[88.81, 122.96]	49.98	[37.33, 72.02]
		30 loci set B	109.87	[94.35, 129.43]	54.86	[38.88, 77.00]
		30 loci set C	109.41	[94.58, 125.37]	50.10	[37.46, 66.39]
	702	30 loci set D	108.97	[92.86, 124.77]	50.09	[36.68, 72.93]
		30 loci set E	112.40	[97.33, 127.83]	52.23	[36.27, 73.79]
		30 loci set F	110.89	[87.82, 127.33]	54.95	[40.48, 79.84]
Stylephorus	1,084	30 loci set A	88.48	[72.87, 105.39]		
		30 loci set B	92.97	[75.31, 112.39]		
		30 loci set C	94.55	[79.52, 110.80]		
	702	30 loci set D	94.04	[78.07, 110.29]		
		30 loci set E	97.74	[82.02, 113.36]		
		30 loci set F	93.74	[73.39, 112.47]		

Gadiformes	1,084	30 loci set A	88.48	[72.87, 105.39	77.01	[61.50, 92.18]
		30 loci set B	92.97	[75.31,112.39]	79.22	[63.54, 97.57]
		30 loci set C	94.55	[79.52, 110.80]	81.29	[65.42, 97.97]
	702	30 loci set D	94.04	[78.07, 110.29]	87.13	[71.95, 103.23]
		30 loci set E	97.74	[82.02, 113.36]	84.64	[68.98, 99.22]
		30 loci set F	93.74	[73.39, 112.47]	80.19	[60.80, 99.93]
Trachichthyiformes	1,084	30 loci set A	137.42	[129.12, 147.30]	46.58	[24.68, 75.50]
		30 loci set B	136.40	[127.79, 144.74]	42.47	[24.82, 72.22]
		30 loci set C	138.07	[129.74, 145.62]	44.99	[25.20, 78.24]
	702	30 loci set D	138.73	[129.73, 147.16]	46.53	[20.28, 78.59]
		30 loci set E	138.45	[129.72, 147.34]	46.02	[23.89, 77.49]
		30 loci set F	138.55	[125.63, 151.42]	51.89	[27.55, 90.99]
Beryciformes	1,084	30 loci set A	132.91	[123.97, 143.13]	100.57	[98.23, 107.44]
		30 loci set B	132.29	[122.95, 141.24]	100.35	[98.28, 107.45]
		30 loci set C	133.93	[126.23, 141.83]	100.57	[98.35, 107.08]
	702	30 loci set D	134.77	[126.10, 144.04]	100.69	[98.18, 108.19]
		30 loci set E	134.80	[125.53, 143.44]	100.70	[98.18, 108.29]
		30 loci set F	134.23	[116.61, 148.64]	100.69	[98.17, 108.06]
Ophidiiformes	1,084	30 loci set A	126.76	[116.96, 135.68]	84.50	[59.31, 111.29]
		30 loci set B	126.31	[117.66, 135.78]	88.86	[66.89, 115.30]
		30 loci set C	127.63	[120.65, 136.57]	92.32	[65.49, 115.42]
	702	30 loci set D	128.36	[119.08, 137.65]	85.49	[57.95, 115.91]
		30 loci set E	127.61	[117.49, 137.46]	83.87	[58.20, 110.70]
		30 loci set F	127.09	[105.34, 141.44]	80.24	[53.46, 114.16]
Batrachoididae	1,084	30 loci set A	121.85	[113.37, 130.94]	49.09	[25.28, 76.27]
		30 loci set B	121.66	[111.66, 130.20]	50.84	[29.93, 78.15]
		30 loci set C	123.25	[114.82, 130.23]	43.56	[23.91, 70.03]
	702	30 loci set D	123.43	[114.13, 133.12]	43.41	[19.20, 76.30]
		30 loci set E	123.23	[113.51, 133.45]	43.46	[18.07, 75.89]
		30 loci set F	121.76	[104.77, 139.03]	50.55	[27.08, 83.20]
Gobiiformes	1,084	30 loci set A	117.81	[108.89, 126.63]	109.64	[98.88, 119.95]
		30 loci set B	118.22	[107.12, 126.70]	111.01	[99.69, 121.14]
		30 loci set C	119.73	[111.67, 127.22]	112.57	[103.28, 121.44]
	702	30 loci set D	119.80	[110.41, 129.24]	111.76	[100.58, 122.53]
		30 loci set E	119.71	[108.92, 129.01]	111.91	[99.63, 122.86]
		30 loci set F	117.80	[97.66, 132.04]	110.32	[94.89, 124.32]

Syngnathiformes	1,084	30 loci set A	110.30	[101.51, 120.65]	104.59	[95.01, 114.75]
		30 loci set B	110.65	[97.59, 119.08]	104.49	[93.39, 114.84]
		30 loci set C	111.82	[101.46, 120.96]	105.30	[92.93, 115.32]
	702	30 loci set D	109.82	[99.69, 119.86]	102.66	[91.04, 112.38]
		30 loci set E	109.64	[98.89, 119.71]	101.48	[88.91, 111.90]
		30 loci set F	107.73	[87.68, 122.92]	98.93	[80.57, 113.81]
Scombriformes	1,084	30 loci set A	110.30	[101.51, 120.65]	65.83	[59.72, 74.36]
		30 loci set B	110.65	[97.59, 119.08]	68.10	[61.74, 79.89]
		30 loci set C	111.82	[101.46, 120.96]	66.96	[60.70, 76.91]
	702	30 loci set D	109.82	[99.69, 119.86]	63.99	[58.44, 71.70]
		30 loci set E	109.64	[98.89, 119.71]	64.74	[59.56, 70.85]
		30 loci set F	107.73	[87.68, 122.92]	63.05	[58.28, 69.03]
Blenniiformes	1,084	30 loci set A	105.90	[96.11, 115.30]	96.20	[86.23, 105.98]
		30 loci set B	107.22	[96.59, 118.94]	96.77	[84.99, 108.06]
		30 loci set C	106.45	[95.78, 117.40]	95.84	[83.69, 106.66]
	702	30 loci set D	107.79	[97.99, 120.19]	98.25	[88.06, 109.92]
		30 loci set E	104.16	[93.40, 114.87]	93.99	[83.25, 104.93]
		30 loci set F	102.17	[87.07, 117.66]	90.17	[78.27, 104.02]
Synbranchiformes	1,084	30 loci set A	98.87	[87.37, 110.69]	86.89	[73.15, 100.03]
		30 loci set B	99.34	[86.57, 113.26]	85.96	[72.16, 98.73]
		30 loci set C	98.46	[85.78, 111.44]	88.14	[75.77, 102.19]
	702	30 loci set D	99.93	[85.23, 111.97]	87.17	[72.00, 101.38]
		30 loci set E	95.32	[81.12, 108.53]	81.86	[66.73, 96.64]
		30 loci set F	97.98	[78.90, 112.10]	83.95	[66.38, 100.05]
Carangiformes	1,084	30 loci set A	98.87	[87.37, 110.69]	75.72	[66.44, 86.53]
		30 loci set B	99.34	[86.57, 113.26]	73.94	[65.91, 85.40]
		30 loci set C	98.46	[85.78, 111.44]	73.12	[65.15, 85.06]
	702	30 loci set D	99.93	[85.23, 111.97]	75.66	[65.74, 88.17]
		30 loci set E	95.32	[81.12, 108.53]	73.30	[64.89, 83.24]
		30 loci set F	97.98	[78.90, 112.10]	71.38	[63.27, 81.47]
Perciformes	1,084	30 loci set A	93.73	[81.70, 107.69]	66.86	[55.18, 78.00]
		30 loci set B	87.35	[77.09, 101.56]	58.70	[48.42, 71.23]
		30 loci set C	86.31	[76.71, 99.62]	61.77	[51.99, 71.14]
	702	30 loci set D	86.27	[76.37, 98.52]	63.53	[52.65, 77.01]
		30 loci set E	87.27	[76.89, 100.23]	59.84	[48.61, 71.50]
		30 loci set F	88.41	[77.47, 104.10]	59.33	[49.69, 72.02]

Centrarchiformes	1,084	30 loci set A	83.17	[75.26, 92.76]	53.26	[35.65, 78.06]
		30 loci set B	80.67	[73.27, 90.20]	50.84	[35.00, 77.08]
		30 loci set C	80.55	[73.40, 89.02]	78.34	[59.02, 88.96]
	702	30 loci set D	81.63	[73.63, 91.51]	54.56	[36.97, 79.62]
		30 loci set E	80.75	[73.11, 89.16]	61.09	[38.33, 84.46]
		30 loci set F	82.97	[73.07, 93.94]	46.08	[31.65, 71.94]
Labriformes	1,084	30 loci set A	81.03	[73.25, 89.30]	76.07	[66.21, 86.95]
		30 loci set B	78.81	[71.72, 87.07]	76.55	[67.89, 85.94]
		30 loci set C	79.34	[72.06, 87.16]	75.25	[65.80, 84.60]
	702	30 loci set D	79.91	[72.33, 88.93]	74.89	[64.69, 85.59]
		30 loci set E	79.06	[71.80, 86.93]	76.45	[73.11, 89.16]
		30 loci set F	81.47	[71.92, 91.68]	77.08	[66.51, 88.21]
Acropomatiformes	1,084	30 loci set A	80.09	[73.10, 88.58]	46.53	[32.55, 60.96]
		30 loci set B	77.12	[70.67, 84.95]	47.39	[33.95, 65.12]
		30 loci set C	78.32	[71.11, 85.72]	46.24	[33.17, 59.99]
	702	30 loci set D	78.83	[71.72, 87.89]	23.78	[14.06, 35.85]
		30 loci set E	77.45	[70.87, 85.19]	22.06	[13.60, 33.15]
		30 loci set F	80.07	[70.93, 89.84]	21.41	[12.44, 31.76]
Acanthuriformes	1,084	30 loci set A	80.09	[73.10, 88.58]	78.52	[72.01, 86.64]
		30 loci set B	77.12	[70.67, 84.95]	75.78	[69.13, 82.30]
		30 loci set C	78.32	[71.11, 85.72]	76.51	[70.12, 84.05]
	702	30 loci set D	78.83	[71.72, 87.89]	76.39	[69.95, 84.70]
		30 loci set E	77.45	[70.87, 85.19]	75.97	[69.71, 83.28]
		30 loci set F	80.07	[70.93, 89.84]	78.16	[69.59, 87.49]
Percomorpha	1,084	30 loci set A	132.91	[123.97, 143.13]	126.76	[116.96, 135.68]
		30 loci set B	132.29	[122.95, 141.24]	126.31	[117.66, 135.78]
		30 loci set C	133.93	[126.23, 141.83]	127.63	[120.65, 136.57]
	702	30 loci set D	134.77	[126.10, 144.04]	128.36	[119.08, 137.65]
		30 loci set E	134.80	[125.53, 143.44]	127.61	[117.49, 137.46]
		30 loci set F	134.23	[116.61, 148.64]	127.09	[105.34, 141.44]

References

- 1 Harrington, R. C. *et al.* Phylogenomic analysis of carangimorph fishes reveals flatfish asymmetry arose in a blink of the evolutionary eye. *BMC Evol. Biol.* **16**, 224, doi:10.1186/s12862-016-0786-x (2016).
- 2 Longo, S. J. *et al.* Phylogenomic analysis of a rapid radiation of misfit fishes (Syngnathiformes) using ultraconserved elements. *Mol. Phylogenet. Evol.* **113**, 33-48, doi:https://doi.org/10.1016/j.ympev.2017.05.002 (2017).
- 3 Alfaro, M. E. *et al.* Explosive diversification of marine fishes at the Cretaceous–Palaeogene boundary. *Nature Ecology & Evolution* **2**, 688-696, doi:10.1038/s41559-018-0494-6 (2018).
- 4 DiBattista, J. D. *et al.* Ice ages and butterflyfishes: Phylogenomics elucidates the ecological and evolutionary history of reef fishes in an endemism hotspot. *Ecology and Evolution* **8**, 10989-11008, doi:10.1002/ece3.4566 (2018).
- 5 Friedman, M. *et al.* A phylogenomic framework for pelagiarian fishes (Acanthomorpha: Percomorpha) highlights mosaic radiation in the open ocean. *Proceedings of the Royal Society B: Biological Sciences* **286**, 20191502, doi:10.1098/rspb.2019.1502 (2019).
- 6 Eschmeyer, W. N. & Fricke, R. (California Academy of Sciences (<http://research.calacademy.org/research/ichthyology/catalog/fishcatmain.asp>), San Francisco, 2021).
- 7 Near, T. J. *et al.* Resolution of ray-finned fish phylogeny and timing of diversification. *Proc. Nat. Acad. Sci. USA* **109**, 13698-13703, doi:10.1073/Pnas.1206625109 (2012).
- 8 Hughes, L. C. *et al.* Comprehensive phylogeny of ray-finned fishes (Actinopterygii) based on transcriptomic and genomic data. *Proc. Nat. Acad. Sci. USA*, doi:10.1073/pnas.1719358115 (2018).
- 9 Glenn, T. C. *et al.* Adapterama I: universal stubs and primers for 384 unique dual-indexed or 147,456 combinatorially-indexed Illumina libraries (iTru & iNext). *PeerJ* **7**, e7755, doi:10.7717/peerj.7755 (2019).
- 10 Faircloth, B. C. PHYLUCe is a software package for the analysis of conserved genomic loci. *Bioinformatics* **32**, 786-788, doi:10.1093/bioinformatics/btv646 (2016).
- 11 Faircloth, B. C. *et al.* Ultraconserved elements anchor thousands of genetic markers spanning multiple evolutionary timescales. *Syst. Biol.* **61**, 717-726, doi:10.1093/sysbio/sys004 (2012).
- 12 Bolger, A. M., Lohse, M. & Usadel, B. Trimmomatic: a flexible trimmer for Illumina sequence data. *Bioinformatics* **30**, 2114-2120 (2014).
- 13 Grabherr, M. G. *et al.* Full-length transcriptome assembly from RNA-Seq data without a reference genome. *Nat Biotechnol* **29**, 644-652, doi:10.1038/nbt.1883 (2011).
- 14 Katoh, K. & Standley, D. M. MAFFT multiple sequence alignment software Version 7: improvements in performance and usability. *Mol. Biol. Evol.* **30**, 772-780, doi:10.1093/molbev/mst010 (2013).
- 15 Capella-Gutiérrez, S., Silla-Martínez, J. M. & Gabaldón, T. trimAl: a tool for automated alignment trimming in large-scale phylogenetic analyses. *Bioinformatics* **25**, 1972-1973, doi:10.1093/bioinformatics/btp348 (2009).

- 16 Nguyen, L. T., Schmidt, H. A., von Haeseler, A. & Minh, B. Q. IQ-TREE: A fast and effective stochastic algorithm for estimating maximum likelihood phylogenies. *Mol. Biol. Evol.* **32**, 268-274, doi:10.1093/molbev/msu300 (2015).
- 17 Kozlov, A. M., Darriba, D., Flouri, T., Morel, B. & Stamatakis, A. RAxML-NG: a fast, scalable and user-friendly tool for maximum likelihood phylogenetic inference. *Bioinformatics* **35**, 4453-4455, doi:10.1093/bioinformatics/btz305 (2019).
- 18 Minh, B. Q., Nguyen, M. A. T. & von Haeseler, A. Ultrafast Approximation for Phylogenetic Bootstrap. *Mol. Biol. Evol.* **30**, 1188-1195, doi:10.1093/molbev/mst024 (2013).
- 19 Kalyaanamoorthy, S., Minh, B. Q., Wong, T. K. F., von Haeseler, A. & Jermiin, L. S. ModelFinder: fast model selection for accurate phylogenetic estimates. *Nat Methods* **14**, 587-589 (2017).
- 20 Lanfear, R., Frandsen, P. B., Wright, A. M., Senfeld, T. & Calcott, B. PartitionFinder 2: New methods for selecting partitioned models of evolution for molecular and morphological phylogenetic analyses. *Mol. Biol. Evol.* **34**, 772-773, doi:10.1093/molbev/msw260 (2017).
- 21 Puigbò, P., Garcia-Vallvé, S. & McInerney, J. O. TOPD/FMTS: a new software to compare phylogenetic trees. *Bioinformatics* **23**, 1556-1558, doi:10.1093/bioinformatics/btm135 (2007).
- 22 Robinson, D. F. & Foulds, L. R. Comparison of phylogenetic trees. *Math. Biosci.* **53**, 131-147 (1981).
- 23 Steel, M. A. & Penny, D. Distributions of tree comparison metrics: Some new results. *Syst. Biol.* **42**, 126-141. (1993).
- 24 Zhang, C., Rabiee, M., Sayyari, E. & Mirarab, S. ASTRAL-III: polynomial time species tree reconstruction from partially resolved gene trees. *BMC Bioinf.* **19**, 153, doi:10.1186/s12859-018-2129-y (2018).
- 25 Mai, U. & Mirarab, S. TreeShrink: fast and accurate detection of outlier long branches in collections of phylogenetic trees. *Bmc Genomics* **19**, 272, doi:10.1186/s12864-018-4620-2 (2018).
- 26 Ane, C., Larget, B., Baum, D. A., Smith, S. D. & Rokas, A. Bayesian estimation of concordance among gene trees. *Mol. Biol. Evol.* **24**, 412-426, doi:10.1093/molbev/msl170 (2007).
- 27 Ronquist, F. *et al.* MrBayes 3.2: efficient Bayesian phylogenetic inference and model choice across a large model space. *Syst. Biol.* **61**, 539-542, doi:10.1093/sysbio/sys029 (2012).
- 28 Bouckaert, R. *et al.* BEAST 2: a software platform for Bayesian evolutionary analysis. *Plos Comput Biol* **10**, e1003537, doi:10.1371/journal.pcbi.1003537 (2014).
- 29 Oliveros, C. H. *et al.* Earth history and the passerine superradiation. *Proceedings of the National Academy of Sciences* **116**, 7916, doi:10.1073/pnas.1813206116 (2019).
- 30 Rambaut, A., Drummond, A. J., Xie, D., Baele, G. & Suchard, M. A. Posterior summarization in Bayesian phylogenetics using Tracer 1.7. *Syst. Biol.* **67**, 901-904, doi:10.1093/sysbio/syy032 (2018).
- 31 Drummond, A. J. & Rambaut, A. BEAST: Bayesian evolutionary analysis by sampling trees. *BMC Evol. Biol.* **7**, 214 (2007).

- 32 Drummond, A. J., Suchard, M. A., Xie, D. & Rambaut, A. Bayesian phylogenetics with BEAUti and the BEAST 1.7. *Mol. Biol. Evol.* **29**, 1969-1973, doi:10.1093/molbev/mss075 (2012).
- 33 Höhna, S., May, M. R. & Moore, B. R. TESS: an R package for efficiently simulating phylogenetic trees and performing Bayesian inference of lineage diversification rates. *Bioinformatics* **32**, 789-791, doi:10.1093/bioinformatics/btv651 (2016).
- 34 Rabosky, D. L. Automatic detection of key innovations, rate shifts, and diversity-dependence on phylogenetic trees. *PLOS One* **9**, e89543, doi:10.1371/journal.pone.0089543 (2014).
- 35 Rabosky, D. L., Donnellan, S. C., Grundler, M. & Lovette, I. J. Analysis and visualization of complex macroevolutionary dynamics: an example from Australian scincid lizards. *Syst. Biol.* **63**, 610-627 (2014).
- 36 Price, S. A. *et al.* Building a body shape morphospace of teleostean fishes. *Integ. Comp. Biol.* **59**, 716-730, doi:10.1093/icb/icz115 (2019).
- 37 Revell, L. J. phytools: an R package for phylogenetic comparative biology (and other things). *Methods Ecol Evol* **3**, 217-223, doi:10.1111/j.2041-210X.2011.00169.x (2012).
- 38 Harmon, L. J., Weir, J. T., Brock, C. D., Glor, R. E. & Challenger, W. GEIGER: investigating evolutionary radiations. *Bioinformatics* **24**, 129-131, doi:10.1093/bioinformatics/btm538 (2008).
- 39 Davesne, D. *et al.* Early fossils illuminate character evolution and interrelationships of Lampridiformes (Teleostei, Acanthomorpha). *Zool. J. Linn. Soc.* **172**, 475-498 (2014).
- 40 Delbarre, D. J., Davesne, D. & Friedman, M. Anatomy and relationships of *Aipichthys pretiosus* and '*Aipichthys*' *nuchalis* (Acanthomorpha: Lampridomorpha), with a review of Late Cretaceous relatives of oarfishes and their allies. *J Syst Palaeontol* **14**, 545-567 (2016).
- 41 Ogg, J. G. & Hinnov, L. A. in *The Geologic Time Scale 2012* Vol. 2 (eds F. Gradstein, J. Ogg, M.D. Schmitz, & G.M. Ogg) 793-853 (Elsevier, 2012).
- 42 Patterson, C. A review of Mesozoic acanthopterygian fishes, with special reference to those of the English Chalk. *Phil. Trans. R. Soc. B* **247**, 213-482 (1964).
- 43 Patterson, C. An overview of the early fossil record of acanthomorphs. *Bull. Mar. Sci.* **52**, 29-59 (1993).
- 44 Owen, E. in *Fossils of the Chalk. Palaeontological Association Field Guides to Fossils: Number 2* (ed A.B. Smith) 9-14 (Oxford University Press, 1987).
- 45 Friedman, M., Beckett, H. T., Close, R. A. & Johanson, Z. The English Chalk and London Clay: two remarkable British bony fish Lagerstätten. *Geological Society, London, Special Publications* **430**, 165, doi:10.1144/SP430.18 (2016).
- 46 Rosen, D. E. & Patterson, C. The structure and relationships of the paracanthopterygian fishes. *Bull. Amer. Mus. Nat. Hist.* **141**, 357-474 (1969).
- 47 Murray, A. M. & Wilson, M. V. H. in *Mesozoic fishes 2 - systematics and fossil record* (eds G. Arratia & H.-P. Schultze) 397-411 (Verlag Dr. Friedrich Pfeil, 1999).
- 48 Armbruster, J. W., Niemiller, M. L. & Hart, P. B. Morphological evolution of the Cave-, Spring-, and Swampfishes of the Amblyopsidae (Percopsiformes). *Copeia* **104**, 763-777, doi:10.1643/CI-15-339 (2016).

- 49 Evanoff, E., McIntosh, W. C. & Murphey, P. C. Stratigraphic summary and $^{40}\text{Ar}/^{39}\text{Ar}$ geochronology of the Florissant Formation, Colorado. *Proc. Denver Mus. Nature Sci. Series 4, no. 1*, 1-16 (2001).
- 50 Danil'chenko, P. G. Kostistye ryby Maikopskikh otlozhenii Kavkaza [Bony fishes of the Maikop deposits of the Caucasus]. *Trudy Paleon. Inst.* **78**, 1-208. [In Russian] (1960).
- 51 Baciu, D.-S., Bannikov, A. F. & Tyler, J. C. Revision of the fossil fishes of the family Zeidae (Zeiformes). *Boll. Mus. Storia Nat. Verona, Geol. Paleon. Preist.* **29**, 95-128 (2005).
- 52 Santini, F., Tyler, J. C., Bannikov, A. F. & Baciu, D. S. A phylogeny of extant and fossil buckler dory fishes, family Zeidae (Zeiformes, Acanthomorpha). *Cybium* **30**, 99-107 (2006).
- 53 Jones, R. W. & Simmons, M. D. A review of the stratigraphy of Eastern Paratethys (Oligocene-Holocene), with particular emphasis on the Black Sea. *AAPG Mem.* **68**, 39-52 (1997).
- 54 Luterbacher, H. P. *et al.* in *A geologic time scale 2004* (eds F. Gradstein, J. Ogg, & A. Smith) 384-408 (Cambridge University Press, 2004).
- 55 Danil'chenko, P. G. in *Ocherki po filogenii i sistematike iskopayemykh ryb i beschelyustnykh [Outlines on the phylogeny and systematics of fossil fishes and agnathans]* (ed D.V. Obruchev) 113-156. [In Russian] (Nauka, 1968).
- 56 Bannikov, A. F. Review of fossil Lampridiformes (Teleostei) finds with a description of a new Lophotidae genus and species from the Oligocene of the northern Caucasus. *Paleontol. J.* **33**, 68-76 (1999).
- 57 Bannikov, A. F. & Parin, N. N. The list of marine fishes from Cenozoic (Upper Paleocene-middle Miocene) localities in southern European Russia and adjacent countries. *J. Ichthyol.* **37**, 150-155 (1997).
- 58 Patterson, C. New Cretaceous berycoid fishes from the Lebanon. *Bull. Brit. Mus. (Nat. Hist.) Geol.* **14**, 69-109 (1967).
- 59 Zehren, S. J. The comparative osteology and phylogeny of the Beryciformes. *Evolutionary Monogr.* **1**, 1-389 (1979).
- 60 Sorbini, L. Gli Holocentridae di Monte Bolca. I: *Eoholocentrum*, nov. gen., *Eoholocentrum macrocephalum* (de Blainville) (Pisces-Actinopterygii). *Stud. Ric. Giaciam. Terz. Bolca* **2**, 205-228 (1975).
- 61 Sorbini, L. Gli Holocentridae di Monte Bolca. II: *Tenuicentrum pattersoni* nov. gen. nov. sp. Nuovi dati a favore dell'origine monofiletica dei beryciformi (Pisces). *Stud. Ric. Giaciam. Terz. Bolca* **2**, 456-472 (1975).
- 62 Sorbini, L. Gli Holocentridae di Monte Bolca. III. *Berybolcensis leptacanthus* (Agassiz). *Stud. Ric. Giaciam. Terz. Bolca* **4**, 19-35 (1979).
- 63 Stewart, J. D. *Taxonomy, paleoecology, and stratigraphy of the halecostome-inoceramid associations of the North American Upper Cretaceous epicontinental seaway*, University of Kansas, (1984).
- 64 Papazzoni, C., Carnevale, G., Fornaciari, E., Giusberti, L. & Trevisani, E. 29-36 (2014).
- 65 Papazzoni, C. A. & Trevisani, E. Facies analysis, palaeoenvironmental reconstruction, and biostratigraphy of the "Pesciara di Bolca" (Verona, northern Italy): An early Eocene *Fossil-Lagerstätte*. *Palaeogeogr. Palaeoclimat. Palaecol.* **242**, 21-35 (2006).

- 66 Sorbini, L. The Cretaceous fishes of Nardò. I°. Order Gasterosteiformes (Pisces). *Boll. Mus. Civ. Stor. Nat. Verona* **8**, 1-27 (1981).
- 67 Orr, J. W. *Phylogenetic relationships of gasterosteiform fishes (Teleostei: Acanthomorpha)*, University of Washington, (1995).
- 68 Pietsch, T. W. Evolutionary relationships of the sea moths (Teleostei: Pegasidae) with a classification of the gasterosteiform families. *Copeia* **1978**, 517-529 (1978).
- 69 Medizza, F. & Sorbini, L. in *I vertebrati fossili italiani—Catalogo dell Mostra* 131-134 (Museo Civico di Storia Naturale, 1980).
- 70 Blot, J. La faune ichthyologique des gisements du Monte Bolca (Province de Vérone, Italie). Catalogue systématique présentat l'état actuel des recherches concernant cette faune. *Bull. Mus. nation. d'Hist. nat., Paris, 4e serie, sec. C* **2**, 339-396 (1980).
- 71 Doiuchi, R. & Nakabo, T. Molecular phylogeny of the stromateoid fishes (Teleostei : Perciformes) inferred from mitochondrial DNA sequences and compared with morphology-based hypotheses. *Mol. Phylogenet. Evol.* **39**, 111-123 (2006).
- 72 Carnevale, G. & Bannikov, A. F. Description of a new stromateoid fish from the Miocene of St. Eugene, Algeria. *Acta Palaeontol Pol* **51**, 489-497 (2006).
- 73 Horn, M. H. Systematic Status and Aspects of the Ecology of the Elongate Ariommid Fishes (Suborder Stromateoidei) in the Atlantic. *Bull. Mar. Sci.* **22**, 537-558 (1972).
- 74 Bannikov, A. F. An new species of stromateoid fishes (Perciformes) the Lower Oligocene of the Caucasus. *Paleontol. J.* **22**, 107-112 (1988).
- 75 Bannikov, A. Morphology and phylogeny of fossil stromateoid fishes (Perciformes). *Geobios* **28**, Supplement 2, 177-181 (1995).
- 76 Doiuchi, R., Sato, T. & Nakabo, T. Phylogenetic relationships of the stromateoid fishes (Perciformes). *Ichthyol. Res.* **51**, 202-212 (2004).
- 77 Carnevale, G. Fossil fishes from the Serravallian (Middle Miocene) of Torricella Peligna, Italy. *Palaeontographia Italica* **91**, 1-67 (2007).
- 78 Santini, F., Carnevale, G. & Sorenson, L. First molecular scombrid timetree (Percomorpha: Scombridae) shows recent radiation of tunas following invasion of pelagic habitat. *Ital. J. Zool.* **80**, 210-221, doi:Doi 10.1080/11250003.2013.775366 (2013).
- 79 Arambourg, C. Resultats scientifiques de la mission C. Arambourg en Syrie et en Iran (1938–1939). II. Les poissons Oligocène de l'Iran. *Notes Mém. Moyen-Orient* **8**, 1-210 (1967).
- 80 Matsui, T. Review of mackerel genera *Scomber* and *Rastrelliger* with description of a new species of *Rastrelliger*. *Copeia* **1967**, 71-83 (1967).
- 81 Monsch, K. A. Revision of the scombroid fishes from the Cenozoic of England. *T Roy Soc Edin-Earth* **95**, 445-489 (2005).
- 82 Monsch, K. A. The PhyloCode, or alternative nomenclature: Why it is not beneficial to palaeontology, either. *Acta Palaeontol Pol* **51**, 521-524 (2006).
- 83 Collette, B. B. & Russo, J. L. Morphology, systematics, and biology of the Spanish Mackerels (*Scomberomorus*, Scombridae). *Fish. Bull.* **82**, 545-692 (1984).
- 84 Leriche, M. Les poissons éocènes de la Belgique. *Memoirs of the Royal Belgian Museum of Natural Sciences* **3**, 49-228 (1905).
- 85 Monsch, K. A. & Bannikov, A. F. New taxonomic synopses and revision of the scombroid fishes (Scombroidei, Perciformes), including billfishes, from the Cenozoic of territories of the former USSR. *Earth Env Sci T R So* **102**, 253-300, doi:Doi 10.1017/S1755691011010085 (2011).

- 86 Bannikov, A. F. Fossil scombrids of the USSR. *Trudy Paleon. Inst.* **210**, 1-111 (1985).
- 87 Murray, A. M. & Thewissen, J. G. M. Eocene actinopterygian fishes from Pakistan, with the description of a new genus and species of channid (Channiformes). *J. Vert. Paleo.* **28**, 41-52 (2008).
- 88 Gingerich, P. D. Stratigraphic and micropaleontological constraints on the middle Eocene age of the mammal-bearing Kuldana Formation of Pakistan. *J. Vert. Paleo.* **23**, 643-651, doi:Doi 10.1671/2409 (2003).
- 89 Rabosky, D. L. *et al.* An inverse latitudinal gradient in speciation rate for marine fishes. *Nature*, doi:10.1038/s41586-018-0273-1 (2018).
- 90 Bannikov, A. The systematic composition of the Eocene actinopterygian fish fauna from Monte Bolca, northern Italy, as known to date. *St. Ric. Giac. Terz. Bolca* **15** (2014).
- 91 Carnevale, G., Bannikov, A., Marramà, G., Tyler, J. C. & Zorzin, R. in *The Bolca Fossil-Lagerstätten: A window into the Eocene World* (eds C. Andrea Papazzoni *et al.*) 37-63 (Rendiconti della Società Paleontologica Italiana, 2014).
- 92 Johnson, G. D. Scombroid phylogeny: an alternative hypothesis. *Bull. Mar. Sci.* **39**, 1-41 (1986).
- 93 Near, T. J. *et al.* Phylogeny and tempo of diversification in the superradiation of spiny-rayed fishes. *Proc. Nat. Acad. Sci. USA* **110**, 12738-12743, doi:10.1073/pnas.1304661110 (2013).
- 94 Friedman, M. & Johnson, G. D. A new species of *Mene* (Perciformes: Menidae) from the Paleocene of South America, with notes on paleoenvironment. *J. Vert. Paleo.* **25**, 770-783 (2005).
- 95 Bonde, N. A distinct fish fauna in the basal ashseries of the Fur/Ølst Formation (U. Paleocene, Denmark). *Aarhus Geoscience* **6**, 33-48 (1997).
- 96 Anthonissen, D. E. & Ogg, J. G. in *The Geologic Time Scale 2012* (eds F. Gradstein, J. Ogg, M.D. Schmitz, & G.M. Ogg) 1083-1127 (Elsevier, 2012).
- 97 Smith-Vaniz, W. F. in *Ontogeny and systematics of fishes* (eds H.G. Moser *et al.*) 522-530 (Allen Press, 1984).
- 98 Eastman, C. R. Descriptions of Bolca fishes. *Bull. Mus. Comp. Zool.* **46**, 1-36 (1904).
- 99 Gushiken, S. Phylogenetic relationships of the perciform genera of the family Carangidae. *Jap. J. Ich.* **34**, 443-461 (1988).
- 100 Friedman, M., Johanson, Z., Harrington, R. C., Near, T. J. & Graham, M. R. An early fossil remora (Echeneoidea) reveals the evolutionary assembly of the adhesion disc. *Proc. R. Soc. B* **280**, 20131200, doi:10.1098/rspb.2013.1200 (2013).
- 101 Micklich, N. R. New information on the fish fauna of the Frauenweiler fossil site. *Ital. J. Zool.* **65**, 169-184 (1998).
- 102 O'Toole, B. Phylogeny of the species of the superfamily Echeneoidea (Perciformes : Carangoidei: Echeneidae, Rachycentridae, and Coryphaenidae), with an interpretation of echeneid hitchhiking behaviour. *Can. J. Zool.* **80**, 596-623 (2002).
- 103 Bannikov, A. F. Fossil carangids and apolectids of the USSR. *Trudy Paleon. Inst.* **244**, 1-106 (1990).
- 104 Friedman, M. The evolutionary origin of flatfish asymmetry. *Nature* **454**, 209-212 (2008).
- 105 Chanet, B. A cladistic reappraisal of the fossil flatfishes record consequences on the phylogeny of the Pleuronectiformes (Osteichthyes: Teleostei). *Ann. Sci. nat., Zool., Paris 13e Sér.* **18** (1997).

- 106 Chanet, B. *Eubuglossus eocenicus* (Woodward 1910) from the Upper Lutetian of Egypt, one of the oldest soleids (Teleostei, Pleuronectiformes). *Neu. Jahrbuch Geolo. Paläon., Monatshefte* **1994**, 391-398 (1994).
- 107 Chapleau, F. & Keast, A. A phylogenetic reassessment of the monophyletic status of the family Soleidae, with comments on the suborder Soleoidei (Pisces, Pleuronectiformes). *Can. J. Zool.* **66**, 2797-2810, doi:DOI 10.1139/z88-408 (1988).
- 108 Baciú, D. S. & Chanet, B. Les poissons plats fossils (Teleostei: Pleuronectiformes) de l'Oligocène de Piatra Neamt (Roumanie). *Oryctos* **4**, 17-38 (2002).
- 109 Sakamoto, K., Uyeno, T. & Micklich, N. *Oligopleuronectes germanicus* gen. et sp. nov., an Oligocene pleuronectid flatfish from Frauenweiler, S-Germany. *Bulletin of the National Science Museum Series C (Geology & Paleontology)* **30**, 89-94 (2004).
- 110 Cooper, J. A. & Chapleau, F. Phylogenetic status of *Paralichthodes algoensis* (Pleuronectiformes: Paralichthodidae). *Copeia* **1998**, 477-481. (1998).
- 111 Carnevale, G., Bannikov, A. F., Landini, W. & Sorbini, C. Volhynian (early Sarmatian sensu lato) fishes from Tsurevsky, North Caucasus, Russia. *J. Paleontol.* **80**, 684-699, doi:Doi 10.1666/0022-3360(2006)80[684:Vesslf]2.0.Co;2 (2006).
- 112 Chanet, B. & Sorbini, C. A male fish *Bothus podas* (Delaroche, 1809) (Pleuronectiformes: Bothidae) in the Pliocene of the Marecchia river (Italy). *Bollettino della Societa Paleontologica Italiana* **40**, 345-350 (2001).
- 113 Murray, A. M. Eocene cichlid fishes from Tanzania, East Africa. *J. Vert. Paleo.* **20**, 651-664 (2000).
- 114 Murray, A. M. The oldest fossil cichlids (Teleostei: Perciformes): Indication of a 45 million-year-old species flock. *Proc. R. Soc. B* **268**, 679-684. (2001).
- 115 Murray, A. M. The fossil record and biogeography of the Cichlidae (Actinopterygii: Labroidei). *Biol. J. Linn. Soc.* **74**, 517-532 (2001).
- 116 Harrison, T. *et al.* in *Eocene biodiversity: Unusual occurrences and rarely sampled habitats* (ed G.F. Gunnell) 39-74 (Kluwer Academic/Plenum Publishers, 2001).
- 117 Benton, M. J. *et al.* Constraints on the timescale of animal evolutionary history. *Palaeontologia Electronica* **18** (2015).
- 118 Bannikov, A., Parin, N. V. & Pinna, J. *Rhamphexocoetus volans*, gen. et sp. nov. a new beloniform fish (Beloniformes, Exocoetidei) from the lower Eocene of Italy. *J. Ichthyol.* **25(2)**, 150-155 (1985).
- 119 Rosen, D. E. The relationships and taxonomic position of the halfbeaks, killifishes, silversides and their relatives. *Bull. Amer. Mus. Nat. Hist.* **127**, 217-268 (1964).
- 120 Rosen, D. E. & Parenti, L. R. Relationships of *Oryzias* and the groups of atherinomorph fishes. *Amer. Mus. Novit.* **2719**, 1-25 (1981).
- 121 Collette, B. B., McGowen, G. E., Parin, N. V. & Mito, S. in *Ontogeny and systematics of fishes* (eds H.G. Moser *et al.*) 335-354 (American Society of Ichthyologists and Herpetologists, 1984).
- 122 Bellwood, D. R. & Schultz, O. A review of the fossil record of parrotfishes (Labroidei: Scaridae) with a description of a new *Calatomus* species from the Middle Miocene (Badenian) of Austria. *Ann. Naturhist. Mus. Wien* **92**, 55-71 (1991).
- 123 Bannikov, A. F. & Tyler, J. C. Phylogenetic revision of the fish families Luvaridae and †Kushlukiidae (Acanthuroidei), with a new genus and two new species of Eocene luvarids. *Smithson. Contrib. Paleobiol.* **81**, 1-45 (1995).

- 124 Blot, J. & Tyler, J. C. New genera and species of fossil surgeon fishes and their relatives (Acanthuroidei, Teleostei) from the Eocene of Monte Bolca, Italy, with application of the Blot Formula to both fossil and recent forms. *St. Ric. Giac. Terz. Bolca* **6**, 13-92 (1990).
- 125 Tyler, J. C. & Bannikov, A. F. Relationships of the fossil and recent genera of rabbitfishes (Acanthuroidei: Siganidae). *Smithson. Contrib. Paleobiol.* **84**, 1-35 (1997).
- 126 Micklich, N. R., Tyler, J. C., Johnson, G. D., Swidnicka, E. & Bannikov, A. F. First fossil records of the tholichthys larval stage of butterfly fishes (Perciformes, Chaetodontidae), from the Oligocene of Europe. *Palaontol. Z.* **83**, 479-497 (2009).
- 127 Carnevale, G. Morphology and biology of the Miocene butterflyfish *Chaetodon ficheuri* (Teleostei: Chaetodontidae). *Zool. J. Linn. Soc.* **146**, 251-267 (2006).
- 128 Blum, S. D. *The osteology and phylogeny of the Chaetodontidae (Teleostei: Perciformes)*, University of Hawaii, (1988).
- 129 Krijgsman, W., Hilgen, F. J., Raffi, I., Sierro, F. J. & Wilson, D. S. Chronology, causes and progression of the Messinian salinity crisis. *Nature* **400**, 652-655 (1999).
- 130 Hilgen, F. J. *et al.* Extending the astronomical (polarity) time scale into the Miocene. *Earth Planet. Sci. Lett.* **136**, 495-510 (1995).
- 131 Carnevale, G. The first fossil ribbonfish (Teleostei, Lampridiformes, Trachipteridae). *Geol. Mag.* **141**, 573-582 (2004).
- 132 Yabumoto, Y. & Uyeno, T. A new Miocene ponyfish of the genus *Leiognathus* (Pisces, Leiognathidae). *Bull. Nat. Sci. Mus., Tokyo Ser. C* **20**, 67-77 (1994).
- 133 Yabumoto, Y. & Uyeno, T. *Euleiognathus*, a new genus proposed for the Miocene ponyfish, *Leiognathus tottori* Yabumoto and Uyeno 1994 (Perciformes: Leiognathidae) from Japan. *Ichthyol. Res.* **58**, 19-23 (2011).
- 134 Chakrabarty, P. & Sparks, J. S. Diagnoses for *Leiognathus* Lacepede 1802, *Equula* Cuvier 1815, *Equulites* Fowler 1904, *Eubleekeria* Fowler 1904, and a new ponyfish genus (Teleostei: Leiognathidae). *Amer. Mus. Novit.*, 1-11 (2008).
- 135 Yamashita, T. & Kimura, S. A new species, *Gazza squamiventralis*, from the East Coast of Africa (Perciformes: Leiognathidae). *Ichthyol. Res.* **48**, 161-166 (2001).
- 136 Sparks, J. S. & Chakrabarty, P. Description of a new genus of ponyfishes (Teleostei: Leiognathidae), with a review of the current generic-level composition of the family. *Zootaxa* **3947**, 181-190 (2015).
- 137 Sparks, J. S., Dunlap, P. V. & Smith, W. L. Evolution and diversification of a sexually dimorphic luminescent system in ponyfishes (Teleostei: Leiognathidae), including diagnoses for two new genera. *Cladistics* **21**, 305-327 (2005).
- 138 Gill, A. C. & Michalski, S. Osteological evidence for monophyly of the Leiognathidae (Teleostei: Acanthomorpha: Acanthuriformes). *Zootaxa; Vol 4732, No 3: 13 Feb. 2020* DOI - 10.11646/zootaxa.4732.3.4 (2020).
- 139 Lourens, L., Hilgen, F., Shackleton, N. J., Laskar, J. & Wilson, D. in *A geologic time scale 2004* (eds F. Gradstein, J. Ogg, & A. Smith) 409-440 (Cambridge University Press, 2004).
- 140 Santini, F. & Tyler, J. C. A phylogeny of the families of fossil and extant tetraodontiform fishes (Acanthomorpha, Tetraodontiformes), Upper Cretaceous to recent. *Zool. J. Linn. Soc.* **139**, 565-617 (2003).
- 141 Bannikov, A. F. & Tyler, J. C. A new genus and species of triggerfish from the Middle Eocene of the northern Caucasus, the earliest member of the Balistidae (Tetraodontiformes). *Paleontol. J.* **42**, 615-620 (2008).

- 142 Carnevale, G. & Pietsch, T. W. An Eocene frogfish from Monte Bolca, Italy: The earliest
known skeletal record for the family. *Palaeontology* **52**, 745-752 (2009).
- 143 Pietsch, T. W. The osteology and relationships of the anglerfish genus *Tetrabrachium*
with comments on lophiiform classification. *Fish. Bull.* **79**, 387-419 (1981).
- 144 Pietsch, T. W. in *Ontogeny and systematics of fishes* (eds H.G. Moser *et al.*) 320-325
(American Society of Ichthyologists and Herpetologists, 1984).
- 145 Alda, F., Ludt, W. B., Elías, D. J., McMahan, C. D. & Chakrabarty, P. Comparing
ultraconserved elements and exons for phylogenomic analyses of Middle American
cichlids: when data agree to disagree. *Genome Biol Evol* **13**, doi:10.1093/gbe/evab161
(2021).
- 146 Meiklejohn, K. A., Faircloth, B. C., Glenn, T. C., Kimball, R. T. & Braun, E. L. Analysis
of a rapid evolutionary radiation using ultraconserved elements: evidence for a bias in
some multispecies coalescent methods. *Syst. Biol.* **65**, 612-627,
doi:10.1093/sysbio/syw014 (2016).
- 147 McCormack, J. E. *et al.* A phylogeny of birds based on over 1,500 loci collected by target
enrichment and high-throughput sequencing. *Plos One* **8**, doi:ARTN e54848
DOI 10.1371/journal.pone.0054848 (2013).
- 148 Lambert, S. M., Reeder, T. W. & Wiens, J. J. When do species-tree and concatenated
estimates disagree? An empirical analysis with higher-level scincid lizard phylogeny.
Mol. Phylogenet. Evol. **82**, 146-155, doi:https://doi.org/10.1016/j.ympev.2014.10.004
(2015).
- 149 Betancur-R, R. *et al.* Phylogenetic classification of bony fishes. *BMC Evol. Biol.* **17**, 162,
doi:10.1186/s12862-017-0958-3 (2017).
- 150 Greenwood, P. H., Rosen, D. E., Weitzman, S. H. & Myers, G. S. Phyletic studies of
teleostean fishes, with a provisional classification of living forms. *Bull. Amer. Mus. Nat.
Hist.* **131**, 341-455 (1966).
- 151 Nelson, J. S., Grande, T. C. & Wilson, M. V. H. *Fishes of the world*. 5th edn, (John
Wiley & Sons, Inc., 2016).
- 152 Betancur-R, R. *et al.* The tree of life and a new classification of bony fishes. *PLOS Cur.
Tree of Life* **2013**, doi:10.1371/currents.tol.53ba26640df0ccaee75bb165c8c26288 (2013).
- 153 Li, B. *et al.* RNF213, a new nuclear marker for acanthomorph phylogeny. *Mol.
Phylogenet. Evol.* **50**, 345-363 (2009).
- 154 Wainwright, P. C. *et al.* The evolution of pharyngognathy: a phylogenetic and functional
appraisal of the pharyngeal jaw key innovation in labroid fishes and beyond. *Syst. Biol.*
61, 1001-1027, doi:10.1093/sysbio/sys060 (2012).
- 155 Malmstrøm, M. *et al.* Evolution of the immune system influences speciation rates in
teleost fishes. *Nat Genet* **48**, 1204-1210, doi:10.1038/ng.3645
<http://www.nature.com/ng/journal/v48/n10/abs/ng.3645.html#supplementary-information>
(2016).
- 156 Johnson, G. D. & Patterson, C. Percomorph phylogeny: a survey of acanthomorphs and a
new proposal. *Bull. Mar. Sci.* **52**, 554-626 (1993).
- 157 Roa-Varón, A. *et al.* Confronting sources of systematic error to resolve historically
contentious relationships: a case study using gadiform fishes (Teleostei,
Paracanthopterygii, Gadiformes). *Syst. Biol.*, doi:10.1093/sysbio/syaa095 (In press).

- 158 Dornburg, A. *et al.* New insights on the sister lineage of percomorph fishes with an anchored hybrid enrichment dataset. *Mol. Phylogenet. Evol.* **110**, 27-38, doi:<https://doi.org/10.1016/j.ympev.2017.02.017> (2017).
- 159 Fricke, R., Eschmeyer, W. N. & Fong, J. D. *Eschmeyer's Catalog of Fishes: species by family/subfamily*, <<http://researcharchive.calacademy.org/research/ichthyology/catalog/SpeciesByFamily.a.sp>> (2021).
- 160 Gill, F., Donsker, D. & Rasmussen, P. *IOC World Bird List (v10.2)*, (2020).
- 161 Burgin, C. J., Colella, J. P., Kahn, P. L. & Upham, N. S. How many species of mammals are there? *J. Mammal.* **99**, 1-14, doi:10.1093/jmammal/gyx147 (2018).
- 162 Uetz, P., Freed, P. & Hošek, J. *The Reptile Database*, <http://www.reptile-database.org> accessed December 2020, (2020).
- 163 Jordan, D. S. A classification of fishes including families and genera as far as known. *Stanford University Publications University Series Biological Sciences* **3**, 77-243 (1923).
- 164 Nelson, J. S. *Fishes of the world, 4th edition*. (John Wiley, 2006).
- 165 Smith, W. L. & Craig, M. T. Casting the percomorph net widely: the importance of broad taxonomic sampling in the search for the placement of serranid and percid fishes. *Copeia* **2007**, 35-55 (2007).
- 166 Nelson, G. in *The hierarchy of life: molecules and morphology in phylogenetic analysis* (eds B. Fernholm, K. Bremer, & H. Jörnvall) 325-336 (Elsevier, 1989).
- 167 Møller, P. R., Knudsen, S. W., Schwarzhans, W. & Nielsen, J. G. A new classification of viviparous brotulas (Bythitidae) – with family status for Dinematchthyidae – based on molecular, morphological and fossil data. *Mol. Phylogenet. Evol.* **100**, 391-408, doi:<http://dx.doi.org/10.1016/j.ympev.2016.04.008> (2016).
- 168 Campbell, M. A. *et al.* Evolutionary affinities of the unfathomable Parabrotulidae: molecular data indicate placement of *Parabrotula* within the family Bythitidae, Ophidiiformes. *Mol. Phylogenet. Evol.* **109**, 337-342, doi:<https://doi.org/10.1016/j.ympev.2017.02.004> (2017).
- 169 Evseenko, S. A., Gordeeva, N. V., Bolshakova, Y. Y. & Kobylansky, S. H. Morphology and molecular phylogenetic relationships of *Barathronus multidentis* (Ophidiiformes: Bythitidae). *Cybium: international journal of ichthyology* **42**, 137-141 (2018).
- 170 Miya, M., Satoh, T. R. & Nishida, M. The phylogenetic position of toadfishes (order Batrachoidiformes) in the higher ray-finned fish as inferred from partitioned Bayesian analysis of 102 whole mitochondrial genome sequences. *Biol. J. Linn. Soc.* **85**, 289-306 (2005).
- 171 Smith, W. L. & Wheeler, W. C. Venom evolution widespread in fishes: a phylogenetic road map for the bioprospecting of piscine venoms. *J. Hered.* **97**, 206-217 (2006).
- 172 Thacker, C. E. Phylogeny of Gobioidae and placement within Acanthomorpha, with a new classification and investigation of diversification and character evolution. *Copeia* **2009**, 93-104 (2009).
- 173 Chakrabarty, P., Davis, M. P. & Sparks, J. S. The first record of a trans-oceanic sister-group relationship between obligate vertebrate troglobites. *Plos One* **7** (2012).
- 174 Kuang, T. *et al.* Phylogenomic analysis on the exceptionally diverse fish clade Gobioidae (Actinopterygii: Gobiiformes) and data-filtering based on molecular clocklikeness. *Mol. Phylogenet. Evol.* **128**, 192-202, doi:<https://doi.org/10.1016/j.ympev.2018.07.018> (2018).

- 175 McCraney, W. T., Thacker, C. E. & Alfaro, M. E. Supermatrix phylogeny resolves goby lineages and reveals unstable root of Gobiaria. *Mol. Phylogenet. Evol.* **151**, 106862, doi:https://doi.org/10.1016/j.ympev.2020.106862 (2020).
- 176 Thacker, C. E. *et al.* Molecular phylogeny of Percomorpha resolves *Trichonotus* as the sister lineage to Gobioidi (Teleostei: Gobiiformes) and confirms the polyphyly of Trachinoidei. *Mol. Phylogenet. Evol.* **93**, 172-179, doi:https://doi.org/10.1016/j.ympev.2015.08.001 (2015).
- 177 Orrell, T. M., Collette, B. B. & Johnson, G. D. Molecular data support separate scombroid and xiphioid clades. *Bull. Mar. Sci.* **79**, 505-519 (2006).
- 178 Song, H. Y. *et al.* Mitogenomic circumscription of a novel percomorph fish clade mainly comprising "Syngnathoidi" (Teleostei). *Gene* **542**, 146-155, doi:10.1016/j.gene.2014.03.040 (2014).
- 179 Gosline, W. A. A reinterpretation of the teleostean fish order Gobiesociformes. *Proc. California Acad. Sci.* **38**, 363-381 (1970).
- 180 Nelson, J. S. *Fishes of the world, 3rd edition*. 3rd edn, (Wiley, 1994).
- 181 Springer, V. G. & Johnson, G. D. Study of the dorsal gill-arch musculature of teleostome fishes, with special reference to the Actinopterygii. *Bull. Biol. Soc. Wash.* **11**, 1-260 (2004).
- 182 Wiley, E. O. & Johnson, G. D. in *Origin and phylogenetic interrelationships of teleosts* (eds J.S. Nelson, H.-P. Schultz, & M.V.H. Wilson) 123-182 (Verlag Dr. Friedrich Pfeil, 2010).
- 183 Johnson, G. D. Percomorph phylogeny: progress and problems. *Bull. Mar. Sci.* **52**, 3-28 (1993).
- 184 Kim, B.-J. Comparative anatomy and phylogeny of the family Mullidae (Teleostei: Perciformes). *Memoirs of the Graduate School of Fisheries Sciences, Hokkaido University* **49**, 1-74 (2002).
- 185 Parenti, L. R. Relationships of atherinomorph fishes (Teleostei). *Bull. Mar. Sci.* **52**, 170-196. (1993).
- 186 Reznick, D. N., Furness, A. I., Meredith, R. W. & Springer, M. S. The origin and biogeographic diversification of fishes in the family Poeciliidae. *PLOS ONE* **12**, e0172546, doi:10.1371/journal.pone.0172546 (2017).
- 187 Bragança, P. H. N., Amorim, P. F. & Costa, W. J. E. M. Pantanodontidae (Teleostei, Cyprinodontiformes), the sister group to all other cyprinodontoid killifishes as inferred by molecular data. *Zoosystematics and Evolution* **94**, 137-145 (2018).
- 188 Pohl, M., Milvertz, F., Meyer, A. & Vences, M. Multigene phylogeny of cyprinodontiform fishes suggests continental radiations and a rogue taxon position of Pantanodon. *Vertebrate Zoology* **65**, 37-44 (2015).
- 189 Parenti, L. R. A phylogenetic and biogeographic analysis of cyprinodontiform fishes (Teleostei: Atherinomorpha). *Bull. Amer. Mus. Nat. Hist.* **168**, 335-557 (1981).
- 190 Costa, W. J. E. M. in *Phylogeny and classification of Neotropical fishes* (eds L.R. Malabarba *et al.*) 537-560 (EDIPUCRS, 1998).
- 191 Lovejoy, N. R. Reinterpreting recapitulation: Systematics of needlefishes and their allies (Teleostei : Beloniformes). *Evolution* **54**, 1349-1362 (2000).
- 192 Lovejoy, N. R., Iranpour, M. & Collette, B. B. Phylogeny and jaw ontogeny of beloniform fishes. *Integ. Comp. Biol.* **44**, 366-377, doi:Doi 10.1093/Icb/44.5.366 (2004).

- 193 Dasilao, J. C. & Sasaki, K. Phylogeny of the flyingfish family Exocoetidae (Teleostei, Beloniformes). *Ichthyol. Res.* **45**, 347-353, doi:10.1007/BF02725187 (1998).
- 194 Bloom, D. D., Unmack, P. J., Gosztonyi, A. E., Piller, K. R. & Lovejoy, N. R. It's a family matter: molecular phylogenetics of Atheriniformes and the polyphyly of the surf silversides (Family: Notocheiridae). *Mol. Phylogenet. Evol.* **62**, 1025-1030 (2012).
- 195 Campanella, D. *et al.* Multi-locus fossil-calibrated phylogeny of Atheriniformes (Teleostei, Ovalentaria). *Mol. Phylogenet. Evol.* **86**, 8-23, doi:https://doi.org/10.1016/j.ympev.2015.03.001 (2015).
- 196 Dyer, B. S. & Chernoff, B. Phylogenetic relationships among atheriniform fishes (Teleostei: Atherinomorpha). *Zool. J. Linn. Soc.* **117**, 1-69 (1996).
- 197 Liem, K. F. & Greenwood, P. H. A functional-approach to the phylogeny of the pharyngognath teleosts. *Am. Zool.* **21**, 83-101 (1981).
- 198 Kaufman, L. & Liem, K. F. Fishes of the suborder Labroidei (Pisces: Perciformes): phylogeny, ecology, and evolutionary significance. *Breviora* **472**, 1-19 (1982).
- 199 Springer, V. G. & Orrell, T. M. Appendix: phylogenetic analysis of 147 families of acanthomorph fishes based primarily on dorsal gill-arch muscles and skeleton. - In: Springer, V.G. & Johnson, G.D. Study of the dorsal gill-arch musculature of teleostome fishes, with special reference to the Actinopterygii. *Bull. Biol. Soc. Wash.* **11**, 236-260 (2004).
- 200 Rosen, D. E. & Patterson, C. On Müller's and Cuvier's concepts of pharyngognath and labyrinth fishes and the classification of percomorph fishes, with an atlas of percomorph dorsal gill arches. *Amer. Mus. Novit.* **2983**, 1-57 (1990).
- 201 Collins, R. A., Britz, R. & Rüber, L. Phylogenetic systematics of leaffishes (Teleostei: Polycentridae, Nandidae). *J. Zool. Syst. Evol. Res.* **53**, 259-272, doi:10.1111/jzs.12103 (2015).
- 202 Lundberg, J. G. in *Biological Relationships between Africa and South America* (ed P. Goldblatt) 156-199 (Yale University Press, 1993).
- 203 Lavoué, S. Origins of Afrotropical freshwater fishes. *Zool. J. Linn. Soc.* **188**, 345-411, doi:10.1093/zoolinnean/zlz039 (2020).
- 204 Stiassny, M. L. J. What are grey mullets? *Bull. Mar. Sci.* **52**, 197-219. (1993).
- 205 Stiassny, M. L. J. Notes on the anatomy and relationships of the bedotiid fishes of Madagascar, with a taxonomic revision of the genus *Rheocles* (Atherinomorpha: Bedotiidae). *Amer. Mus. Novit.* **2979**, 1-33 (1990).
- 206 Lin, H. C. & Hastings, P. A. Phylogeny and biogeography of a shallow water fish clade (Teleostei: Blenniiformes). *BMC Evol. Biol.* **13**, doi:Unsp 210 Doi 10.1186/1471-2148-13-210 (2013).
- 207 Kawahara, R. *et al.* Interrelationships of the 11 gasterosteiform families (sticklebacks, pipefishes, and their relatives): a new perspective based on whole mitogenome sequences from 75 higher teleosts. *Mol. Phylogenet. Evol.* **46**, 224-236 (2008).
- 208 Mabuchi, K., Miya, M., Azuma, Y. & Nishida, M. Independent evolution of the specialized pharyngeal jaw apparatus in cichlid and labrid fishes. *BMC Evol. Biol.* **7**, - (2007).
- 209 Britz, R. & Johnson, G. D. "Paradox Lost": Skeletal ontogeny of *Indostomus paradoxus* and its significance for the phylogenetic relationships of Indostomidae (Teleostei, Gasterosteiformes). *Amer. Mus. Novit.* **3383**, 1-43 (2002).

- 210 Travers, R. A. A review of the Mastacembeloidei, a suborder of synbranchiform teleost fishes. Part II: Phylogenetic analysis. *Bull. Br. Mus. Nat. Hist. (Zool.)* **47**, 83-150 (1984).
- 211 Gosline, W. A. The suborders of perciform fishes. *Proceedings of the United States National Museum* **124**, 1-78 (1968).
- 212 Datovo, A., de Pinna, M. C. C. & Johnson, G. D. The infrabranchial musculature and Its bearing on the phylogeny of percomorph fishes (Osteichthyes: Teleostei). *Plos One* **9**, e110129, doi:10.1371/journal.pone.0112600 (2014).
- 213 Li, C. H., Ricardo, B. R., Smith, W. L. & Ortí, G. Monophyly and interrelationships of snook and barramundi (Centropomidae *sensu* Greenwood) and five new markers for fish phylogenetics. *Mol. Phylogenet. Evol.* **60**, 463-471 (2011).
- 214 Sanciangco, M. D., Carpenter, K. E. & Betancur-R, R. Phylogenetic placement of enigmatic percomorph families (Teleostei: Percomorphaceae). *Mol. Phylogenet. Evol.* **94**, Part B, 565-576, doi:http://dx.doi.org/10.1016/j.ympev.2015.10.006 (2016).
- 215 Girard, M. G., Davis, M. P. & Smith, W. L. The phylogeny of carangiform fishes: morphological and genomic investigations of a new fish clade. *Copeia* **108**, 265-298, doi:10.1643/CI-19-320 (2020).
- 216 Smith, W. L., Stern, J. H., Girard, M. G. & Davis, M. P. Evolution of venomous cartilaginous and ray-finned fishes. *Integ. Comp. Biol.* **56**, 950-961, doi:10.1093/icb/icw070 (2016).
- 217 Chen, W.-J., Bonillo, C. & Lecointre, G. Repeatability of clades as a criterion of reliability: a case study for molecular phylogeny of Acanthomorpha (Teleostei) with larger number of taxa. *Mol. Phylogenet. Evol.* **26**, 262-288 (2003).
- 218 Dettai, A. & Lecointre, G. In search of notothenioid (Teleostei) relatives. *Antarctic Sci.* **16**, 71-85 (2004).
- 219 Miya, M. *et al.* Major patterns of higher teleostean phylogenies: a new perspective based on 100 complete mitochondrial DNA sequences. *Mol. Phylogenet. Evol.* **26**, 121-138, doi:10.1016/S1055-7903(02)00332-9 (2003).
- 220 Matschiner, M., Hanel, R. & Salzburger, W. On the origin and trigger of the notothenioid adaptive radiation. *Plos One* **6**, e18911 (2011).
- 221 Lautredou, A.-C. *et al.* New nuclear markers and exploration of the relationships among Serraniformes (Acanthomorpha, Teleostei): the importance of working at multiple scales. *Mol. Phylogenet. Evol.* **67**, 140-155 (2013).
- 222 Johnson, G. D. *Niphon spinosus*: A primitive epinepheline serranid, with comments on the monophyly and intrarelationships of the Serranidae. *Copeia*, 777-787 (1983).
- 223 Johnson, G. D. *Niphon spinosus*, a primitive epinepheline serranid: corroborative evidence from the larvae. *Jap. J. Ich.* **35**, 7-18 (1988).
- 224 Johnson, G. D. in *Ontogeny and systematics of fishes* (eds H.G. Moser *et al.*) 464-498 (American Society of Ichthyologists and Herpetologists, 1984).
- 225 Near, T. J. *et al.* Identification of the notothenioid sister lineage illuminates the biogeographic history of an Antarctic adaptive radiation. *BMC Evol. Biol.* **15**, 109, doi:10.1186/s12862-015-0362-9 (2015).
- 226 Smith, W. L., Elizabeth, E. & Clara, R. Phylogeny and taxonomy of flatheads, scorpionfishes, sea robins, and stonefishes (Percomorpha: Scorpaeniformes) and the evolution of the lachrymal saber. *Copeia* **106**, 94-119, doi:10.1643/CG-17-669 (2018).

- 227 Clardy, T. R. *Phylogenetic systematics of the prickleback family Stichaeidae (Cottiformes: Zoarcidae) using morphological data* Ph.D. thesis, The College of William & Mary, (2014).
- 228 Kwun, H. J. & Kim, J.-K. Molecular phylogeny and new classification of the genera *Eulophias* and *Zoarchias* (PISCES, Zoarcoidei). *Mol. Phylogenet. Evol.* **69**, 787-795, doi:https://doi.org/10.1016/j.ympev.2013.06.025 (2013).
- 229 Radchenko, O. A. The system of the suborder Zoarcoidei (Pisces, Perciformes) as inferred from molecular genetic data. *Russian Journal of Genetics* **51**, 1096-1112, doi:10.1134/S1022795415100130 (2015).
- 230 Near, T. J. *et al.* Nuclear gene-inferred phylogenies resolve the relationships of the enigmatic Pygmy Sunfishes, *Elassoma* (Teleostei: Percomorpha). *Mol. Phylogenet. Evol.* **63**, 388-395, doi:10.1016/j.ympev.2012.01.011 (2012).
- 231 Chen, W.-J., Lavoué, S., Beheregaray, L. B. & Mayden, R. L. Historical biogeography of a new antitropical clade of temperate freshwater fishes. *J. Biogeogr.* **41**, 1806-1818, doi:10.1111/jbi.12333 (2014).
- 232 Greenwood, P. H. A revised familial classification for certain cirrhitoid genera (Teleostei, Percoidae Cirrhitidae), with comments on the group's monophyly and taxonomic ranking. *Bull. Nat. Hist. Mus. Lond. (Zool.)* **61**, 1-10 (1995).
- 233 Burrige, C. P. & Smolenski, A. J. Molecular phylogeny of the Cheilodactylidae and Latridae (Perciformes: Cirrhitidae) with notes on taxonomy and biogeography. *Mol. Phylogenet. Evol.* **30**, 118-127 (2004).
- 234 Kimura, K., Imamura, H. & Kawai, T. Comparative morphology and phylogenetic systematics of the families Cheilodactylidae and Latridae (Perciformes: Cirrhitidae), and proposal of a new classification. *Zootaxa* **4536**, doi:10.11646/zootaxa.4536.1.1 (2018).
- 235 Ludt, W. B., Burrige, C. P. & Chakrabarty, P. A taxonomic revision of Cheilodactylidae and Latridae (Centrarchiformes: Cirrhitidae) using morphological and genomic characters. *Zootaxa* **4585**, doi:10.11646/zootaxa.4585.1.7 (2019).
- 236 McDowall, R. M. Relationships and taxonomy of the New Zealand torrent fish, *Cheimarrichthys fosteri* Haast (Pisces: Mugiloididae). *Journal of the Royal Soc NZ* **3**, 199-217 (1973).
- 237 Pietsch, T. W. Phylogenetic relationships of trachinoid fishes of the family Uranoscopidae. *Copeia* **1989**, 253-303 (1989).
- 238 Pietsch, T. W. & Zabatien, C. P. Osteology and interrelationships of the sand lances (Teleostei: Ammodytidae). *Copeia* **1990**, 78-100 (1990).
- 239 Imamura, H. & Matsuura, K. Redefinition and phylogenetic relationships of the family Pinguipedidae (Teleostei : Perciformes). *Ichthyol. Res.* **50**, 259-269 (2003).
- 240 McDowall, R. M. Biogeography of the New Zealand torrentfish, *Cheimarrichthys fosteri* (Teleostei : Pinguipedidae): a distribution driven mostly by ecology and behaviour. *Envir. Biol. Fishes* **58**, 119-131 (2000).
- 241 Last, P. R. in *FAO species identification guide for fishery purposes: The living marine resources of the Western Central Pacific, Volume 6. Bony fishes part 4 (Labridae to Latimeriidae)* (eds K.E. Carpenter & V.H. Niem) 3517 (FAO, 2001).
- 242 Davis, M. P., Sparks, J. S. & Smith, W. L. Repeated and widespread evolution of bioluminescence in marine fishes. *PLoS ONE* **11**, e0155154, doi:10.1371/journal.pone.0155154 (2016).

- 243 Prokofiev, A. M. Osteology and some other morphological characters of *Howella sherborni*, with a discussion of the systematic position of the genus (Perciformes, Percoidei). *J. Ichthyol.* **47**, 413-426 (2007).
- 244 Patterson, C. & Rosen, D. E. in *Papers on the systematics of gadiform fishes* Vol. 32 *Natural History Museum of Los Angeles County Science Series* (ed D.M. Cohen) 5-36 (Natural History Museum of Los Angeles County, 1989).
- 245 Chanet, B. *et al.* Evidence for a close phylogenetic relationship between the teleost orders Tetraodontiformes and Lophiiformes based on an analysis of soft anatomy. *Cybium* **37**, 179-198 (2013).
- 246 Baldwin, C. C. The phylogenetic significance of colour patterns in marine teleost larvae. *Zool. J. Linn. Soc.* **168**, 496-563 (2013).
- 247 Winterbottom, R. The familial phylogeny of the Tetraodontiformes (Acanthopterygii: Pisces) as evidenced by their myology. *Smithson. Contrib. Zool.* **No. 155**, 1-201 (1974).
- 248 Leis, J. M. in *Ontogeny and systematics of fishes* (eds H.G. Moser *et al.*) 459-463 (American Society of Ichthyologists and Herpetologists, 1984).
- 249 Holcroft, N. I. A molecular analysis of the interrelationships of tetraodontiform fishes (Acanthomorpha : Tetraodontiformes). *Mol. Phylogenet. Evol.* **34**, 525-544 (2005).
- 250 Alfaro, M. E., Santini, F. & Brock, C. D. Do reefs drive diversification in marine teleosts? Evidence from the pufferfish and their allies (Order Tetraodontiformes). *Evolution* **61**, 2104-2126 (2007).
- 251 Yamanoue, Y. *et al.* Phylogenetic position of tetraodontiform fishes within the higher teleosts: Bayesian inferences based on 44 whole mitochondrial genome sequences. *Mol. Phylogenet. Evol.* **45**, 89-101 (2007).
- 252 Santini, F., Sorenson, L. & Alfaro, M. E. A new phylogeny of tetraodontiform fishes (Tetraodontiformes, Acanthomorpha) based on 22 loci. *Mol. Phylogenet. Evol.* **69**, 177-187, doi:Doi 10.1016/J.Ympev.2013.05.014 (2013).
- 253 Arcila, D., Pyron, R. A., Tyler, J. C., Orti, G. & Betancur-R, R. An evaluation of fossil tip-dating versus node-age calibrations in tetraodontiform fishes (Teleostei: Percomorphaceae). *Mol. Phylogenet. Evol.* **82**, 131-145 (2015).
- 254 Arcila, D. & Tyler, J. C. Mass extinction in tetraodontiform fishes linked to the Palaeocene-Eocene thermal maximum. *Proc. R. Soc. B* **284** (2017).
- 255 Miya, M. *et al.* Evolutionary history of anglerfishes (Teleostei: Lophiiformes): a mitogenomic perspective. *BMC Evol. Biol.* **10** (2010).
- 256 Pietsch, T. W. & Orr, J. W. Phylogenetic relationships of deep-sea anglerfishes of the suborder Ceratioidei (Teleostei: Lophiiformes) based on morphology. *Copeia* **2007**, 1-34 (2007).
- 257 Derouen, V., Ludt, W. B., Ho, H.-C. & Chakrabarty, P. Examining evolutionary relationships and shifts in depth preferences in batfishes (Lophiiformes: Ogcocephalidae). *Mol. Phylogenet. Evol.* **84**, 27-33, doi:https://doi.org/10.1016/j.ympev.2014.12.011 (2015).
- 258 Swann, J. B., Holland, S. J., Petersen, M., Pietsch, T. W. & Boehm, T. The immunogenetics of sexual parasitism. *Science* **369**, 1608, doi:10.1126/science.aaz9445 (2020).
- 259 Pietsch, T. W. *Oceanic anglerfishes extraordinary diversity in the deep sea.* (University of California Press, 2009).

- 260 Lanfear, R. Calculating and interpreting gene- and site-concordance factors in
phylogenomics. http://www.robertlanfear.com/blog/files/concordance_factors.html
(2018).
- 261 Minh, B. Q., Hahn, M. W. & Lanfear, R. New methods to calculate concordance factors
for phylogenomic datasets. *Mol. Biol. Evol.* **37**, 2727-2733, doi:10.1093/molbev/msaa106
(2020).
- 262 de la Estrella, M., Forest, F., Wieringa, J. J., Fougère-Danezan, M. & Bruneau, A.
Insights on the evolutionary origin of Detarioideae, a clade of ecologically dominant
tropical African trees. *New Phytologist* **214**, 1722-1735,
doi:<https://doi.org/10.1111/nph.14523> (2017).
- 263 Jetz, W. & Pyron, R. A. The interplay of past diversification and evolutionary isolation
with present imperilment across the amphibian tree of life. *Nature Ecology & Evolution*
2, 850-858, doi:10.1038/s41559-018-0515-5 (2018).
- 264 Thomson, R. C., Spinks, P. Q. & Shaffer, H. B. A global phylogeny of turtles reveals a
burst of climate-associated diversification on continental margins. *Proceedings of the
National Academy of Sciences* **118**, e2012215118, doi:10.1073/pnas.2012215118 (2021).
- 265 Condamine, F. L., Nel, A., Grandcolas, P. & Legendre, F. Fossil and phylogenetic
analyses reveal recurrent periods of diversification and extinction in dictyopteran insects.
Cladistics **36**, 394-412, doi:<https://doi.org/10.1111/cla.12412> (2020).
- 266 May, M. R., Höhna, S. & Moore, B. R. A Bayesian approach for detecting the impact of
mass-extinction events on molecular phylogenies when rates of lineage diversification
may vary. *Methods Ecol Evol* **7**, 947-959, doi:<https://doi.org/10.1111/2041-210X.12563>
(2016).
- 267 Moore, B. R., Höhna, S., May, M. R., Rannala, B. & Huelsenbeck, J. P. Critically
evaluating the theory and performance of Bayesian analysis of macroevolutionary
mixtures. *Proceedings of the National Academy of Sciences* **113**, 9569-9574 (2016).
- 268 Rabosky, D. L., Mitchell, J. S. & Chang, J. Is BAMM Flawed? Theoretical and Practical
Concerns in the Analysis of Multi-Rate Diversification Models. *Syst. Biol.* **66**, 477-498
(2017).
- 269 Venditti, C., Meade, A. & Pagel, M. Multiple routes to mammalian diversity. *Nature* **479**,
393-396, doi:Doi 10.1038/Nature10516 (2011).
- 270 Chang, J., Rabosky, D. L. & Alfaro, M. E. Estimating Diversification Rates on
Incompletely Sampled Phylogenies: Theoretical Concerns and Practical Solutions. *Syst.
Biol.* **69**, 602-611, doi:10.1093/sysbio/syz081 (2020).
- 271 Louca, S. & Pennell, M. W. Extant timetrees are consistent with a myriad of
diversification histories. *Nature* **580**, 502-505, doi:10.1038/s41586-020-2176-1 (2020).